IMPERIAL COLLEGE LONDON

FACULTY OF NATURAL SCIENCES

DIVISION OF BIOLOGY

REGULATION AND LOCALISATION OF PSP PROTEINS IN E. COLI

CHRISTOPH ENGL

SUBMITTED FOR THE DEGREE OF DOCTOR OF PHILOSOPHY

DECLARATION OF AUTHORSHIP

I certify that this thesis entitled "Regulation and Localisation of Psp proteins in *E. coli*" is written entirely by myself and that the research to which it refers to is my own. I confirm that all main sources of help have been acknowledged and that any ideas or quotations from the work of others have always clearly been referenced.

Christoph Engl

ABSTRACT

The phage shock protein (Psp) response is found in many Gram-negative enterobacteria, where it helps to maintain the proton motive force (PMF) when the integrity of the inner membrane (IM) is impaired and promotes virulence of pathogens such as *Yersinia* or *Salmonella*. In *Escherichia coli,* Psp comprises seven genes (*pspF pspABCDE* and *pspG*) which are organised in a regulon under the control of two Sigma54-dependent promoters. Despite considerable advances, neither the mechanism of Psp induction nor the functioning of the Psp response is fully understood. Recent findings comparing the roles of ArcB in *Yersinia enterocolitica* and *E. coli* caused a dispute over the requirement of the two-component system ArcAB in Psp signal-transduction. The present study now establishes that ArcAB involvement is conditional and appears to be mediated via protein-protein interactions between ArcB and PspB. The study further suggests that the cellular ubiquinone pool, which acts upstream of ArcAB, may also play a role in Psp signalling whereas dissipation of proton motive force (PMF), generally inferred to be the inducing signal, is not sufficient to mount a Psp response. To gain further insight into its functioning, PspA (a negative regulator and effector of Psp) and PspG (an effector of Psp) were visualised *in vivo* using fusions to Green fluorescent protein (GFP). To maintain PMF, PspA was proposed to uniformly cover the cytoplasmic face of the IM. However, the present study demonstrates that PspA (and PspG) is highly organised into distinct complexes at the cell pole and the lateral cell membrane. Real-time observations revealed lateral PspA and PspG complexes are highly mobile, but absent in cells lacking MreB. Without the MreB cytoskeleton,

induction of the Psp response is still observed, yet these cells fail to maintain PMF under stress conditions.

ACKNOWLEDGEMENTS

I would like to thank my supervisor Martin Buck for providing such an interesting project, for his continuous support, advice and guidance throughout my PhD and also for giving me the chance to present my work at conferences.

A big thank you goes out to Trish for being immensely supportive inside and outside the lab, for the great time we had and for helping to organise the lab - especially me and my bench. I also want to thank all the past and present members of Martin's lab. It was a fun, enjoyable and stimulating experience working with you guys. Special thanks to Goran for his help with the project, for lively discussions on the Psp response and for his fatherly advice beyond work.

I also want to thank all my collaborators, Liming Ying and Martin Spitaler at Imperial College, Heath Murray and Jeff Errington at the University of Newcastle as well as Alex Ter Beek, Martijn Bekker and Joost Teixeira de Mattos at the University of Amsterdam (The Netherlands) for providing their equipment and expertise without which this project would not have been possible.

Ganz besonders moechte ich meinen Eltern danken. Ohne ihre fortwaehrende uneingeschraenkte Unterstuetzung von Beginn an haette ich das nicht geschafft.

CONTENTS

DECLARATION OF AUTHORSHIP 2
ABSTRACT 3
ACKNOWLEDGEMENTS 5
CONTENTS 6
LIST OF TABLES 9
LIST OF FIGURES 10
ABBREVIATIONS 12

CHAPTER 1 INTRODUCTION 15
1.1 OVERVIEW 16
1.2 COMPOSITION OF THE GRAM-NEGATIVE CELL ENVELOPE 17
1.2.1 The outer membrane (OM) 17
1.2.2 The periplasm 19
1.2.3 The inner membrane (IM) 19
1.2.3.1 Chemotaxis 22
1.2.3.2 Energy conservation 22
1.3 PROTEIN SECRETION SYSTEMS IN GRAM-NEGATIVE BACTERIA 26
1.3.1 Translocation into or across the IM 26
1.3.1.1 The Sec pathway 26
1.3.1.2 The Tat (Twin-arginine translocation) pathway 28
1.3.2 Translocation into the OM 30
1.3.2.1 Insertion of OMPs into the OM 30
1.3.2.2 The Lol system 33
1.3.3 Secretion into the extracellular milieu 35
1.3.3.1 The Type I Secretion 35
1.3.3.2 The Type II Secretion 36
1.3.3.3 The Type III Secretion 36
1.3.3.4 The Type IV Secretion 37
1.3.3.5 The Type V Secretion 38
1.3.3.6 The Type VI Secretion 38
1.4 THE ROLE OF THE CELL ENVELOPE IN BACTERIAL ADHESION AND PATHOGENESIS 41
1.4.1 Pili/Fimbria 41
1.4.2 Invasion proteins 42
1.5 STRESS RESPONSES OF THE CELL ENVELOPE 43
1.5.1 The SigmaE response 43
1.5.2 The Cpx system 46
1.5.3 The BaeSR system 47
1.5.4 The Phage-shock protein (Psp) response 49
1.5.4.1 Inducers of the Psp response 50
1.5.4.2 The function of the Psp response 53
1.5.4.2.1 PMF maintenance under envelope stress 53
1.5.4.2.2 Role in virulence of pathogenic Gram-negative bacteria 54
1.5.4.3 Conservation of Psp proteins 55
1.5.4.4 The Psp response in Escherichia coli 56
1.5.4.4.1 Components 56
1.5.4.4.2 Regulation of psp gene expression 59
1.6 OBJECTIVES OF THIS STUDY 63

CHAPTER 2 MATERIALS AND METHODS 64
2.1 MATERIALS 65
2.1.1 Media 65
2.1.2 Antibiotics 65
2.1.3 Kits 66

2.1.4 Dyes and Chemicals 66
2.2 BACTERIAL STRAINS 67
2.2.1 Generation of bacterial strains 67
2.3 DNA METHODS 69
2.3.1 Purification of DNA 70
2.3.1.1 Chromosomal DNA 70
2.3.1.2 Plasmid DNA 70
2.3.2 Polymerase Chain Reaction (PCR) 71
2.3.2.1 PCR for molecular cloning 71
2.3.2.2 Analysis of cloned or deleted genes 72
2.3.3 Agarose Gel electrophoresis 73
2.3.4 Gel extraction of DNA 74
2.3.5 TA cloning 74
2.3.6 DNA sequencing 75
2.3.7 Restriction digest of DNA 76
2.3.8 Ligation 76
2.3.9 Preparation of competent cells 76
2.3.10 Heat shock transformation of competent cells 77
2.3.11 Site-directed mutagenesis 77
2.4 IN VITRO METHODS 79
2.4.1 Small scale protein expression 79
2.4.2 SDS Polyacrylamid Gel electrophoresis (SDS-PAGE) 79
2.4.3 Immunoblotting 80
2.4.4 β-Galactosidase assay 81
2.4.5 Extraction and measurement of quinones 84
2.4.6 Triton X-100 cell fractionation 85
2.4.6.1 Extraction of soluble proteins 85
2.4.6.2 Extraction of inner membrane proteins 86
2.4.6.3 Extraction of outer membrane proteins 86
2.4.6.4 Extraction of aggregated proteins 86
2.5 IN VIVO METHODS 88
2.5.1 Growth of bacterial cells 88
2.5.2 Bacterial two-hybrid analysis 89
2.5.3 Motility assay 91
2.5.4 Separation of mini- and rod-shaped cells 91
2.5.5 In vivo cross-linking 91
2.5.6 PMF measurement 92
2.5.7 Oxygen measurement 93
2.5.8 Fluorescence microscopy to analyse subcellular protein localisation 94
2.5.8.1 The Green Fluorescent Protein GFPmut2 94
2.5.8.2 Epi- and confocal fluorescence microscopy 97
2.5.8.3 Single molecule fluorescence imaging 98

CHAPTER 3 PHYSICAL, FUNCTIONAL AND CONDITIONAL INTERACTIONS BETWEEN ARCAB AND PSP 100
3.1 INTRODUCTION AND RECAP 101
3.2 OBJECTIVES 103
3.3 RESULTS 105
3.3.1 pIV-dependent induction of Psp under different growth conditions 105
3.3.2 Activation of ArcA facilitates pIV-dependent induction of Psp 111
3.3.3 An active form of ArcB promotes low-level induction of Psp independent of pIV 118
3.3.4 Activation of ArcAB results in decreased electron potential ($\Delta\psi$) 119
3.3.5 ArcB and PspB interact in vivo 122
3.3.6 $ArcB^{LeuZm}$ is in an active kinase form 129
3.3.7 PspBC propagates the signal onwards from the Arc system 132
3.4 DISCUSSION 135
3.4.1 Conditional requirement for Arc activation in pIV-dependent induction of Psp 135
3.4.2 ArcB communicates with PspB 137

3.4.3 Integration of the Arc system in the PspB/C-specific signalling pathway 139
3.4.4 PspA-PspF is a minimal Psp system 140

CHAPTER 4 CORRELATIONS BETWEEN QUINONE POOLS AND INDUCTION OF PSP **142**
4.1 INTRODUCTION AND RECAP **143**
4.2 OBJECTIVES **147**
4.3 RESULTS **148**
4.3.1 The electron transport mutants differ in their ubiquinone content under both, aerobic and microaerobic growth 148
4.3.2 Under microaerobic growth, the level of Psp induction in the electron transport mutants correlates with changes in the ubiquinone pool 151
4.3.3 DMK_8 and MK_8 are not required to mount the Psp response 155
4.3.4 Production of the pIV secretin affects the redox state of the ubiquinone pool 157
4.3.5 Psp can be induced at WT PMF levels 161
4.3.6 The PMF dissipating agents Valinomycin and actetate do not induce Psp 164
4.4 DISCUSSION **171**

CHAPTER 5 IN VIVO LOCALISATIONS OF PSP INNER MEMBRANE STRESS CONTROLLERS PSPA AND PSPG **175**
5.1 INTRODUCTION AND RECAP **176**
5.2 OBJECTIVES **177**
5.3 RESULTS **178**
5.3.1 GFP-PspA and PspG-GFP are functional 178
5.3.2 GFP-PspA and PspG-GFP are localised to the cell poles and traffic between both poles 187
5.3.3 GFP-PSpA and PspG-GFP trafficking is affected by A22 195
5.3.4 Psp induction can occur independently of an assembled MreB scaffold whereas PMF maintenance by Psp requires the MreB scaffold 203
5.3.5 PspA and PspG form oligomers in vivo 206
5.4 DISCUSSION **209**
5.4.1 GFP-PspA and PspG-GFP accumulate at the cell poles 209
5.4.2 MreB-dependent lateral complexes and the trafficking of GFP-PspA and PspG-GFP 212
5.4.3 PspA does not form a scaffold-like structure which evenly coats the IM 213

CHAPTER 6 OVERVIEW AND FUTURE DIRECTIONS **215**
6.1 OVERVIEW **216**
6.2 FUTURE DIRECTION **223**

REFERENCES **225**

APPENDIX **258**
APPENDIX A (STRAINS) **259**
APPENDIX B (PLASMIDS) **262**
APPENDIX C (PRIMER) **264**
APPENDIX D (ANALYSIS OF KNOCK-OUT STRAINS) **265**
APPENDIX E (ANTIBODIES) **266**
APPENDIX F (HPLC TRACES FROM THE QUINONE MEASUREMENT) **268**
APPENDIX G (ORIGINAL IMAGES FROM THE LOCALISATION STUDY) **275**
APPENDIX H (PUBLICATIONS ARISING FROM THIS WORK) **277**

LIST OF TABLES

CHAPTER 2 MATERIALS AND METHODS
Table 2.1: Media used in this study 65
Table 2.2: Antibiotics used in this study 65
Table 2.3: Kits used in this study 66
Table 2.4: Dyes and chemicals used in this study 67

CHAPTER 3 PHYSICAL, FUNCTIONAL AND CONDITIONAL INTERACTIONS BETWEEN ARCAB AND PSP
Table 3.1: Biochemical phenotypes of arcB alleles 111
Table 3.2: Interactions of Psp and ArcB proteins in vivo 123

LIST OF FIGURES

CHAPTER 1 INTRODUCTION

Figure 1.1: The cell envelope of Gram-negative bacteria 21
Figure 1.2: Energy conservation 25
Figure 1.3: The Sec and Tat pathway 29
Figure 1.4: Insertion of OMPs into the OM 32
Figure 1.5: The Lol system 34
Figure 1.6: The Type secretion systems 40
Figure 1.7: The SigmaE response 45
Figure 1.8: TheCpx system 48
Figure 1.9: The Psp regulon in E. coli 58
Figure 1.10: Regulation of the Psp response 62

CHAPTER 2 MATERIALS AND METHODS

Figure 2.1: Reactions catalysed by LacZ (β-galactosidase) 83
Figure 2.2: Flow-chart of the Triton X-100 based cell fractionation procedure 87
Figure 2.3: The BACTH System 90
Figure 2.4: The β-barrel and chromophore structure of WT GFP 96

CHAPTER 3 PHYSICAL, FUNCTIONAL AND CONDITIONAL INTERACTIONS BETWEEN ARCAB AND PSP

Figure 3.1: Regulation of the ArcAB two-component system 104
Figure 3.2: pIV-dependent induction of psp expression under different growth conditions 107
Figure 3.3: Production and localisation of pIV under microaerobic growth 108
Figure 3.4: Percentage of oxygen in MG1655 (WT) vs. ΔarcB and effect of global regulator mutants on Psp induction under microaerobic growth 110
Figure 3.5: Schematic representation of ArcB and ArcA with the locations of the amino acid substitutions used in this study 112
Figure 3.6: Expression and localisation of $ArcB_{WT}$ and ArcB mutants 114
Figure 3.7: Control of ArcA-P activated pfl expression by Arc protein variants 115
Figure 3.8: Bipartite role of ArcB activation in pIV-dependent Psp induction and production of pIV in cells co-expressing the Arc proteins 116
Figure 3.9: Activation of ArcAB reduces the electron potential ($\Delta\psi$) 121
Figure 3.10: Subcellular localisation of ArcB and PspB Cya-fusion proteins 124
Figure 3.11: In vivo cross-linking to test the interaction between PspB and ArcAB 126
Figure 3.12: Functionalities of T25-$ArcB_{WT}$, T25-ArcB and T25-$ArcB^{LeuZm}$ fusion proteins* 128
Figure 3.13: Activities and expression of the $ArcB^{LeuZm}$ proteins 130
Figure 3.14: $ArcB^{LeuZm}$ reduces the $\Delta\psi$ of the cell 131
Figure 3.15: Roles of PspB and PspC in transducing the psp-inducing signal(s) 134

CHAPTER 4 CORRELATIONS BETWEEN QUINONE POOLS AND INDUCTION OF PSP

Figure 4.1: The menaquinone and ubiquinone biosynthetic pathway 145
Figure 4.2: Ubiquinones play a central role as electron carrier in the electron transport chain under aerobic and also microaerobic growth 146
Figure 4.3: A typical HPLC trace of the quinone measurements and standard curve used to calculate the amount of ubiquinone 150
Figure 4.4: Psp induction and ubiquinones in the electron transport mutants 154
Figure 4.5: Psp induction in strains deleted for menA 156
Figure 4.6: Ubiquinones in MG1655 and MG1655ΔpspF in absence (-) and presence (+) of pIV 158
Figure 4.7: IM mislocalisation of the pIV secretin 160
Figure 4.8: PMF measurement in the electron transport mutants 162
Figure 4.9: Measurement of Psp induction by various agents 167
Figure 4.10: PMF measurement in MG1655 cells 169

CHAPTER 5 IN VIVO LOCALISATIONS OF PSP INNER MEMBRANE STRESS CONTROLLERS PSPA AND PSPG
Figure 5.1: Expression of GFP-PspA and PspG-GFP 180
Figure 5.2: Negative regulatory function of GFP-PspA is comparable to plasmid-borne PspA 181
Figure 5.3: GFP-PspA and PspG-GFP are functional effectors of the Psp response 184
Figure 5.4: GFP-PspA and PspG-GFP are not localised in inclusion bodies 185
Figure 5.5: PspG is an integral IM protein 186
Figure 5.6: GFP-PspA and PspG-GFP localise at both cell poles 188
Figure 5.7: Model for the MinCDE system 190
Figure 5.8: PspG-GFP can be found in minicells 191
Figure 5.9: GFP-PspA and PspG-GFP traffic between the cell poles 193
Figure 5.10: Lateral complexes of GFP-PspA and PspG-GFP are affected by A22 treatment 198
Figure 5.11: Positioning of polar complexes 199
Figure 5.12: Weak or transient interactions occur between PspA or PspB and MreB 202
Figure 5.13: Psp induction and maintenance of PMF in cells lacking the MreB scaffold 205
Figure 5.15: GFP-PspA and PspG-GFP form high-order oligomers in vivo 208

CHAPTER 6 OVERVIEW AND FUTURE DIRECTIONS
Figure 6.1: Summary of the findings on the signalling pathway of the Psp response 222

APPENDIX G (ORIGINAL IMAGES FROM THE LOCALISATION STUDY)
Original epi-fluorescence images of Figure 5.9 275
Original epi-fluorescence images of Figure 5.10 276

ABBREVIATIONS

α: anti

aa: amino acid

Agg: fraction containing aggregated proteins

APS: Ammoniumpersulphate

ATP: Adenosine triphosphate

A22: S-(3.4-dichlorobenzyl)-isothiourea

BACTH: bacterial two-hybrid

bp: base pair

°C: degree centigrade (Celsius)

Da: Dalton

DAPI: 4',6-diamidino-2-phenylindole

Δ: delta; gene deletion

DNA: Deoxyribonucleic acid

dNTP: deoxy nucleotide triphosphate

$\Delta\psi$: electron potential

DMK_8: demethylmenaquinone-8

DSP: dithiobis(succinimydylpropionate)

DTT: Dithiothreitol

EDTA: Ethylendiaminetetraacetic acid

ETC: electron transport chain

ϕ: gene fusion

g: gram

g: gravity

GFP: Green fluorescent protein

GTP: Guanosine triphosphate

HRP: Horse-radish peroxidase

IM: inner membrane

IPTG: Isopropyl β-D-1-thiogalactopyranoside

k: kilo

l: litre

LB: Luria-Bertani broth

LeuZ: leucine zipper

LeuZm: leucine zipper mutant

µ: micro

m: milli

M: Molar

MK_8: menaquinone-8

OM: outer membrane

ONPG: ortho-Nitrophenyl-β-galactoside

P_i: inorganic phosphate

pIV: protein IV from filamentous phage f1

PMF: proton motive force

Psp: phage shock protein

RNA: Ribonucleic acid

rpm: revolutions per minute

Sol: soluble fraction (cytoplasmic and periplasmic proteins)

SDS: Sodium dodecyl sulphate

TBS: Tris-buffered saline

TCA: Tri-chloro acetic acid

TEMED: Tetramethylethylenediamine

TIRF: total internal reflection fluorescence

TM: trans-membrane

Tris: Tris(hydroxymethyl)aminomethane

TTBS: Tris-buffered saline with Tween-20

UQ_8: ubiquinone-8

U Q_8-H_2: ubiquinol-8

V: Volts

v/v: volume per volume

WT: wild-type

w/v: weight per volume

CHAPTER 1

INTRODUCTION

1.1 OVERVIEW

Having colonised every ecological niche, microorganisms such as bacteria are one of the most versatile and successful life forms on earth. In their native habitats they encounter a plethora of stresses, e.g. extreme temperatures, pH or high salt concentrations. Being the barrier between the inside of the cell and the environment the cell envelope is often directly subjected to these adverse conditions. In addition to its function as a barrier, the cell envelope accommodates a third of all cellular proteins involved in various fundamental processes (Lopez-Campistrous, *et al*., 2005). Integrity of the cell envelope therefore is vital for the cell to survive. Thus, microorganisms such as the Gram-negative bacterium *Escherichia coli* have evolved various systems to counteract cell envelope stress, one of which is the Phage-shock protein (Psp) response, the subject of the present study.

In Chapter 1 key properties of the Gram-negative cell envelope are introduced, followed by a characterisation of the Psp response and an overview of the objectives of this study. Materials and Methods are summarised in Chapter 2. Results are then presented in Chapter 3, 4 and 5. Chapter 6 provides directions for future work.

1.2 COMPOSITION OF THE GRAM-NEGATIVE CELL ENVELOPE

The cell envelope of Gram-negative bacteria (e.g. *Escherichia coli*) comprises the outer membrane (OM), the periplasm and the inner membrane (IM) (Figure 1.1) and is composed of phospholipids (in *E. coli*: 70-75% phosphatidylethanolamine, 20-25% phosphatidylglycerol and 5% cardiolipin), lipopolysaccharide, peptidoglycan and proteins.

1.2.1 The outer membrane (OM)

The OM is an asymmetrical lipid bilayer of unique composition containing lipids, proteins (β-barrel proteins and lipoproteins) and polysaccharides. The inner leaflet is formed by a monolayer of phospholipids and the outer leaflet (in direct contact with the extracellular medium) consists of phospholipids and lipopolysaccharide (LPS) (Figure 1.1) (Mulhradt and Golecki, 1975).

LPS can generally be sub-divided into 3 structural domains:

- Lipid A (with fatty acids linked to *N*-acetylglucosamine)
- core polysaccharide
- O-specific polysaccharide

} The structure of the core and the O-specific polysaccharide is variable and species-specific.

The OM also contains lipoproteins and outer membrane proteins (OMPs).

Lipoproteins are surface exposed proteins anchored into the OM (and IM) via three hydrophobic acyl chains attached to a cysteine residue in their N-terminus (Tokuda, 2009). So far, 90 different lipoproteins (e.g. BamA, LolB or Lpp) have been identified

in *E. coli* (Tokuda *et al.*, 2007). OM lipoproteins connect the OM with the peptidoglycan in the periplasm below (see section 1.2.2) and are implicated in the biogenesis of the OM by aiding sorting of OMPs, LPS and lipoproteins (Tokuda, 2009). In order to localise into their destined lipid layer (OM or IM), lipoproteins require the Lol system (see section 1.3.2.2), which facilitates integration into the IM or the transport across the periplasmic space and subsequent insertion into the OM (Tanaka *et al.*, 2007).

OMPs typically exhibit a cylindrical β-barrel structure formed by antiparallel amphiphatic β-strands. One such class of OMPs are porins (e.g. PhoE), which span the inner and outer leaflet allowing the exchange of abundant small hydrophilic molecules (< 0.6 kDa) between the outside of the cell and the periplasmic space through passive diffusion (Bos *et al.*, 2007). Molecules larger than 0.6 kDa or at low concentrations, e.g. Vitamin B12 or siderophores (iron-carriers), pass through the OM via energy-dependent active uptake (Schauer *et al.*, 2008). This uptake is facilitated by receptors (e.g. FecA), OMPs with a β-barrel structure and an additional plug-domain at its periplasmic face enabling a gated passage of the substrate through the OM. Upon substrate-binding, the plug-domain of the receptor is rearranged to allow the subsequent release of the substrate into the periplasm. However for larger molecules, such as enzymes, the OM is impermeable. This ensures that proteins required in the periplasm remain in the space between the IM and OM.

1.2.2 The periplasm

The periplasm (Figure 1.1) contains an array of proteins involved in a variety of cellular processes such as substrate transport or degradation of nutrients. The periplasm also contains a polysaccharide, called peptidoglycan. Peptidoglycan is formed by layers of alternating *N*-acetylglucosamine and *N*-acetylmuramic acid. The individual layers are inter-connected by peptides containing the amino acids D-alanine, L-alanine, D-glutamic acid and di-aminopimelic acid. The main function of peptidoglycan is to confer rigidity to the bacterial cell.

1.2.3 The inner membrane (IM)

The IM separates the periplasm from the cytoplasm (Figure 1.1). It consists of a bilayer of phospholipids with a hydrophobic inner core (formed by the fatty acid part of the lipids) framed by the hydrophilic glycerol-phosphate backbone facing the exterior. The IM contains around 15 % of all cellular proteins (Lopez-Campistrous *et al.*, 2005) that are required for e.g. translocation of small molecules and proteins, chemotaxis and motility, respiration and energy generation.

In contrast to the OM, the IM is only semi-permeable owing to its amphiphatic character and the lack of un-gated protein channels (such as the porins found in the OM). The exchange of molecules between the periplasm and cytoplasm is highly selective and requires active energy-dependent transport of the substrate across the IM through dedicated transport systems formed by α-helical integral IM proteins.

There are 3 classes of transport systems:

- Simple transporter (no modification of the substrate)
    - Uniporter (only the substrate crosses the IM)
    - Symporter (a second molecule is co-transported together with the substrate in the same direction; e.g. LacY)
    - Antiporter (the second molecule is transported in the opposite direction to the substrate; e.g. the Na^+/H^+ antiporter NhaB in *E. coli*)
- Group translocator (the substrate is chemically modified during transport)
- ABC-transporter (e.g. the maltose transport system)

  It involves more than one protein and requires several steps:

  i) Substrate-binding by a periplasmic protein

  ii) Transfer to the IM transporter

  iii) Substrate translocation through, and release from, the IM transporter coupled with ATP-hydrolysis by an ATPase at the cytoplasmic face of the IM

The IM however is not just a semipermeable barrier for the selective exchange of molecules between the cell and the environment it also plays a role in other fundamental cellular processes, such as chemotaxis or energy conservation.

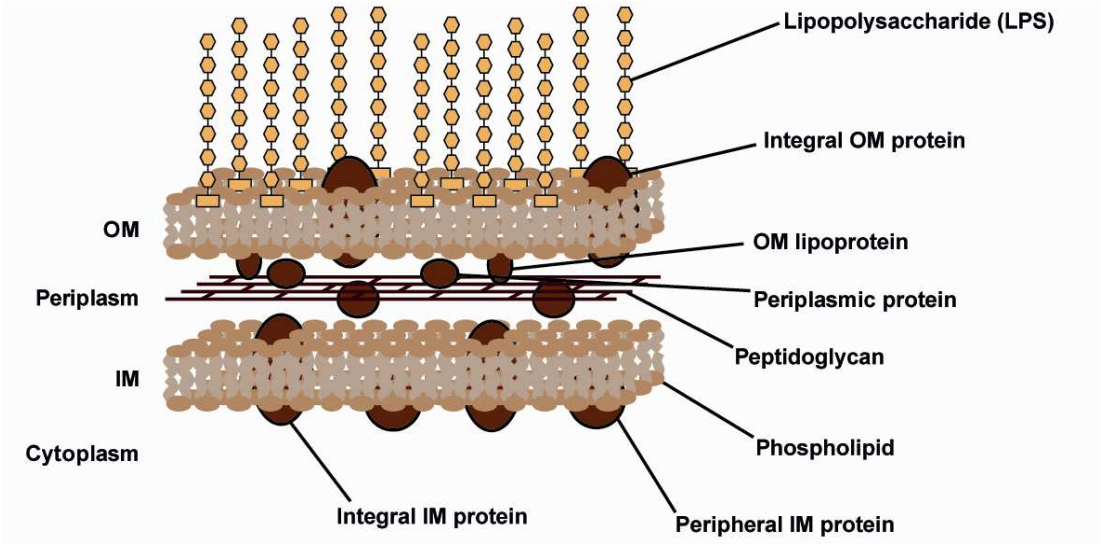


Figure 1.1: The cell envelope of Gram-negative bacteria. The cell envelope of Gram-negative bacteria consists of the outer membrane (OM), the periplasm and the inner membrane (IM). The OM is in direct contact with the extracellular milieu and contains proteins, phospholipids and LPS. The periplasm underneath contains proteins and layers of peptidoglycan that confer rigidity to the bacterial cell. The IM separates the cytoplasm from the periplasm. It consists of a bilayer of phospholipids as well as proteins either embedded or associated with the phospholipid-bilayer.

1.2.3.1 Chemotaxis

Chemotaxis is the process which allows the cell to detect and respond to attractants and repellents present in the extracellular milieu (Wolanin *et al.*, 2002; Wolanin and Stock, 2004). Transmembrane receptor clusters, e.g. Tsr or Tar (Kim *et al.*, 2002) bind such attractants or repellents at the periplasmic face of the IM. At the cytoplasmic face, the receptors are in contact with CheA, part of a typical two-component system consisting of a sensor-kinase (CheA) and its response regulator (CheY). Ligand-binding by the chemoreceptor results in autophosphorylation-dependent activation of CheA, which in turn modifies CheY through phosphorelay. Binding of attractants by the chemoreceptor decreases the phosphorylation of CheA and hence CheY, whereas repellents increase CheA-P and CheY-P. CheY directly impacts in a phoshorylation dependent-manner on the cell motility by regulating the activity of the flagellar motor located within the IM (Berg, 2003). Unphosphorylated CheY is unable to interact with the motor, which leads to counter-clockwise flagellar rotation (run) enabling the cell to swim towards attractants. CheY-P in contrast can bind to the motor. The resulting clockwise rotation of the flagella increases tumbling which helps the cell to move away from repellents (Wolanin *et al.*, 2002; Wolanin and Stock, 2004).

1.2.3.2 Energy conservation

One of the most important functions of the IM is to generate the energy that drives vital cellular processes such as those mentioned above. Energy is conserved in 2

different ways: as the proton motive force (PMF) and as hydrolysable ATP. Both energy sources are directly linked to respiration. Respiration is the mechanism of energy conservation used in the presence of external electron acceptors (oxygen for aerobic respiration and e.g. nitrate or fumarate for anaerobic respiration). In contrast to fermentation (used in the absence of external electron acceptors), where ATP is generated by substrate-level phosphorylation during biochemical pathways such as glycolysis, respiration generates ATP in a process called oxidative phosphorylation. The integral part of respiration is the electron transport chain (ETC), a sequence of reductases and oxidases located within the IM and linked through membrane soluble electron carriers. These carriers are the quinones (ubiquinone, menaquinone and demethylmenaquinone) used to transfer electrons from primary electron donors to terminal electron acceptors through alternating reduction / oxidation reactions. Being a facultative bacterium, *E. coli,* for example, can use various primary electron donors and terminal electron acceptors. Thus, *E. coli* contains a set of dehydrogenases specific for a certain electron donor and oxidases specific for a certain electron acceptor. Which combination of enzymes is used depends on the availability of donor and acceptor and is regulated on the level of gene expression. Under aerobic respiration, electrons are transferred from the electron donor NADH (oxidised by NADH dehydrogenase) via ubiquinone to cytochrome oxidases, which subsequently reduce the terminal electron acceptor oxygen, yielding H_2O. Under anaerobic conditions, i.e. when molecular oxygen is absent, *E. coli* produces e.g. nitrate reductase enabling the use of nitrate as a terminal electron acceptor (nitrate reductase reduces nitrate to nitrite).

Simultaneously with the flow of electrons within the IM through the ETC, H^+ ions are translocated across the IM from inside to outside (Figure 1.2). The subsequent accumulation of H^+ ions at the outside face of the IM results in i) a separation of charge (positive charge outside and negative charge inside) and ii) a H^+ ion gradient (with an increased concentration of H^+ ions outside compared to inside). The ETC therefore energises the IM, referred to as proton motive force (PMF). The level of PMF generated by the ETC however is dependent on the type of respiration used and the enzymes involved in the electron transport. During the anaerobic nitrate respiration for example, fewer H^+ ions are translocated across the IM compared to aerobic oxygen respiration and hence the resulting PMF is lower.

Generation of PMF is one of the most important functions of the IM since PMF is directly used as an energy source for many cellular processes, such as chemotaxis, where it drives the rotation of the flagellar motor (see above), or the secretion of proteins through the Sec pathway (Section 1.3.1.1). Additionally, PMF also drives the synthesis of the energetic chemical compound ATP. An enzyme called ATPsynthase transfers the H^+ ion along the gradient back into the cytoplasm thereby generating ATP (chemiosmotic theory by Mitchell, 1961). The energy stored in ATP is released through hydrolysis (to form the products ADP + P_i) by ATPases that are involved in a plethora of cellular functions.

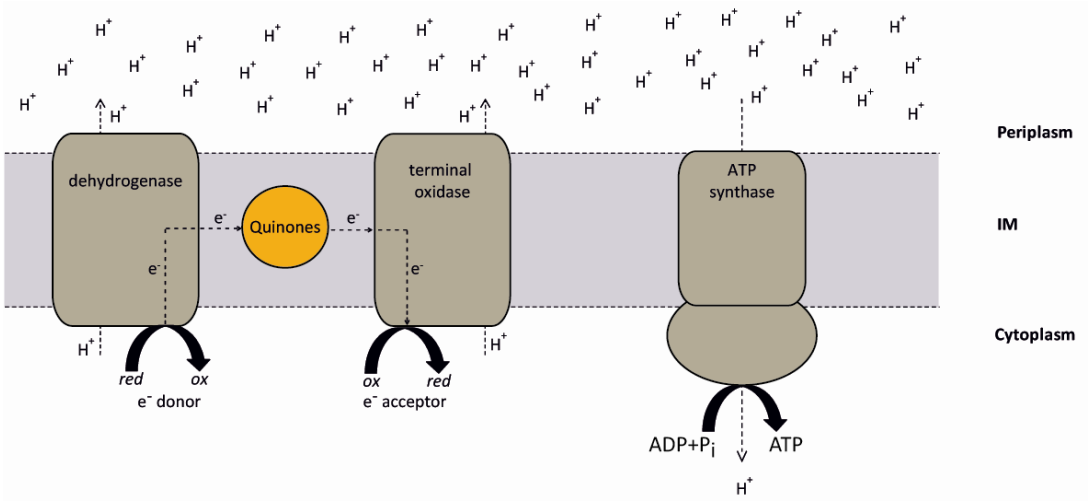


Figure 1.2: Energy conservation. The IM is the site of energy conservation via oxidative phosphorylation. This requires the ETC composed of dehydrogenases, which transfer electrons (e^-) from an electron-donor (e^--donor) via quinones to terminal oxidases that ultimately transfer the e^- onto an e^--acceptor. During this course, H^+ ions are translocated from the cytoplasm into the periplasm. This causes a separation of charge and H^+ ions across the IM. The resulting energy is called the proton-motive force (PMF). The H^+ ions are pumped back (across the gradient) into the cytoplasm via the ATPsynthase, which simultaneously produces ATP.

1.3 PROTEIN SECRETION SYSTEMS IN GRAM-NEGATIVE BACTERIA

1.3.1 Translocation into or across the IM

In order to translocate cell envelope proteins from the cytoplasm across or into the IM, the bacterial cell uses two different systems, Sec (for unfolded proteins) and Tat (for folded proteins) (Figure 1.3) (Beckwith and Silhavy, 1983; Danese and Silhavy, 1998; Sargent, *et al.*, 1998, 1999 & 2001; Luirink, *et al.*, 2005; Pohlschroeder *et al.* 2005; Natale *et al.*, 2008; Kuhn, 2009). Both systems have not only been found in the IM of bacteria but also in archeae, the ER and mitochondria of eukaryotes and in thylakoid membranes of plants. Importantly, defects in protein secretion are linked to induction of the Psp response (see section 1.5.4.1).

1.3.1.1 The Sec pathway

Protein translocation using the Sec pathway occurs either co- or post-translationally via a funnel-like integral IM channel composed of SecYEG, through which the unfolded protein is pushed by SecA - an ATPase (ATP hydrolysis drives the translocation process) peripherally bound to the cytoplasmic face of SecYEG (Natale *et al.*, 2008; Kuhn, 2009).

During co-translational translocation (in bacteria mainly used for integral IM proteins) the newly-synthesised peptide is bound (while it emerges from the ribosome) by the signal recognition particle (SRP), a ribunucleoprotein consisting of Ffh and 4.5S RNA (Poritz *et al.*, 1990; Wild *et al.*, 2004). Translation is halted and the

peptide/SRP/ribosome complex transferred to the SecA-YEG channel via the peripheral IM GTPase FtsY. At the channel, translation is resumed and the peptide subsequently translocated (Halic *et al.*, 2004).

For the SRP-independent post-translational translocation the chaperone SecB binds to the unfolded peptide while it emerges from the ribosome to prevent its aggregation. After translation, SecB transfers the peptide to SecA. SecA then pushes the peptide through SecYEG.

Proteins destined for the Sec pathway contain an N-terminal signal sequence that is recognised by the Sec machinery and proteolytically cleaved off from the translocated protein by a type-I signal peptidase (leader peptidase) (Paetzel *et al.*, 2002). The signal sequence consists of approximately 20 amino acids comprising a polar n-region, a hydrophobic h-region (both of which have been shown to be recognised by SRP and SecA; Cunningham and Wickner, 1989; Lee and Bernstein, 2001; Peterson *et al*., 2003) and a polar c-region, recognised by the signal peptidase. (Paetzel *et al.*, 2002).

Additional components - the IM proteins SecDF-YajC and YidC - have been found to copurify with the Sec complex (Nouwen and Driessen, 2002). SecDF-YajC appears to modulate SecA activity (Doung and Wickner, 1997), increase SecG stability (Kato *et al.*, 2003) and mediate the release of mature proteins (Matsuyama *et al.*, 1993). YidC facilitates the insertion of proteins into the IM in both a Sec-dependent and Sec-independent manner (Sammuelson *et al.*, 2000 & 2001; Urbanus *et al.*, 2001). Celebi *et al*. (2006) and Kol *et al*. (2008) showed that IM insertion of both the subunit II of cytochrome *bo* oxidase (CyoA) and the ATPsynthase are dependent on

YidC. YidC appears to also play a role in the assembly of components of the anaerobic ETC and hence growth of YidC-depleted cells is impaired under anaerobiosis (Price and Driessen, 2008).

1.3.1.2 The Tat (Twin-arginine translocation) pathway

In *E. coli*, the Tat translocation machinery consists of 3 IM proteins TatA, TatB and TatC (Sargent *et al.*, 1998). Additional Tat (TatD, TatE and TatF) factors have been identified but appear to be non-essential for the translocation process (Lindenstrauss and Brueser, 2006). Tat substrates, folded proteins of the cell envelope (DeLisa *et al.*, 2003) often containing co-factors (Berks *et al.*, 2005), are recognised by their N-terminal signal sequence ((S/T)-**R**-**R**-x-F-L-K; x = variable amino acid) (Berks, 1996) and translocated in a PMF-dependent manner. The folded protein is bound by TatBC at the cytoplasmic face of the IM (Alami *et al.*, 2003). TatA, which forms an oligomer with a ring-like structure, is then recruited to the TatBC complex and the substrate transported through the TatA pore (Natale *et al.*, 2008). It has been suggested that this transport is driven by TatBC and that TatC is the motor of this process (Brueser *et al.*, 2003).

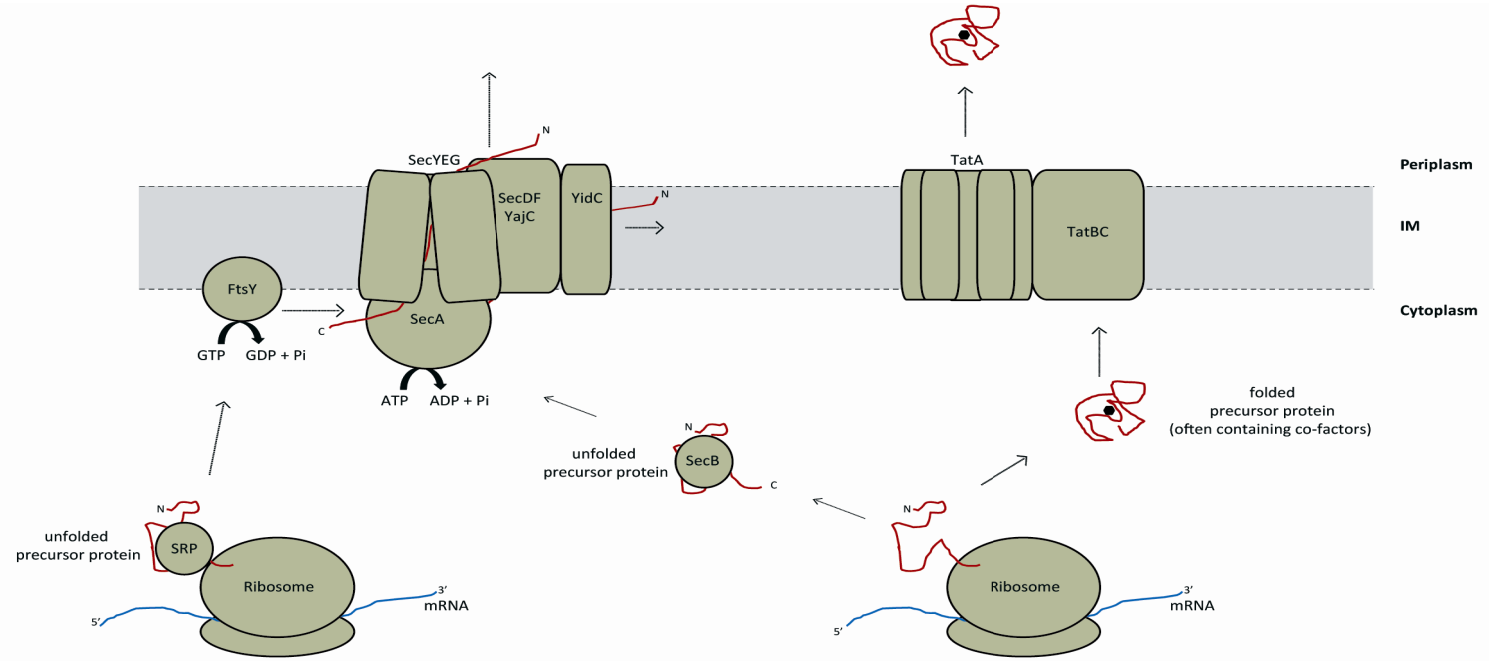


Figure 1.3: The Sec and Tat pathway. The Sec- and Tat pathways are used to translocate proteins from the cytoplasm either across the IM into the periplasm or into the IM. The Sec-pathways translocates unfolded proteins either cotranslationally via SRP and FtsY or posttranslationally via SecB to the Sec-translocase (SecA,SecYEG). The proteins are realeased from SecYEG via SecDF,YajC. YidC is required to insert components of the ETC into the IM. Proteins which are already folded (often containing co-factors) prior to the passage through the IM are translocated via the Tat pathway, which consists of the TatA pore and TatBC which guide the protein to the TatA pore.

1.3.2 Translocation into the OM

Upon transfer across the IM, insertion of OMPs into the OM occurs either directly or is mediated via a set of periplasmic chaperones. Lipoproteins employ the so-called Lol system, which facilitates sorting of lipoproteins destined for OM and IM (Tokuda, 2009).

1.3.2.1 Insertion of OMPs into the OM

OMPs generally use the Sec pathway to cross the IM (Mogensen and Otzen, 2005). As a result, OMPs enter the periplasm structurally unfolded (see section 1.3.1.1). The mechanism by which OMPs are integrated into the OM is not yet well established, however the following model is proposed (Figure 1.4) (Mogensen and Otzen, 2005). In order to prevent their aggregation and mediate their proper folding, upon release into the periplasmic space OMPs are bound by chaperones such as Skp, SurA, PpiD or FkpA (Mogensen and Otzen, 2005). Insertion into the OM then occurs either directly or via Omp85/YaeT (Voulhoux *et al.*, 2003). With the exception of TolC that appears to integrate into the OM via Omp85/YaeT independent of periplasmic chaperones (Mogensen and Otzen, 2005). A direct route for OMPs from the IM into the OM has also been suggested (Mogensen and Otzen, 2005). The periplasm contains an additional factor, DegP (Lipinska *et al*., 1988; Pallen and Wren, 1997; Clausen *et al.*, 2002). DegP functions as both protease and chaperone (Spiess *et al.*, 1999) and is involved in OMP biogenesis and

homeostasis through degradation or unfolding of aggregated and misfolded OMPs (Mogensen and Otzen, 2005).

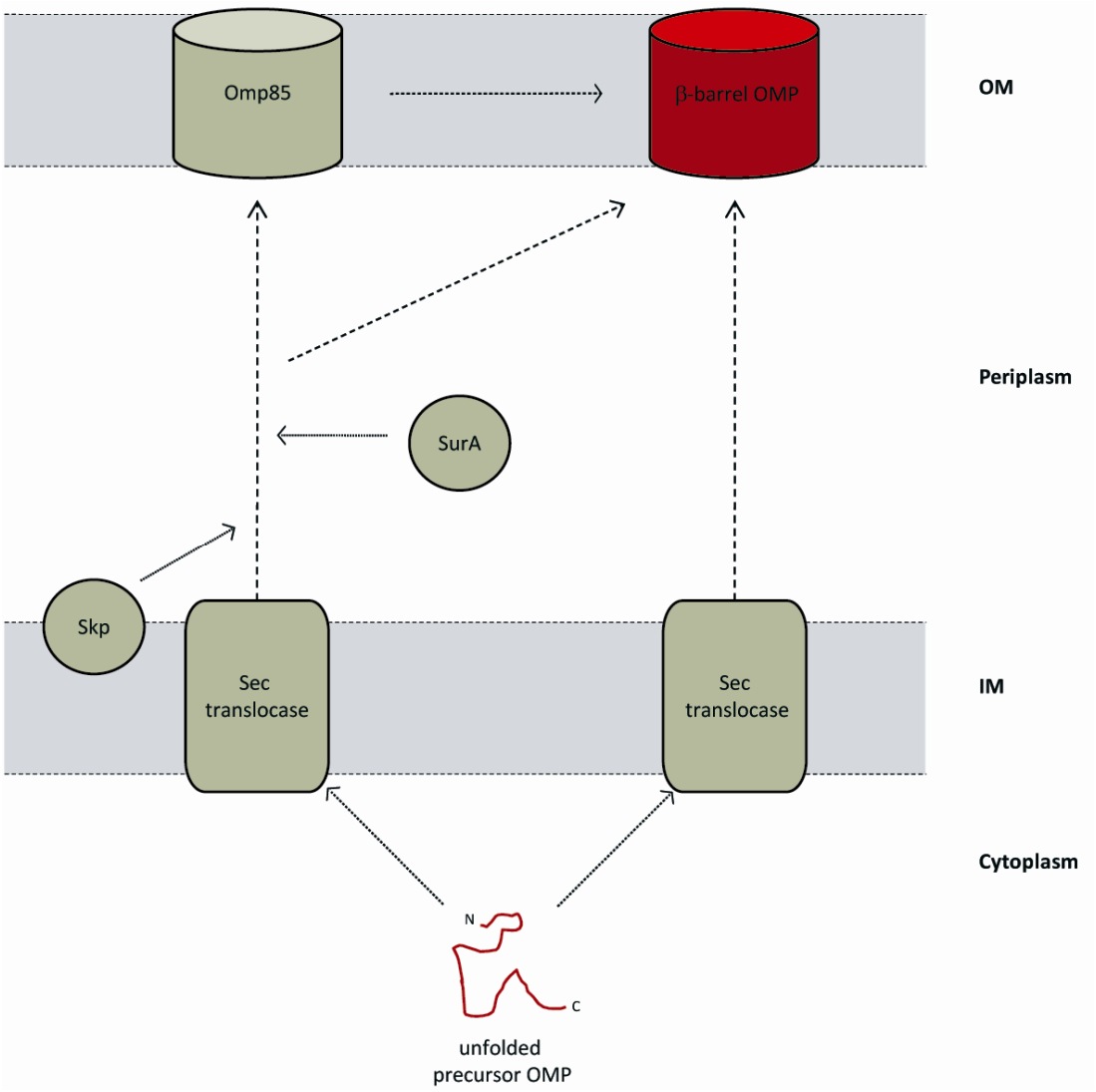


Figure 1.4: Insertion of OMPs into the OM. The β-barrel outer membrane proteins (OMP) are tarnslocated across the IM into the periplasm via the Sec pathway. In the periplasm, they are bound by chaperones (e.g. Skp or SurA) and inserted into the OM either directly or via Omp85. Direct insertion via Omp85 without periplasmic chaperones has also been reported for TolC.

1.3.2.2 The Lol system

The Lol system (Figure 1.5) is required for sorting and translocation of lipoproteins destined for either the IM or the OM. Following their synthesis in the cytoplasm, precursor lipoproteins are translocated across the IM via the Sec pathway (see section 1.3.1.1). In addition to the Sec-signal sequence, the N-terminus of lipoproteins contains a lipobox with an L-(A/S)-(G/A)-C motif. This motif is recognised by a diacylglyceryl transferase (Lgt), a signal peptidase (LspA) and a transacylase (Lnt) at the periplasmic face of the IM, which removes the signal sequence and lipobox and adds 3 acyl chains to the cysteine residue at position 1. Whether lipoproteins remain at the IM or are translocated to the OM, depends on their residues at position 2 and 3 (Yamaguchi *et al.*, 1988; Terada *et al.*, 2001). Aspartate at position 2 appears to be crucial for lipoprotein insertion into the IM (Gennity and Inouye, 1991), aided by acidic D or E and polar N or Q residues at position 3 (Terada *et al.*, 2001). Lipoproteins that do not have an aspartate at position 2, and hence are destined for the OM, are then bound by the LolCDE complex at the IM. Upon ATP-hydrolysis by the LolD ATPase, the lipoprotein is transferred to LolA, which facilitates the passage of the lipoprotein through the periplasm. LolA then passes the lipoprotein to the OM-anchored lipoprotein LolB, which inserts the lipoprotein into the OM (Matsuyama *et al.*, 1997).

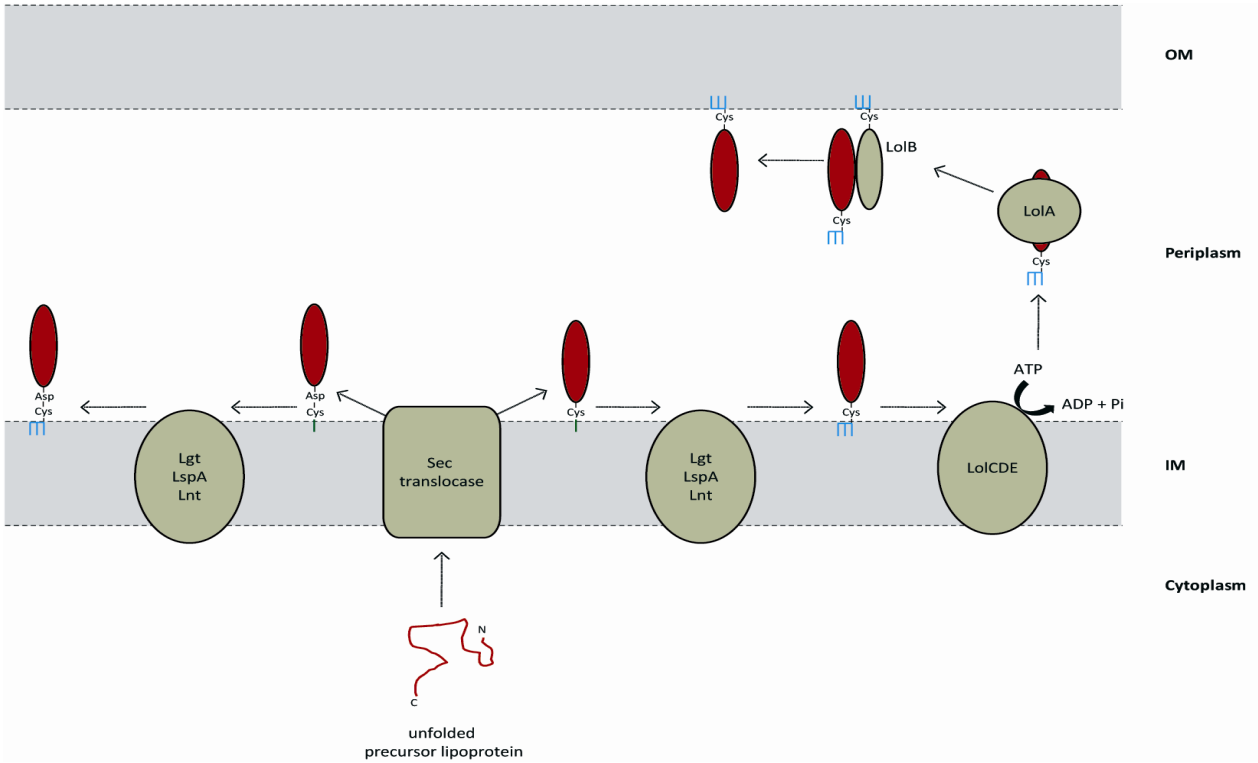


Figure 1.5: The Lol system. The Lol system is used for sorting and directing of lipoproteins to their destination, either the OM or the IM. Translocation of lipoprotein precursors occurs via the Sec pathway. Lgt, LspA and Lnt then modify the lipoprotein at the periplasmic face of the IM by replacing the N-terminal signal sequence with 3 acyl chains. Lipoproteins containing an aspartate residue at position 2 remain at the IM whilst lipoprotein lacking aspartate at position 2 are transported to and inserted into the OM via the Lol proteins.

1.3.3 Secretion into the extracellular milieu

Secretion into the extracellular milieu is governed by 6 different mechanisms, termed type I through to type VI secretion systems (Figure 1.6). Type I, III, IV and VI resemble a one-step process, where secreted factors are transported directly from the cytoplasm to the cell surface. Secretion via the type II and V systems occurs in two steps, which involves substrate translocation across the IM via the Sec or Tat pathway and subsequent transport to, and export across, the OM (Filloux *et al.*, 2008).

1.3.3.1 The Type I Secretion

Type I secretion systems are tripartide protein complexes consisting of an ATP-binding cassette (ABC) transporter in the IM, a channel in the OM and a periplasmic protein in contact with both the ABC transporter and the OMP (Gerlach and Hensel, 2007). They assemble into a contiguous protein channel spanning the IM, periplasm and OM and facilitate the secretion of proteins and non-protein molecules (Thanabalu *et al.*, 1998; Gerlach and Hensel, 2007). Best characterised is the type I secretion system required for the export of the virulence factor α-hemolysin (HlyA) from uropathogenic *E. coli* (Thanabalu *et al.*, 1998). The ABC transporter is formed by a homo-dimer of HlyB. HlyD bridges the periplasm and is in contact with TolC, a trimeric pore in the OM (Schulein *et al.*, 1992; Koronakis *et al*., 2001; Schmitt *et al.*, 2003). HlyA is recognised and bound by HlyB. Upon HlyA-binding, HlyB hydrolyses

ATP. The energy is then used to drive the transport of HlyA through the HlyD channel and is exported via TolC (Gerlach and Hensel, 2007).

1.3.3.2 The Type II Secretion

Another mechanism used for the secretion of molecules into the extracellular milieu is the type II secretion system. The pullulanase (PulA) secretion in *Klebsiella oxytoca* serves as a model for its functioning (Pugsley *et al.*, 1997). It forms a multi-subunit IM complex, comprising PulG-J,F,K-N, which is in contact with PulD via PulC. PulD belongs to the secretin protein family, which assemble into homo-multimeric ring-like channels in the OM (see section 1.5.4.1). Its substrate, PulA, crosses the IM via the Sec pathway (see section 1.3.1.1), is then passed to the Pul complex and finally secreted through PulD.

1.3.3.3 The Type III Secretion

The type III secretion System (TTST) is a protein complex consisting of more than 20 subunits forming a needle-like “injectisome” spanning the IM, periplasm and OM of Gram-negative pathogens. It is used to inject virulence factors into the target cell upon cell-cell contact in order to regulate the host cell physiology (Galan and Bliska, 1996; Kubori *et al.*, 1998 & 2000; Blocker *et al.*, 1999; Aldon *et al.*, 2000; Tamano *et al.*, 2000; Galan, 2001; Enninga, *et al.*, 2005). Pathogenic *E. coli* (EHEC and EPEC) for example, use the TTST to integrate a receptor (Tir) into the host cell membrane specific for the invasion protein Intimin in the OM of bacterium. Binding of Intimin

to Tir then results in the formation of pedestals, an outgrowth of the host cytoplasmic membrane through the recruitment of cytoskeletal proteins such as actin at the adhesion site of the bacterium (Kenny *et al*, 1997, Finlay and Cossart, 1997). In *Yersinia*, the injected virulence factors - 6 different proteins called Yops - inhibit phagocytosis of and downregulate the inflammatory response by the host cell in order to promote the survival of the bacterium (Cornelis, 1998 & 2002).

1.3.3.4 The Type IV Secretion

Type IV secretion systems (evolved from bacterial conjugation) are used to secrete single proteins or protein complexes as well as DNA into target cells. Best characterised is the VirB system from *Agrobacterium tumefaciens* used to transfer T-DNA into host plant cells (Burns, 1999). It consists of 10 subunits. The IM platform is composed of VirB4, VirB6/8, VirB11 and VirD4 and is in direct contact with a needle-like structure containing the OM proteins VirB2, VirB5, VirB7, VirB9 and VirB10. The T-DNA is transferred directly into the host cell in complex with another protein, VirE2, where it integrates into the host genome and stimulates uncontrolled cell division and tumour foramtion (Lai and Kado, 1998; Gerlach and Hensel, 2007). Type IV systems have also been described in human pathogens such as *Bordetella pertussis* and *Helicobacter pylori* (Gerlach and Hensel, 2007).

1.3.3.5 The Type V Secretion

Prototypes for type V secretion systems are OMPs called autotransporters (Gerlach and Hensel, 2007). They cross the IM via the Sec pathway and integrate into the OM as typical β-barrels. Autotransporters contain a passenger domain which is transported through the β-barrel pore to the outside face of the OM (where it is occasionally cleaved off) where it interacts with surface structures on the target cell. In some cases, the two components of the autotransporter, the β-barrel pore and the passenger domain are separated. An example for this two-partner pathway is TpsA and TpsB (Jacob-Dubuisson *et al.*, 2004).

1.3.3.6 The Type VI Secretion

Recently, a new mechanism for protein transport across membranes, the type VI secretion system (T6SS), has been described (Filloux *et al.*, 2008). Details of its functioning are yet unknown, some aspects however have been elucidated. T6SS is used by Gram-negative pathogens such as *Vibrio cholera* or *Pseudomonas aeruginosa* to transfer effectors into eukaryotic cells (Das and Chaudhuri, 2003; Mougous *et al.*, 2006; Pukatzki *et al.*, 2006). So far, 9 components of the T6SS have been identified. Central to most T6SS is an IM ATPase associated with various cellular activities (AAA+), ClpV. It is speculated that ATP hydrolysis by ClpV drives the secretion process (Filloux *et al.*, 2008). Secretion is regulated via the phosphrylation state of the IM protein Fha, which may in turn be controlled by the antagonising Ser/Thr kinase (STK) and Ser/Thr phosphatase (STP) (Mukhopadhyay *et*

al., 1999). The IM channel may be formed by IcmF and DotU. An OM lipoprotein (VasD in *V. cholera*) often associated with T6SS may play a role in formation of the OM pore. VgrG (found in *V. cholera*) and hexameric Hcp rings have been proposed to form a needle-like structure that may be used to inject effectors into the host. Attachment to the target cell may be mediated by VgrG (Pukatzki *et al.*, 2007) and a domain of VgrG may be released into the target cell (Filloux *et al.*, 2008).

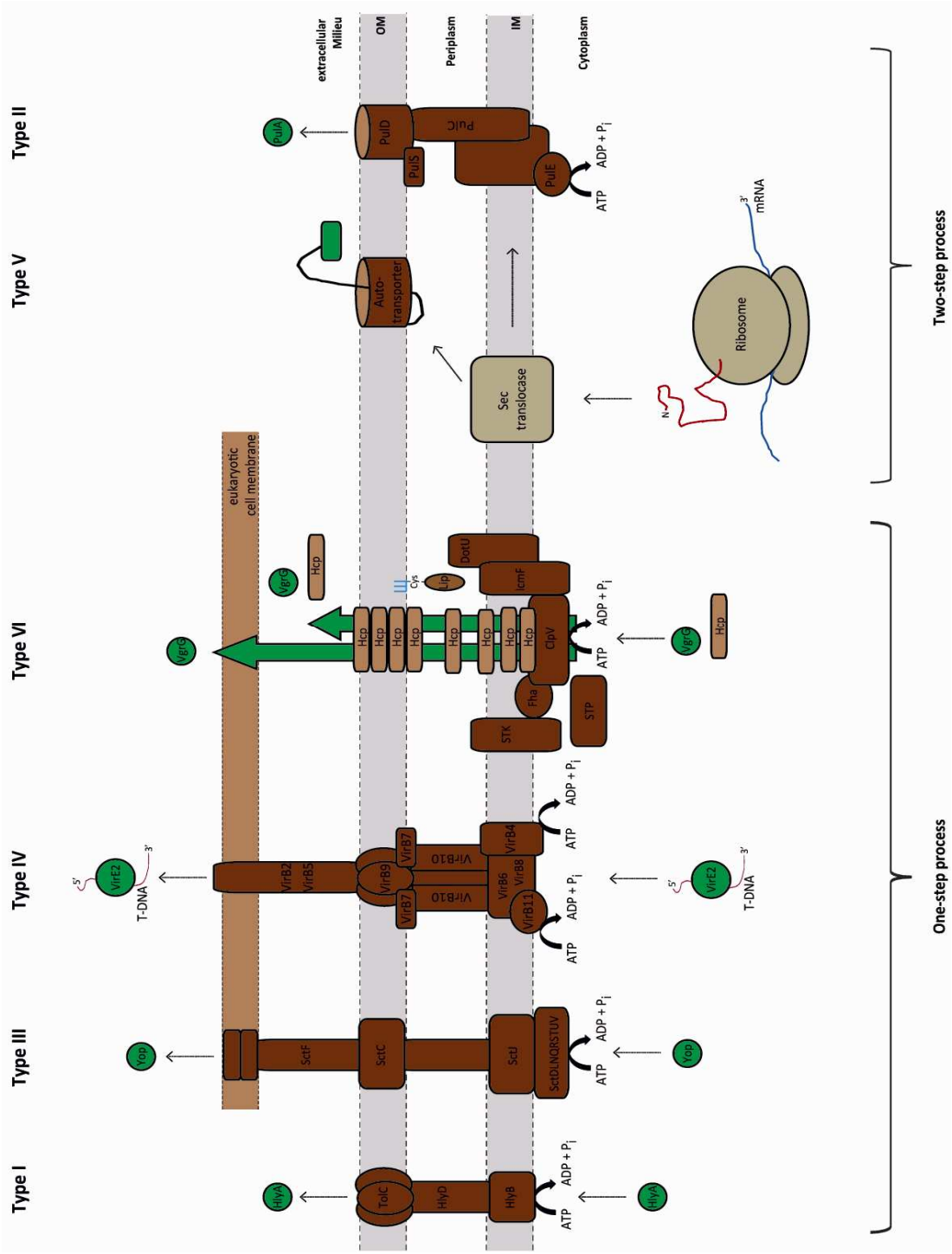


Figure 1.6: The Type secretion systems. To date, 6 different secretion systems have been identified. In Type I, III, IV and VI secretion across the IM, periplasm and OM occurs in one process. In contrast, Type II and V secretion additionally involves translocation of the substrate across the IM via the Sec pathway. Type II and III systems contain an OM secretin (here: SctC and PulD), which forms a pore in the OM facilitating secretion. Importantly, such secretins have been found to induce the Psp response (see section 1.5.4.1).

1.4 THE ROLE OF THE CELL ENVELOPE IN BACTERIAL ADHESION AND PATHOGENESIS

The cell envelope of bacteria contains a set of factors that facilitate adhesion to surfaces and cells enabling biofilm formation as well as the colonisation and/or invasion of host tissues (Pizzaro-Cerda and Cossart, 2006). Factors, such as the TTST, autotransporters or the T6SS have been described in section 1.3.3. Additional factors include Pili/Fimbria and invasion proteins are described below.

1.4.1 Pili/Fimbria

Pili/Fimbria are multimeric filaments of the cell envelope protruding into the extracellular milieu. They consist of a homo-multimeric rod anchored in the OM linked with an adhesin (a molecule that can interact with specific target structures, e.g. at the surface of the host cell) at its tip.

Several types of pili/fimbria are known that differ in their biogenesis and function:

- P (pyelonephritis-associated) and type I pili are synthesised by the so-called "Chaperone/Usher Pathway", best described for the P pilus assembly (Sauer *et al.*, 2000). The P pilus is encoded by the *pap* gene cluster. The periplasmic chaperone PapD binds to pilus subunits (thereby preventing their aggregation and mediating their proper folding) and sequesters them to the PapC usher, which forms a pore in the OM where the pilus subunits are assembled (Thanassi *et al.*, 1998). The rod is formed by a PapA polymer

while the tip contains PapEFG, where PapG mediates the adhesion to structures on the target surface (Hultgren *et al.*, 1991). Pilus biogenesis occurs in an ordered fashion with the subunits forming the tip of the pilus being assembled first, followed by a continual addition of several PapA subunits (rod) before the final PapH anchors the pilus at the OM (Sauer *et al.*, 2000).

- In contrast to P and type I pili, type IV pili are fully assembled at the IM and subsequently inserted into the OM where they protrude into the extracellular milieu (Wolfgang *et al.*, 2000). A further characteristic of type IV pili is that the rod of the pilus can be retracted, while the tip remains target-bound (Pizzaro-Cerda and Cossart, 2006). This facilitates improved contact between the bacterium and target surface. Type IV pili have been described in e.g. pathogenic *E. coli* and *Salmonella enterica* serovar Typhi (Craig *et al.*, 2004).

1.4.2 Invasion proteins

Invasion proteins are produced by the bacterium to facilitate its uptake into the host cell. A typical invasion protein is Invasin found in the OM of *Y. enterocolitica*. Invasin interacts with β1-integrin in the extracellular matrix of the target cell (Isberg and Leong, 1990). This mediates re-arrangements of the cytoskeleton within the host at the site of adhesion, the subsequent engulfment of the bacterium by the cytoplasmic membrane and its internalisation into the host cell (Pizzaro-Cerda and Cossart, 2004).

1.5 STRESS RESPONSES OF THE CELL ENVELOPE

As described above, the cell envelope has many different functions. Hence, its robustness is vital for the cell to survive. Bacteria have therefore evolved a number of partially overlapping systems (e.g. the SigmaE response, the Cpx system or the Psp response) to maintain cell envelope integrity (Ruiz and Silhavy, 2005; Rowley *et al.*, 2006; Darwin, 2005 & 2007).

1.5.1 The SigmaE response

The cell envelope stress response involving the alternative sigma factor SigmaE is induced under conditions such as high or low temperatures, exposure to ethanol or detergents, osmotic and oxidative stress as well as biofilm formation, stationary phase growth and the overexpression of OM proteins (Raivio and Silhavy, 1999; Ruiz and Silhavy, 2005; Rowley *et al.*, 2006). It has been proposed that these conditions cause misfolding of OM proteins resulting in the activation of the SigmaE response. Although recently other activation pathways have been suggested (Grigorova *et al.*, 2004), the best understood mechanism of induction of the SigmaE response is DegS-dependent regulated intramembrane proteolysis (RIP; Figure 1.7) (Alba and Gross, 2004; Ehrmann and Clausen, 2004; Ades, 2008).

In the absence of stress/misfolded OM proteins, SigmaE is bound to the integral IM α-sigma factor RseA at the cytoplasmic face of the IM and hence is unable to promote transcription of SigmaE-dependent genes. The periplasmic protein RseB is also bound to RseA at its periplasmic domain, which prevents proteolysis of RseA

and stabilises the inhibitory effect of RseA on SigmaE. Under stress conditions, misfolded OM proteins expose C-terminal peptides containing a YxF motif (x = variable amino acid) that are recognised by the PDZ domain of the IM protease DegS. Additionally, RseB is removed from RseA to allow for DegS-dependent proteolysis of RseA. DegS then cleaves RseA at the periplasmic face of the IM. A second IM protease, RseP (formerly YeaL), subsequently cleaves RseA at the cytoplasmic face of the IM. The RseA-SigmaE complex is the released into the cytoplasm and bound by SspB, which sequesters the complex to the ClpXP protease (Flynn *et al.*, 2004). SspB is released (ready to bind another RseA-SigmaE), RseA degraded and SigmaE is free to bind to core RNA polymerase and hence direct SigmaE-dependent gene expression. Dartigalongue, *et al.* (2001) identified 20 promoters regulated by SigmaE. The gene products are mostly involved in folding and degradation of proteins in the cell envelope. Examples are DsbC, SurA, FkpA and DegP (Lipinska *et al.*, 1988; Erickson and Gross, 1989; Danese and Silhavy, 1997; Dartigalongue *et al.*, 2001) (see section 1.3.2.1).

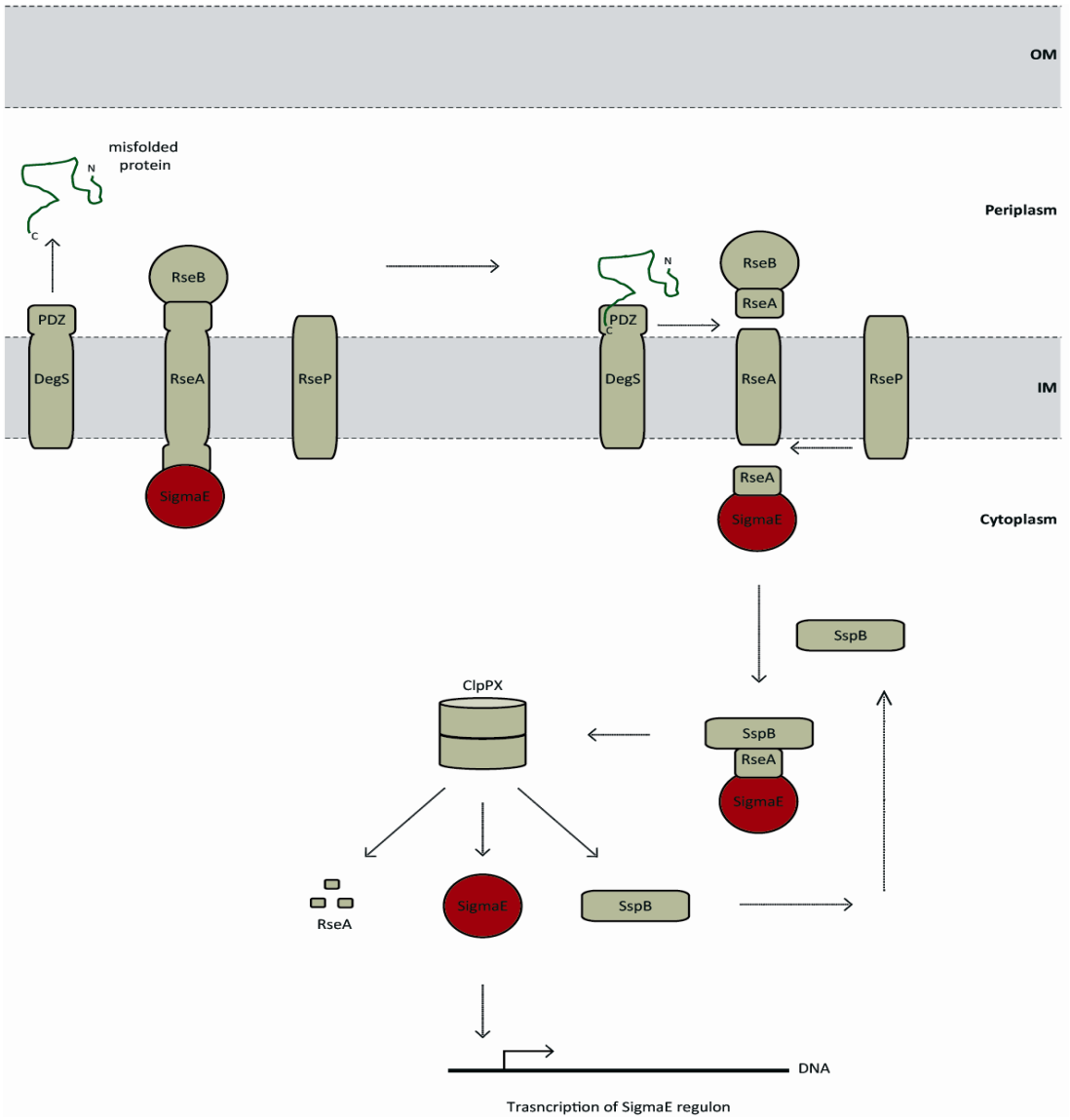


Figure 1.7: The SigmaE response. The SigmaE response is stimulated by misfolded proteins in the periplasm. In absence of stimulus, SigmaE is bound to the IM by the α-sigma factor RseA. The interaction of RseA and SigmaE is stabilised by RseB, which binds to the periplasmic domain of RseA. Upon cell envelope stress, DegS recognises the C-terminus of misfolded proteins via its PDZ domain. DegS then cleaves RseA at the periplasmic face of the IM, releasing RseB. A second protease, RseP, then cleaves RseA at the cytoplasmic face of the IM. SigmaE (in complex with the cytoplasmic domain of RseA) is released into the cytoplasm. This complex is then bound by SspB and sequestered to ClpPX. The cytoplasmic domain of RseA is degraded and SigmaE and SspB are released. SspB is ready to bind another RseA-SigmaE complex, while SigmaE directs transcription of the SigmaE regulon.

1.5.2 The Cpx system

DegP expression is also activated by a second response to cell envelope stress, the Cpx system. The Cpx system (Figure 1.8) is induced by alteration in the cell envelope caused e.g. through cell adhesion, P pili synthesis, misfolded envelope proteins, overproduction of the lipoprotein NlpE and alkaline pH (Danese *et al.*, 1995; Nakayama and Watanabe, 1995; Jones *et al.*, 1997; Raivio and Silhavy, 1997; Danese and Silhavy, 1998; Ravio *et al.*, 1999 & 2000; Ruiz and Silhavy, 2005; Rowley *et al.*, 2006). The Cpx system is a two-component system involving an IM sensor kinase (CpxA) and a cytoplasmic response regulator (CpxR). An additional level of regulation is provided by the periplasmic CpxP, which binds to CpxA under non-stress conditions thereby inhibiting its kinase activity (Ruiz and Silhavy, 2005; Rowley *et al.*, 2006). Under stress conditions, the sensor kinase CpxA senses the above mentioned alterations in the cell envelope, by an unknown mechanism. The binding affinity of CpxP to CpxA is altered and CpxA released (Ruiz and Silhavy, 2005; Rowley *et al.*, 2006). This activates the autophosphorylation of CpxA by transfer of a phosphate-group from ATP onto a histidine residue within its cytoplasmic domain. Subsequently, this phosphate is transferred onto CpxR in the cytoplasm (Ruiz and Silhavy, 2005; Rowley *et al.*, 2006). Phosphorylated CpxR-P then activates or represses gene expression of the Cpx-regulon. Upregulated genes include proteins involved in e.g. protein secretion (*secA*) and folding (*dsbA*), lipid biosynthesis (*psd*) or virulence and adherence (*pap*), while genes involved in e.g. chemotaxis and motility (*aer*, *motAB*, *cheAW*) or cell-division (*minCDE*) are down-regulated (Rowley *et al.*, 2006). From this transcriptomic profile it has been

suggested that the Cpx system plays a role in the early stages of infection and in the switch from a mobile to a sessile life in a biofilm (Dorel *et al.*, 2006).

1.5.3 The BaeSR system

Recently, an additional two-component system sensing cell envelope stress has been identified, the BaeSR system, with the IM sensor kinase BaeS and the response regulator BaeR (Raffa and Raivio, 2002). It appears to respond to alterations in the cell envelope caused by antimicrobials such as novobiocin and renders the cell resistant to such substances by activation of multi-drug-resistance transporters (Baranova and Nikaido, 2002; Hirakawa *et al.*, 2003).

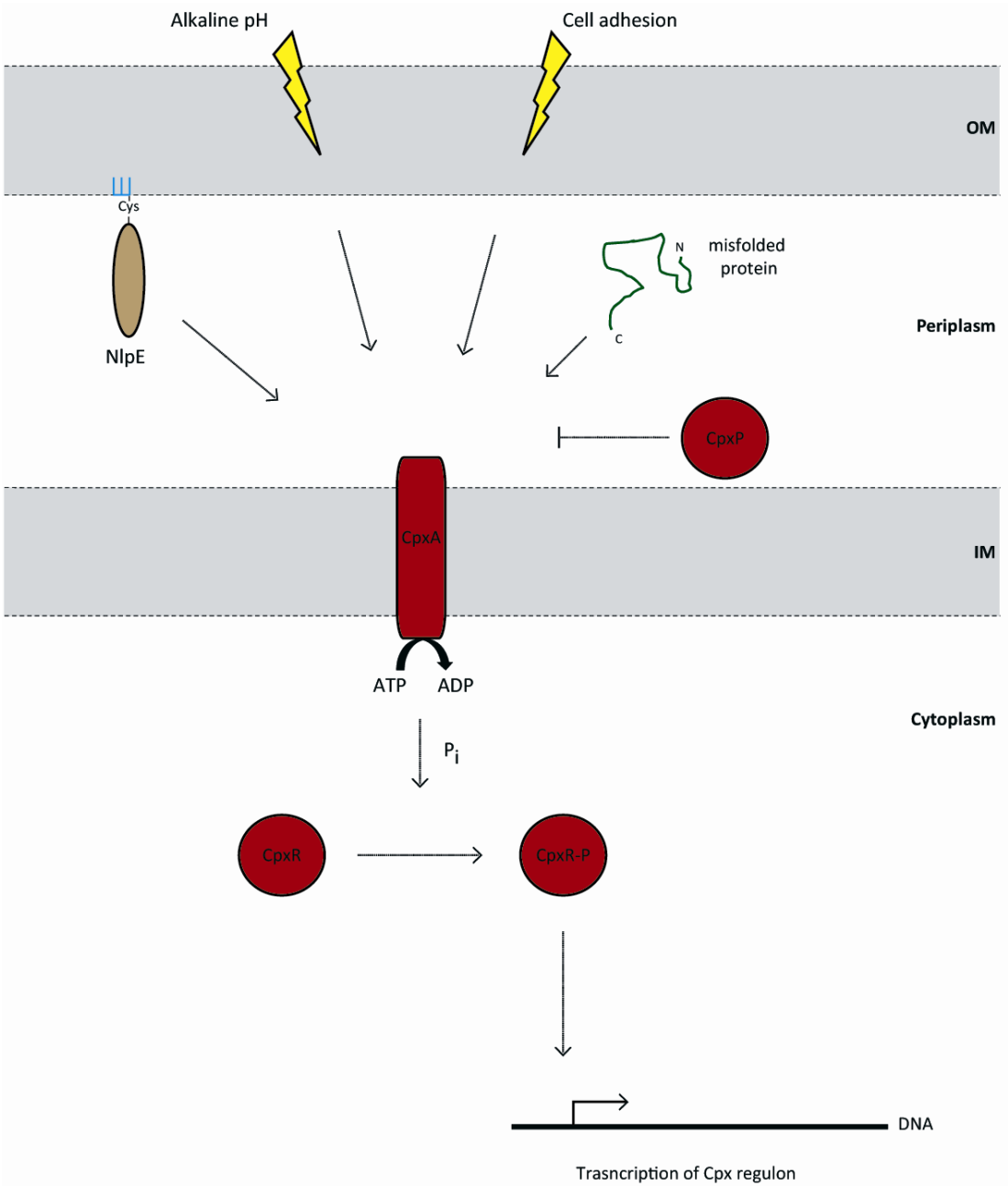


Figure 1.8: TheCpx system. The Cpx system is stimulated by e.g. overproduction of the OM lipoprotein NlpE, alkaline pH, cell adhesion or misfolded proteins in the periplasm. The CpX system resembles a typical two-component system comprising the CpxA sensor kinase and the CpxR response regulator. In the absence of stimulus, CpxA is bound by periplasmic CpxP, which inhibits CpxA kinase activity. Upon stimulation, the CpxA is released from CpxP, CpxA then phosphorylates CpxR, which then activates the transcription of the Cpx regulon.

1.5.4 The Phage-shock protein (Psp) response

Another system counteracting cell envelope stress is the Phage-shock protein (Psp) response - highly conserved in Gram-negative bacteria (Model *et al.*, 1997; Darwin, 2005 & 2007). Maxson *et al.* (2004) showed that in *Y. enterocolitica* Psp mainly responds to stresses that do not activate the SigmaE or Cpx system. Additionally, deletion of *cpxA* in *E. coli* had no effect on Psp induction (Jovanovic *et al.*, 2006). However, a *Salmonella* mutant lacking RpoE (SigmaE) exhibited increased Psp expression and a double-knock out of *rpoE* and *pspA* (coding for a central component of the Psp response) resulted in impaired survival at stationary phase upon CCCP treatment (Becker *et al.*, 2005). CCCP is a proton-ionophore in the IM that causes an unregulated influx of H^+ ions into the cytoplasm thereby discharging the PMF. The authors proposed therefore a compensatory role of Psp in the absence of a functional SigmaE response (Becker *et al.*, 2005). Jovanovic *et al.* (2006) suggested that Psp acts in concert with the SigmaE and Cpx system.

The Phage-shock protein (Psp) response was originally discovered during studies of the infection of *Escherichia coli* with filamentous phage f1 (Brissette *et al.*, 1990). Upon f1 infection, *E. coli* produces a 25 kDa protein in such amounts that it becomes one of the major proteins in the cell. Due to its relation to phage infection, the authors called it Phage-shock protein A (PspA) (Brissette *et al.*, 1990). Since then, much progress has been made in terms of its *in vivo* and *in vitro* characterisation.

1.5.4.1 Inducers of the Psp response

The OM secretin pIV from filamentous phage f1 was the first identified inducer of the Psp response (Brissette *et al.*, 1990; Russel and Kazmierczak, 1993). pIV has been well characterised due to its role in f1 infection and as a model OM secretin. The lysogenic f1 phage replicates within Gram-negative bacteria such as *E. coli* (Russel, 1994a). The f1 genome contains 11 open reading frames coding for phage proteins pI through pXI, required for replication of the phage genome, assembly of the phage particle as well as its release from the host (Russel, 1994a). Following assembly, the mature particles are exported from the cell via an exit-channel, which facilitates the crossing of the IM and OM barrier without killing the bacterium (Russel, 1994a; Feng *et al.*, 1999). The pIV protein forms the OM part of the exit channel (Russel, 1994a). The structure of pIV has been revealed using a combination of Scanning Transmission Electron Microscopy (Linderoth *et al.*, 1997) and Cryo-electron Microscopy (Opalka *et al.*, 2003). The pIV secretin is a gated (Russel *et al.*, 1997) homo-multimeric channel consisting of 14 subunits. The channel is 24 nm long, with a pore-size of 6.0 to 8.8 nm, wide enough to accommodate the exit of the rod-like f1 particle (diameter of 6.5 nm) (Linderoth *et al.*, 1997; Opalka *et al.*, 2003). In line with this, Marcino *et al.* (2001) showed that the pIV pore is blocked by the exit of f1 particles.

Despite being encoded by the phage chromosome, the sequence and structure of pIV is homologous to bacterial OM secretins of the type II and type III secretion systems (see section 1.3.3) (Russel, 1994a). pIV homologues include PulD, an OM secretin from *Klebsiella oxytoca* (see section 1.3.3.2), OutD from *Erwinia*

chrysanthemi or HrpH from *Pseudomonas syringae* (Russel, 1994a). Notably, PulD and OutD also induced the Psp response (Possot *et al.*, 1992; Russel and Kazmierczak, 1993) and in *Y. enterocolitica* Psp is induced by synthesis of the Ysc type III secretion system (Darwin and Miller, 2001). Moreover, overexpression of YscC, the OM secretin of the Ysc TTST, alone resulted in increased Psp expression (Darwin and Miller, 2001).

Indications of how pIV (and other OM secretins) might induce the Psp response were drawn from reports, where pIV was found to be evenly distributed between both the IM (25%) and the OM (25%) when using a Triton X-100 based cell fractionation method (Russel and Kazmierczak, 1993). The remainder was found in the soluble (8%) and insoluble (42%) fraction (Russel and Kazmierczak, 1993). Furthermore, variants of pIV, which remained within the cytoplasm or were unable to multimerise, did not induce Psp (Russel and Kazmierczak, 1993; Russel, 1994b). Additionally, multimeric (but not monomeric) PulD activated Psp expression when it mislocalised to the IM in the absence of its cognate chaperone-pilotin PulS (Hardie *et al*., 1996a & 1996b; Guilvout *et al.*, 2006). Hence, it seems likely that it is the location of OM secretin channels (such as pIV) within the IM which stimulates Psp induction.

In addition to the mislocalisation of OM secretins into the IM, Psp is also induced by a variety of other conditions:

- Treatment with uncouplers of PMF such as CCCP, dinitrophenol or free fatty acids (Weiner and Model, 1994)

- Exposure to hydrophobic organic solvents such as n-hexane or cyclooctane (Kobayashi *et al.*, 1998)
- Inhibition of fatty acid biosynthesis (Bergler *et al.*, 1994)
- Late stationary phase growth (Weiner and Model, 1994)
- Extreme heat shock (50°C), 10 % ethanol, hyper-osmotic shock (0.75 M NaCl) (Brissette *et al.*, 1990)
- Impaired protein secretion
    - Blockage of the Tat pathway (DeLisa *et al.*, 2004)
    - Knocking-out components of the Sec pathway (SecA, SecD, SecF, SecM) and depletion of YidC (Kleerebezem and Tommassen, 1993; Jones *et al.*, 2003; van der Laan *et al.*, 2003)

Taken together, all stimuli which induce the Psp response can be assumed to have the potential to affect the integrity of the IM. In a number of cases it has been shown that these conditions also decrease the level of PMF (see section 1.2.3.2), eg. pIV- production in cells lacking the Psp response, treatment with the proton ionophore CCCP (Weiner and Model, 1994; Jovanovic *et al.*, 2006), knocking-out SigmaE in *S. enterica* (Becker *et al.*, 2005) or the expression of a mislocalising form of the OM porin PhoE (Kleerebezem and Tommassen, 1993; Kleerebezem, *et al.*, 1996). Depletion of YidC also dissipates the PMF since YidC is required for proper IM assembly of the cytochrome *o* oxidase and the F_1F_0-ATPase (van der Lann *et al.*, 2003; Celebi *et al*., 2006; Kol *et al*. 2008). It is therefore generally proposed that

dissipation of PMF may well serve as the inducing signal to mount the Psp response (Darwin *et al.*, 2005 & 2007).

1.5.4.2 The function of the Psp response

1.5.4.2.1 PMF maintenance under envelope stress

Although bacteria lacking the Psp response are still viable, their tolerance to envelope stresses that decrease the energy state of the cell is markedly reduced (Model *et al.*, 1997; Darwin, 2005 & 2007). For example, cells deleted for Psp exhibit impaired growth in stationary phase at alkaline pH (Weiner and Model, 1994) or on bile salts (Adams *et al.*, 2003). Additionally, in the absence of a functional Psp response, efficiency of PMF- and ATP-dependent protein secretion is decreased (Kleerebezem and Tommassen, 1993; Kleerebezem *et al.*, 1996) and PMF is lowered under stress conditions (Kleerebezem *et al.*, 1996). This implies that Psp functions in maintaining the cell's energy state under stress (Kleerebezem *et al.*, 1996; Model *et al.*, 1997; Darwin, 2005 & 2007). Indeed, when measuring the membrane potential in living cells using a tetraphenylphosphonium (TPP^+)-sensitive electrode, Kleerebezem *et al.* (1996) showed that PspA counteracts proton loss caused by translocation of a mutant form of the OM porin PhoE. These results were supported by the observation that purified PspA blocks proton-leakage of membrane vesicles reconstituted from total lipids from *E. coli* (Kobayashi *et al.*, 2007). Furthermore, PspA can directly and specifically bind to the IM phospholipids phosphatidylglycerol (PG) and phosphatidylserine (PS) (Kobayashi *et al.*, 2007). How PspA repairs proton leakage is still unknown, the authors however proposed that under membrane

stress PspA forms a scaffold covering the cytoplasmic face of the IM by binding to PG and PS in the lipid layer. This may change the rigidity of the IM and as such facilitate PMF maintenance (Kobayashi *et al.*, 2007). Recently, scaffold-like networks composed of homo-multimeric PspA have been reported from structural studies (Standar *et al.*, 2008).

Transcriptome analysis (Jovanovic *et al.*, 2006) demonstrated that Psp effectors downregulated genes involved in chemotaxis / motility (e.g. *che, tap, tar, tsr, fli, flg, flh, motA*) and aerobic respiration (e.g. *glp, arcB, cyoC, cadA, icdA*), and upregulated anaerobic respiration (e.g. *flu, hlyE, nirB, dmsAB, yfiD, focA*), cation (e.g. H^+) (*nikE, modF*) uptake as well as protein assembly and secretion (e.g. *dnaK, grpE, clpB, lon, secE*) and cell envelope integrity (*lpp, murG, cutF, ddg*). It was therefore concluded that under stress, the Psp response also indirectly maintains PMF by improving cell envelope integrity, subtly switching the metabolism to anaerobic respiration and fermentation as well as downregulating PMF consuming processes such as motility (Jovanovic *et al.*, 2006).

1.5.4.2.2 Role in virulence of pathogenic Gram-negative bacteria

Psp is found in many Gram-negative pathogens (Darwin, 2005 & 2007) and is induced by OM secretins that are often part of type II and type III secretion (see section 1.3.3). These systems are used during the infection process for cell adherence and for the export of virulence factors into the extracellular milieu or into target cells. Psp may therefore protect the cell envelope of pathogens during infection. Indeed, in *Yersinia enterocolitica* mutation of a component of the Psp

response, *pspC*, resulted in attenuated virulence and impaired growth upon type III secretion (Darwin and Miller, 2001). Furthermore, *psp* gene expression is elevated during swarming and macrophage infection of *Salmonella typhimurium* and *Shigella flexneri* (Eriksson *et al.*, 2003; Wang *et al.*, 2004; Lucchini *et al.*, 2005) and during biofilm formation in *E. coli* (Beloin *et al.*, 2004). Additionally, *E. coli* unable to mount a Psp response (by deleting the transcriptional activator PspF; see section 1.5.4.4.2) are defective for biofilm formation (Beloin *et al.*, 2004).

1.5.4.3 Conservation of Psp proteins

An *in silico* search within available genomic sequences (Darwin, 2005) as well as experimental data show that Psp is not just highly conserved among Gram-negative bacteria, but also present in a number of organisms throughout all three domains of life. Darwin (2005) found Psp systems in Gamma-, Delta-, and Alpha-proteobacteria. However, whilst PspFABC (see section 1.5.4.4.1) were always conserved, other Psp members appeared to be dispensable. It was therefore concluded that the minimal Psp system comprises PspFABC (Darwin, 2005). Recent *in silico* analysis of the evolutionary divergence of members of the Psp response across 129 bacterial species also found a high degree of co-conservation of PspA and PspF, other Psp proteins in contrast appear to be far less conserved (Huvet *et al.*, 2009). Other organisms show an even higher degree of Psp reduction, containing only homologues of PspA. In the Gram-positive bacterium *Streptomyces lividans* the expression of a PspA homologue was induced upon membrane stress (Vrancken *et al.*, 2008). *Bacillus subtilis* contains a PspA homologue, LiaH, which responds to

alkaline shock (pH 9) (Wiegert *et al.*, 2001). A PspA homologue was also found in the halophilic archeae *Haloferax volcanii* where it was upregulated under high-salt (3.5 M NaCl) conditions (Bidle *et al.*, 2008). Furthermore, a PspA homologue, Vipp1 (Vesicle-inducing protein in plastids 1), is essential in plants and *Synechocystis* for thylakoid membrane formation and photosynthesis (Westphal *et al*., 2001; Aseeva *et al.*, 2007). Upon Vipp1 deletion, the structure of thylakoids in *Synechocystis* is impaired and the cells are unable to perform photosynthesis (Westphal *et al*., 2001). Recently it has been reported that Vipp1's effect on the photosynthetic activity of cells may be independent of its effect on thylakoid formation (Gao and Xu, 2009). Notably, Vipp1 can complement for the loss of PspA in an *E. coli pspA* mutant strain, suggesting that PspA function is conserved within Vipp1 and hence across pro- and eukaryotic organisms (DeLisa *et al.*, 2004). Taken together, it appears that PspA may play a fundamental role in membrane physiology and energy conservation in all three domains of life.

1.5.4.4 The Psp response in *Escherichia coli*

1.5.4.4.1 Components

The Psp response in *E. coli* comprises 7 genes, which are organised in a regulon consisting of the polycistronic *pspABCDE* operon and the monocistronic *pspG* as well as the *pspF* gene adjacent but divergently transcribed to the *pspABCDE* operon (Figure 1.9) (Brissette *et al.*, 1991; Jovanovic *et al.*, 1996; Lloyd *et al.*, 2004).

The *pspA* gene (669bp) encodes a peripheral IM protein of 25.5 kDa (222aa), which can be found in both the cytoplasmic and the IM fractions of the cell (Brissette *et al.*, 1990). PspA is bifunctional, acting as a negative transcriptional regulator and an effector protein of the Psp response (Model *et al.*, 1997; Darwin, 2005 & 2007). Both, *pspB* (225bp) and *pspC* (360bp) encode integral IM proteins (PspB: 74aa; 8.7 kDa and PspC: 119aa; 13 kDa), which are positive transcriptional regulators relieving PspA-negative regulation (Brissette *et al.*, 1991; Weiner *et al.*, 1991 & 1995). PspD (73aa; 8 kDa), encoded by the 4th open-reading-frame (222bp) in the *pspABCDE* operon, is also associated with the IM and acts as effector, synergistically to PspA (Adams *et al.*, 2003; Jones *et al.*, 2003; Jovanovic *et al.*, 2006). *pspE* (315bp) encodes a 11.5 kDA (104aa) rhodanase which transfers sulphur onto sulphur-containing enzymes in the periplasm (Brissette *et al.*, 1990; Adams *et al.*, 2002; Cheng *et al.*, 2008). To date, neither its precise physiological function nor its role in the Psp response is known (Brissette *et al.*, 1991; Model *et al.*, 1997; Lloyd *et al.*, 2004; Cheng *et al.*, 2008). The *pspF* (993bp) gene upstream of the *pspABCDE* operon encodes for PspF (330aa; 36,9 kDa), a bacterial enhancer binding protein (bEBP) belonging to the AAA+ (ATPase Associated with a variety of cellular Activities) family and activates transcription of the Psp regulon (Jovanovic *et al.*, 1996; Neuwald *et al.*, 1999; Zhang *et al.*, 2002). Recently, a new member of the Psp response, *pspG* (243 bp), was identified (Green and Darwin, 2004; Loyd *et al.*, 2004). It encodes an integral IM protein (80aa; 9 kDa) with Psp effector function (Lloyd *et al.*, 2004; Jovanovic *et al.*, 2006).

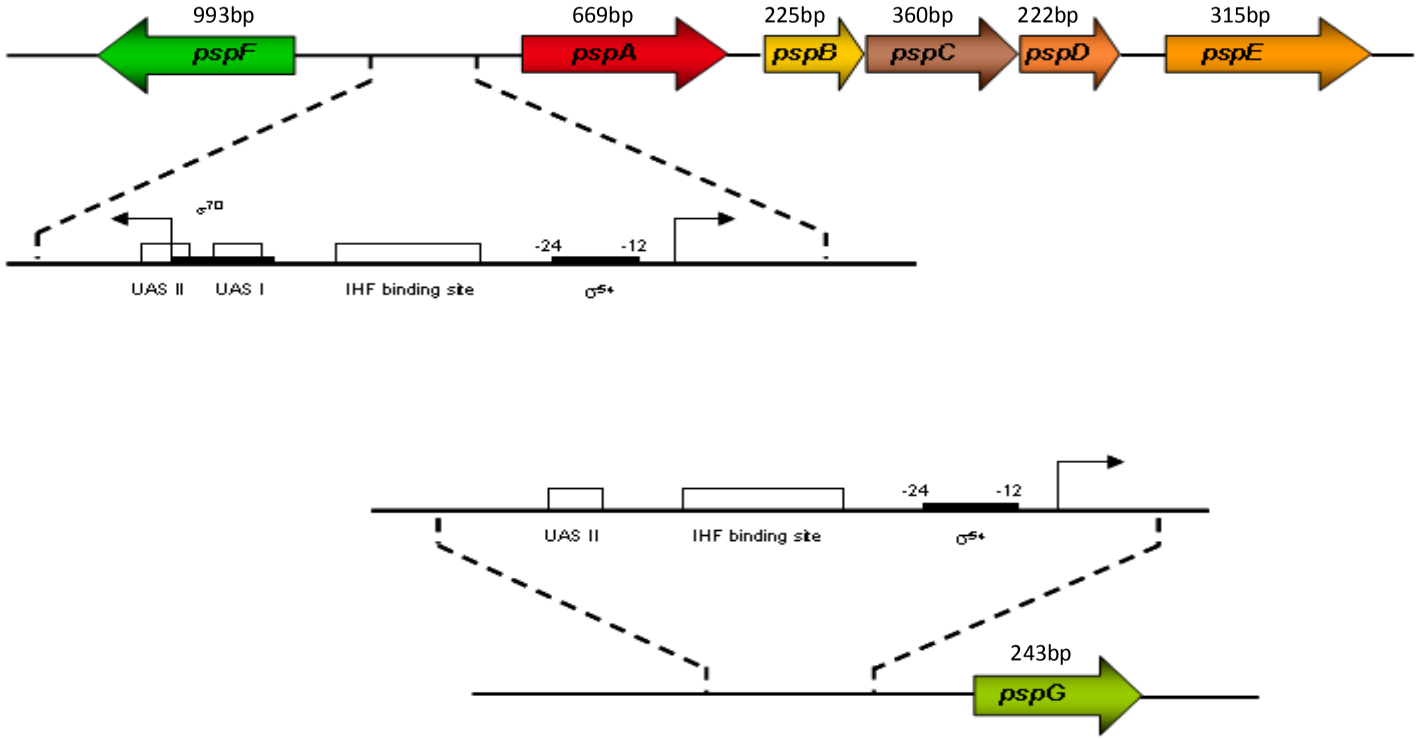


Figure 1.9: The Psp regulon in *E. coli.* The Psp regulon comprises the *pspABCDE* operon, the *pspG* gene and *pspF*, which is divergently transcribed upstream of the *pspABCDE* operon. The *pspABCDE* and *pspG* genes are under the control of a Sigma54-promoter. Upstream of the promoter is a binding site for IHF and upstream activation sequences (UASII and I upstream of *pspABCDE* and UASII upstream of *pspG*) to which the bEBP PspF binds. Notably, UASI and II upstream of *pspABCDE* partially overlap with the Sigma70-promoter and transcription start site of *pspF*, hence PspF autogenously regulates its own expressin by binding to UAS I and II. Gene sizes in bp are indicated.

1.5.4.4.2 Regulation of *psp* gene expression

Gene expression involves two major steps, the transcription of coding DNA into messenger-RNA and the subsequent translation of the messenger-RNA into proteins. This is a highly energy-consuming process and hence constitutive expression of non-essential genes is unfavourable. Cells have therefore evolved mechanisms for its adjustment by limiting the expression of genes to those essential for survival in present environmental conditions. Genes therefore contain specific upstream sequences (e.g. promoters) that enable regulation of their transcription through DNA-dependent RNA polymerase (RNAP). Prior to transcription, core RNAP interacts with a sigma factor, which facilitates specific promoter recognition by the holoenzyme (Sigma-RNAP). *E. coli* for example contains 2 classes of sigma factors (Sigma70 and Sigma54) with differing promoter-specificity directing gene transcription. Housekeeping genes (essential genes which are constitutively expressed) contain Sigma70-dependent promoters with a typical -35 box (5'-TTGACA-3') and a -10 box (5'-TATAAT-3') (Helmann and Chamberlin, 1988). Sigma54-specific promoters are characterised by 5'-GG-3' at position -24 and 5'-GC-3' at position -12 sequenences and are typically located upstream of non-essential genes whose expression is only required under specific growth conditions (Morett and Buck, 1989; Buck *et al.*, 2000). Transcription by Sigma70-RNAP can occur spontaneously and independent of any additional factors. In contrast, transcription from Sigma54-dependent promoters requires activation through ATP-hydrolysis provided by bacterial enhancer binding proteins (bEBPs) which bind upstream

activation sequences (UAS) typically 80-200bp upstream of the promoter (Buck *et al.*, 2000; Reitzer and Schneider, 2001).

Transcription of the Psp regulon is under the control of such a Sigma54-specific promoter (Weiner *et al.*, 1991) with 2 UAS (UAS I and II) located upstream of the *pspA* promoter and 1 UAS (UAS II) upstream of the *pspG* promoter (Weiner *et al.*, 1995; Lloyd *et al.*, 2004) to which the bEBP PspF binds (Figure 1.9) (Jovanovic *et al.*, 1996). Notably, UAS I and II of the *pspA* promoter partially overlap with the Sigma70-promoter, transcriptional start and ribosome-binding site of *pspF* and hence PspF autogenously regulates its own expression by binding to UAS I and II (Jovanovic *et al.*, 1997). In both *pspA* and *pspG* promoters an IHF binding site is present between the UAS and promoter (Weiner *et al.*, 1995). IHF bends the DNA facilitating close contact of PspF and RNAP-Sigma54 thereby stimulating *psp* transcription (Weiner *et al.*, 1995; Jovanovic and Model, 1997). ATP-hydrolysis by PspF is used to remodel the initial closed DNA-RNAP-Sigma54 complex to an open complex (where the DNA strands are separated) from which transcription can be initiated (Buck *et al.*, 2006). Typically, bEPBs contain an N-terminal domain for self-regulation (Studholme and Dixon, 2003). PspF, however, belongs to a group of bEPBs that lack this domain (Studholme and Dixon, 2003). Regulation of PspF therefore requires a second protein, PspA (Dworkin *et al.*, 2000).

In absence of membrane stress, PspA interacts with PspF (mediated via residue W56 of PspF) thereby inhibiting PspF ATPase activity and *psp* transcription (Elderkin *et al.*, 2002; Darwin, 2005 & 2007). The inhibitory complex appears to consist of 6 PspA subunits associated with 1 PspF hexamer (Rappas *et al.*, 2005; Joly *et al.*,

2009). Upon membrane stress, PspF is somehow released from negative control and can activate transcription of the *psp* genes (Figure 1.10) (Darwin, 2005 & 2007). PspB and PspC are positive regulators of *psp* transcription (Brissette *et al.*, 1991; Weiner *et al.*, 1991 & 1995). Interestingly, PspB and PspC have been predicted to contain a leucine zipper motif, while PspA is a predicted coiled-coil protein (Weiner *et al.*, 1991; Model *et al.*, 1997). Both structures are often involved in protein-protein interactions. Indeed, Adams *et al.* (2003) showed binary interactions of PspA with PspB (in the presence of PspC) and PspA with PspC. It is therefore assumed that PspB and PspC might somehow sense the membrane stress, e.g. the mislocalisation of pIV in the IM (see section 1.5.4.1), transduce the signal via protein-protein interactions to the inhibitory complex, which subsequently causes conformational changes within PspAF (Figure 1.10). This relieves the negative control imposed by PspA on PspF, freeing PspF to activate *psp* transcription (Darwin, 2005 & 2007). PspA, PspD and PspG act as effectors to counteract the stress caused by impaired cell envelope integrity (Figure 1.10) (Jovanovic *et al.*, 2006). How PspA switches between negative regulatory and effector functions is still unknown. However, some findings suggest that PspA functioning may correlate with its oligomeric state. Kobayashi *et al.* (2007) showed that only higher-order oligomers of PspA are able to block proton leakage from membrane vesicles and hence have effector function (see section 1.5.4.2.1), while monomeric PspA fails. In line with this, Joly *et al.* (2009) only observed a stable interaction between PspF and PspA (negative regulator function) with lower-order oligomers of PspA.

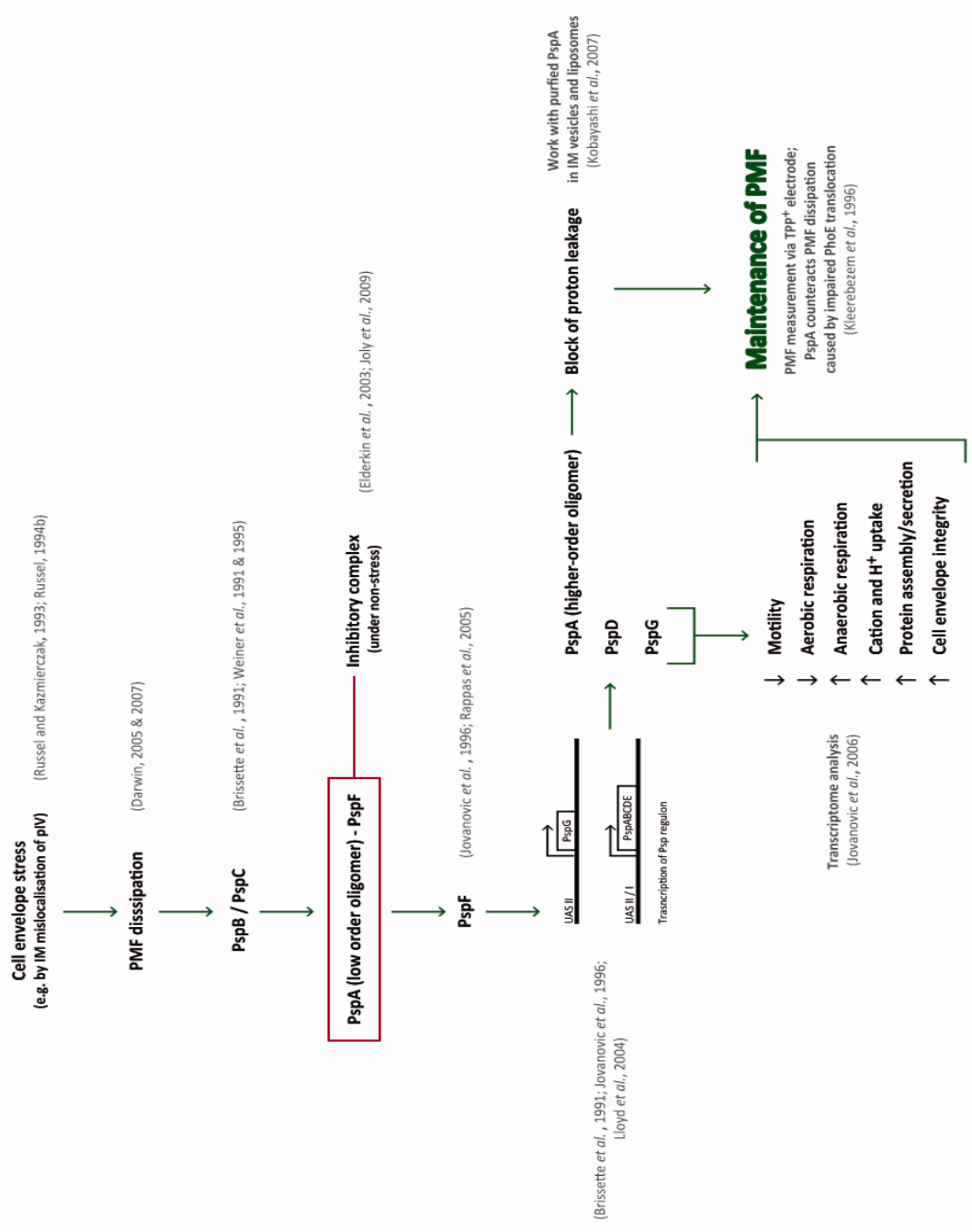


Figure 1.10: Regulation of the Psp response. The Psp response is induced upon cell envelope stress which may cause dissipation of PMF. The inducing signal (green arrows) is sensed by PspB/PspC and relayed to the PspAF inhibitory complex. Subsequently, PspF is released and activates transcription of the Psp regulon genes. Psp effectors (PspA, PspD, PspG) help to maintain PMF under stress by adjusting the transcription profile of genes involved in the indicated cellular processes. Additionally, PspA (as a high-order oligomer) is proposed to directly block proton leakage. Publications upon which the signal transduction is based on are shown in grey.

1.6 OBJECTIVES OF THIS STUDY

Recently, it was concluded from the profile of genes affected by either deletion or overexpression of Psp effector proteins that the ArcAB two component system (more specifically the ArcB sensor kinase), required for the switch from aerobic to anaerobic respiration, plays a role in Psp signal transduction (Jovanovic *et al.*, 2006). This hypothesis was supported by a marked reduction of transcription from the *pspA* promoter in an *arcB* deletion strain (Jovanovic *et al.*, 2006). However, these findings could not be confirmed in either *Y. enterocolitica* or *E. coli* (Seo *et al.*, 2007). One aim of this study therefore was to further elaborate the requirement of ArcAB in the signalling cascade from the stress stimulus to the Psp complex (see Chapter 3).

Reports suggest that ArcAB respond to the redox state of the cell by sensing changes in the ubiquinone and menaquinone pool (Georgellis *et al.*, 2001; Malpica *et al.*, 2004; Bekker *et al.*, 2009). It was therefore assumed that, if ArcAB are involved in Psp signalling, changes in quinones may also affect the expression of Psp proteins. Hence, the impact of changes in the quinone pool on the Psp response was assessed (see Chapter 4).

Bacteria show a remarkable subcelluar organisation. Correct localisation of proteins is often crucial for the functioning of cellular processes. Moreover, members of interrelated pathways often co-localise within the cell. An additional aim of the present study therefore was to analyse the spatial organisation of Psp proteins to gain further insights into the physiological role of the Psp response and its integration in the network of other cellular systems (see Chapter 5).

CHAPTER 2

MATERIALS AND METHODS

2.1 MATERIALS

2.1.1 Media

Media used for growing the bacterial strains are shown in Table 2.1:

Medium	Contents
LB (Luria Bertani Broth)	10 g/L peptone, 5 g/L NaCl, 5 g/L yeast extract
LB agar	10 g/L peptone, 5 g/L NaCl, 5 g/L yeast extract, 18 g/L agar
N^-C^- minimal medium	1 g/L K_2SO_4, 13.5 g/L K_2HPO_4, 4.7 g/L KH_2PO_4, 0.1 g/L $MgSO_4$ (suppl. 0.4% glucose, 10mM NaH_4Cl)
Trace elements	0.5 g/L $FeCl_2$, 0.05 g/L $ZnCl_3$, 0.01 g/L $CuCl_2$, 0.01 g/L $CoCl_2 \bullet 6H_2O$, 0.01 g/L H_3BO_3, 0.5 g/L EDTA pH 7.0
Motility agar SA (soft agar)	10 g/L tryptone, 5 g/L NaCl, 3 g/L agar
TA7 (Top Agar)	10 g/L tryptone, 5 g/L NaCl, 7 g/L Difco agar

Table 2.1: Media used in this study.

2.1.2 Antibiotics

Antibiotics were filter sterilised and used at the following final concentrations:

Antibiotic	Concentration
Ampicillin	100 µg/ml
Kanamycin	50 µg/ml
Chloramphenicol	25 µg/ml
Tetracyclin	10 µg/ml
Erythromycin	200 µg/ml

Table 2.2: Antibiotics used in this study.

2.1.3 Kits

The following commercially available kits were used in this study:

Kit	Company	Used for
DNeasy® Blood & Tissue Kit	Qiagen	Purification of chromosomal DNA
QIAprep® Spin Miniprep Kit	Qiagen	Purification of plasmid DNA
QIAquick® PCR Purification Kit	Qiagen	Gel extraction of DNA
Bio-X-ACT DNA Polymerase Kit	Bioline	PCR for molecular cloning
GoTaq® Hot Start Polymerase Kit	Promega	Analysis of cloned and deleted genes
pGEM®-T Easy Vector Kit	Promega	TA cloning of DNA
LigaFast™ Rapid DNA Ligation Kit	Promega	Ligation of DNA
QuikChange™ kit	Stratagene	Site-directed mutagenesis
ECL Plus™ Western Blotting Detection Kit	GE Healthcare	Immunoblotting

Table 2.3: Kits used in this study.

2.1.4 Dyes and chemicals

The following commercially available dyes and chemicals were used in this study:

Dye	Company	Used for
SYBR® Safe	Invitrogen	DNA Gel stain
Isopropyl-D-1-thiogalactopyranoside (IPTG)	Sigma	Induction of gene expression
5-Bromo-4-chloro-3-indolyl-β-D-galactopyranoside (X-gal)	Sigma	Blue/White screening of bacterial colonies
ortho-Nitrophenyl-β-galactoside (ONPG)	Sigma	Substrate for β-galactosidase assay
Valinomycin	Sigma	Dissipation of electron potential
4',6-diamidino-2-phenylindole (DAPI)	Molecular Probes	*In vivo* DNA stain
N-(3-trimethylammoniumpropyl)-4-(6-(4-(diethylamino)phenyl)hexatrienyl)pyridinium	Molecular Probes	*In vivo* IM stain

dibromide (FM® 5-95)		
5,5',6,6'-tetrachloro-1,1',3,3'-tetraethylbenzimidazolylcarbocyanine iodide (JC-1)	Molecular Probes	*In vivo* indicator of electron potential

Table 2.4: Dyes and chemicals used in this study.

2.2 BACTERIAL STRAINS

2.2.1 Generation of bacterial strains

All strains used in this study are listed in Appendix A.

Baba *et al.* (2006) have created a library of 3985 mutant strains of *E. coli* K-12 BW25113 containing single-gene deletions by inserting a kanamycin cassette into non-essential genes using the λ Red system (Datsenko and Wanner, 2000) (see Figure 2.1). Strains from this library, called the Keio collection, were used as donors in a bacteriophage $P1_{vir}$ general-transduction method (described below) to delete chromosomally encoded *E. coli* genes by replacing the coding sequence of the interest with a kanamycin cassette. The bacteriophage $P1_{vir}$ lyses the host cell upon infection and is prone to package 90 kb (approx. 2 minutes)-long segments of the bacterial chromosome instead of its own phage genome. This "false" packaging is a random event and creates a diversity of phages containing various sections of the bacterial DNA including a sub-population harbouring the desired gene. This sub-population is used as a carrier to introduce the manipulated DNA into the recipient strain where it is then integrated into the chromosome via homologous recombination - when a phage carries in a segment of DNA carrying the deletion of interest resulting in deletion of the gene of interest. When using strains from the

Keio collection as donors, the gene of interest in the recipient is replaced by the kanamycin cassette. Strains harbouring the desired chromosomal deletion can therefore be selected through their aquired resistance to kanamycin.

One caveat of using phages for the transfer of DNA between bacterial cells is to prevent the re-infection and lysis of already transduced cells. Hence, the infection needs to be controlled. Since infectivity of $P1_{vir}$ requires free calcium, this can be achieved by varying the amount of free calcium during the infection process through a combination of incubation steps with $CaCl_2$ and then Na-citrate (citrate chelates free calcium). A typical protocol for $P1_{vir}$ transduction is described below:

Protocol:

a) Preparation of the $P1_{vir}$ bacteriophage lysate from the donor strain

0.2 ml of an overnight culture of the donor strain (from the Keio collection harbouring the gene to be deleted replaced by a kanamycin resistance cassette grown in LB supplemented with kanamycin) is incubated for 25 minutes at RT with 0.2 ml of a $P1_{vir}$ bacteriophage lysate (to allow for binding of the phage to the bacterial cell). 18.5 ml LB, 0.5 ml 40% glucose and 1.0 ml 0.1 M $CaCl_2$ is added and the cells incubated at 37°C with shaking until the suspension becomes clear (upon phage replication, bacterial cells are lysed and can be seen as debris). 1-2 ml chloroform is then added (to kill any remaining bacteria). After 30 minutes incubation at RT, the lysate is centrifuged at 16,100 x g at RT for 10 minutes. The supernatant contains the $P1_{vir}$ phages including a sub-population of phages containing the bacterial DNA of interest (in this case the desired *E. coli* gene replaced by the kanamycin cassette) and is subsequently used to infect the recipient strain (typically, E. *coli* K-12 MG1655 or MC1061 and derivatives).

b) Infection of the recipient strain

Cells from a 5 ml overnight culture of the recipient strain are harvested by centrifugation (5 minutes, RT, 4,500 x g) and primed for transduction by 15 minutes incubation in 5 ml 0.1 M $MgSO_4$, 0.25 ml 0.1 M $CaCl_2$ at 37°C with shaking. Then, 0.2 ml of the recipient strain are mixed with 0.2 ml of the $P1_{vir}$ bacteriophage lysate (see above) and incubated for 20 minutes at 37°C without shaking (during this time transduction occurs). Transduction is stopped with 0.4 ml 1 M Na-Citrate. The suspension is mixed with 3 ml TA7 agar and poured onto LB plates containing kanamycin and 0.5 M Na-Citrate. The plates are then incubated overnight at 37°C. Per transduction, 4 colonies are re-streaked on LB plates containing kanamycin, their chromosomal DNA is isolated (see section 2.3.1.1) and the replacement of the desired gene with the kanamycin cassette is detected by PCR (see section 2.3.2) using a combination of gene- and kanamycin cassette-specifc primers.

2.3 DNA METHODS

DNA manipulations (overview)

Gene-specific sets of forward and reverse primers harbouring restriction sites for sub-cloning the fragment were used to amplify the desired gene from either chromosomal or plasmid DNA (see section 2.3.1) via Polymerase Chain Reaction (PCR; see section 2.3.2). Following agarose gel purification (see section 2.3.3) and TA cloning (see section 2.3.5), the DNA construct was verified by sequencing (see section 2.3.6), digested with the appropriate restriction enzymes (see section 2.3.7) and ligated into the desired vector (see section 2.3.8). After transformation

(typically using the heat-shock method; see section 2.3.10), 4 different clones were re-streaked under antibiotic selection, the plasmids purified and again analysed using restriction digest or PCR, before being used in subsequent studies. Where appropriate, gene sequences were modified by site-directed mutagenesis PCR using the QuikChange™ kit (Stratagene; see section 2.3.11) or deleted by inserting a kanamycin cassette using the P1 transduction method (see section 2.2.1). Typically, DNA was visualised on 0.8-1.0% (w/v) agarose (BDH) gels (in 1xTBE) supplemented with 10 µl SYBR® Safe DNA Gel Stain (Invitrogen) per 100 ml gel (see section 2.3.3).

All plasmids and primers used in this study are listed in Appendix B and C.

2.3.1 Purification of DNA

2.3.1.1 Chromosomal DNA

Genomic DNA from 1-2 x 10^9 cells was purified from a 5 ml overnight culture in LB (containing the appropriate antibiotic if required) using a DNeasy® Blood & Tissue Kit (Qiagen), according to the manufacturer's guidelines, and eluted in a final volume of 200 µl water.

2.3.1.2 Plasmid DNA

Plasmids used were purified from a 5 ml overnight culture in LB containing the appropriate antibiotic using a QIAprep® Spin Miniprep Kit (Qiagen), according to the

manufacturer's guidelines, and eluted in a final volume of 50 µl or 30 µl water as required.

2.3.2 Polymerase Chain Reaction (PCR)

2.3.2.1 PCR for molecular cloning

For molecular cloning, the desired DNA fragment was amplified from chromosomal or plasmid DNA using specific primer sets and the Bio-X-ACT DNA Polymerase (Bioline). Bio-X-ACT uses a blend of enzymes with 5'-3' DNA polymerase and 3'-5' proof reading activity which dramatically increases the fidelity of the PCR reaction compared to normal *Taq* polymerase.

The PCR reaction mix used for molecular cloning comprised:

Component	**Final Concentration or Volume**
Optibuffer	1x
Hi Spec. Additive Specificity Enhancer	1x
$MgCl_2$	2.0 mM
PCR Nucleotide Mix	2.0 µM (per nucleotide)
forward and reverse primer	0.3 µM (per primer)
Bio-X-ACT DNA Polymerase	2.5 units
purified chromosomal or plasmid DNA	2.0 µl

⇨ Add to a final volume of 50 µl with distilled nuclease free water

The PCR reaction was run in an Eppendorf Mastercycler gradient thermal cycler PCR machine at the following conditions:

PCR Step	Temperature and Duration
Denaturation	94 °C for 5 minutes (initial step)
	94 °C for 45 seconds (subsequent cycles)
Annealing	55 °C for 45 seconds
Extension	72 °C for 60 seconds
	72 °C for 10 minutes (final step)
Cycle number	34

2.3.2.2 Analysis of cloned or deleted genes

To analyse gene cloning or knock-out, the desired fragment was amplified from chromosomal or plasmid DNA using specific primer sets and the GoTaq® Hot Start Polymerase kit (Promega).

The PCR reaction mix used to analyse cloned and deleted genes comprised:

Component	Final Concentration or Volume
Green GoTaq® Flexi Buffer	1x
$MgCl_2$	1.0 mM
PCR Nucleotide Mix	0.2 mM (per nucleotide)
forward and reverse primer	0.5 µM (per primer)
GoTaq® Hot Start Polymerase	1.25 units
purified chromosomal or plasmid DNA	2.0 µl

⇨ Add to a final volume of 50 µl with distilled nuclease free water

The reaction mix was placed in an Eppendorf Mastercycler gradient thermal cycler PCR machine and run using the following conditions:

PCR Step	Temperature and Duration
Denaturation	94°C for 5 minutes (initial step)
	94°C for 45 seconds (subsequent cycles)
Annealing	55°C for 45 seconds
Extension	72°C for 60 seconds
	72°C for 10 minutes (final step)
Cycle number	34

The results of the test for successful replacement of the gene of interest with the kanamycin cassette from the Keio collection are shown in Appendix D.

2.3.3 Agarose Gel electrophoresis

DNA fragments were separated using agarose gel electrophoresis. Agarose gels were prepared according to the size of the DNA fragments. Typically, 0.8 % (w/v) agarose (BDH) were dissolved by heating in 100 ml of 1x TBE (Sigma). SYBR® Safe DNA Gel Stain (Invitrogen) was added at a final concentration of 1:10,000 and the solution was poured into a gel tank containing an appropriate comb and left to cool. Samples were mixed with 5x loading buffer (Sigma) and loaded onto the gel alongside the appropriate molecular weight marker (Invitrogen). The gel was run at 75 V in 1x TBE until the dye front (bromophenol blue) of the marker reached the bottom of the gel.

2.3.4 Gel Extraction of DNA

If required, DNA fragments were excised from agarose gels and extracted using a QIAquick® PCR Purification Kit (Qiagen). The DNA (about 1 µg) was eluted in a final volume of 30 µl water.

2.3.5 TA-cloning

In the process of molecular cloning, restriction digest of linear DNA fragments produced by PCR can be challenging. The pGEM®-T Easy Vector System allows for the integration of linear PCR products to form a circular plasmid, thereby facilitating the restriction digest and subsequent cloning of the desired DNA fragment. The linear pGEM®-T Easy vector contains a single thymidine overhang on both 3'-ends, compatible with the single 5'- adenosine overhang produced by e.g. the *Taq* polymerase during PCR. Following PCR (and clean-up by gel extraction), the amplified DNA fragment can directly be inserted into the vector via the T-A overhangs. The insertion-site (flanked by the T7 and SP6 promoter, as well as a multiple cloning site) lies within the α-peptide gene sequence of LacZ (β-galactosidase) encoded on the vector. Hence, insertion results in the disruption of the *lacZ* gene. This can be detected after transformation of XL1-blue cells using blue/white screening on indicator plates supplemented with 5-Bromo-4-chloro-3-indolyl-β-D-galactopyranoside (X-gal). Cells containing the pGEM®-T Easy vector with insert produce white colonies, blue colonies are formed by cells harbouring the re-ligated vector (lacking insertion). After purification of the plasmids from white

colonies, the inserted DNA can be sequenced using T7 and SP6 promoter specific primers.

Protocol:

The integration of the linear PCR fragment is carried out in a final reaction mix as follows:

Component	Final Concentration or Volume
Rapid Ligation Buffer for T4 DNA Ligase	1x
pGEM®-T Easy vector	1 µl (50 ng)
PCR product	3 µl
T4 DNA Ligase (3 Weiss units/µl)	1 µl

⇨ Add to a final volume of 10 µl with distilled nuclease free water

After 1 hour incubation at RT, 5 µl of the ligation mix is used to transform 50 µl of XL1-blue cells as described in section 2.3.10.

2.3.6 DNA sequencing

For sequencing, a mix of 7 µl purified plasmid DNA and 3 µl 10 µM sequencing primer was submitted to the DNA Core Laboratory of the Medical Research Council (Clinical Sciences Centre, Hammersmith Hospital, London, W12 0NN). Sequences were analysed using the EcoGene Database of *E. coli* Sequence and Function (http://ecogene.org/) in combination with the MultAlin software (http://bioinfo.genotoul.fr/multalin/multalin.html).

2.3.7 Restriction digest of DNA

Typically, 10-16 µl of purified plasmid DNA were digested in a 20 µl final reaction volume supplemented with the appropriate buffer (NEB or Promega) at 37°C for 2 hours using 10-20 units per restriction enzyme (NEB or Promega). The digest was then run on an agarose gel and the desired DNA fragment extracted and purified.

2.3.8 Ligation

After restriction digest, vector and insert (molar ratio = 1:3) were ligated at RT for 1 hour in a final reaction volume of 20µl using the LigaFast™ Rapid DNA Ligation system (Promega). The reaction mix contained 10 µl of 2x Reaction buffer, 1 µl of T4 DNA ligase , X µl vector, Y µl insert and was made up to a final volume of 20 µl with distilled water. After ligation, 1-5 µl of the reaction was used to transform competent *E. coli* cloning cells (see section 2.3.10).

2.3.9 Preparation of competent cells

5ml of LB (supplemented with the appropriate antibiotic) in a universal tube were inoculated with a single colony of the desired strain and grown overnight at 37°C with shaking. The overnight culture was diluted 1:100 in 30ml of LB (supplemented with the appropriate antibiotic) and grown at 37°C with shaking until mid-log phase. Cells were harvested by centrifugation (4,500 x g for 10 minutes at 4°C) and washed with 10ml of 20 mM $CaCl_2$, 15 % (v/v) glycerol. After washing, cells were

resuspended in 10 ml of 20 mM $CaCl_2$, 15 % (v/v) glycerol, incubated on ice for 15 minutes and pelleted by centrifugation (4,500 x g for 10 minutes at 4°C). The pellet was resuspended in 1 ml of 20 mM $CaCl_2$, 15 % (v/v) glycerol and kept on ice for one hour. The cells were then either directly transformed using the heat-shock method or stored at -80°C until required.

2.3.10 Heat shock transformation of competent cells

Typically, 30 µl of competent cells were mixed with 1–5 µl of plasmid DNA and incubated on ice for 40 minutes. After 90 seconds heat shock at 42°C and 2 minutes incubation on ice, cells were left to recover for 1 hour in 0.5 ml LB at 37°C with shaking. Cells were then spread onto LB plates containing the appropriate antibiotic to select for the plasmid of interest and incubated overnight at 37°C.

2.3.11 Site-directed mutagenesis

Site-directed mutagenesis (QuikChange™ Site-Directed mutagenesis kit; Stratagene) was used to exchange or insert nucleotides in plasmid-borne DNA fragments to either mutate genes, create gene deletions or to integrate linker regions into fused gene sequences. The DNA modification was performed on plasmids isolated from a *dam*$^+$ *E. coli* strain (the Dam methylase transfers a methyl group from S-adenosylmethionine to the adenine in the GATC-sequence) using PCR with the *PfuTurbo* high-fidelity DNA polymerase and primer pairs containing the desired

mutation or insertion flanked by sequences complementary to the area of interest. Following amplification of the entire plasmid, the PCR mixture contained the parental template sequence and the newly-synthesised mutant plasmid. These could be distinguished by the GATC-methylation of the parental DNA. The non-modified template was degraded using the restriction enzyme *Dpn*I, which specifically recognises methylated GATC-sites. In a final step, an aliquot of the mixture was transformed into *E. coli* XL1-blue cells to propagate the mutant plasmid.

Protocol:

The DNA modification is carried out by PCR in a final reaction mix as follows:

Component	**Final Concentration or Volume**
PfuTurbo reaction buffer	1x
PCR Nucleotide Mix	10 mM (per nucleotide)
forward and reverse primer	10 µM (per primer)
PfuTurbo DNA polymerase	2.5 units
plasmid DNA (from a *dam*$^+$ *E. coli* strain)	4.0 µl

⇨ Add to a final volume of 50 µl with distilled nuclease free water

PCR Step	**Temperature and Duration**
Denaturation	95°C for 1 minute (initial step)
	95°C for 30 seconds (subsequent cycles)
Annealing	58°C for 1 minute
Extension	68°C for 12 minutes
Cycle number	16

After amplification, the parental DNA was degraded by incubation of the PCR mix with 3,000 units *Dpn*I (NEB) in 1x NEB buffer 4 (NEB) for 1 hour at 37°C. Competent

E. coli XL1-blue cells were transformed with 5 µl of the mix using the transformation method as described in section 2.2.10.

2.4 IN VITRO METHODS

2.4.1 Small scale protein expression

5 ml of LB or minimal medium supplemented with the appropriate antibiotics were inoculated with 50 µl of an overnight culture. Cultures were grown at 37°C or 30°C with shaking until OD_{600nm} 0.4-0.6 was reached. Unless indicated otherwise, pIV was constitutively (without inducer) expressed from pGJ4, a plasmid harbouring *gIV* under the control of a leaky *lacUV5* promoter. Expression of other proteins was induced either with 0.1 mM IPTG or 0.001% arabinose for 1 hour at 37°C or 30°C, as indicated. The bacterial pellet of 1 ml was resuspended in 50 µl dH_2O and 50 µl 2x Laemmli sample buffer (Sigma), the solution boiled for 5 minutes at 95°C and the proteins separated electrophoretically by SDS-PAGE.

2.4.2 SDS Polyacrylamide Gel electrophoresis (SDS-PAGE)

10-20 µl of samples from small scale protein expressions (see section 2.4.1) were loaded on either a 7.5%, 12.5% or 15% (depending on the expected protein size) SDS polyacrylamide gel, using the BioRAD mini-protein gel II system. The gel was run at 200 V for 50 minutes in 1x Tris/SDS/Glycine (National Diagnostics).

	Stacking Gel	Separating Gel		
Component	**4.5%**	**7.5%**	**12.5%**	**15.0%**
Solution I	0.3 ml	1.25 ml	2.05 ml	2.5 ml
Solution II	-	1.25 ml	1.25 ml	1.25 ml
Solution III	0.5 ml	-	-	-
Water	1.2 ml	2.5 ml	1.7 ml	1.25 ml
Temed (Sigma)	2 µl	5 µl	5 µl	5 µl
10 % APS (BDH)	20 µl	50 µl	50 µl	50 µl

Solution I	ProtoGel® (National Diagnostics) 30% (w/v) Acrylamide
Solution II	1.5 M Tris-HCl, pH 8.8, 0.3 % (w/v) SDS
Solution III	0.5 M Tris-HCl, pH 6.8, 0.3 % (w/v) SDS

2.4.3 Immunoblotting

Following SDS-PAGE, the separating gel (together with Whatman filter paper (Merck)) was equilibrated in transblot buffer (10 mM Tris base, 100 mM glycine, 10% (v/v) methanol) for 10 minutes. Proteins were transferred from the gel onto a methanol-activated and transblot buffer-equilibrated Immun- Blot™ PVDF membrane (Ge Healthcare) using a Trans-Blot® SD Semi-Dry Transfer Cell (BIO-RAD). The cell was run for 30 minutes to 1 hour at ≥100 mA. After confirming protein transfer onto the membrane using Ponceau S (Sigma) and blocking of unspecific binding-sites with 5% (w/v) milk-powder in TBS (50 mM Tris-HCl (pH 7.5), 150 mM NaCl) overnight at 4°C, the membrane was washed with TTBS (TBS, 0.1% Tween-20) and TBS and incubated for 1 hour at RT with the primary antibody (diluted in 5% (w/v) milk-powder in TBS) specific for the analysed protein. The membrane was washed as above and incubated for 1 hour at room temperature with horseradish peroxidase (HRP) conjugated secondary antibody (diluted in 5% (w/v) milk-powder

in TBS) specific for the FC-domain of the primary antibody. Following 5 final washing steps with TTBS, the detected proteins were visualised via the ECL Plus™ Western Blotting Detection System (GE Healthcare) using the Luminescent Image Analyzer LAS-3000 (FujiFilm) or by exposure of the membrane to a Biomax XR film (Fisher). All antibodies (including the dilution) used in this study are listed in Appendix E.

2.4.4 β-galactosidase assay

The β-galactosidase assay is a colorimetric test to assess the level of transcription of certain genes. For that, *lacZ*-based reporter fusions are created enabling β-galactosidase (LacZ) production under the control of the promoter of interest. Under physiological conditions LacZ catalyses the hydrolysis of the di-saccharide lactose to the mono-saccharides glucose and galactose. In β-galactosidase assays, lactose is substituted by its non-physiological analogue ONPG (*o*-nitrophenyl-*β*-D-galactoside) as substrate. Hydrolysis of the colourless ONPG results in production of the yellow orthonitrophenol (2,4-di-nitrophenol). The amount of orthonitrophenol produced is proportional to the number of LacZ molecules (β-galactosidase activity) in the solution. The more LacZ available, the faster the solution turns yellow. Hence, the activity of the promoter of interest can be assessed by measuring the time between the addition of ONPG to the reaction and the colour-change from colourless to yellow and is expressed as Miller units (MU) taking into account the number of LacZ expressing cells used in the assay and the time of incubation.

Protocol:

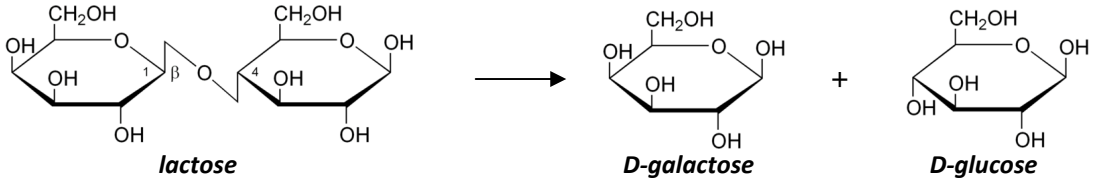
Day-cultures (in triplicate) of *E. coli* strains containing the promoter-l*acZ* transcriptional reporter fusion were grown to mid-log phase in LB with the appropriate antibiotic(s). The cell-density (by measuring the OD_{600nm}) was determined and 500 µl of the culture were added to 500 µl of Z buffer (60 mM Na_2HPO_4, 40 mM NaH_2PO_4, 10 mM KCl, 1 mM $MgSO_4$, 50 mM β-mercaptoethanol). Following addition of 50 µl of chloroform and vortexing for 30 seconds (to lyse the cells), the solution was incubated at 30°C with 200 µl of ONPG (4 mg/ml dissolved in Z buffer minus β-mercaptoethanol and pre-warmed to 30°C). The reaction was quenched by 500 µl of 1 M Na_2CO_3 to raise the pH once the solution has turned yellow and the time between addition of ONPG and quenching was recorded. The reaction was analysed at OD_{420nm} and OD_{550nm}. The activity of the promoter of interest was expressed as Miller units (MU) calculated based on the following equation:

$$\text{Miller Units (MU)} = [(OD_{420} - (1.75 \times OD_{550})) \times 1000] / (OD_{600} \times t \times v)$$

OD_{420} = absorbance of reaction at 420nm; OD_{550} = absorbance of reaction at 550nm

OD_{600} = absorbance of culture at 600nm; t = reaction time (minutes); v = volume of cells used in the assay (ml)

Physiological



Non-physiological (β-Galactosidase Assay)

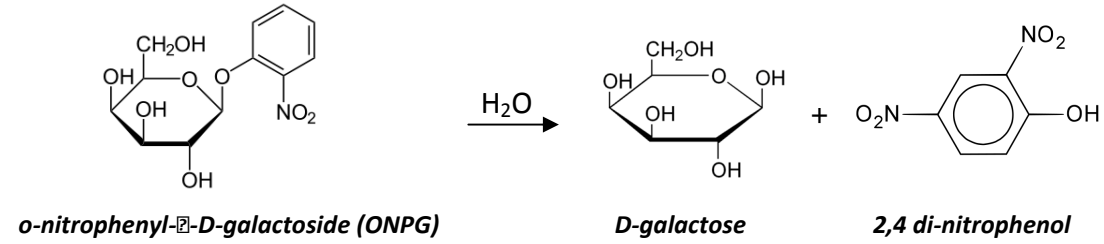


Figure 2.1: Reactions catalysed by LacZ (β-galactosidase). Under physiological conditions, LacZ (β-galactosidase) hydrolyses lactose to D-galactose and D-glucose. In β-galactosidase assays, lactose is substituted by its analogue o-nitrophenyl-β-D-galactoside (ONPG). One product of the hydrolysis of ONPG is the yellow 2,4 di-nitrophenol. Its production can be measured spectroscopically at an OD_{440nm}.

2.4.5 Extraction and measurement of quinones

Ubiquinone and menaquinone extraction and measurement was adapted from Bekker *et al.*, 2007. A 30 ml day-culture was set up in LB containing the appropriate antibiotic using an 1:100 inoculum of an overnight culture. Depending on the aeration needed, cells were grown at 37°C in 250 ml (aerobic growth) or 100 ml (microaerobic growth) Erlenmeyer flasks at either 200rpm (aerobic growth) or 100rpm (microaerobic growth) in an Innova® shaking incubator (New Brunswik Scientific). To quench the sample, 8 ml of the culture (OD_{600nm} ~ 0.5) was added quickly (within 2 seconds to prevent reduction of the quinones) to 24 ml of ice-cold methanol. Quinones were extracted by adding 8 ml of petroleum ether (40-60°C). Samples were votexed and centrifuged at 900 x g for 2 minutes. The upper phase (petroleum ether) was removed into a clean tube and evaporated under constant nitrogen flow. The lower phase was again treated with 8ml of petroleum ether and the additional steps repeated 4 times to extract any remaining quinones. The extracted and dried quinones were resuspended in 50 µl of 99.9% ethanol using a glass rod. A 30 µl sample of this solution was loaded onto a reverse phase Lichrosorb (Chrompack) 10 RP 18 column (4.6 mm i.d., 2500 mm length) equilibrated with ethanol : methanol (1:1 v/v), also used as mobile phase. Quinone contents were analysed using the Pharmacia LKB gradient pump 2249 HPLC system.

Peaks were identified by UV-Vis spectroscopy (Bekker *et al.*, 2007). The amount of quinones was calculated from the area-size below a corresponding peak using a standard curve for UQ_{10}.

2.4.6 Triton X-100 cell fractionation

5 ml of minimal medium supplemented with 0.4% glucose, 10 mM NH_4Cl, 10 ml/L trace elements and the appropriate antibiotic was inoculated with 50 µl of an overnight culture and incubated at 30°C with shaking until OD_{600nm} 0.7-0.9 was reached.

2.4.6.1 Extraction of soluble proteins

A 1 ml of cells was drained by centrifuging at 16,100 x g for 5 minutes and the pellet resuspended in 20 µl 200 mM Tris-HCl (pH 8.0), 5 µl 10 mM EDTA and vortexed. To this 30 µl of 40% sucrose and 5 µl of 5 mg/ml egg white lysozyme (Sigma) was added. After 10 minutes incubation at RT, the cells were lysed by performing 2-3 cycles of freezing (dry ice with ethanol) and thawing (42°C). After such time, 400 µl dH_2O, 12 µl $MgCl_2$ and 2 µl DNaseI (5 u/µl; GE Healthcare) was added and the samples incubated for a further 20 minutes at RT. Soluble and insoluble fractions were separated by centrifuging for 5 minutes at 16,100 x g at RT. The supernatant, containing the cytoplasmic and periplasmic fraction, was removed into 500 µl 10% TCA, incubated at 4°C for 10 minutes, centrifuged for 10 minutes at 16,100 x g and 4°C, washed with 500 µl acetone, spun again for 10 minutes at 4°C, drained and air-dried. The proteins of the soluble fraction were resuspended in 30 µl 4% SDS.

2.4.6.2 Extraction of IM proteins

The pellet (inner membrane, outer membrane and aggregates) was resuspended in 100 µl 1% Triton, 10mM $MgCl_2$, 50 mM Tris-HCl (pH 8.0) and incubated for 20 minutes at 37°C to extract the proteins from the IM. Samples were centrifuged for 5 minutes at 16,100 x g at RT. The IM proteins (in the supernatant) were precipitated with 100 µl chloroform and 240 µl methanol and pelleted for 5 minutes at 16,100 x g at RT. Subsequently, the air-dried pellet containing the IM proteins was resuspended in 30 µl 4% SDS.

2.4.6.3 Extraction of OM proteins

OM proteins were obtained by incubating the pellet, containing OM and insoluble fraction, in 100 µl of 1% Triton, 10 mM EDTA, 50 mM Tris-HCl (pH 8.0) for 20 minutes at 37°C. The sample was centrifuged for 5 minutes at 16,100 x g at RT. The proteins of the OM (in the supernatant) were precipitated with 100 µl chloroform and 240 µl methanol. After 5 minutes centrifugation at 16,100 x g at RT, the protein pellets were drained, air-dried and resuspended in 30 µl 4% SDS.

2.4.6.4 Extraction of aggregated proteins

The remaining pellet, containing the aggregated fraction, was also air-dried and resuspended in 30 µl 4% SDS.

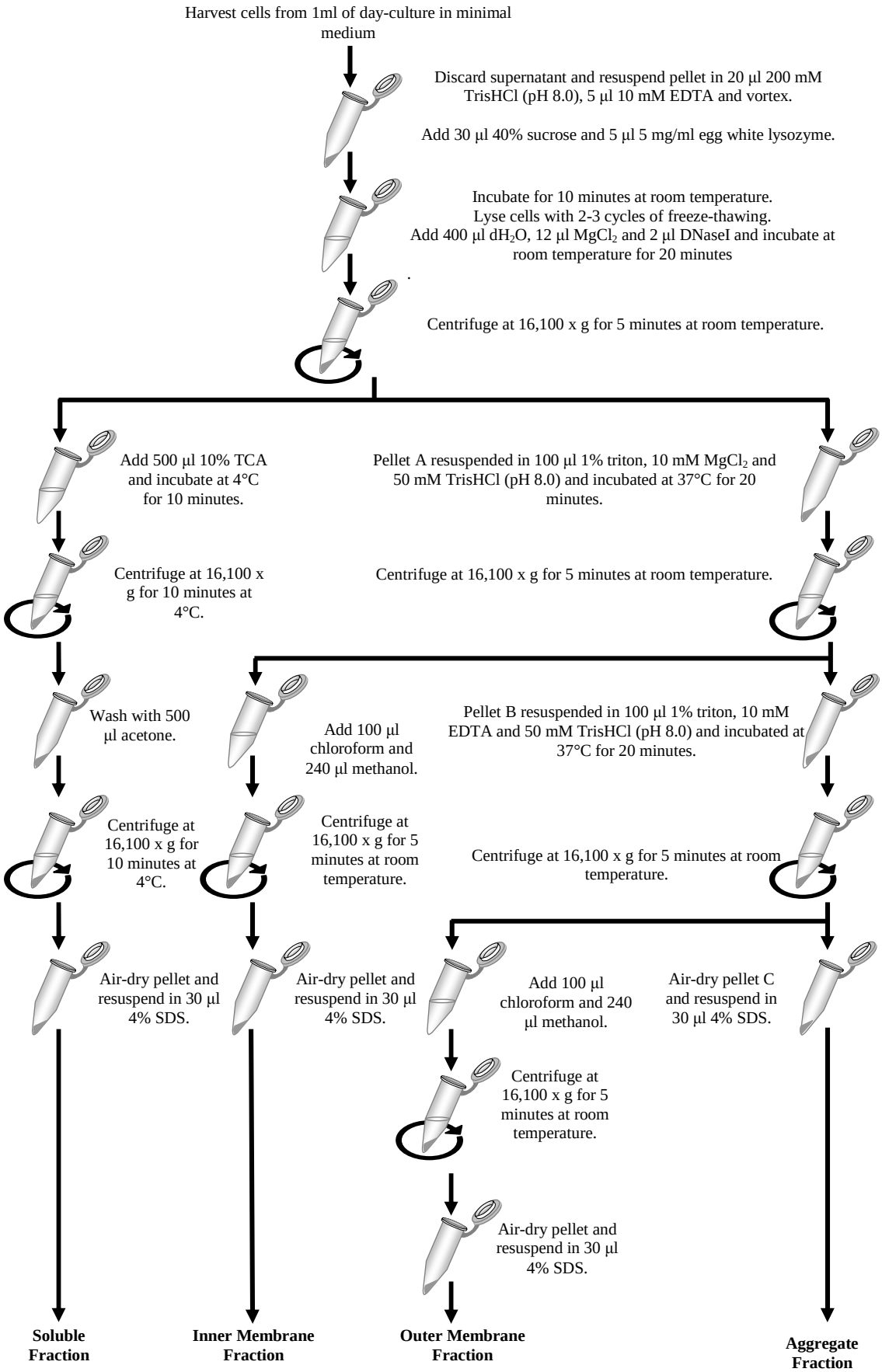


Figure 2.2: Flow-chart of the Triton X-100 based cell fractionation procedure.

2.5 IN VIVO METHODS

2.5.1 Growth of bacterial cells

In general and unless indicated otherwise, cells were grown in 5 ml LB (supplemented with the appropriate antibiotic) in 30 ml universal tubes at 37°C and 200 rpm on an Innova® shaking platform (New Brunswik Scientific). Overnight cultures were inoculated with a single colony from a freshly streaked plate (supplemented with the appropriate antibiotic). Day- (sample-) cultures were inoculated with 50 µl (1:100-dilution) of an overnight culture and grown to mid-log phase (OD_{600nm} ~ 0.6) prior to analysis. In chapter 3, cells were grown aerobically by placing the lid loosely onto the universal tube (without tightening) and shaking at 200 rpm, microaerobically by tightening the lid and shaking at 100 rpm, and anaerobically by growing the cells in a sealed (Suba-seal®; Sigma) universal tube fully filled with LB (supplemented with the appropriate antibiotic) overnight without shaking. In chapter 4, aerobic growth was achieved by growing the cells in 30 ml LB (supplemented with the appropriate antibiotic) in a 250 ml Erlenmyer flask at 200 rpm. For microaerobic growth, 30 ml cells were grown in a 100 ml Erlenmeyer flask at 100 rpm (see section 2.4.5). Anaerobic growth was as in chapter 3. In general, samples for analysis were taken from technical duplicates of three independently grown cultures of each strain tested.

2.5.2 Bacterial two-hybrid analysis

The *cya*-based bacterial two-hybrid (BACTH) system (Karimova *et al.*, 1998) exploits the physical separation of the T18 and T25 fragments into inactive parts of the adenylate-cyclase (*cya*) from *Bordetella pertussis*. T18 and T25 can only form an active enzyme when in close proximity to each other. Effective reconstitution of the adenylate-cyclase is a direct consequence of the interaction of 2 proteins fused to T18 and T25 and is reported via LacZ expression, which can be analysed in the BTH101 (cya^-) strain either by using blue-white screening on XGal plates or β-galactosidase assays.

Protocol:

BTH101 cells were co-transormed with the 2 plasmids encoding the proteins of interest fused to the T18 and T25 fragments. Cells were grown in LB medium with the appropriate antibiotic at 30°C and expression of the fusion proteins was induced with 0.5 mM IPTG at mid-log phase growth. After 1 hour induction LacZ activity was measured by β-galactosidase assays, performed in triplicate per strain tested. A ≥2-fold increase in LacZ activity compared to the negative control was scored as a positive interaction. BTH101 cells carrying pUT18C and pKT25 vectors alone were used as the negative control and as the positive control we assayed cells containing pUT18C-zip and pKT25-zip plasmids carrying a fused GCN4 leucine-zipper sequence (Karimova *et al.*, 1998).

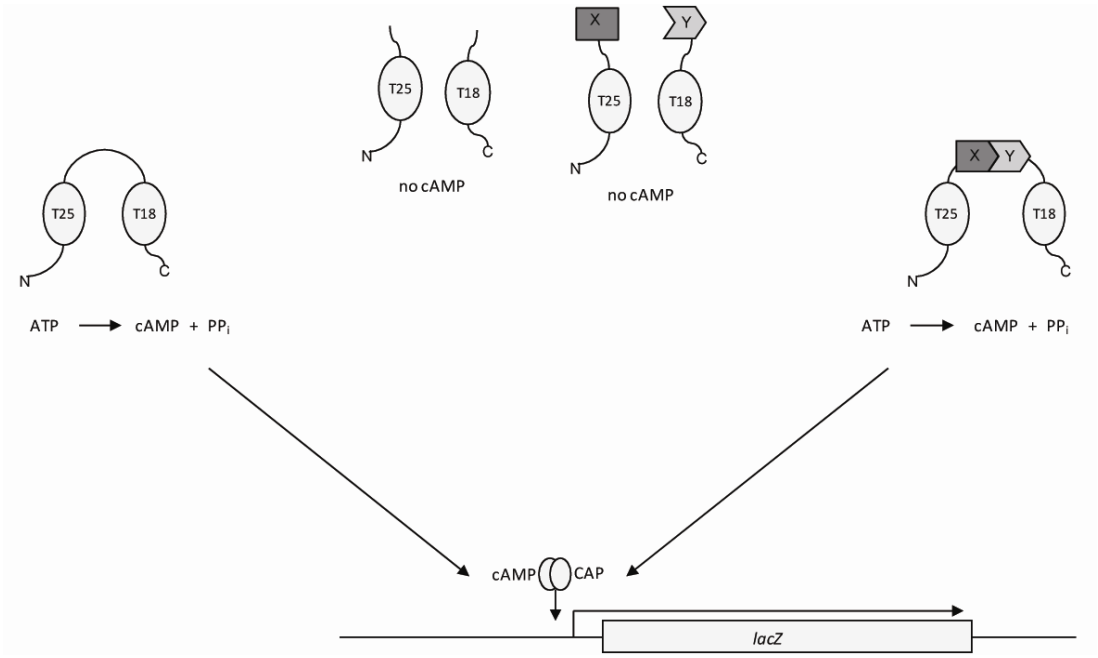


Figure 2.3: The BACTH System (adapted from Karimova *et al.*, 1998)**.** The BACTH system uses the production of cAMP by the adenylate-cyclase (Cya) from *B. pertussis* to test the interaction of two proteins of interest (X and Y). The CyaA protein is only active when its T18 and T25 domain are in close proximity to each other. For the assay, both domains have been physically separated and are therefore unable to synthesise cAMP. The enzymatic activity of Cya can only be restored if the two proteins of interest fused to T18 and T25 interact. Subsequent cAMP synthesis results in the formation of complexes between cAMP and CAP (catabolite gene activator protein). These complexes can activate transcription of e.g. the *lac* operon, in particular l*acZ*, which can be measured by β-galactosidase assays.

2.5.3 Motility assay

Motility assays were performed as described (Lloyd *et al.*, 2004). Briefly, 2 µl of an overnight LB culture was pipetted onto soft agar plates (1% tryptone (w/v), 0.5% NaCl (w/v), and 0.3% agar (w/v)) containing the appropriate antibiotic and 1 mM IPTG where required. Plates were incubated overnight at RT, and zones of motility were measured in mm. Each strain was assayed six times. Standard errors of the mean are indicated.

2.5.4 Separation of mini- and rod shaped cells

E. coli YLS1 (MC1000Δ*minCDE*) (a gift from Shih, Y-L) cells were grown in minimal medium supplemented with 25 µg/ml leucine and 5 µg/ml thiamine at 30°C. At mid-log phase, the cells were separated by differential centrifugation (Lai *et al.*, 2004) and proteins visualised by immunoblotting.

2.5.5 In vivo cross-linking

In vivo cross-linking was performed as described (Adams *et al.*, 2003) using the thiol-reactive cross-linking agent dithiobis(succinimydylpropionate) DSP (PIERCE). Cells were grown in minimal medium at 30°C to an OD_{600nm} of 1.0, harvested and washed in 0.9% NaCl. Proteins were exposed to the cross-linker for 30 minuntes (100 µM DSP in 125 mM HEPES (pH 7.3) at 25°C). To quench the reaction, 50 µl of 1

M Tris-HCl (pH 8.0) were added and the reaction was transferred to ice for 5 minutes. Proteins were separated on a 7.5% SDS-gel (run at 200 V for 50 minutes) and cross-linked species detected by immunoblotting.

2.5.6 PMF measurement

PMF measurements were performed as described by Jovanovic *et al.* (2006) using JC-1 (Molecular probes). This membrane-permeable dye can be found in two different fluorescent states depending on the electron potential of the cell. JC-1 forms red aggregates at high electron potential and remains a green monomer at low electron potential. The ratio between both forms can be used as a measure for the PMF of the cell.

Protocol:

Cells from a 1ml day-culture (OD_{600nm} ~ 0.8) grown in LB supplemented with the appropriate antibiotic were harvested (4,500 x g) and resuspended in 1ml of permeabilisation buffer (10 mM Tris-HCl (pH 7.5), 1 mM EDTA, 10 mM glucose). Following 30 minutes incubation with 2 µl JC-1 (5 mg/ml) at RT, cells were again harvested at 4,500 x g and resuspended in 500 µl of permeabilisation buffer. Cells across three different microscopic fields were imaged using confocal fluorescence microscopy.

2.5.7 Oxygen measurement

The oxygen content in cultures of bacterial cells was measured using the Oxy_2Dot™ sensor (OxySense® 4000B system; Air Monitors) (as in Jovanovic *et al.*, 2009). The sensor was placed within the tubes used for growing the day-cultures. It contains a metal organic fluorescent dye which emits light at 610 nm upon excitation with light at 470 nm. The OxySense® 4000B system calculates the oxygen concentration by measuring the intensity as well as the fluorescence lifetime of the emitted light which depends on fluorescence quenching caused by oxygen surrounding the sensor. The sensor was excited and output fluorescence was measured by an OxySense® reader-pen (through the growth tube). Read-outs for the oxygen content within the cultures can be obtained as percentage of oxygen (% O_2), p.p.b. (1000 p.p.b. = 1 mg of O_2 l^{-1}) or as oxygen concentration in mg/L. Cells were grown microaerobically at 37°C (see 2.5.1) from an initial OD_{600nm} ~ 0.025 for 2.5 hours to OD_{600nm} ~ 0.6 with similar growth rates. Per measurement, 100 signals were captured using the OxySense® reader-pen. Per strain, 10 measurements were taken to calculate the mean values of the oxygen content.

2.5.8 Fluorescence microscopy to analyse subecullar protein localisation

In the recent years, fluorescence microscopy has become a popular tool in biology. It is used to study fluorescently labelled biological molecules (such as proteins or DNA) both *in vitro* and *in vivo* and has been applied to a broad range of organisms. Advances in the properties of fluorescent labels as well as the development of new microscopes and software constantly help to push the boundaries of sensitivity and resolution of this technique. Currently, it is possible to study biological processes at single-cell and single-molecule level.

In this work, a combination of epi-, confocal and Total Internal Reflection Fluorescence (TIRF) microscopy was used to study PspA and PspG in its cellular context. For this, both proteins were fluorescently labelled with GFPmut2, a bright variant of the commonly used Green Fluorescent Protein (GFP).

2.5.8.1 The Green Fluorescent Protein GFPmut2

After its isolation from the jellyfish *Aequorea victoria* in the 1960s by Osamu Shimomura, GFP became one of the most commonly used fluorescent labels. Its simple handling (specific labelling of target proteins by gene fusion), the independence of co-factors and the absence of toxicity when expressed in living cells was the basis for studying proteins in their native environment. In 2008, the contributions of Osama Shimomura, Martin Chalfie and Roger Y. Tsien through their extensive studies of GFP were acknowledged with the Nobel Prize in Chemistry.

GFP is a 26.9kDa protein which emits green light (with an emission peak at 509nm and a shoulder at 540nm) upon excitation with blue light (with a major excitation peak at 395nm and a minor peak at 475nm). The 238 amino acids form a β-barrel structure (Figure 2.4). Inside the barrel resides a α-helix containing the chromophore, composed of the amino acids 65-67 (Ser-Tyr-Gly). To form an excitable chromophore, these 3 amino acids need to undergo a post-translational cyclisation process, called maturation, involving a nucleophilic attack from the amino group of Gly67 on the carbonyl group of Ser65 followed by a hydrolysation and an oxidation step. The post-translational maturation can take several hours and is dependent on the nature of the amino acids surrounding the chromophore. Site-directed changes in these surrounding amino acids led to the development of GFP variants with various properties such as faster maturation time (e.g. Venus) or differences in excitation and emission spectra (e.g. YFP).

One of the variants is GFPmut2 (Cormack *et al.*, 1996). The excitation spectrum of WT GFP contains 2 peaks with maximum excitation at 395nm and a smaller peak at 470nm (Figure 2.4). The most commonly used light-source, the argon laser, excites at a wavelength of 488nm. Hence, excitation of WT GFP and therefore fluorescence yield is not optimal. Cormack *et al.* (1996) have therefore mutagenised GFP and isolated GFPmut2 (S65A, V68L, S72A), a variant which exhibits 100-fold increased fluorescence due to a red-shift of the excitation maximum from 395nm to 481nm allowing optimal excitation of the chromophore when using an argon laser. Additionally, the GFPmut2 variant was reported to facilitate protein folding compared to the WT form (Cormack *et al.*, 1996). GFPmut2 fusion proteins should therefore be more stable and tend to form less protein aggregates.

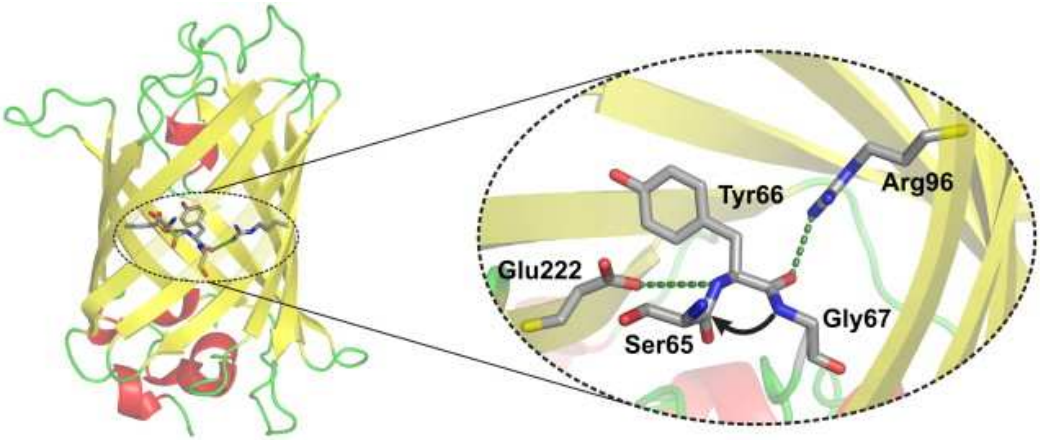


Figure 2.4: The β-barrel and chromophore structure of WT GFP (taken from Pakhomov *et al.* 2008)**.** GFP adopts a β-barrel structure with a single α-helix buried inside containing the chromophore. The image also shows a magnification of the chromophore which consists of the 3 amino acids Ser65, Tyr66 and Gly67. The nucleophilic attack from Gly67 to Ser65 is indicated by an arrow.

2.5.8.2 Epi- and confocal fluorescence microscopy

Epi- and confocal fluorescence microscopy are common techniques to visualise fluorescently labelled biological molecules. In principle, the set-up of both microscopes is similar as the instruments contain a light-source, an objective, filters and a detector. In epi-fluorescence microscopes, fluorescence from in- and out-of-focus fluorophores is detected. In confocal fluorescence microscopes an additional pinhole is placed in front of the detector, which can only be passed by light emitted from fluorophores in the focal plane. This allows for improved signal-to-noise resolution along the axial and lateral axes.

Protocol:

On the day prior to an imaging experiment using epi- or confocal fluorescence microscopy, 80 µl of melted agarose (BDH) (0.8% in water) were pipetted onto a microscope slide (VWR) and sandwiched with a sigmacoted (Sigma) coverglass (VWR) to obtain a thin and evenly spread layer of agarose. The coverglass was removed after 30 minutes at RT and the microscope slide (covered with the agarose-layer) was left to dry overnight at 37°C. For imaging, 5µl of a mid-log phase (OD_{600nm} ~ 0.5) culture grown at 30°C in minimal medium (see section 2.1.1) supplemented with the appropriate antibiotics was mounted onto the agarose-coated microscope slide and covered with a coverglass. Where indicated, cell membranes were stained by adding 1 µl FM 5-95 dye (Molecular Probes) to 9 µl cells and DNA was stained using DAPI (300 nM) (Molecular Probes). When treated with A22 to disrupt the MreB cytoskeleton, cells were grown in minimal medium at 30°C until OD_{600nm} ~ 0.3. After 12 hour or 24 hour incubation with 50 µg/ml of A22

(suspended in 100% methanol), the cells were immobilised by adding 2 µl of 0.1% (w/v) poly-L-lysine to 8 µl of cells and spotted onto a coverglass. Addition of poly-L-lysine rendered the cells immobile after approximately 10-15 minutes, but had no significant effect on the Psp response as judged by β-galactosidase assays (data not shown)

Confocal fluorescence images were taken using a Leica SP2 upright microscope fitted with a HCX PL APO CS 63.0x1.32 Oil Ph3 objective. Epi-fluorescence images were taken using inverted epi-fluorescence microscopes and either a Zeiss Axiovert 200M fitted with a Plan-Neofluar objective (Zeiss 100x/1.30 Oil Ph3), a 300 W xenon arc-lamp transmitted through a liquid light guide (Sutter Instruments), a Sony CoolSnap HQ cooled CCD camera (Roper Scientific), modified magnetron ET filter sets (Chroma); or a Nikon TE-2000 microscope equipped with a CoolView EM 1000/TV camera (Photonic Science) and a tuneable argon ion laser. Digital images were acquired and analysed using either METAMORPH (version V.6.2r6) or ImageJ software (http://rsbweb.nih.gov/ij/).

2.5.8.3 Single molecule fluorescence imaging

Single PspA and PspG complexes *in vivo* were imaged using objective-type total internal reflection fluorescence (TIRF) on a Nikon TE-2000 inverted optical microscope equipped with a CoolView EM 1000/TV camera (Photonic Science) and a tuneable argon ion laser.

TIRF microscopy is especially suited to visualise membrane bound proteins since only fluorophores residing within 100 nm from the surface of the specimen are

excited. This is achieved through an instrument set-up where the incident laser light is positioned in a way that it is totally reflected at the glass-water interface. Hence, and in contrast to, other fluorescence microscopes, the excitatory light does not directly pass through the specimen. Instead, fluorophores are excited by the evanescent wave (the electromagnetic field of the laser). Since this wave decays exponentially with increased distance from the point of reflection, only fluorophores proximal to the interface are excited. This results improved resolution and sensitivity up to single molecule level.

Protocol:

E. coli MG1655 cells harbouring pDSW209 (GFP), *E. coli* MG1655Δ*pspA*/GFP-PspA (for GFP-PspA) and *E. coli* MG1655Δ*pspG*/PspG-GFP (for PspG-GFP) cells were grown in minimal medium at 30°C until OD_{600nm} ~ 0.6. GFP cell lysates were prepared by sonication (50 mM Tris-HCl (pH 8.0), 100 mM NaCl, 1 mM EDTA (pH 8.0), 1 mM DTT). GFP cell lysates, GFP-PspA and PspG-GFP expressing cells were mounted on coverglass and immobilised by adding 2 µl of 0.1% (w/v) poly-L-lysine to 8 µl of cells. Images were taken at 80 milliseconds per frame and analysed manually using the ImageJ software.

CHAPTER 3

PHYSICAL, FUNCTIONAL AND CONDITIONAL INTERACTIONS BETWEEN ARCAB AND PSP

3.1 INTRODUCTION AND RECAP

Bacteria in their native habitats encounter a plethora of stresses, which challenge their cellular integrity. Robustness of the cytoplasmic membrane is required for it to function as a barrier between the inside of the cell and the environment. Bacteria have therefore evolved a number of systems to maintain membrane integrity (see section 1.5), one of which is the Psp response (see section 1.5.4), highly conserved in Gram-negative bacteria. In *E. coli,* Psp genes are organised in a regulon (*pspF pspABCDE* and *pspG*) that is under the control of a Sigma54-dependent promoter activated by PspF, positively controlled by PspBC and negatively regulated by PspA (Model *et al*., 1997; Darwin, 2005). Psp expression is induced upon IM stress which dissipates the PMF (potentially resulting in a reduced energy status of the cell). Psp effector proteins (e.g., PspA – effector upon stress, PspD and PspG) subsequently help to conserve PMF (Kleerebezem *et al.*, 1996; Jovanovic *et al.*, 2006, Kobayashi *et al.*, 2007). Understanding the mechanism of Psp induction and its biological function is important since the Psp system is significant in protein translocation and in the growth and virulence of pathogenic enterobacteria (Darwin, 2005 & 2007; Rowley *et al.*, 2006). The PspA homologue Vipp1 has been shown to be essential in plants and *Synechocystis* for thylakoid biogenesis and photosynthesis (Westphal *et al*., 2001). Further, PspA homologues have been reported in Gram-positive bacteria and archea (Bidle *et al.*, 2008; Vrancken *et al.*, 2008). PspA therefore appears to have a fundamental role in the three domains of life.

The nature of the stress signal and how it is detected by the Psp system remains unknown (Darwin, 2005). Previously it has been observed that ArcB (the sensor

kinase of the two-component ArcAB system) is required for full pIV-dependent *psp* expression in *E. coli* (Jovanovic *et al.*, 2006). The ArcAB system (Figure 3.1) - of particular importance under microaerobic growth conditions, where oxygen is limiting rather than being completely absent (Alexeeva *et al.*, 2003) - regulates the transition from aerobic to anaerobic respiration and fermentation (Malpica *et al.*, 2006) in response to the redox state of the cell potentially sensed through changes in the ubiquinone pool (Georgellis *et al.*, 2001; Malpica *et al.*, 2004). Hence, the following model for the induction of the Psp response has been proposed (Jovanovic *et al.*, 2006):

Psp inducing stress conditions such as pIV-secretin production result in impaired IM integrity and a proton influx into the cytoplasm. The subsequent dissipation of PMF and the increased redox state of the cell is sensed by ArcB through changes in the ratio between UQ and UQH_2. This causes an initial activation of the ArcAB system at a low level. The subtle switch from aerobic to anaerobic gene transcription mediated by the low levels of phosphorylated ArcA helps to amplify the signal by generating a more pronounced drop in PMF. Psp induction then occurs via the positive regulators PspBC, which re-arrange the PspAF inhibitory complex. PspF activates transcription of the *psp* genes and Psp effectors (PspA, PspD and PspG) will ultimately conserve PMF by favouring anaerobic respiration, by down-regulating PMF consuming processes such as chemotaxis/motility and by improving the cell integrity through production of cell wall components (Jovanovic *et al.*, 2006).

3.2 OBJECTIVES

Recently, Seo *et al.* (2007) reported that ArcB was dispensable for Psp induction in contrast to Jovanovic *et al.* (2006). A general transposon mutagenesis-based search for gene products involved in Psp signal transduction as well as a specific analysis using Δ*arcB* strains of both *Y. enterocolitica* and *E. coli* failed to detect ArcB as a component of the signalling cascade. Instead, the authors concluded from microarray data that Psp proteins alone are capable of mounting a response to inner membrane stress, largely independent of any other proteins (Seo *et al.*, 2007). The present study therefore aimed at solving the apparent controversy on the relevance of ArcB for Psp.

The main objectives for this work were to:

1) Explore further the relationship(s) between the Psp and Arc system under different growth conditions (aerobic, microaerobic and anaerobic growth)

2) Find evidence for a physical and functional interaction between Psp and ArcAB *in vivo*

3) Establish the determinants for a potential cross-talk between Psp and ArcAB

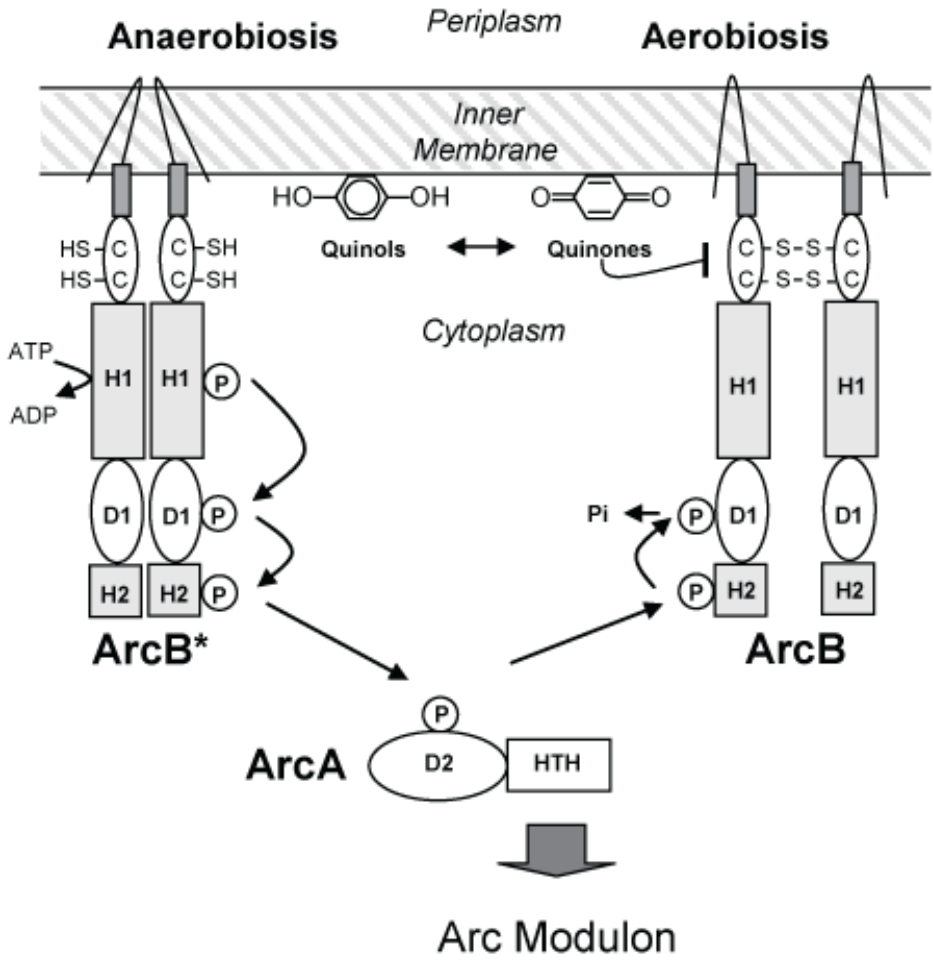


Figure 3.1: Regulation of the ArcAB two-component system (adapted from Malpica *et al.*, 2004)**.** The sensor kinase ArcB is an IM localised dimer. Its kinase activity is diminished by UQ and elevated in the presence of UQH_2 leading to reduction of the ArcB Cys180 and Cys241 thiol groups in the PAS (Per-Arnt-Sim) domain (PAS domains are signalling domains and they function as input modules in proteins that sense oxygen, redox potential, light, and several other stimuli) and an increased interaction between the two ArcB trans-membrane domains. Reduction of ArcB is followed by autophosphorylation of H292 (H1) and the phosphorelay *via* D576 (D1) and H717 (H2) to residue D54 (D2) within the response regulator ArcA. Phosphorylated ArcA then down-regulates transcription of genes involved in aerobic respiration and activates transcription of genes involved in anaerobic respiration (Arc Modulon).

3.3 RESULTS

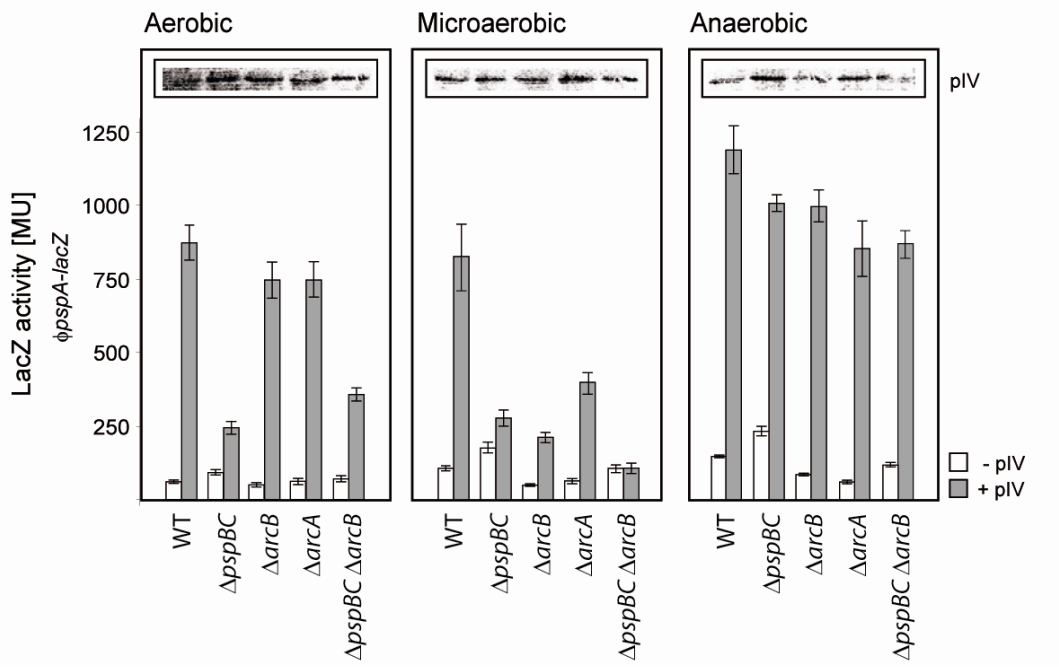
3.3.1 pIV-dependent induction of Psp under different growth conditions

To test whether the requirement of ArcAB for pIV-secretin induced *psp* expression is dependent on the growth condition, strains with different complements of *arc* and *psp* genes were grown aerobically, microaerobically and anaerobically (see Chapter 2) where the ArcAB proteins are known to have differing importance (Figure 3.2). The induction of Psp is dependent on ArcAB only in microaerobiosis and on PspBC (positive regulators) in microaerobiosis and aerobiosis (Figure 3.2A). In aerobiosis, any requirement for the ArcAB system is not apparent (Figure 3.2A). Under anaerobic growth, full pIV-dependent Psp induction is largely independent of PspBC and the Arc system compared to microaerobiosis (Figure 3.2A). These differing dependencies on Arc are consistent with the ArcAB system functioning as a microaerobic redox regulator, required under microaerobic but not aerobic or anaerobic conditions (Alexeeva *et al.*, 2003).

Notably, under microaerobic growth conditions, the requirement for ArcB is more pronounced then for ArcA. Importantly, control reactions demonstrate that the different growth conditions *per se* do not affect the activity from the *psp* promoter since *psp* expression in Δ*pspA* cells is similar under aerobic, microaerobic and anaerobic conditions (Figure 3.3B). Further, since the level of *psp* expression in

control strains Δ*pspA*Δ*arcB* ϕ*pspA-lacZ* and Δ*pspA*Δ*arcA* ϕ*pspA-lacZ* are unaffected by ArcB and ArcA, we infer that the Arc proteins may contribute to relieving PspA negative regulation in microaerobiosis (Figure 3.2B). In these strains the OM secretin pIV was used to induce *psp* expression. It is believed that pIV mislocalises to the IM thereby impairing cell membrane integrity and resulting in a *psp*-inducing stress signal similar to PulD (Guilvout *et al.*, 2006). To ascertain that the strains assayed were exposed to equivalent (pIV-induced) levels of "stress", pIV expression was tested and the amount of pIV localised within the IM determined. As shown in Figure 3.2A (inset), pIV expression did not change in the different backgrounds tested or when the cells were grown under differing aeration. Additionally, the distribution of pIV between the IM and OM was similar in microaerobiosis in the WT, *arcA*, *arcB* and *pspBC* deletion backgrounds (Figure 3.3).

A



B

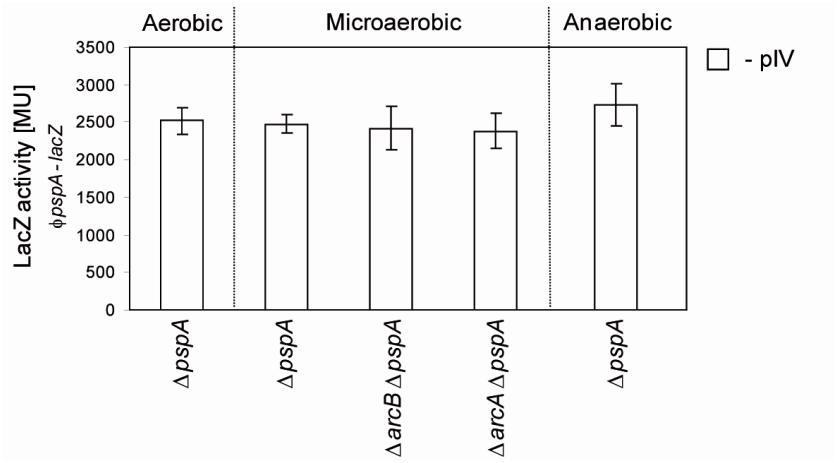


Figure 3.2: **pIV-dependent Psp induction under different growth conditions. (A)** pIV-induced *psp* expression in *E. coli* cells containing ϕ*pspA-lacZ* grown under aerobic, microaerobic or anaerobic conditions as measured using a β-galactosidase assay (see section 2.4.4). WT (wild-type). Insets: Immunoblotting of pIV expression in corresponding cells using pIV-specific antibodies. **(B)** *psp* expression in *E. coli* MG1655 Δ*pspA*, Δ*arcB*Δ*pspA* and Δ*arcA*Δ*pspA* cells containing ϕ*pspA-lacZ* grown under aerobic, microaerobic or anaerobic conditions as measured using β-galactosidase assays.

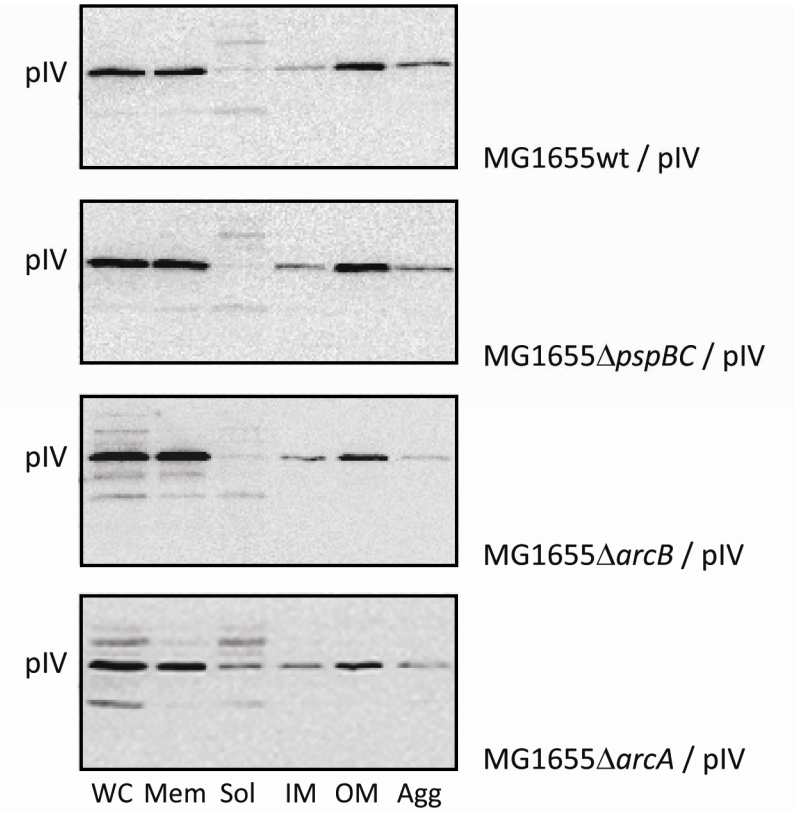
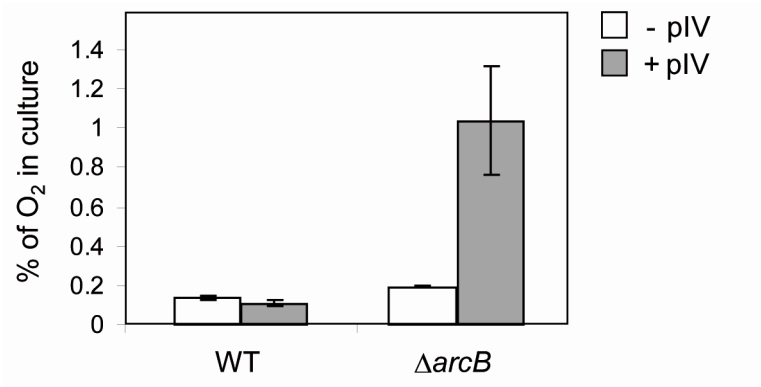


Figure 3.3: Production and localisation of pIV under microaerobic growth. The pIV production and its subcellular localisation under microaerobic conditions are not affected in Δ*pspBC*, Δ*arcB* or Δ*arcA* mutants compared to WT. The bacterial cells expressing pIV were fractionated using a Triton X-100-based extraction method and analysed by immunoblotting using antibodies specific to pIV. WC (whole cell), Mem (Membranes, IM+OM), Sol (soluble fraction; cytoplasmic and periplasmic proteins), IM (inner membrane), OM (outer membrane) and Agg (aggregated) proteins (inclusion bodies).

Since Psp effector proteins (PspA, PspD and PspG) alter expression levels of genes associated with aerobic growth (Jovanovic *et al.*, 2006) and ArcAB regulates the switch from aerobic to anaerobic respiration and fermentation, effects of (i) pIV on oxygen consumption in microaerobiosis (Figure 3.4A) and (ii) other global regulators associated with aerobicity (e.g. FNR or Nar; Figure 3.4B) on Psp induction (chromosomal knock-out of the genes encoding the global regulators analysed in this study was confirmed by PCR; see Appendix D) were tested. The results show that pIV changes oxygen consumption in an ArcB-dependent manner and that amongst the global regulators tested, the Arc system has the greatest effect on *psp* expression, supporting the idea of specific crosstalk between the Psp and ArcAB systems. Taken together, these results indicate a growth condition specific requirement for ArcAB and PspBC proteins in Psp induction. In addition since under anaerobiosis Psp induction is independent of PspBC (positive regulators), the PspAF regulatory complex may (itself) be capable of perceiving a pIV-dependent inducing signal. Importantly, all subsequent experiments reported here were conducted under the microaerobic conditions where the roles of PspBC and ArcAB were most prominent.

A



B

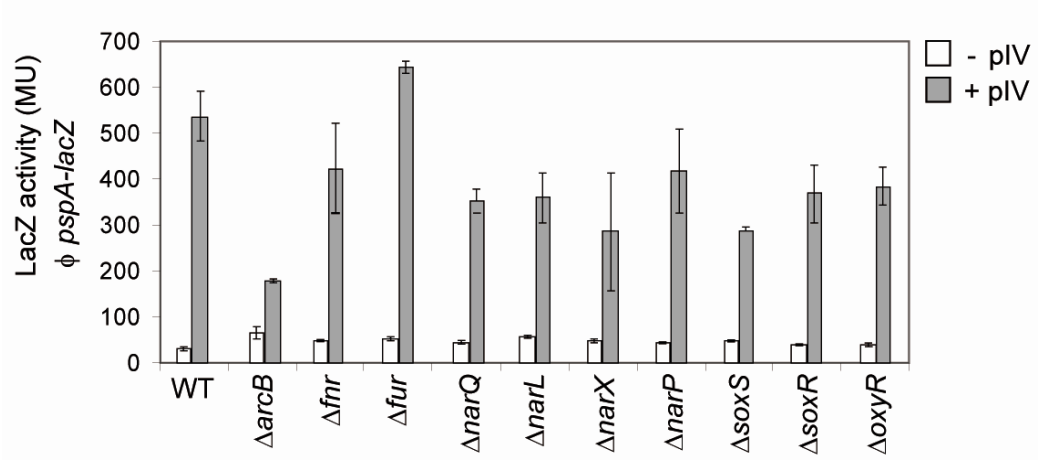


Figure 3.4: Percentage of oxygen in MG1655 (WT) vs. Δ*arcB* and effect of global regulator mutants on Psp induction under microaerobic growth. (A) pIV production causes an increase in oxygen content of a Δ*arcB* culture. Presented is the percentage of oxygen (% O_2) within the bacterial culture which corresponds to the following oxygen concentrations (according to manufacturers guidelines): WT (0.065±0.004 mg/L), WT/pIV (0.056±0.002 mg/L), Δ*arcB* (0.095±0.009 mg/L), Δ*arcB*/pIV (0.418±0.014 mg/L). WT (wild-type). **(B)** *psp* expression in different global regulator mutants grown microaerobically at 37°C was measured using β-galactosidase assays (see section 2.4.4) in cells containing ϕ*pspA-lacZ*.

3.3.2 Activation of ArcA facilitates pIV-dependent induction of Psp

To further assess the roles of ArcAB in pIV-dependent Psp induction in microaerobiosis, mutants of ArcB (Table 3.1) and ArcA were constructed, which: (i) had a constitutively active kinase: $ArcB_{C180A/C241A}$ (termed ArcB*), (ii) disrupted the phosphorelay from ArcB to ArcA: $ArcB_{H292A}$, $ArcB_{H717A}$, $ArcB^{*}_{H292A}$ and $ArcB^{*}_{H717A}$ and (iii) inactivated ArcA (by disrupting phosphorylation and preventing binding to target promoters): $ArcA_{D54A/\Delta HTH}$ (Figure 3.5). WT and mutant forms of ArcB proteins were similarly expressed (Figure 3.6A and data not shown) and appropriately localised within the IM (Figure 3.6B and data not shown).

	Motif(s) Mutation(s)	ArcB Activation[a]	ArcB Const. active[b]	ArcA Activation[c]
$ArcB_{WT}$	Wild-type	+	-	+
$ArcB_{H292A}$	H292A	+	-	-
$ArcB_{H717A}$	H717A	+	-	-
$ArcB^{*}$	C180A, C241A	-	+	+
$ArcB^{*}_{H292A}$	C180A, C241A, H292A	-	+	-
$ArcB^{*}_{H717A}$	C180A, C241A, H717A	-	+	-
$ArcB^{LeuZm}$	L87A, L90A, L94A, M97A	+	+	+
$ArcB^{LeuZm}_{H292A}$	L87A, L90A, L94A, M97A, H292A	+	+	-
$ArcB^{LeuZm}_{H717A}$	L87A, L90A, L94A, M97A, H717A	+	+	-

[a] Kinase "on":, wild type C180 and C241 (apo form); [b] Kinase constitutively "on"; [c] Phosphorelay "on"

Table 3.1: Biochemical phenotypes of *arcB* alleles.

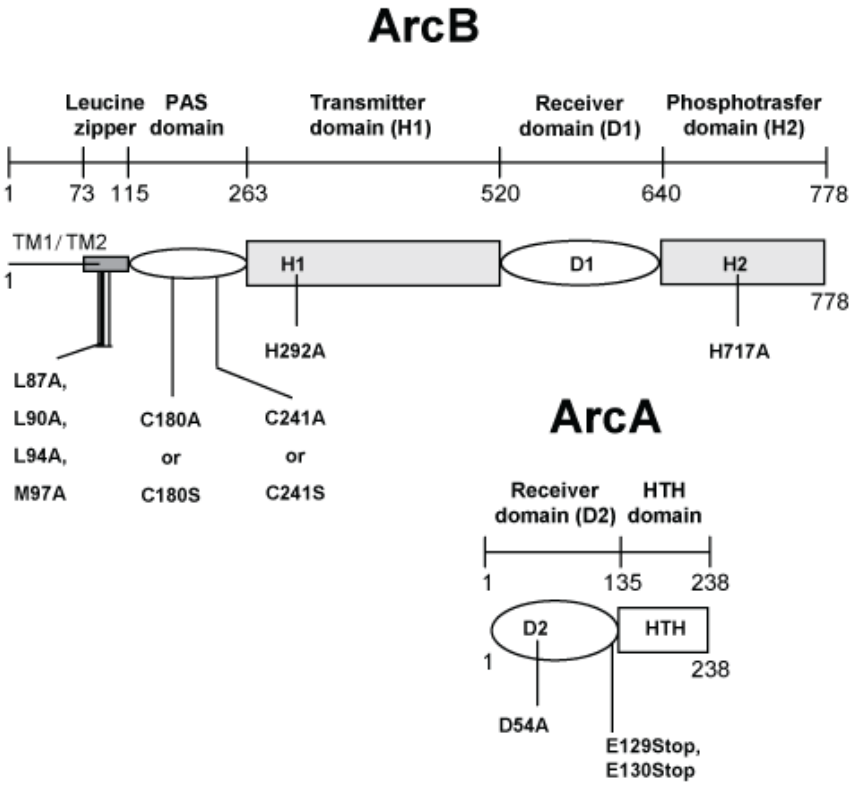


Figure 3.5: Schematic representation of ArcB and ArcA (adapted from Malpica *et al*., 2004) **with the locations of the amino acid substitutions used in this study. ArcB:** *activation mutants* (C180A/S and C241A/S substitutions within the PAS domain); *phosphorelay mutants* (H292A or H717A); *leucine zipper mutant* (LeuZm; L87A, L90A, L94A and M97A). **ArcA:** *a phosphorylation defective mutant* (D54A) and *DNA-binding deficient mutant* (ΔHTH; introduction of two stop codons, E129Stop and E130Stop).

Furthermore, WT and certain mutant ArcB and ArcA proteins (only those with intact phosphorelay systems) were able to activate ArcA-P-dependent *pfl* transcription (Figure 3.7). Subsequently, the ability of Arc mutants to complement Δ*arcB* or Δ*arcA* mutations and support pIV-dependent Psp induction was assayed. As shown in Figure 3.8A, $ArcB_{WT}$ and ArcB* or $ArcA_{WT}$ fully complemented Δ*arcB* or Δ*arcA* mutations respectively for pIV-dependent induction of *psp* expression. None of the phosphorelay mutants in ArcB or the inactive ArcA variant fully supported pIV-dependent induction of *psp* expression (Figure 3.8A), indicating that ArcA-P has a role in promoting pIV-dependent induction. Importantly, control reactions demonstrated that similar levels of pIV secretin were present in all the samples tested (Figure 3.8B). Over-expression of ArcB proteins ($ArcB_{WT}$ and ArcB*) in a Δ*arcAB* strain demonstrates that in the absence of $ArcA_{WT}$ lower levels of pIV-dependent induction of *psp* expression were obtained (similar to the ArcB* phosphorelay mutants) (Figure 3.8A). These data indicate that ArcB has an activity with respect to Psp that is partially ArcA independent. In contrast, over-expression of $ArcA_{WT}$ in the Δ*arcAB* strain led to strong pIV-dependent induction of *psp* (Figure 3.8A), indicating that there are two levels of Arc involvement in *psp* expression, one mediated by ArcB independent of ArcA, and one directed by ArcA.

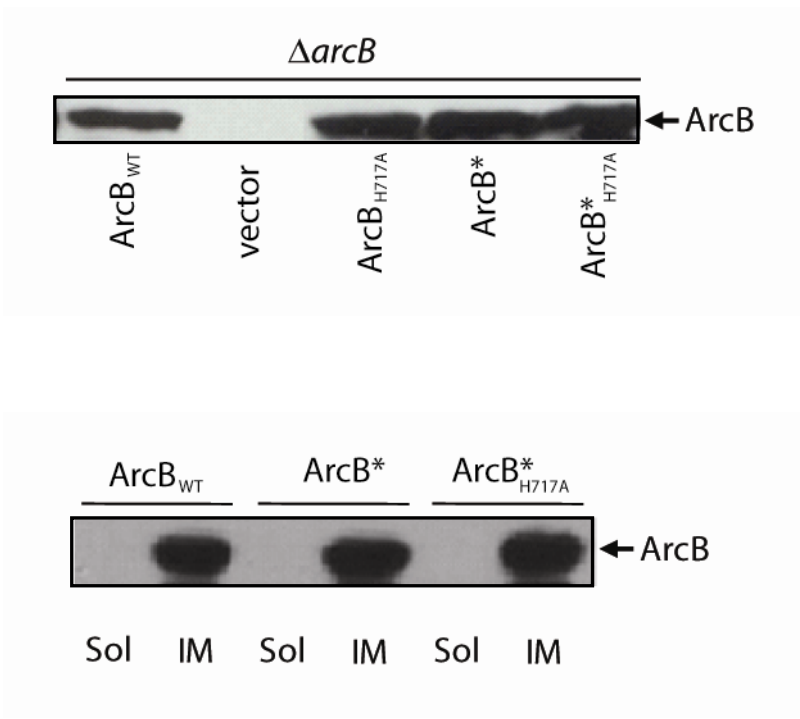


Figure 3.6: Expression and localisation of ArcB$_{WT}$ and ArcB mutants. (A) ArcB or ArcB mutants over-expressed in an Δ*arcB* strain grown microaerobically were detected by immunoblotting (see section 2.4.3) and ArcB-specific antibodies (arrow). **(B)** Triton X-100 fractionated bacterial cells (see section 2.4.6) over-expressing ArcB$_{WT}$ and ArcB mutants (arrow) were analysed by immunoblotting and ArcB-specific antibodies. Sol (soluble fraction; cytoplasmic and periplasmic proteins), IM (inner membrane), OM (outer membrane) and Agg (aggregated) proteins (inclusion bodies). In both cases, protein production was induced by 0.1 mM IPTG for 1h at 37°C prior to analysis.

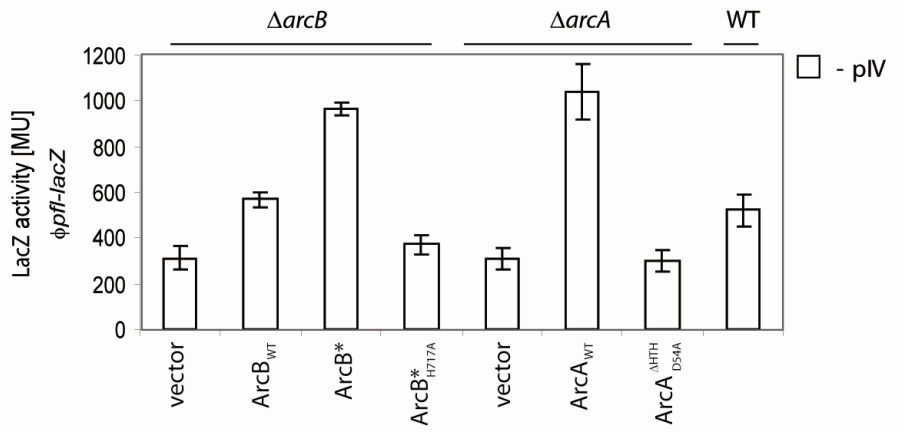


Figure 3.7: Control of ArcA-P activated *pfl* expression by Arc protein variants. Activities of over-expressed Arc proteins were assessed by β-galactosidase assays (see section 2.4.4) in microaerobically grown cells containing the plasmid (pGJ46) borne *pfl-lacZ* transcriptional fusion, ϕ*pfl-lacZ*. WT (wild-type). Protein production was induced by 0.1 mM IPTG for 1h at 37°C prior to analysis.

A

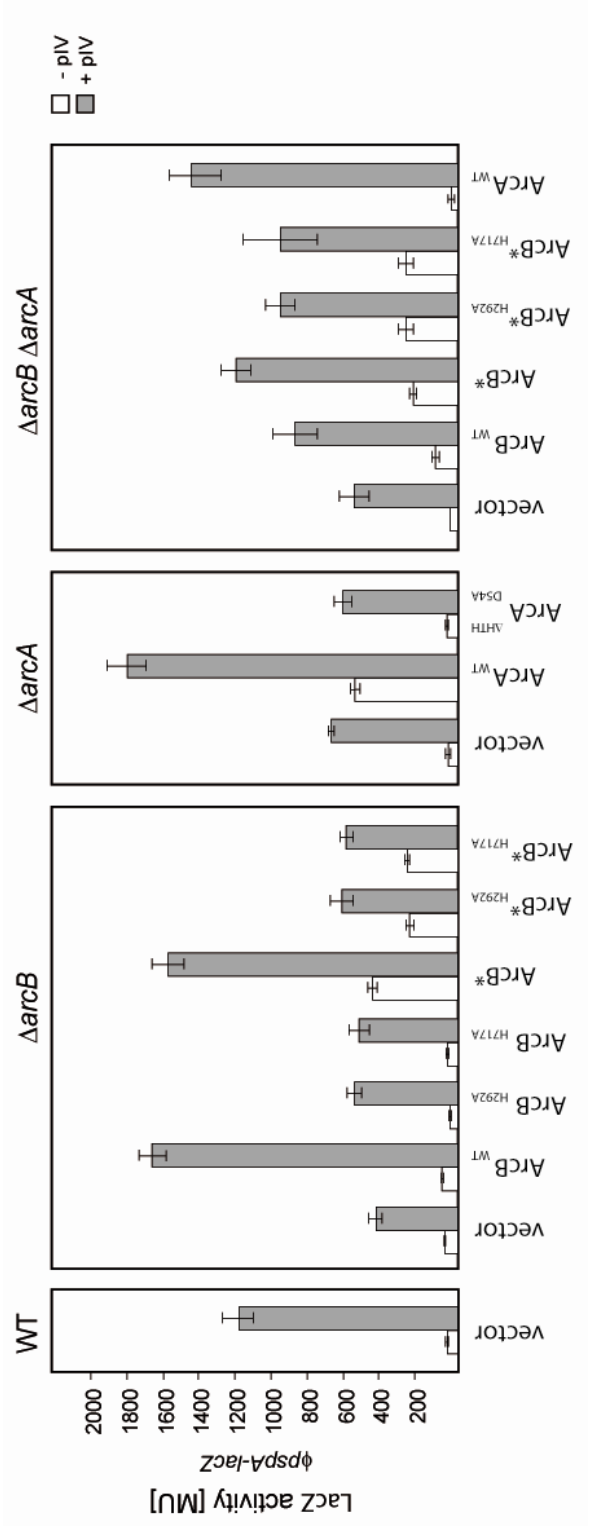


Figure 3.8: Bipartite role of ArcB activation in pIV-dependent Psp induction and production of pIV in cells co-expressing the Arc proteins (Full legend see next page)**.**

B

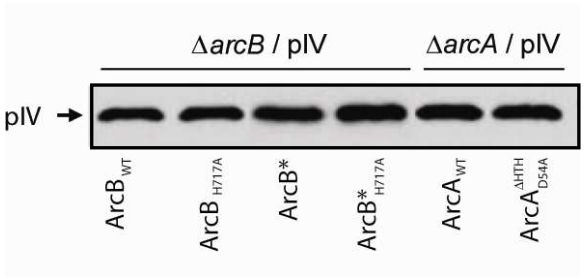


Figure 3.8: Bipartite role of ArcB activation in pIV-dependent Psp induction and production of pIV in cells co-expressing the Arc proteins (continued)**. (A)** Psp induction in Δ*arcB*, Δ*arcA* and a double mutant Δ*arcAB* strains expressing $ArcB_{WT,}$ $ArcA_{WT}$ and their mutants (which where induced by 0.1 mM IPTG for 1h at 37°C prior to analysis) was measured using β-galactosidase assays (see section 2.4.4) under microaerobic conditions in the absence or presence of pIV. WT (wild-type). **(B)** pIV production in microaerobically grown cells co-expressing Arc proteins was detected by immunoblotting with pIV-specific antibodies (see section 2.4.3).

3.3.3 An active form of ArcB promotes low-level induction of Psp *independent of pIV*

In the absence of pIV (-pIV; white bars in Figure 3.8A), over-expression of either $ArcB_{WT}$ or the ArcB phosphorelay mutants ($ArcB_{H292A}$ or $ArcB_{H717A}$) did not significantly induce *psp* expression. However, over-expression of either activated ArcB (ArcB*) or the ArcB* phosphorelay mutants (e.g., $ArcB^*_{H717A}$) were able to induce a low-level of *psp* expression (compared to $ArcB_{WT}$). When ArcB* is over-expressed in the Δ*arcAB* strain, a similar low-level of pIV independent *psp* expression was observed (Figure 3.8A), suggesting that the low-level Psp induction caused by the ArcB* phosphorelay mutants appears to be due to an effect of activated ArcB*, which is completely independent of ArcA or ArcA-P action.

Over-expression of $ArcA_{WT}$ in a Δ*arcA* strain in the absence of pIV results in Psp induction (Figure 3.8A). Notably, this elevation of *psp* expression by over-expression of $ArcA_{WT}$ is ArcB-dependent (compare Δ*arcA* and Δ*arcAB* strains) (Figure 3.8A). However in the presence of pIV, over-expression of $ArcA_{WT}$ in the Δ*arcAB* strain results in strong *psp* expression even in the absence of ArcB (although this activity is probably due to ArcA-P where phosphorylation has occurred by acyl phosphatase). Together with the results implying that low-level Psp induction can occur in an ArcA-independent manner in the presence of the ArcB* phosphorelay mutants, these data again strongly suggest that activation of the Arc system results in two distinct outcomes (one *via* ArcA-P, the other *via* an active form of ArcB) that

generate the Arc-dependencies in the signalling pathway for pIV-dependent Psp induction.

3.3.4 Activation of ArcAB results in decreased electron potential (Δψ)

Next, the electron potential (Δψ) of strains expressing either WT or mutant ArcB or ArcA proteins in the presence and absence of pIV (Figure 3.9) was measured (see section 2.5.6), to address the nature of the signal that is responsible for low-level Psp induction by ArcB* and to potentially discriminate between roles of ArcB* and ArcA-P.

In the absence of a functioning Psp system (i.e. no effectors present, Δ*pspAG;* or no Psp proteins present, Δ*pspF*), a clear decrease in Δψ under pIV stress is observed (Figure 3.9) that appears to be ArcB-dependent (Jovanovic *et al.*, 2006). As shown in Figure 3.9, over-expression of $ArcB_{WT}$, ArcB* or $ArcA_{WT}$ in Δ*pspF*Δ*arcB* or Δ*pspF*Δ*arcA* strains resulted in a clear drop in Δψ under pIV stress conditions. Interestingly, in phosphorelay ArcB and ArcA mutants a drop in Δψ could no longer be observed, suggesting that phosphorylation of ArcA could therefore be a pre-requisite for the pIV-dependent drop in PMF.

Notably, in the absence of pIV, over-expression of ArcB* or $ArcA_{WT}$ (which also results in *psp* expression; Figure 3.9A) was also sufficient to significantly reduce Δψ (Figure 3.9). In contrast, over-expression of $ArcB_{WT}$, ArcB* phosphorelay mutants

(e.g., ArcB*$_{H717A}$) or inactive ArcA (ArcA$_{D54A/\Delta HTH}$) did not reduced $\Delta\psi$ in the absence of stress (Figure 3.9).

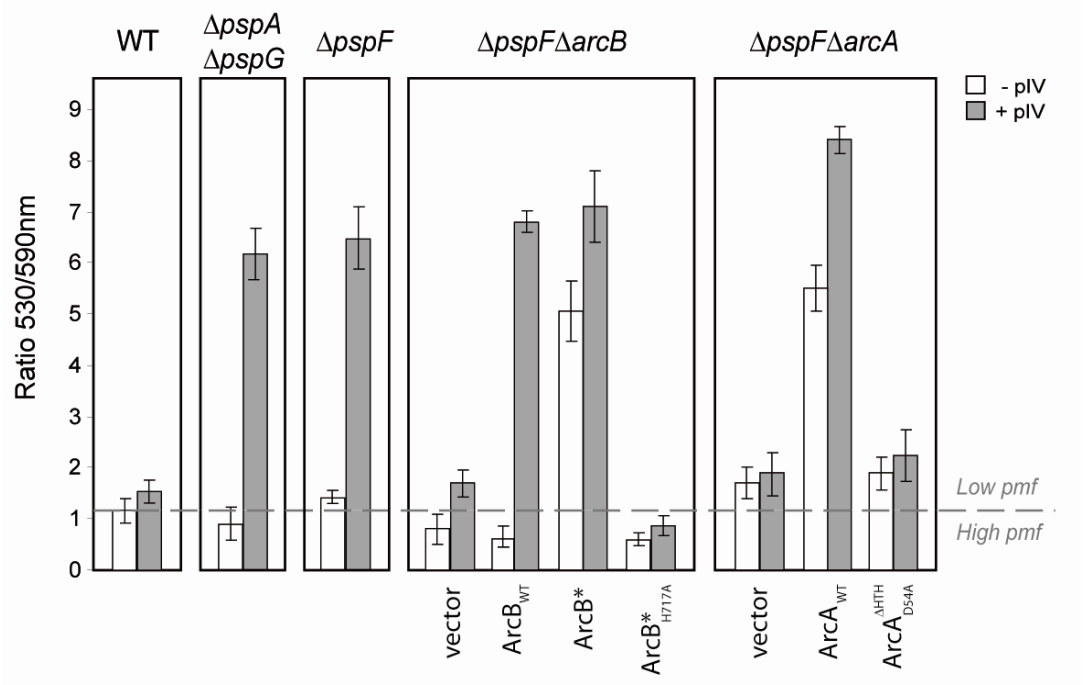


Figure 3.9: Activation of ArcAB reduces the electron potential (Δψ). Cells were grown microaerobically, treated with JC-1 dye (Molecular Probes), and the change in Δψ calculated as the 530/590 nm ratio (see section 2.5.6). $ArcB_{WT}$, $ArcA_{WT}$ and key variants (induced by 0.1 mM IPTG for 1h at 37°C prior to analysis) were expressed in the absence or presence of pIV. An increase in the 530/590 ratio indicates a decrease in Δψ compared to WT (wild-type).

3.3.5 ArcB and PspB interact in vivo

To understand how ArcB*-dependent signalling might be integrated into the PspBC-specific signal transduction pathway, a Cya-based bacterial two-hybrid system (BACTH; see section 2.5.2) was used to study potential Arc-Psp protein-protein interactions *in vivo* (Karimova *et al.*, 1998 & 2005).

$ArcB_{WT}$, ArcB*, PspA, PspB, PspC, and PspF fusion proteins with Cya T18, T18C and T25 fragments were constructed. As a control, the ability of ArcB and ArcB* to self-associate (since ArcB forms dimers; Malpica *et al*., 2006) was analysed. $ArcB_{WT}$ and ArcB* fusion proteins are capable of self-associating (Table 3.2). It was then tested whether $ArcB_{WT}$ or ArcB* could interact with several key members of the Psp regulon (PspA, B, C, F). Additionally, known interactions between PspA-PspF, PspA-PspC and PspB-PspC (Table 3.2) were detected, showing that the fusion proteins used are capable of native interactions (Darwin, 2005). We demonstrated that a clear interaction between either $ArcB_{WT}$ or ArcB* (T25-fused protein) occurs with the C-terminal PspB fusion protein (PspB-T18) (Table 3.2).

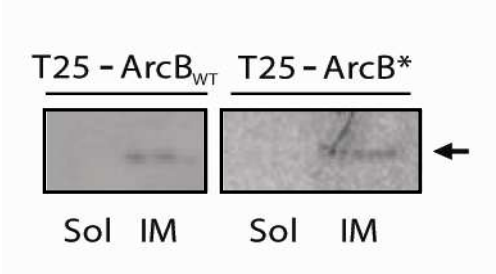
A weak, but detectable, interaction between $ArcB_{WT}$ or ArcB* and N-terminal T18-fusions to either PspA or PspC (Table 3.2), but no interaction between ArcB, ArcB* and PspF was detected (Table 3.2). Since interactions between PspF, PspA, PspB, PspC have previously been established (see section 1.5.4.4.2; Adams *et al.*, 2003; Elderkin *et al*., 2005; Maxson and Darwin, 2006), ArcB (potentially regardless of its state) could interact with members of a Psp[FABC] complex via PspB.

	T25- $ArcB_{WT}$	***T25-*** *ArcB**	***T25-*** $ArcB^{LeuZm}$	***T25-*** *PspC*
T18C- $ArcB_{WT}$	+/-	ND	ND	+/-
T18C- *ArcB**	ND	+	ND	+/-
PspB ***-T18***	++	++	+	++
$PspB^{LeuZm}$ ***-T18***	-	-	-	++
T18C- *PspA*	+/-	+/-	+/-	+
T18C- *PspC*	+/-	+/-	+/-	-
T18C- $ArcB^{LeuZm}$	ND	ND	+/-	+/-
T18C- *PspF*	-	-	-	-

Table 3.2: Interactions of Psp and ArcB proteins *in vivo.* The BACTH system (see section 2.5.2) (Karimova *et al.*, 1998 & 2005) was used to detect the protein-protein interactions between the Psp and ArcB proteins. *Negative control*: BTH101/pKT25+pUT18C vectors alone (74±4 MU); *Positive control:* BTH101/pKT25-zip+pUT18C-zip (1017±34 MU); *Interaction estimates were as follows:* **(+/-)** weak interaction (235-350 MU); **(+)** interaction (350-700 MU); **(++)** strong interaction (>700 MU); **(-)** no interaction (≤234 MU); **(ND)** not determined.

A Triton X-100 based cell fractionation and Western blotting method (see section 2.4.3 and 2.4.6) was used to provide evidence that the interaction between ArcB, ArcB* and PspB occurs in the IM (Figure 3.10). As a control, an N-terminal T18C (T18C-PspB) PspB fusion (where T18C is now embedded in the IM) did not interact with ArcB (data not shown). Using an *in vivo* cross-linking assay (see section 2.5.5), we demonstrate that a higher molecular weight cross-linked "Psp complex" (labelled DSP-specific cross-linked species in Figure 3.11) can be detected with PspB antibodies in a MG1655 WT and Δ*arcA* strain but not in a Δ*arcB* deletion strain (Figure 3.11), providing further evidence that an interaction between ArcB and PspB occurs.

A



B

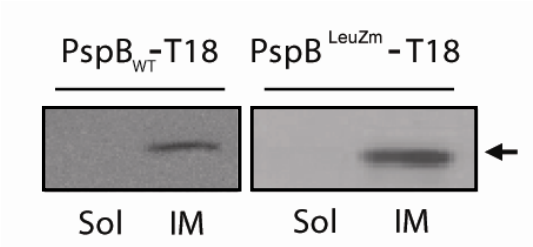


Figure 3.10: Subcellular localisation of ArcB and PspB Cya-fusion proteins. Triton X-100 fractionation (see section 2.4.6) of BTH101 cells followed by immunoblotting shows that the fusion proteins T25-ArcB$_{WT}$, T25-ArcB*, PspB-T18, and PspB^{LeuZm}-T18 localise within the IM (consistent with the subcellular localisation of ArcB and PspB). Cells were grown at 30°C and fusion proteins induced by 0.5 mM IPTG for 1h prior to analysis. **(A)** ArcB fusion proteins (arrow) detected in the IM fraction using Cya T25-specific antibodies. **(B)** PspB fusion proteins (arrow) detected in the IM fraction using PspB-specific antibodies. Sol (soluble fraction; cytoplasmic and periplasmic proteins), IM (inner membrane).

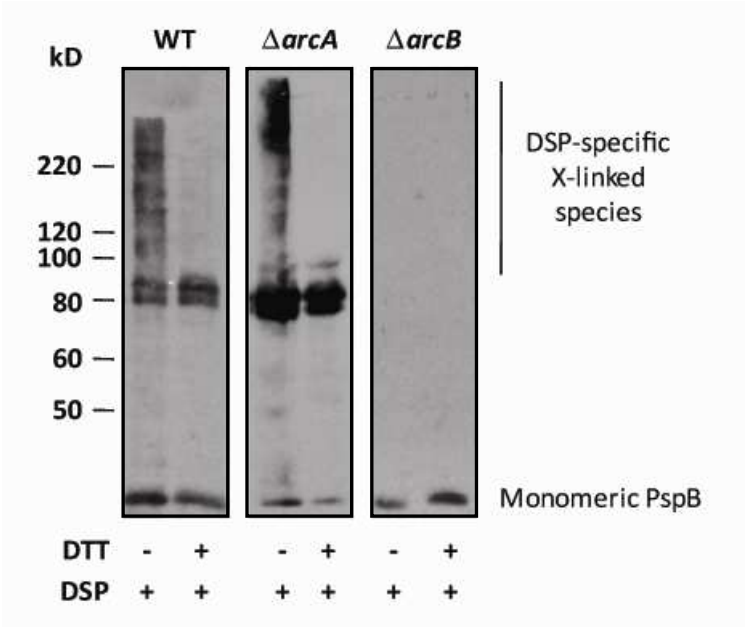


Figure 3.11: *In vivo* cross-linking to test the interaction between PspB and ArcAB. Upon *in vivo* cross-linking (see section 2.5.5), PspB-specific antibodies recognise a higher molecular weight complex (labelled DSP-specific X-linked species) in a WT and Δ*arcA* mutant strain but not in a Δ*arcB* strain.

Since both ArcB and PspB contain putative leucine zipper motifs that are most likely positioned at the IM/cytoplasm interface, the interaction observed between ArcB and PspB may be occurring directly through these sequences. To determine whether this could be the case, the leucine zipper motifs (LeuZm) of both ArcB (ArcB^{LeuZm}; L87A, L90A, L94A, M97A) were mutated and PspB (PspB^{LeuZm}; L10A L15A L18A) and fused these mutants to T25- and -T18 respectively. Importantly, the PspB^{LeuZm}-T18 fusion protein remained localised within the IM (Figure 3.10B), however PspB^{LeuZm} is no longer able to interact with either ArcB$_{WT}$ or ArcB* (Table 3.2). Interestingly, PspB^{LeuZm} retained the ability to interact with PspC (Table 3.2), indicating that the interaction with PspC is not dependent on the leucine zipper sequences. These results support a physical interaction between ArcB and PspB mediated by the PspB leucine zipper motif.

Like PspB^{LeuZm}-T18, the T25-ArcB^{LeuZm} fusion protein remained localised within the IM (data not shown) and importantly retained the ability to activate *pfl* transcription (Figure 3.12), similar to T25-ArcB*. However, T25-ArcB^{LeuZm} showed reduced pIV-independent and pIV-dependent Psp induction compared to T25-ArcB* (Figure 3.12). Interestingly, the ArcB^{LeuZm} mutant was still able to interact with PspB (albeit not as strongly, Table 3.2), implying that the site of PspB interaction on ArcB does not solely require the integrity of the putative ArcB leucine zipper motif. Like ArcB$_{WT}$, ArcB^{LeuZm} self-associates (Table 3.2), suggesting that the ArcB leucine zipper motif does not play a major role in self-association. Finally, ArcB^{LeuZm} retained a very weak interaction with PspA and PspC (Table 3.2), at a similar level to those observed with ArcB$_{WT}$ or ArcB*, suggesting no role for the ArcB leucine zipper in these interactions.

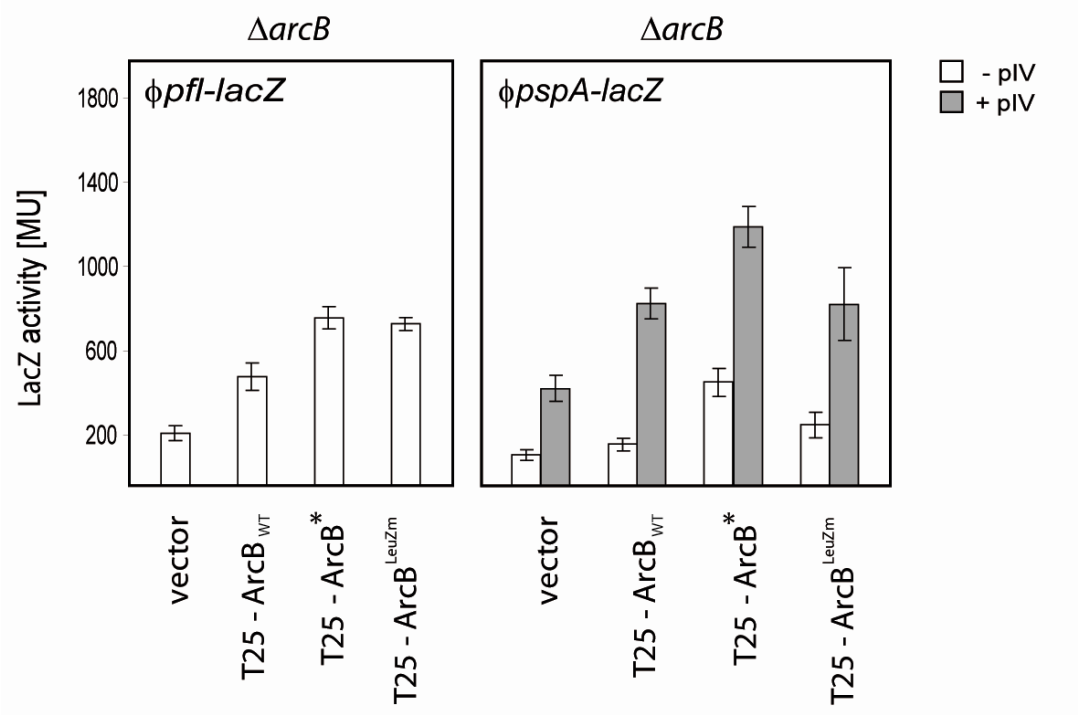


Figure 3.12: Functionalities of T25-ArcB$_{WT}$, T25-ArcB* and T25-ArcB^{LeuZm} fusion proteins. *Left panel:* Activity of over-expressed T25-ArcB$_{WT}$, T25-ArcB* or T25-ArcB^{LeuZm} fusion protein was measured in a Δ*arcB* strain containing the ArcA-P-regulated *pfl-lacZ* transcriptional fusion plasmid, grown microaerobically at 30°C. Expression of the fusion proteins was induced by 0.5 mM IPTG for 1h prior to analysis. *Right panel:* Psp induction of *psp* expression by T25-ArcB$_{WT}$, T25-ArcB* or T25-ArcB^{LeuZm} (either in the absence or presence of pIV) in a Δ*arcB* strain containing the ϕ*pspA-lacZ* transcriptional fusion. For both panels: *pfl* or *psp* expression was measured using β-galactosidase assays (see section 2.4.4).

3.3.6 ArcB^{LeuZm} is in an active kinase form

Since the primary role of the putative LeuZm in ArcB is not in binding to PspB, the role of this sequence was investigated further. Initially, the activity of ArcB^{LeuZm} in a Δ*arcB* strain was tested. In contrast to ArcB$_{WT}$, ArcB^{LeuZm} is able to significantly upregulating activity from the *pfl* promoter (Figure 3.13A) similar to ArcB* (Figure 3.7). Importantly, upregulation of the *pfl* promoter by ArcB^{LeuZm} is dependent on the phosphorelay residues H292 and H717, since ArcB$^{LeuZm}_{H292A}$ and ArcB$^{LeuZm}_{H717A}$ do not show elevated *pfl-lacZ* activities (Figure 3.13A), but are expressed at similar levels (Figure 3.13B).

Over-expression of ArcB^{LeuZm} in a Δ*arcB* strain resulted in elevated *psp* expression in the absence of pIV and full induction in the presence of pIV (Figure 3.13A), similar to ArcB* (Figure 3.8). Consistent with the *pfl-lacZ* findings, phosphorelay in the ArcB^{LeuZm} (Figure 3.13A compare ArcB^{LeuZm} with ArcB$^{LeuZm}_{H292A}$ and ArcB$^{LeuZm}_{H717A}$) appears critically important for pIV-dependent Psp induction, but less so for pIV-independent elevation of *psp* expression. Over-expression of ArcB^{LeuZm} in a Δ*pspF*Δ*arcB* strain (Figure 3.14) complemented the *arcB* mutation and reduced Δψ in the presence and absence of pIV (similar to ArcB*). However as shown in Figure 3.14, over-expression of ArcB$^{LeuZm}_{H717A}$ neither complemented the *arcB* mutation in the presence of pIV, nor reduced Δψ in the absence of pIV, consistent with the inability of ArcB$^{LeuZm}_{H717A}$ to upregulate *pfl* transcription or to stimulate *psp* expression (Figure 3.13A).

A

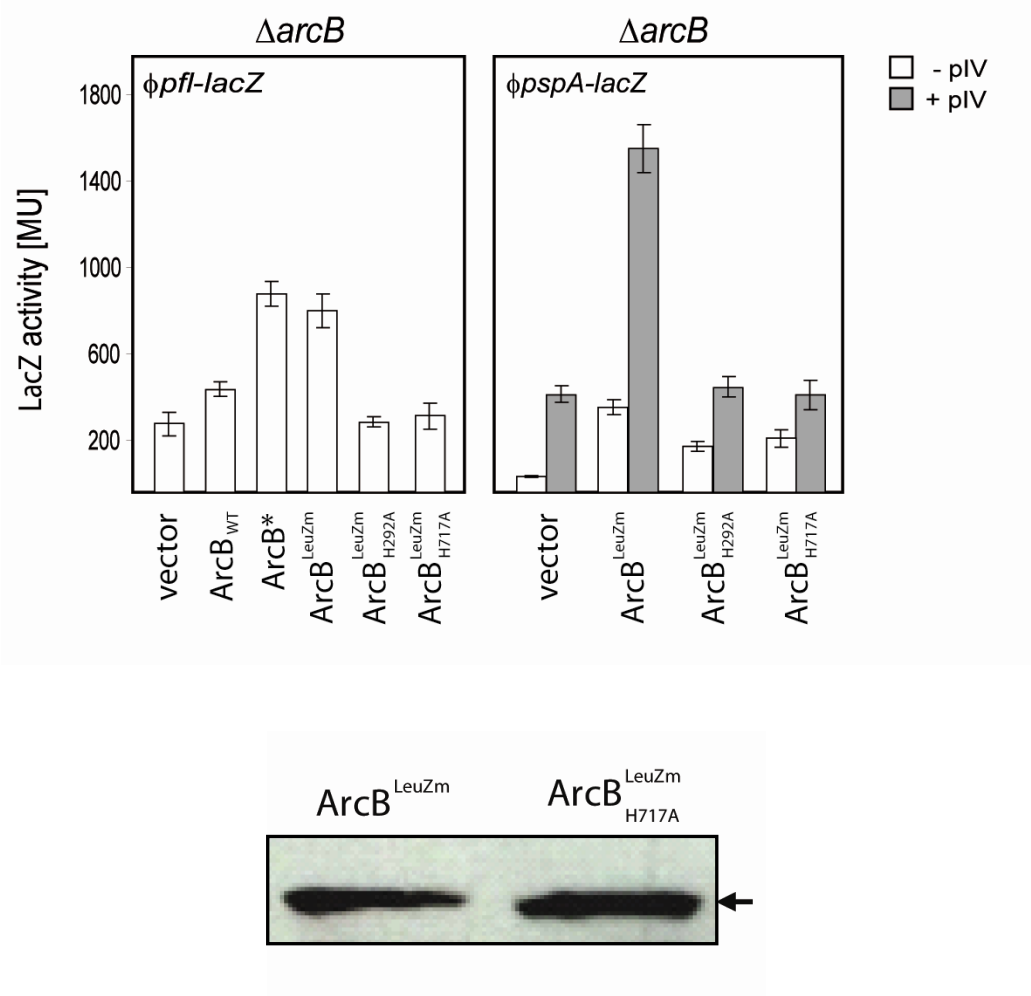


Figure 3.13: Activities and expression of the ArcB^{LeuZm} proteins. (A) ArcB LeuZm has a 'kinase on' activity and supports Psp induction. *Left panel:* Activities of overexpressed ArcB^{LeuZm} and its corresponding phosphorelay mutants were assessed in a Δ*arcB* strain also carrying the ϕ*pfl-lacZ* transcriptional fusion construct grown microaerobically at 37°C. Expression of ArcB and its variants was induced by 0.1 mM IPTG for 1h prior to analysis. *Right panel*: pIV -independent and -dependent Psp induction after complementation of the Δ*arcB* mutation with ArcB^{LeuZm} and its variants. *pfl* or *psp* expression was measured using β-galactosidase assays (see section 2.4.4). **(B)** Expression of ArcB^{LeuZm} and its phosphorelay mutant variant in Δ*arcB* cells grown microaerobically. Arc proteins were over-expressed and detected (arrow) using immunoblotting with ArcB-specific antibodies.

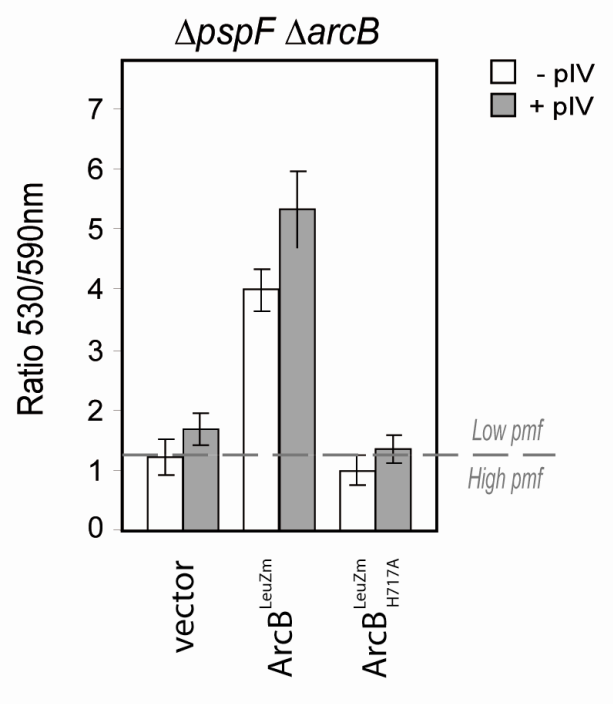


Figure 3.14: ArcB^{LeuZm} reduces the Δψ *of the cell*. *E. coli* Δ*pspF*Δ*arcB* cells expressing ArcB^{LeuZm} and its variants in the presence and absence of pIV were treated with JC-1 dye and changes in Δψ were calculated (see section 2.5.6). An increase in the 530/590 nm ratio indicates a decrease in Δψ compared to Δ*pspF*Δ*arcB* strain containing the vector control. Cells were grown microaerobically at 37°C and protein production induced by 0.1 mM IPTG for 1h prior to analysis.

It seems that ArcB^{LeuZm} resembles ArcB* (the active ArcB form) in the upregulation of *pfl* transcription (compare Figure 3.7 and Figure 3.13A) and Psp induction (compare Figure 3.8, and Figure 3.13A) activities, as well as the effect on $\Delta\psi$ (compare Figure 3.9 and Figure 3.14). Introduction of the H292A or H717A mutations in ArcB^{LeuZm} led to the same reduction in activity seen for ArcB*, demonstrating the importance of an intact phosphorelay system for ArcB^{LeuZm} activity.

3.3.7 PspBC propagates the signal onwards from the Arc system

Since a specific binding interaction between ArcB and PspB is evident, the relationship between ArcB and PspB in the context of a PspBC-specific signal transduction pathway resulting in Psp induction was explored.

In the absence of PspB (Δ*pspB*) neither pIV nor over-expression of ArcB* or ArcA$_{WT}$ significantly induced *psp* expression (Figure 3.14). Over-expression of ArcB* in the presence of pIV in Δ*pspB* cells failed to induce *psp* expression (Figure 3.14). PspB$_{WT}$ but not PspB^{LeuZm} complemented Δ*pspB* for pIV-dependent Psp induction (Figure 3.14), consistent with the inability of PspB^{LeuZm} to interact with ArcB (Table 3.2). Importantly, both PspB$_{WT}$ and PspB^{LeuZm} are stably expressed and localised within the IM (data not shown). Further, in the absence of PspC (Δ*pspC*), Psp induction by pIV and by ArcB* was also abolished (Figure 3.14). The Arc and Psp systems may

therefore be integrated via the PspB leucine zipper motif and as such, ArcB may form part of the PspBC-specific signal transduction pathway.

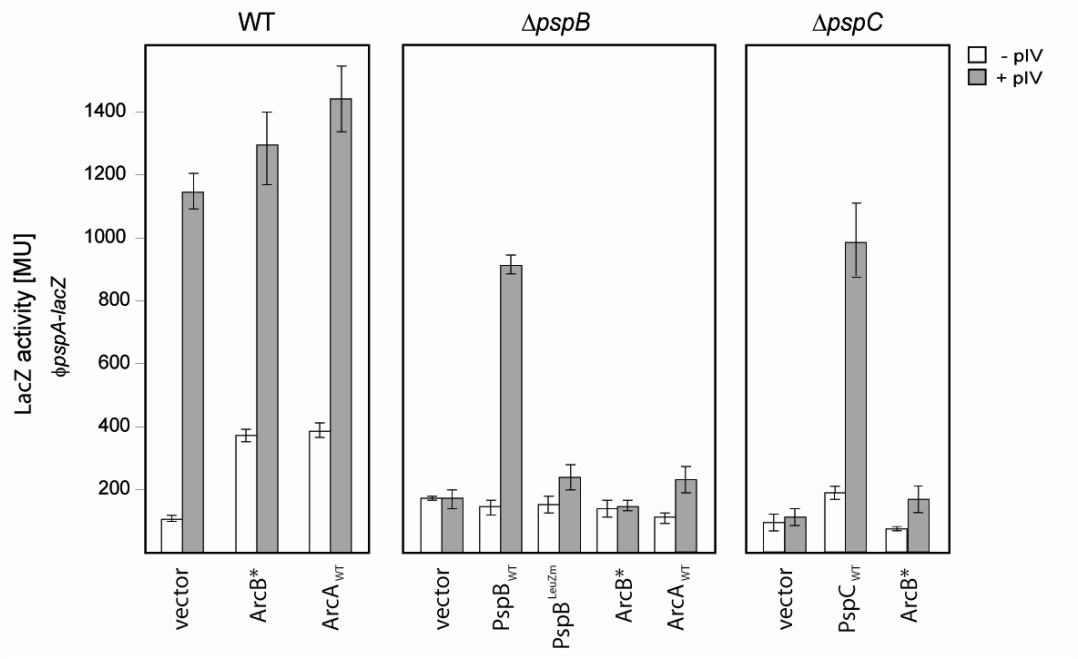


Figure 3.15: Roles of PspB and PspC in transducing the *psp*-inducing signal(s). WT, Δ*pspB* or Δ*pspC* cells containing ϕ*pspA-lacZ* were grown microaerobically at 37°C and the expression of *psp* was measured using β-galactosidase assays (see section 2.4.4). The Δ*pspB* mutation was complemented either with PspB or PspB^{LeuZm}, the Δ*pspC* mutation was complemented by PspC. Production of PspB, PspB^{LeuZm} and PspC was induced by 0.001% arabinose, production of ArcB* and ArcA$_{WT}$ was induced by 0.1 mM IPTG for 1h prior to analysis.

3.4 DISCUSSION

3.4.1 Conditional requirement for Arc activation in pIV-dependent induction of Psp

In this work, several lines of evidence demonstrate that the ArcAB system in microaerobiosis is required to facilitate pIV-dependent Psp induction and may potentially contribute to maintaining PMF (via the Psp response). ArcB activation is clearly important for pIV-dependent Psp induction as is the integrity of the phosphorelay signalling cascade (which results in phosphorylation of ArcA) and ArcA itself. However, the Arc system may not directly control the expression of the *psp* genes, since neither of the 2 *E. coli psp* promoters contain recognisable ArcA binding sites and the absence of Arc proteins does not affect transcription of *psp* genes in Δ*pspA* cells (i.e., in the absence of negative control).

In microaerobiosis, Arc-dependent Psp induction in the presence of pIV correlates with a decrease in $\Delta\psi$ (PMF), which is dependent on both the phosphorelay activity of ArcB and on ArcA itself. Under pIV stress conditions, the Psp response is not able to conserve PMF when the Arc proteins are absent, activation of the ArcAB system may therefore help with generating and/or propagating a pIV-dependent *psp*-inducing signal threshold needed to mount the Psp response. Since the Psp response helps to maintain the cells PMF (and energy status) (see section 1.5.4.2.1) and is implicated in the growth and virulence of enterobacteria (see section 1.5.4.2.2) (Darwin, 2005; Rowley *et al.*, 2006; Darwin, 2007), the crosstalk between

the Arc and Psp systems is of particular physiological relevance given that changes in oxygen availability often prevail e.g. during pathogenesis and during changes in cell density.

The requirement for ArcAB activation in pIV-dependent Psp induction significantly decreases in aerobiosis and anaerobiosis, consistent with the proposed major importance of the ArcAB regulators in microaerobic growth and in managing transitions between aerobic and anaerobic conditions (Alexeeva *et al.*, 2003; Partridge *et al.*, 2007). Conditional use of ArcAB can explain results in which involvement of Arc in Psp-induction was not evident under aerobic growth conditions (Seo *et al.*, 2007).

In anaerobiosis, the more reducing environment in the cytoplasm may decrease the *psp*-inducing signal threshold resulting in increasingly Arc-independent pIV-dependent *psp* expression, consistent with the cellular redox state (as defined by the NADH/NAD ratio) favouring a reducing environment in anaerobiosis *versus* an oxidising environment in aerobiosis (de Graef *et al.*, 1999). In addition under anaerobic conditions, the contribution of UQ to the respiratory chain is significantly lower (and is in fact largely replaced by menaquinone) (Gennis and Stewart, 1996) and so may contribute to a decreased requirement for Arc in pIV-dependent induction of *psp* expression. Hence, Arc-dependent induction of *psp* expression under pIV stress depends on specific growth conditions. Other examples of conditional effects of Arc on certain genes are known (Mika and Hengge, 2005).

3.4.2 ArcB communicates with PspB

Clearly, there are two observable separate actions of the Arc system in pIV-dependent Psp induction. One is related to activation of ArcA (and subsequent expression of ArcA-P target genes) required for full Psp induction under pIV stress. The other action relates to a more direct effect of activated ArcB that promotes low-level Psp induction, where ArcB*, in the absence of pIV, can induce low-level *psp* expression in a Δ*arcA* strain as can ArcB* phosphorelay mutants in Δ*arcB* cells. ArcB interacts with PspB and this interaction is dependent on the integrity of the PspB leucine zipper motif. Further, mutational analysis revealed that the PspB leucine zipper is important for pIV-dependent Psp induction, but not required for direct binding interactions between PspB and PspC, suggesting that PspB may be directly involved in receiving (or transducing) an inducing signal from activated ArcB.

The linker region of ArcB which connects the TM domain with the catalytic domain of ArcB (Figure 3.2 and 3.6) contains a putative leucine zipper motif (conserved leucine residues at positions 73, 80, 87, and 94) and a PAS domain. It has been suggested that Leu87 functions in intra-molecular signal-propagation in ArcB kinase activation (Malpica *et al.*, 2006). The ArcB leucine zipper motif is functionally important in intra-molecular activation of ArcB. The results indicate that the ArcB leucine zipper mutant ($ArcB^{LeuZm}$) is in a constitutive 'kinase on' state, capable of inducing the *pfl* promoter, but not if the phosphorelay residues H292 or H717 are

compromised (e.g., $ArcB^{LeuZm}_{H717A}$). $ArcB^{LeuZm}$ also facilitates pIV-dependent and increases pIV-independent Psp induction. However, Psp induction by $ArcB^{LeuZm}_{H717A}$ (for example) is significantly lower when compared to $ArcB^{*}_{H717A}$. In addition, the $ArcB^{LeuZm}$ mutant exhibits a decreased affinity for PspB, further suggesting that under specific *psp*-inducing conditions, the leucine zipper motifs of both ArcB and PspB are involved in ArcB-PspB communication.

The PAS domain of ArcB may allow ArcB to respond to a number of factors related to changes in e.g. oxygen supply and associated metabolic processes (Malpica *et al.*, 2006). Since ArcB specifically interacts with PspB, in principle this would allow PspB to respond to signals received by ArcB, and *vice versa*. A similar relationship between signalling and control components has been described for other systems (e.g., for PhoP and PmrD) (Kato *et al.*, 2007) where communication often occurs through membrane interactions (Szurmant *et al.*, 2008).

3.4.3 Integration of the Arc system in the PspB/C-specific signalling pathway

In vivo it has been shown that PspB, PspC and PspA and PspA and PspF interactions occur under non-stress conditions (see section 1.5.4.4.2) (Darwin, 2005 & 2007). ArcB and PspB interact, which may correspond to a ArcB-Psp[B/C/A/F] regulatory complex. Stress-induced activation of ArcB may result in conformational changes in either PspB or PspC (or both) and presumably through altered protein-protein interactions releases the PspA-imposed negative regulation of PspF.

The precise nature of the signal(s) that induces *psp* expression remains to be determined. It is possible that under stress conditions, besides changes in the integrity of the IM and/or $\Delta\psi$ (PMF) (see section 1.5.4.1), the redox state of respiratory chain components specifically quinones, may also contribute to Arc-dependent Psp induction. One possibility is that alongside Arc-independent signalling, *psp*-inducing stimuli reduce quinones and, following an increased diffusion of H^+ ions into the cytosol, consequently dissipates PMF, which may then activate ArcB. This view is supported by the observation that both UQ and ArcAB are required to detect a drop in $\Delta\psi$ in the presence of pIV (Jovanovic *et al.*, 2006; this study). Notably, Psp induction and a significant down-regulation of aerobic respiration and PMF occur simultaneously in cells undergoing contact-dependent growth inhibition (Aoki *et al.*, 2009).

In microaerobiosis, activation of the Arc system greatly facilitates pIV-dependent Psp induction in a PspBC-dependent manner. However, since part of the induction process is Arc-independent but still PspBC-dependent (Figure 3.3A) it seems likely that one (or both) of the *psp* encoded sensors (PspB and or PspC) can receive a signal. Therefore, a "double check point" potentially exists to regulate pIV-dependent Psp induction. This arrangement of sensors would help the Psp system maintain specificity to stimuli, as described for unorthodox two-component systems which maintain their robustness to noises (Kim and Cho, 2006).

3.4.4 PspA-PspF is a minimal Psp system

This study clearly shows that in anaerobiosis, pIV-dependent Psp induction is PspBC-independent, consistent with the observation that some *psp*-inducing stimuli are PspBC-independent (e.g., extreme heat shock, CCCP) or only partially PspBC-dependent (ethanol treatment and hyperosmotic shock) (Model *et al*., 1997; Darwin, 2005; Jovanovic *et al.*, 2006). These results strongly suggest that either PspA (and/or PspF) can (i) directly receive the inducing signal and relieve the PspA-imposed negative regulation or (ii) that other factors substitute for PspBC and ArcAB. That a minimal PspAF system is capable of responding to extracytoplasmic stimulus is consistent with a high degree of PspAF co-conservation found via an *in silico* analysis across 129 bacterial species (Huvet *et al.*, 2009) and with a regulated PspA stress response in Gram-positive bacteria and archebacteria where PspBC are absent (Darwin, 2005; Bidle *et al.*, 2008; Vrancken *et al.*, 2008). PspA homologues are found amongst Gram-positive bacteria, cyanobacteria, archea and higher plants

(see section 1.5.4.3) (Darwin, 2005; Bidle *et al.*, 2008; Vrancken *et al.*, 2008). In all these organisms, PspA homologues often respond to stress conditions similar to those described for inducing the Psp response in a partially PspBC-dependent or -independent manner in enterobacteria (e.g., extreme heat shock, ethanol treatment, hyperosmotic shock, CCCP).

CHAPTER 4

CORRELATIONS BETWEEN QUINONE POOLS AND INDUCTION OF PSP

4.1 INTRODUCTION AND RECAP

Despite detailed *in vitro* data regarding the mechanism of transcriptional regulation of the Psp response (Buck *et al.*, 2000; Darwin, 2005 & 2007; Joly, *et al.*, 2009) vital information explaining its onset *in vivo* still remains elusive. The results from Chapter 3 show a direct cross-talk, via protein-protein interactions, between the ArcAB and Psp systems. Moreover, these results further elaborate previous findings on the involvement of ArcB in the signalling cascade to Psp (Jovanovic *et al.*, 2006). In microaerobiosis, activation of ArcB and the subsequent phosphorelay to its response regulator ArcA are factors that influence expression of the *psp* genes (Jovanovic *et al.*, 2006 & 2009). The ArcAB system consequently appears to be important for the amplification of one Psp-inducing signal. Although the nature of the primary signal for the induction is still unknown, the findings imply that it may be sensed by the ArcB sensor kinase. It has been shown that the kinase activity of ArcB is regulated through the redox state of the quinones (Georgellis *et al.,* 2001; Malpica *et al.*, 2004; Bekker *et al.*, 2009). The quinone pool may therefore be a component of the Psp signalling cascade acting upstream of ArcB. The reduced Psp expression in cells deleted for *ubiG*, part of the ubiquinone-biosynthesis pathway (Figure 4.1), lends some support to this idea (Jovanovic *et al.*, 2006).

Quinones – ubiquinones (UQ), menaquinones (MK) and demethyl-menaquinones (DMK) are part of the electron transport chain, where they act as electron carriers by accepting electrons from dehydrogenases and transferring electrons onto terminal reductases (see section 1.2.3.2). Quinones cycle between their reduced and oxidised forms thereby creating a defined quinone pool (reduced

/ oxidised). Which quinone is used as an electron carrier and what its redox state is, depends on the level of aeration of the cell. Under aerobic growth conditions, ubiquinone is the main electron carrier and hence its concentration is 4-5 fold increased in comparison to the menaquinones. In contrast, anaerobic respiration mainly relies on menaquinones as electron carriers and hence anaerobically grown cells produce about 3 times more menaquinones than ubiquinone (Wallace and Young, 1977; Wissenbach *et al.*, 1992).

Ubiquinone is reduced (to ubiquinol) by the NADH dehydrogenases NDH-1 and NDH-2 (Figure 4.2). Ubiquinol then transfers the electrons to the oxidases Cyt *bd*-I, Cyt *bo* and Cyt *bd*-II, which ultimately pass them onto O_2 to create H_2O (Figure 4.2). The dehydrogenases and oxidases each differ in their capacity to reduce or oxidise the ubiquinones. The redox state of the ubiquinone pool therefore is a result of the combined activity of these enzymes.

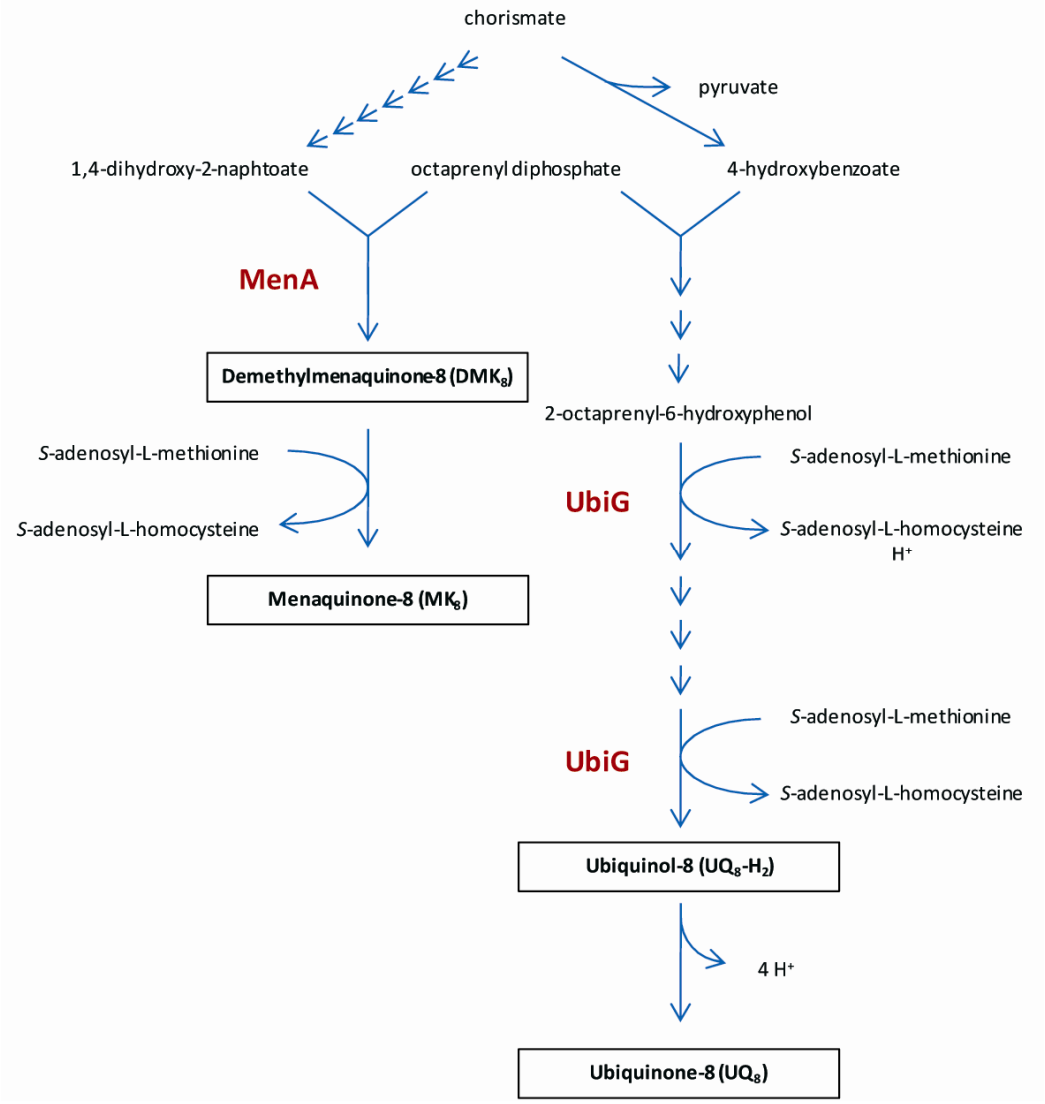


Figure 4.1: The menaquinone and ubiquinone biosynthetic pathway. Both, menaquinones (DMK_8 and MK_8) and ubiquinones (UQ_8-H_2 and UQ_8) are derived from the same precursors, chorismate and octaprenyl diphosphate. The reactions catalysed by MenA and UbiG are shown. Deletion of MenA and UbiG results in the loss of menaquinones and ubiquinones, respectively.

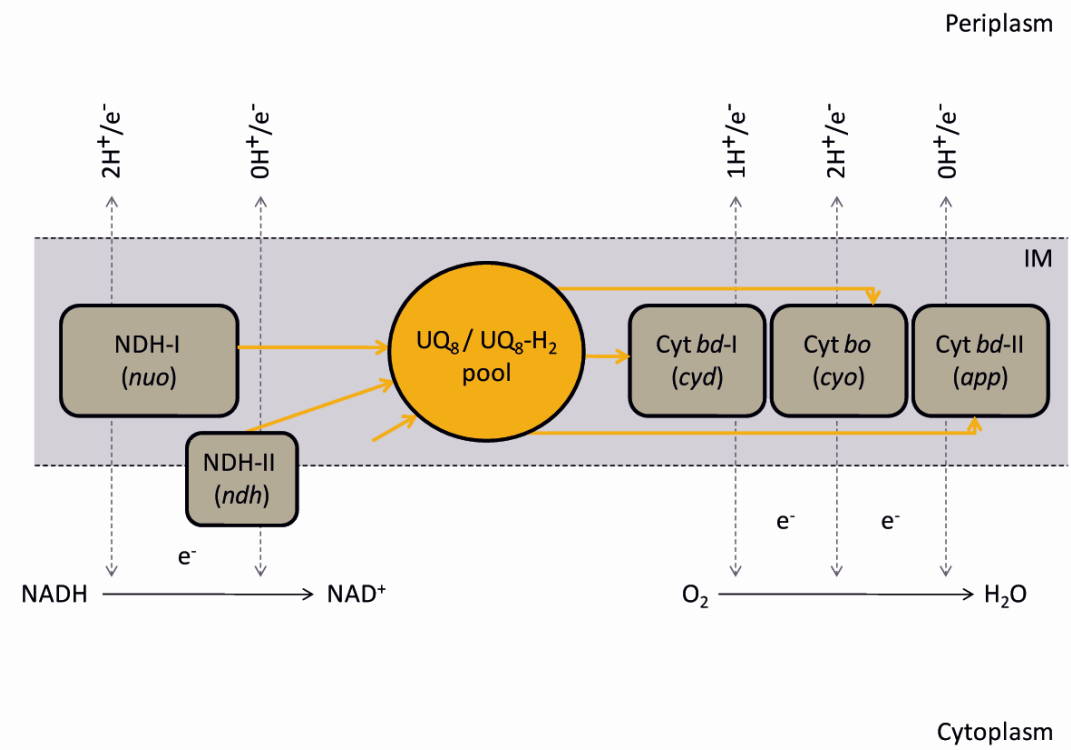


Figure 4.2: Ubiquinones play a central role as electron carrier in the electron transport chain under aerobic and also microaerobic growth. Shown are the UQ_8 reducing dehydrogenases NDH-I and NDH-II as well as the UQ_8-H_2 oxidising cytochrome oxidases Cyt *bd*-I, Cyt *bo* and Cyt *bd*-II. UQ_8 and UQ_8-H_2 cycle between their reduced and oxidised forms thereby creating a defined quinone pool (reduced / oxidised; orange).

4.2 OBJECTIVES

The present study aimed to investigate a potential correlation between the cellular quinone pool and the induction of the Psp response (under aerobic and/or microaerobic growth conditions), therby finding evidence whether changes in the quinone pool are part of the signalling cascade to Psp acting upstream of ArcB.

The main objectives for this work were to:

1) Analyse the quinone content in a set of electron transport mutants (proposed to show differences in their quinone pool; Edwards *et al.*, 2006)

2) Measure the level of Psp induction in the above mutants and correlate this with their variations in the quinone pool

3) Determine whether a similar correlation between the quinone pool and Psp induction is found in cells with intact electron transport chain but containing the well established Psp inducer pIV (see section 1.5.4.1)

3) Assess whether PMF dissipation is sufficient to induce Psp

4.3 RESULTS

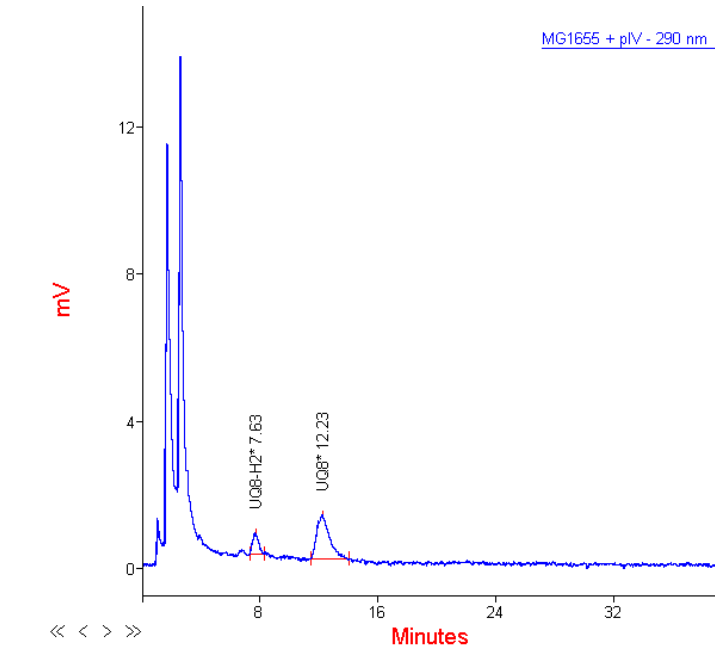
4.3.1 The electron transport mutants differ in their ubiquinone content under both, aerobic and microaerobic growth

In order to explore whether changes in the quinone pool might affect Psp expression the quinone content was determined and the level of Psp induction measured in *E. coli* RP437 variants, which contained binary deletions of either NDH-1 or NDH-2 and Cyt *bd*-I or Cyt *bo* (Edwards *et al.*, 2006). It was reasoned that the quinone pool of these electron transport mutants may differ (with respect to each other), thereby enabling any correlation between the quinones and Psp induction to be addressed.

To analyse the quinone content, all strains tested were treated as described by Bekker *et al.* (2007) (see section 2.4.5). Briefly, the cells were grown either aerobically or microaerobically, rapidly quenched with ice-cold methanol, the total quinones extracted using petroleoum ether (40-60°C) and analysed using HPLC (see Appendix F). Quinones were detected using UV/Vis spectroscopy at a 290 nm wavelength and identified by comparison to their previously established elution times (Bekker *et al.*, 2007) - reduced ubiquinol (UQ_8-H_2) eluting after 8 minutes, oxidised ubiquinone (UQ_8) after 12.5 minutes, demethylmenaquinone (DMK_8) after 18 minutes and menaquinone (MK_8) after 21 minutes (both detected at 248 nm). The amount of ubiquinones (oxidised and reduced) were calculated by measuring

the area below the UQ_8 and UQ_8-H_2 peak, where 1 AU of the area corresponds to 0.0122 nmol of quinone (derived using defined concentrations of ubiquinone-10 as references; Figure 4.3).

In line with previous reports (Wallace and Young, 1977; Unden, 1988; Wissenbach *et al.*, 1992; Soballe and Poole, 1999) MK_8 and DMK_8 production could be detected under microaerobic growth conditions (see Apendix F); however under aerobic growth only the ubiquinones were observed. Furthermore, the electron transport mutants all showed variations in their ubiquinone pools compared to the WT RP437 ($RP437_{WT}$) strain (Figure 4.4). Based on this observation, a comparison of BT3402, BT3406 and BT3408 was judged to be useful in the analysis of a potential correlation between changes in the quinone pool and the induction of the Psp response.



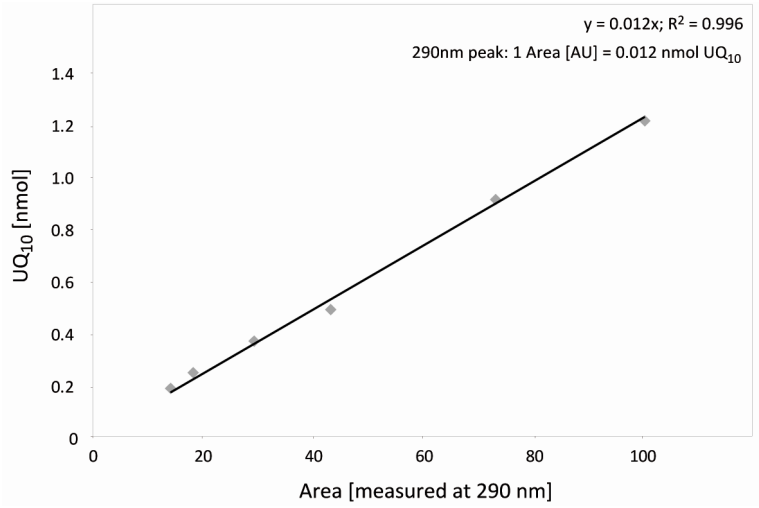


Figure 4.3: A typical HPLC trace of the quinone measurements (here: MG1655 + pIV at aerobic growth; for complete data set see Appendix F) **and standard curve used to calculate the amount of ubiquinone.** Defined concentrations of UQ_{10} were used as reference points to calculate the amount of ubiquinone. 1 area unit [AU] of the peak at 290 nm corresponds to 0.012 nmol UQ_{10}.

4.3.2 Under microaerobic growth, the level of Psp induction in the electron transport mutants correlates with changes in the ubiquinone pool

After establishing that the electron transport mutants BT3402, BT3406 and BT3408 differ in their ubiquinone content (Figure 4.4), a ϕ*pspA-lacZ* reporter fusion was introduced into the chromosome of each mutant and the parental $RP437_{WT}$ strain. The activity of the *pspA* promoter, under aerobic and microaerobic growth conditions, was then measured using β-galactosidase assays (see section 2.4.4; Figure 4.4).

All 3 electron transport mutants maintain the ability to activate the Psp response under both aerobic and microaerobic growth, however the levels of induction are markedly different. The *pspA* promoter is most active in the BT3406 strain, with an 8-fold increase of LacZ activity compared to RP437 under aerobic growth and an 18-fold increase under microaerobic growth. In contrast, Psp induction in the BT3408 strain is 2-fold increased under aerobic and 6-fold under microaerobic growth in comparison to RP437. BT3402 shows the lowest level of Psp induction compared to RP437 with a 2-fold increase under aerobic and a 4-fold increase under microaerobic growth (Figure 4.4).

The amount of oxidised UQ_8 and reduced UQ_8-H_2 forms was simultaneously measured with *pspA-lacZ* under either aerobic and microaerobic growth and the redox state of the ubiquinones (% UQ_8-H_2) was determined. Under aerobic

conditions (Figure 4.4), a correlation between Psp induction and ubiquinones is evident for the reduced form, UQ_8-H_2, the higher the amount of UQ_8-H_2, the higher the level of Psp induction. Accordingly, Psp induction also correlated with a shift in the redox state of the ubiquinones towards being more reduced (Figure 4.4) (although this effect is somewhat masked by the large standard deviations). Under microaerobic growth, Psp induction appeared to be inversely proportional to the amount of oxidised UQ_8 (Figure 4.4), the lower the amount of UQ_8 the higher the level of Psp induction (for example the BT3406 strain contained the lowest amount of UQ_8 molecules, but exhibited the highest level of activity from the *pspA* promoter). Under these growth conditions, the reduced form of ubiquinone (UQ_8-H_2) appeared to have little effect on the level of Psp induction. Similar to the aerobic growth results, under microaerobiosis Psp induction correlated with a shift towards a more reduced redox state of the ubiquinones. Furthermore, this correlation was more pronounced under microaerobic than under aerobic growth (Figure 4.4).

The redox state of the ubiquinones is generally (in all strains tested) shifted towards a more reduced state under microaerobic growth (Figure 4.4), consistent with the changed respiration mode under such conditions compared to full aerobiosis (see section 1.2.3.2). Additionally, when cells were grown microaerobically, both demethylmenaquinone (DMK_8) and menaquinone (MK_8) could be measured at 18 and 21 minutes elution time in agreement with previous results (Bekker *et al.*, 2007) (Figure 4.3A). This observation is fully in line with the role of DMK_8 and MK_8 as the main electron carriers of the electron transport chain under conditions with low aeration (Unden, 1988; Wissenbach et al., 1992). Together with the observed redox

states, these results indicate that the quinone measurements generated in this study appear to be faithfully representative of the metabolic and respiratory state of the cell.

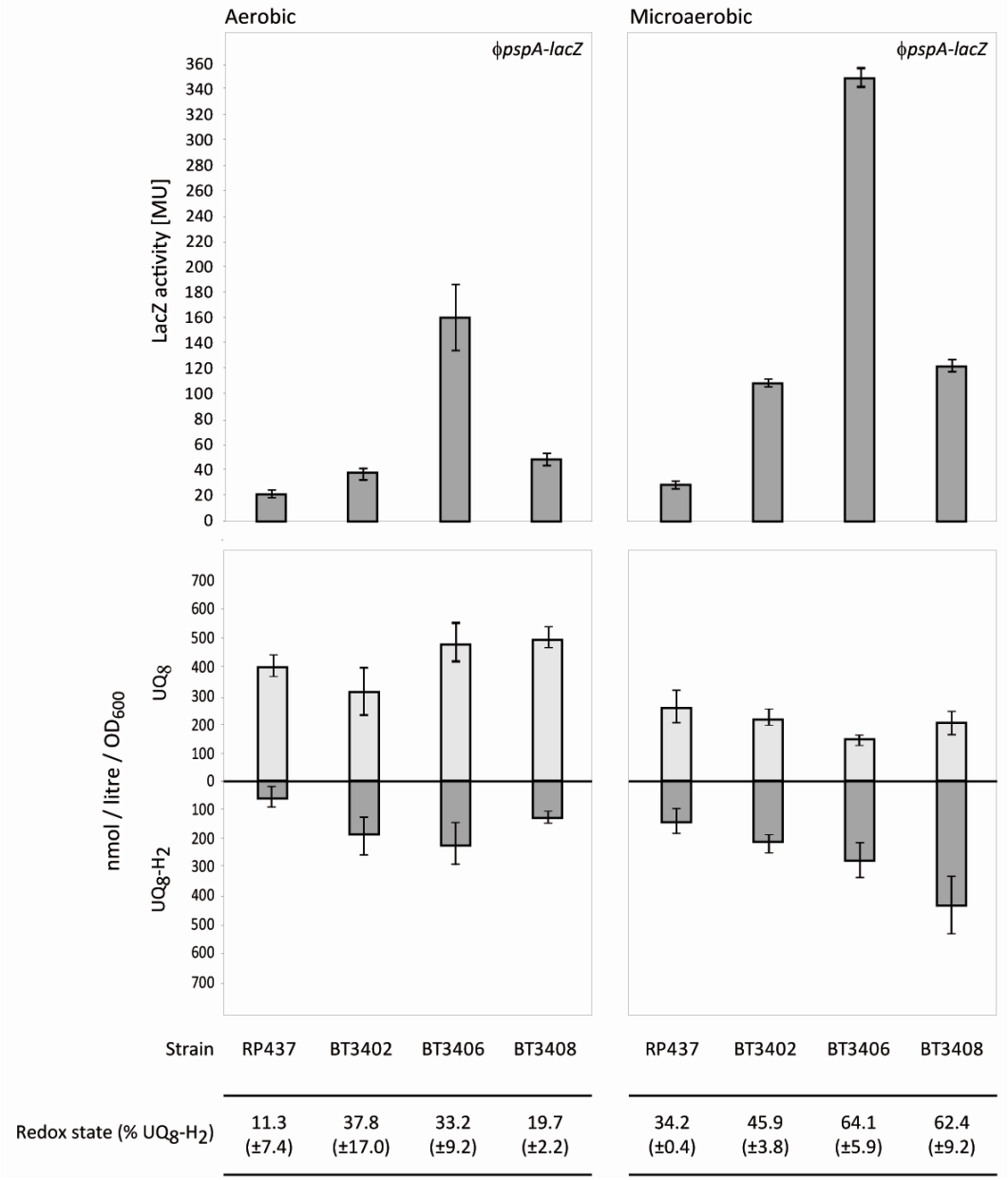


Figure 4.4: Psp induction and ubiquinones in the electron transport mutants. Comparison of **(Top)** the level of Psp induction and **(Bottom)** the amount of oxidised (UQ_8; light grey) and reduced (UQ_8-H_2; dark grey) ubiquinone as well as the redox state (% UQ_8-H_2) in WT RP437 and the electron transport mutants BT3402, BT3406 and BT3408. Cells were grown aerobically or microaerobically at 37°C until mid-log phase. Values for the standard deviation are included.

4.3.3 DMK_8 and MK_8 are not required to mount the Psp response

DMK_8 and MK_8 were both observed under microaerobic growth, a condition where ArcB is required to activate *psp* transcription (Jovanovic *et al*., 2009). The kinase activity of ArcB is stimulated by the ubiquinone analogue UQ_0 and is also responsive to menadione, an analogue of menaquinone (Georgellis *et al*., 2001). In line with this, Bekker *et al.* (2009) showed recently that ArcAB is regulated by the redox state of both, the ubi- and the menaquinone pool. It is therefore conceivable that DMK_8 and MK_8 may play a role in Psp induction under such conditions. Hence, the ability to induce Psp was analysed in *E. coli* MG1655 cells deleted for *menA*. MenA functions in the menaquinone-biosynthesis pathway (Figure 4.1) and catalyses the formation of DMK_8 by 1,4-dihydroxy-2-naphtoate and octaprenylpyrophosphate. MK_8 is the result of the subsequent methylation of DMK_8. Cells lacking *menA* therefore lack DMK_8 and MK_8. Notably, *E. coli* MG1655 Δ*menA* cells maintained the ability to mount the Psp response to pIV secretin stress under anaerobic, microaerobic and aerobic growth. It therefore seems unlikely that either DMK_8 or MK_8 are required for Psp induction (Figure 4.5) - assuming no alternative route to menaquinone synthesis is operating.

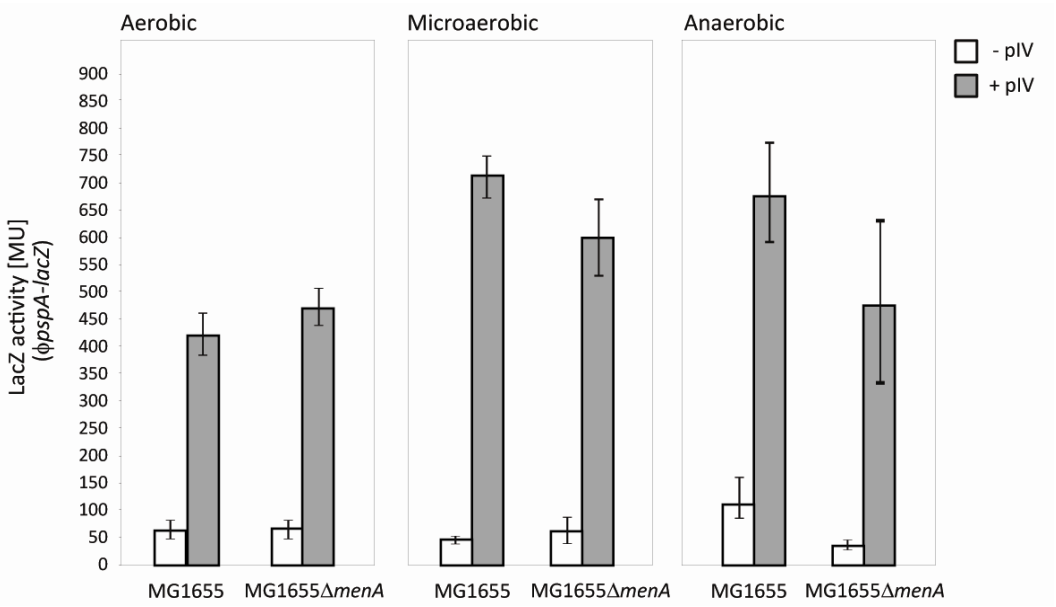


Figure 4.5: Psp induction in strains deleted for *menA*. The ability of pIV-dependent Psp induction in strains deleted for *menA*, hence lacking both DMK_8 and MK_8, has been assessed under aerobic, microaerobic and anaerobic growth using β-galactosidase assays (see section 2.4.4). Cells were grown at 37°C until mid-log phase. The lack of MenA appears to have no effect on Psp induction under the growth conditions tested. White bars: pIV absent; Grey bars: pIV present. Values for the standard deviation are included

4.3.4 Production of the pIV-secretin affects the redox state of the ubiquinone pool

The above data suggest that changes in the ubiquinone pool (here a consequence of mutations in the electron transport chain) may cause induction of the Psp response. To further explore this it was determined, in cells where the electron transport chain remains intact, whether the presence of the Psp inducing stress agent, pIV-secretin (see section 1.5.4.1), might also influence the ubiquinones (Figure 4.6). The results clearly show that under aerobic and microaerobic growth pIV influences the ubiquinone pool of the cell. The effects of pIV are much more pronounced under microaerobic growth akin to the electron transport mutants. In cells where pIV is produced UQ_8 is slightly decreased under aerobic and increased under microaerobic growth. In contrast, UQ_8-H_2 is consistently decreased in the presence of pIV under aerobic and microaerobic growth. Accordingly, the redox state of the ubiquinones is shifted towards more oxidised (with the total percentage of the reduced form UQ_8-H_2 being almost halved under microaerobic growth when pIV is present). Intriguingly, this appears to be purely an effect of pIV and independent of the activity of the Psp response (compare WT MG1655 cells with those lacking the ability to activate the Psp response, MG1655Δ*pspF*) (Figure 4.6), suggesting the Psp response does not act to counter effects of pIV on ubiquinones.

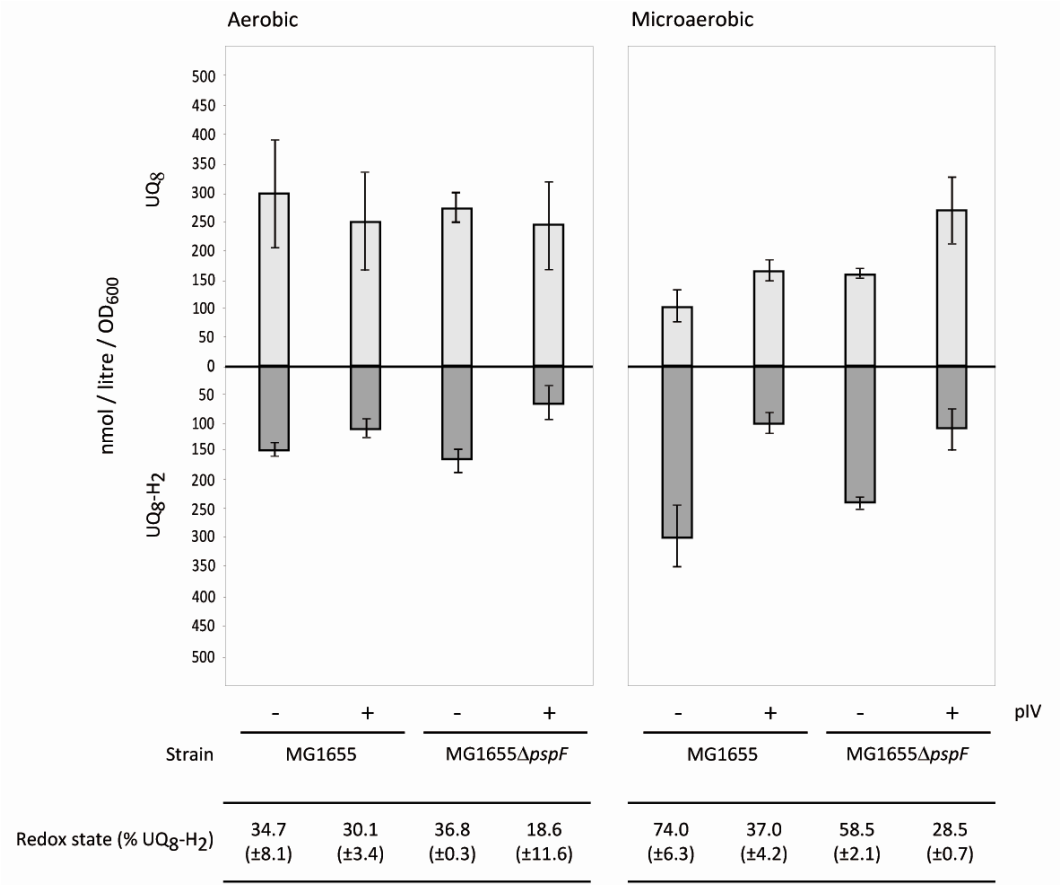


Figure 4.6: Ubiquinones in MG1655 and MG1655Δ*pspF* in absence (-) and presence (+) of pIV. Shown is the effect of pIV production on the amount of oxidised (UQ_8; light grey) and reduced (UQ_8-H_2; dark grey) ubiquinone as well as the redox state (% UQ_8-H_2) in WT MG1655 cells (with the ability to mount the Psp response) and in MG1655Δ*pspF* cells (lacking the PspF transcriptional activator, hence unable to mount the Psp response; see section 1.5.4.4.2). Cells were grown aerobically or microaerobically at 37°C until mid-log phase. Values for the standard deviation are included.

pIV is an OM secretin which can mislocalise into the IM (see section 1.5.4.1) (Russel and Kazmierczak, 1993). It has been proposed that this mislocalisation event impairs the integrity of the IM thereby creating an inducing signal for the Psp response (see section 1.5.4.1). This view is supported by the observation that the OM secretin PulD induces Psp in the absence of its cognate chaperone PulS as it mislocalises into the IM (see section 1.5.4.1) (Guilvout *et al.*, 2006). In the present work it was examined whether (or not) Psp can actively remove pIV from the IM by measuring the percentage of pIV in the IM (in comparison to the OM) in WT MG1655 and MG1655Δ*pspF* cells. No difference in this ratio was found in the presence and absence of an active Psp response (Figure 4.7). In both strains about 20% of the pIV produced was detected in the IM fraction. Alongside the above observation, that pIV changes the ubiquinone pool independent from an active Psp response; the results suggest that the mislocalisation of pIV into the IM causes the changes in the ubiquinone pool. Clearly the Psp response does not alter the IM so as to cause less mislocalisation of pIV.

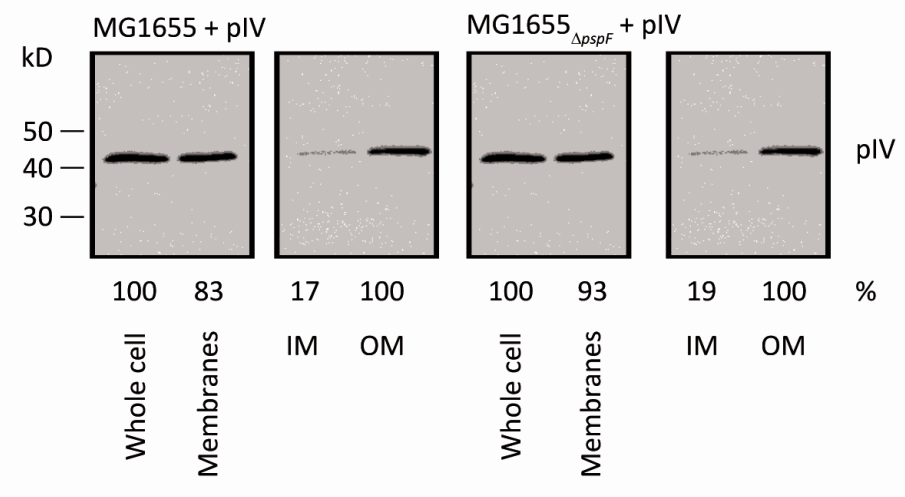


Figure 4.7: IM mislocalisation of the pIV secretin. The IM mislocalisation of pIV was assessed in WT MG1655 and MG1655Δ*pspF* cells. At mid-log phase, cells grown microaerobically at 37°C were fractionated using a Triton X-100 based cell fractionation method (see section 2.4.6) and pIV detected using immunoblotting with pIV specific antibodies (see section 2.4.3). The protein bands were quantified using the AIDA software. The amount of pIV in the inner membrane (IM) was expressed as percentage with respect to the amount of pIV found in the outer membrane (OM). As a control for the reliability of the fractionation method, the amount of pIV recovered in the total membrane fraction (Membranes; corresponding to IM and OM) was compared to the amount of pIV in the whole cell.

4.3.5 Psp can be induced at WT PMF levels

Edwards *et al.*, (2006) reported no significant differences in the electron potential ($\Delta\psi$) of the electron transport mutants under aerobic growth when measured using tetraphenyl phosphonium (TPP^+) in combination with a TPP^+-sensitive electrode. In the present work the cellular $\Delta\psi$ was measured via the JC-1 dye (see section 2.5.6) (Figure 4.8) (Becker *et al.*, 2005). JC-1 changes its oligomeric state in response to the level of the electron potential. It can only form red fluorescent JC-1 aggregates (measured as emission at 590 nm) if the cellular $\Delta\psi$ is equal or greater than WT levels. When the $\Delta\psi$ is decreased, JC-1 remains monomeric, emitting fluorescence at 530 nm. Cells with decreased $\Delta\psi$ will therefore appear mostly green. Since the conversion between both states is not 100%, cells with WT $\Delta\psi$ will emit light at both wavelengths and hence simultaneously appear green and red. Furthermore, the values for $\Delta\psi$ obtained using the JC-1 dye represent the cellular PMF since measurements were taken at pH 7.6 (corresponding to the pH inside the bacterial cell).

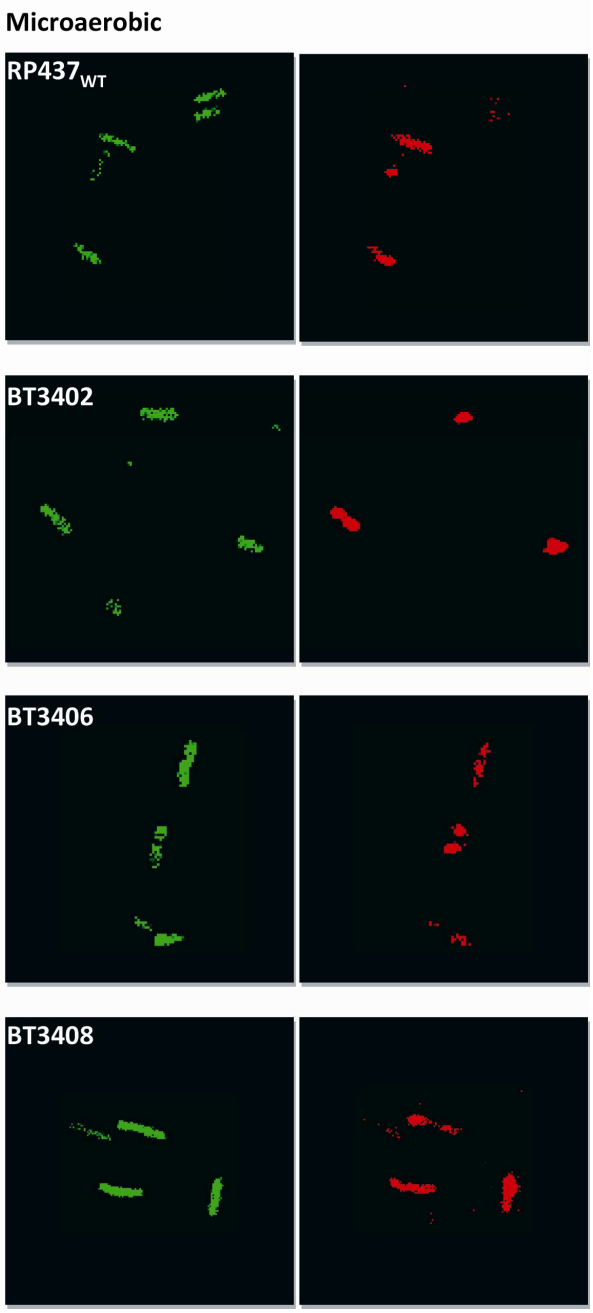


Figure 4.8: PMF measurement in the electron transport mutants. The PMF in $RP437_{WT}$ BT3402, BT3406 and BT3408 was measured at mid-log phase growth using the JC-1 dye (see section 2.5.6). JC-1 changes its oligomeric state in response to the level of cellular $\Delta\psi$. It forms red fluorescent JC-1 aggregates (measured as emission at 590 nm) if the $\Delta\psi$ is equal or higher than WT levels. Cells with decreased $\Delta\psi$ will be mostly green since JC-1 remains monomeric, emitting fluorescence at 530 nm. Conversion between both states is not 100%, cells with WT $\Delta\psi$ will therefore emit light at both wavelengths and hence simultaneously appear green and red (continued on next page).

The values for the $\Delta\psi$ obtained using JC-1 represent the cellular PMF since measurements were taken at pH 7.6 (corresponding to the pH inside the bacterial cell). The electron transport mutants show no marked decrease in the number of red fluorescent cells compared to the parental $RP437_{WT}$ strain indicating WT PMF levels of BT3402, BT3406 and BT3408. Cells were grown microaerobically at 37°C until mid-log phase.

The measurements of the cellular $\Delta\psi$ under the growth conditions used for this Psp study were in full agreement with the data reported in Edwards *et al.* (2006). The electron potential of all mutant strains was similar to $RP437_{WT}$ under both aerobic (data not shown) and microaerobic growth (Figure 4.8). Taken together, both methods used to estimate the cellular PMF, JC-1 (this study) and TPP^+ (Edwards *et al.*, 2006), demonstrate the electron transport mutants are comparable to the WT strain (Figure 4.8) (under aerobic and microaerobic growth) and yet their Psp induction levels are markedly different (Figure 4.4). This indicates that the differences in Psp induction observed between the electron transport mutants may not be caused by a drop in PMF. This is in conflict with prior proposals, in which the Psp response is mounted upon dissipation of PMF (see section 1.5.4.1) (Darwin, 2005 & 2007). Therefore whether (or not) a drop in PMF is sufficient to induce Psp was addressed next.

4.3.6 The PMF dissipating agents Valinomycin and acetate do not induce Psp

It has been shown that CCCP dissipates the PMF and induces Psp (see section 1.5.4.1) (Jovanovic *et al.*, 2006 and Figures 4.9 and 4.10). CCCP is a protonophore causing an influx of H^+ ions into the cytoplasm, thereby discharging both $\Delta\psi$ and the H^+ ion gradient across the inner membrane. Hence, it is conceivable that changes in one of the 2 PMF components may be required to trigger induction of the Psp response. Therefore, the effect of both components on the Psp induction was tested individually (Figure 4.9 and 4.10).

Paul *et al.* (2008) reported the use of Valinomycin and acetate (at an external pH 5 and pH 7) to separate $\Delta\psi$ from the H^+ ion gradient. Valinomycin is a K^+-ionophore which specifically dissipates the $\Delta\psi$ component of PMF by facilitating the influx of K^+ ions into the cytoplasm whilst leaving the H^+ ion gradient unchanged. Acetate in contrast disrupts the H^+ ion gradient by protonating the cytoplasm after crossing the IM. Using the chromosomal ϕ*pspA-lacZ* reporter the *pspA* promoter activity was measured in cells treated with either Valinomycin or acetate at an external pH 5 (LB buffered with MES) and pH 7 (LB buffered with MOPS) (Figure 4.9A).

Neither cells (primed for K^+-uptake by the addition of 150 mM KCl / 120 mM Tris) incubated with 10 μM Valinomycin for 10 or 30 minutes (Figure 5A and Figure 5B), nor cells grown in the presence of 34 mM acetate (at an external pH 5 and 7) showed any increase in activity from the *pspA* promoter (Figure 4.9A). Furthermore, measurement of PMF using JC-1 clearly demonstrates that Valinomycin markedly dissipates $\Delta\psi$ of the cell (MG1655 + Valinomycin; Figure 4.10).

To differentiate between whether the lack of *pspA* promoter activity is due to (i) the inability of Valinomycin to induce Psp, or (ii) because Valinomycin simply inhibits Psp induction, cells were simultaneously subjected to pIV-secretin stress (in the presence of Valinomycin) (Figure 4.9B). Despite the presence of Valinomycin, pIV production caused increased *pspA* promoter activity (as measured by β-galactosidase assays) and a significant increase in PspA expression (as measured by immunoblotting with PspA specific antibodies) (Figure 4.9B). Hence, Valinomycin *per se* does not hinder Psp induction.

Moreover, the PMF measurements of these cells (MG1655 + pIV + Valinomycin; Figure 6) show that, although the Psp response is “on”, it can not maintain PMF

comparable to WT cells which are subject to only the pIV stress (MG1655 + pIV; Figure 4.10). This is either because the dissipation of PMF is so severe (due to the presence of 2 discharging agents) that Psp can not cope with it or because Psp can not counteract the mechanism by which Valinomycin dissipates PMF (similar is seen with CCCP, where the induced Psp response can not maintain PMF; Figure 4.10).

The above data on the effects of PMF discharging agents Valinomycin and acetate (pH 5) on Psp induction fully support the observations using the electron transport mutants – indicating that PMF dissipation is not sufficient to cause Psp induction. As demonstrated with Valinomycin, PMF can be dissipated but Psp induction remains low (Figures 4.9 and 4.10).

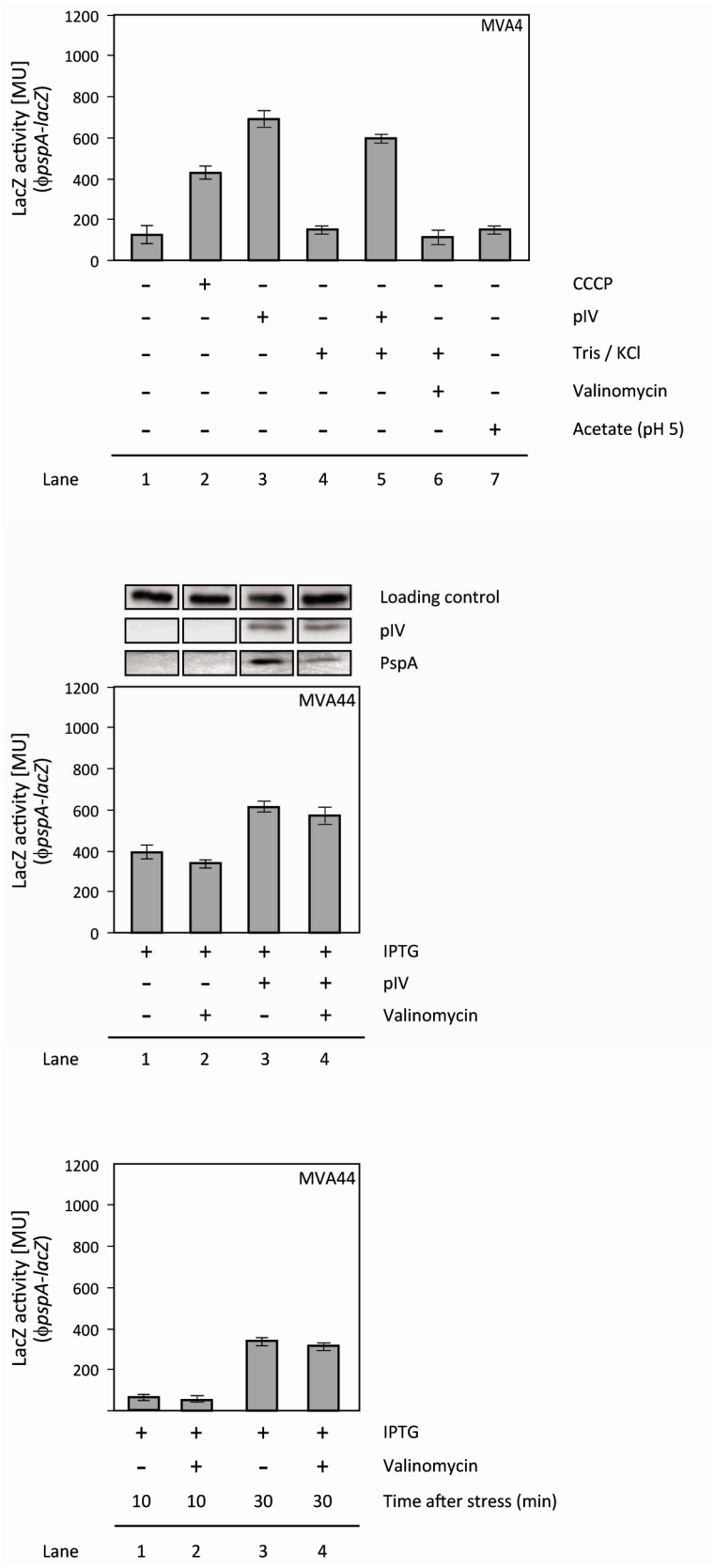


Figure 4.9: Measurement of Psp induction by various agents (Figure legend on next page)**.**

Figure 4.9: Measurement of Psp induction by various agents (continued). (A) The level of Psp induction was measured as LacZ activity in cells containing a chromosomal ϕ*pspA-lacZ* either in **(A)** MVA4 or **(B)** and **(C)** MVA44. **(A)** The Psp response is induced by CCCP (40 μM for 30 minutes; Lane 2) and pIV (constitutively expressed from pGJ4; Lane 3 and 5), but not by KCl/Tris (a combination of 150 mM KCl/ 120 mM Tris was used to prime cells for Valinomycin treatment; Lane 4), Valinomycin (10 μM for 30 minutes; Lane 6) or 34 mM acetate (at external pH 5, Lane 7 or at external pH 7, data not shown). Additionally, KCl/Tris does not inhibit Psp induction by pIV (Lane 5). **(B)** The effect of Valinomycin on the ability of pIV to induce Psp was assessed in MVA44 (MG1655ϕ*pspA-lacZ*) cells. To test this, plasmid-borne (pPMR129) pIV was set under the control of a tight IPTG-inducible promoter. All cells were incubated with 1 mM IPTG for 30 minutes. Cells in Lane 2 and 4 were treated with Valinomycin (10 μM for 30 minutes). IPTG and Valinomycin addition occurred simultaneously. IPTG treatment in cells containing the pIV plasmid induced the production of the pIV secretin (Lane 3 and 4). Note, that the basal level of LacZ activity in MVA44 is increased compared to MVA4. This is due to the native *lacZ* located on the chromosome of MVA44. In addition to reporting the induction of the *pspA* promoter through the measurement of LacZ, expression of PspA protein was assessed by immunoblotting with PspA-specific antibodies. Cells in lane 4 and 5 clearly show increased PspA production (due to the presence of pIV as determined by immunoblotting with pIV-specific antibodies). **(C)** To test, whether "time after stress" was important for Psp induction by Valinomycin, the LacZ activity in MVA44 was measured after 10 and 30 minutes incubation with Valinomycin (10 μM) and compared to MVA44 cells without Valinomycin treatment. To cross-compare with results from **(B)** all cells were incubated with 1 mM IPTG for the indicated length of time. Valinomycin does not induce Psp after 10 and 30 minutes (Lane 2 and 4).

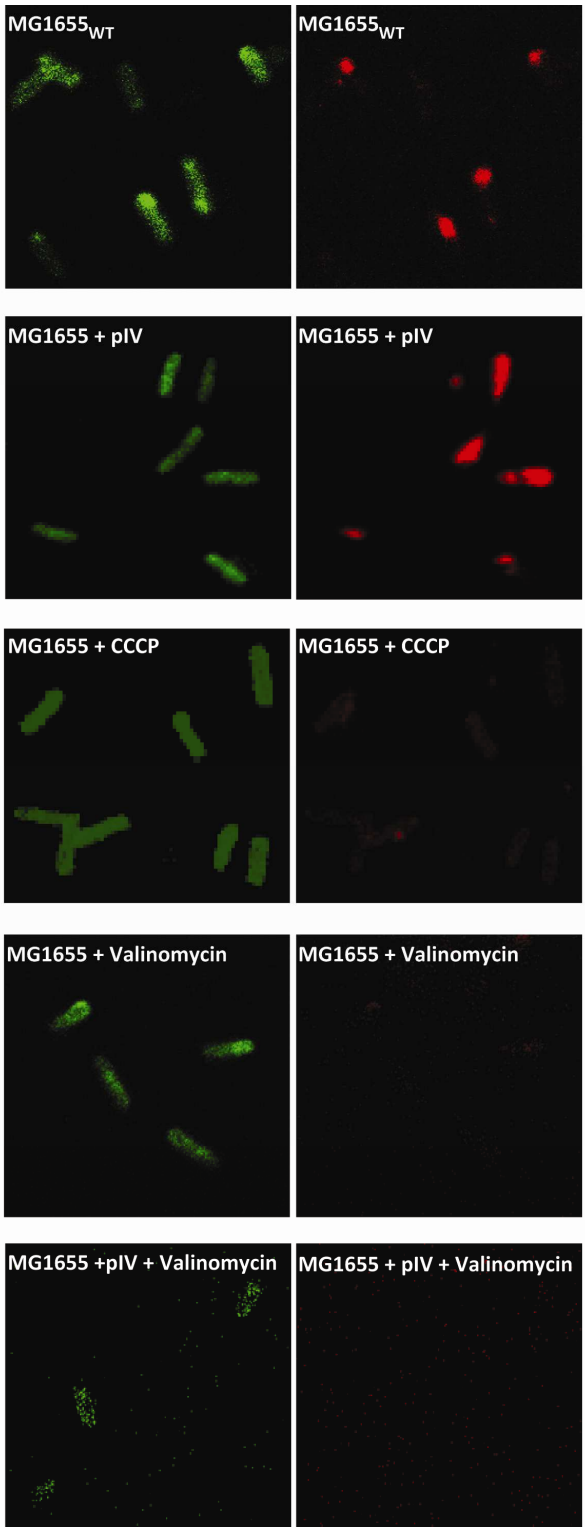


Figure 4.10: PMF measurement in MG1655 cells (Figure legend on next page).

Figure 4.10: PMF measurement in MG1655 cells (continued). The PMF was measured in MG1655 grown microaerobically at 37°C until mid-log phase using the JC-1 dye (see section 2.5.6). Cells were either untreated ($MG1655_{WT}$), or grown in the presence of pGJ4-borne pIV (MG1655 + pIV), CCCP (40 μM for 30 minutes; MG1655 + CCCP), Valinomycin (10 μM for 30 minutes; MG1655 + Valinomycin) or simultaneously with both pIV (pGJ4) and Valinomycin (10 μM for 30 minutes; MG1655 + pIV + Valinomycin). WT cells expressing pIV show no apparent drop in PMF compared to $MG1655_{WT}$ cells. CCCP and Valinomycin dissipate PMF (as seen through the marked decrease in red fluorescent cells). Additionally, Psp effector proteins (induced by pIV) can not overcome dissipation of PMF in the presence of Valinomycin.

4.4 DISCUSSION

Since its discovery nearly 2 decades ago (Brissette *et al.*, 1990), the Psp response has been studied extensively (see section 1.5.4). Today, much is known about its transcriptional regulation (Buck *et al.*, 2000; Dworkin *et al.*, 2000; Rappas *et al.*, 2005; Wigneshweraraj *et al.*, 2008, Joly *et al.*, 2009), its degree of conservation as well as its incidence throughout bacteria, archeae and plants (Westphal *et al*., 2001; Darwin, 2005; Bidle *et al.*, 2008; Vrancken *et al.*, 2008). Its role in maintenance of PMF (Kleerebezem *et al.*, 1996; Darwin, 2005; Jovanovic *et al.*, 2006, Kobayashi *et al.*, 2007) and its implications in bacterial pathogenicity (Darwin, 2005; Rowley *et al.*, 2006; Darwin, 2007) have also been established. A variety of conditions have been found which stimulate Psp expression, all of which may combine impaired IM integrity and the subsequent dissipation of PMF (Darwin, 2005). Due to the often global cellular effects stimuli that induce Psp cause, the nature of the initial inducing signal as well as how it is perceived still remains elusive.

As demonstrated in Chapter 3, the ArcAB two-component system involved in the switch from aerobic to anaerobic respiration is specifically required for Psp induction under microaerobic growth (Jovanovic *et al.*, 2006 & 2009). Moreover, in order to induce Psp the sensor kinase ArcB needs to be activated (Jovanovic *et al.*, 2009). It was therefore concluded that, at least under microaerobic growth, stimulation of Psp induction occurs through activation of ArcB. It has been reported that ArcB activation is responsive to the redox state of quinones - the electron carriers of the electron transport chain (Georgellis *et al.*, 2001; Malpica *et al.*, 2004; Bekker *et al.*, 2009). These observations point towards quinones playing a role in

induction of the Psp response. In the present study, the correlation between quinones and the Psp response was analysed, initially using *E. coli* RP437 derivatives containing binary deletions of NADH I or II dehydrogenase and Cytochrome *bd* or *bo* oxidase. These components of the electron transport chain are linked by quinones, which transfer electrons from the dehydrogenases to the oxidases (see section 1.2.3.2). Hence, it was considered that the quinone pool of these mutants would vary significantly. Indeed, both the oxidised and reduced forms of the ubiquinones exhibited marked differences, depending on which combination of dehydrogenase and oxidase was deleted. Intriguingly, the electron transport mutants also showed strong variations in Psp induction levels, in the absence of any obvious stimulation by IM stress and independent from PMF. Intriguingly, under both, aerobic and microaerobic growth, these variations appeared to be related to changes in the ubiquinone pool. Psp induction increased as the percentage of the reduced form of ubiquinones also increased. Importantly, in cells where the electron transport chain remained intact, pIV-secretin a potent and well characterised inducer of Psp, also impacted on the ubiquinones under aerobic and microaerobic growth. In contrast to the electron transport mutants, pIV appeared to decrease the percentage of reduced UQ_8-H_2. These results suggest that Psp may in general respond to changes in the ubiquinone pool in either direction, towards a more reduced or more oxidised state, indicative of a homeostatic role for the Psp response.

Georgellis *et al.* (2001) showed that menadione, a menaquinone-8 analogue, was able to suppress ArcB activation. Additionally, Bekker *et al.* (2009) reported that ArcAB is regulated by the redox state of menaquinones. Concentration of both,

DMK_8 and MK_8, significantly increased during microaerobic growth. It was therefore formally possible that activation of Psp is mediated by menaquinones. Cells lacking DMK_8 and MK_8 however were able to activate *pspA* transcription demonstrating that menaquinones are dispensable for Psp induction and indicating that the observed effects were specific for ubiquinones.

Induction of the Psp response is stimulated by a number of stresses mainly affecting the integrity of the IM or energy state of the cell (see section 1.5.4.1). It was assumed that the common effect that combines all these stimuli is the dissipation of PMF, and that Psp generally responds to a drop in PMF (Darwin *et al.*, 2005 & 2007). However, to date it is still not clear whether Psp is directly induced by low levels of PMF or whether Psp responds to a secondary effect caused by decreased PMF. Alternatively, PMF dissipation may in many cases simply be a side-effect of the actual stimulus and may not be sufficient to cause Psp induction.

The present study lends support to the latter scenario. When measured using JC-1 dye, the PMF of the electron transport mutants appeared to be similar to WT $RP437_{WT}$ cells under both aerobic and microaerobic growth conditions. In agreement with reports from Edwards *et al.* (2006) where under aerobiosis, the strains showed no major difference in PMF. Nevertheless, the level of Psp induction varied significantly indicating that PMF dissipation is not sufficient to induce Psp. Further support for this emerges from using Valinomycin and/or actetate to analyse the contribution of each individual component of PMF in relation to induction of the Psp response. The results also strongly suggest that dissipation of neither $\Delta\psi$ nor of the H^+ ion gradient is sufficient to induce Psp. Additionally, these results can help to

explain the apparent paradox of why the Psp response is still induced in MG1655 cells producing pIV, despite measurements of $\Delta\psi$ with JC-1 clearly showing that PMF remains at WT levels (compare Figure 5A and Figure 6; Jovanovic *et al.*, 2006). PMF maintenance under pIV stress can be attributed to a functioning Psp response, which is consistent with Psp's proposed role under stress (see section 1.5.4.2.1) (Kleerebezem *et al.*, 1996; Jovanovic *et al.*, 2006; Kobayashi *et al.*, 2007). A drop in PMF is only evident in cells where the Psp activator protein PspF is deleted. These cells then fail to maintain WT PMF in the presence of pIV (Jovanovic *et al.*, 2006). Recovery of PMF by the induced Psp effectors would, in principle result in a loss of the inducing signal should it be the drop in PMF. These considerations rather suggest that pIV should cause a constant physiological change in the cell that can not be relieved by Psp effectors. Something of this change in cell physiology may serve as the Psp inducing signal.

In contrast to the drop in PMF, the effect of pIV on the redox state of ubiquinones is consistent in both WT MG1655 and MG1655Δ*pspF* cells, and thus unaffected by a prolific Psp response (Figure 4.6). Hence, changes in the redox state of the ubiquinone pool meet the proposed criteria of a constant physiological effect by pIV and as such, may therefore be one part of the signalling cascade of the Psp response. Notably, changes in the redox state of the ubiquinone pool are involved in ArcB activation (Georgellis *et al.*, 2001; Malpica *et al.*, 2004; Bekker *et al.*, 2009), a requirement for Psp induction under microaerobic growth (Jovanovic *et al.*, 2009), where the effect of pIV on the redox state of the ubiquinones is much more pronounced than under aerobic growth (Figure 4.6).

CHAPTER 5

IN VIVO LOCALISATION OF PSP INNER MEMBRANE STRESS CONTROLLERS PSPA AND PSPG

5.1 INTRODUCTION AND RECAP

The Psp response is strongly induced by the OM secretin protein IV (pIV) from filamentous phage f1 (Brissette *et al.*, 1990), bacterial secretins and IM stresses including conditions that block or reduce the efficiency of the protein export apparatus, extreme heat shock, hyper-osmotic shock, and uncouplers of PMF (see section 1.5.4.1) (Model *et al.*, 1997; Darwin, 2005). It is assumed that PMF-dissipation is the unifying Psp-inducing signal, however the results from Chapter 4 suggest that PMF-dissipation alone is not sufficient to induce Psp and that changes in the redox state of ubiquinones may also be involved in Psp induction. Several lines of evidence lend support to maintenance of PMF in cells under envelope stress conditions being the major physiological role of Psp (see section 1.5.4.2.1) (Kleerebezem *et al.*, 1996; Darwin, 2005 & 2007; Jovanovic *et al.*, 2006). Recently, work with *E. coli* IM vesicles and liposomes provide evidence that higher–order oligomers of PspA mitigate proton loss across membrane bilayers and that PspA (which is a peripheral protein at the cytoplasmic face of the IM) can directly interact with phosphatidylserine (PS) and phosphatidylglycerol (PG) (Kobayashi *et al.* 2007). It was therefore proposed that PspA may form a scaffold-like structure below the IM to alter its rigidity (Kobayashi *et al.*, 2007). Based on structural studies, Standar *et al.* (2008) reported a scaffold-like network composed of homo-multimeric PspA. Additionally, transcription profiling of cells over-expressing PspA or PspG suggest these proteins also indirectly maintain PMF by causing a subtle switch towards anaerobic respiration and fermentation as well as a downturn of PMF consuming cellular processes such as motility (Jovanovic *et al.*, 2006). In this work, fusions to

the GFP were used to visualise PspA and PspG in the living cell in order to further elaborate their mode of action.

5.2 OBJECTIVES

Although lacking the confined cellular compartments of eukaryotes, *in vivo* localisation studies using fluorescence microscopy have revealed a remarkable organisation within the bacterial cell. Based on asymmetric protein distribution, rod-shaped cells such as *E. coli* can be divided into different sub-cellular domains: the polar, lateral and septal regions. Correct spatial localisation of proteins within these regions is often crucial for the functioning of cellular processes. Furthermore, members of interrelated pathways often co-localise, hence studying the spatial organisation of a protein can provide insights into its role within the complex network of cell physiology.

The main objectives for this work were to:

1) Construct and visualise PspA and PspG fusions to the green fluorescent protein (see section 2.5.6), GFPmut2 (herein termed GFP) (Cormack *et al.,* 1996) within *E. coli*.

2) Probe the mode of action and the relationship between the Psp response and other cellular proteins and processes.

5.3 RESULTS

5.3.1 GFP-PspA and PspG-GFP are functional

PspA was fused to the C-terminus of GFPmut2 in pDSW209 (plasmid pLL5), and PspG-GFP was created by cloning *pspG* into pDSW210 (plasmid pGJ7) creating an N-terminal fusion. The GFP fusions underwent rigorous quality control by testing their stability, functionality and the extent of inclusion body formation to confirm their native state and to rule out artefacts due to accumulation of fluorescent aggregates or proteolytic cleavage products within inclusion bodies caused by over-expression (Ventura and Villaverde, 2006; Bardy and Maddock, 2007).

GFP-PspA expressed from pLL5 was not functional with respect to PspA activity and so a serine / glycine linker region was introduced between GFPmut2 and PspA to create plasmid pEC1 since including a flexible linker region could result in a more functional fusion protein. To allow relatively low protein levels, the fusion genes were expressed without induction under the control of a weak P_{trc} promoter down-regulated by the constitutive $LacI^{q}$ repressor encoded on plasmids (Weiss *et al.*, 1999).

Immunoblotting demonstrated that the expression level of GFP-PspA (from pEC1) is very similar to that of the native PspA protein upon pIV-induced membrane stress (Figure 5.1) and hence the fusions represent native Psp protein levels. Furthermore, the fusions appeared stably expressed. Neither MG1655Δ*pspA*/GFP-PspA nor MG1655Δ*pspG*/PspG-GFP cells contained detectable amounts of free PspA, PspG or GFP (Figure 5.1A). PspA is a bi-functional protein (negative regulator and effector of

Psp). The negative regulator function of GFP-PspA was tested using β-galactosidase assays (see section 2.4.4) in MG1655Δ*pspA*/GFP-PspA cells containing pSJ1 (ϕ*pspA-lacZ* transcriptional reporter fusion) (Figure 5.2A) and immunoblotting with PspC-specific antibodies (see section 2.4.3) (Figure 5.2A). GFP-PspA behaves very similarily to WT PspA when produced *in trans* in partially inhibiting PspF activity and reducing PspC expression (Figure 5.2B).

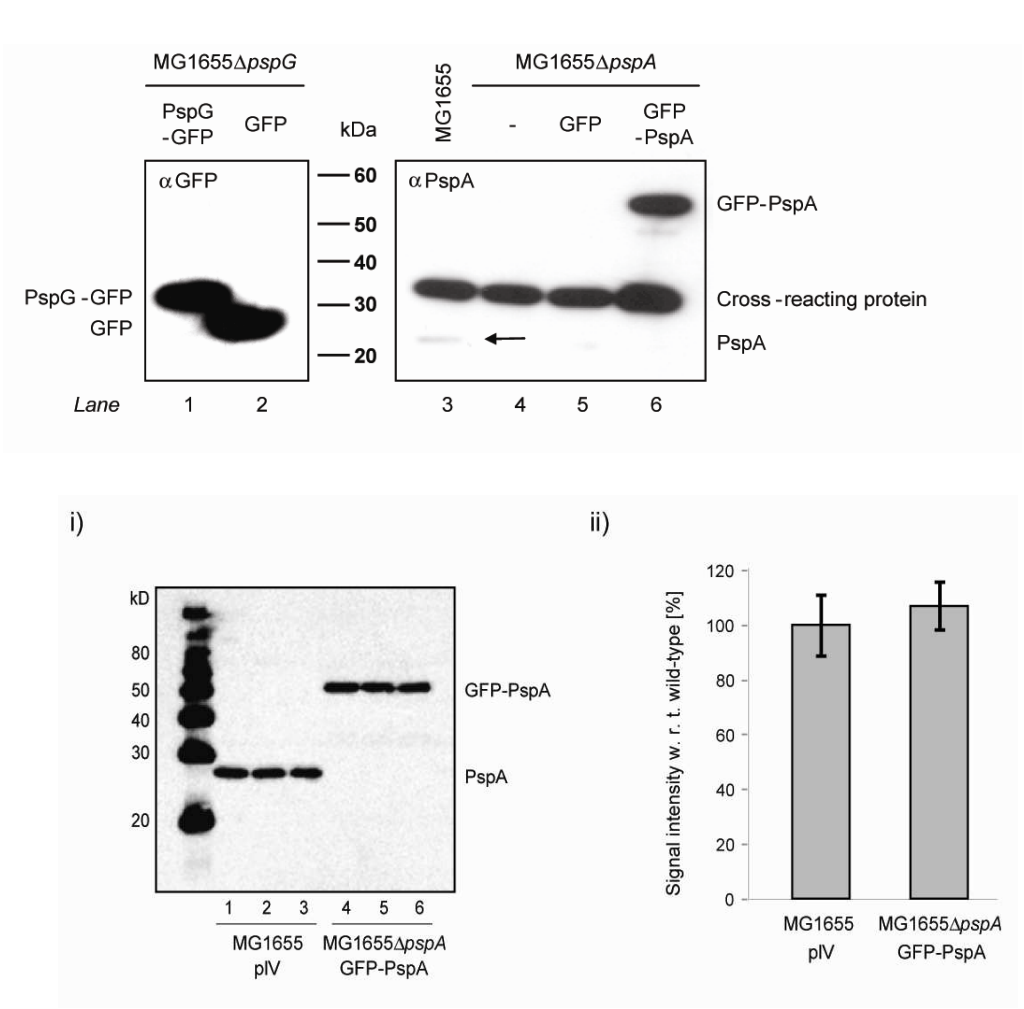
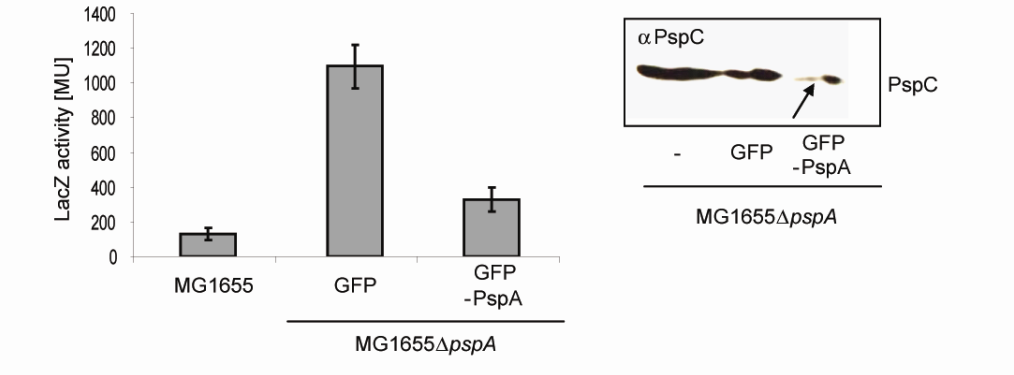


Figure 5.1: Expression of GFP-PspA and PspG-GFP. (A) The stability of GFP-PspA and PspG-GFP fusion proteins were tested by immunoblotting with antibodies against PspA and GFP (see section 2.4.3). Proteins corresponding to GFP-PspA (53 kDa, lane 6), PspG-GFP (37 kDa, lane 1), GFP (28 kDa, lane 2) and PspA (25 kDa, lane 3) are indicated. The PspA antibody cross-reacts with an unknown 35 kDa *E. coli* protein (labelled cross-reacting protein). **(B)** i) The leaky expression (as used for microscopy) of GFP-PspA (from pEC1; Lanes 4-6) was comparable to chromosomal PspA levels from WT MG1655 cells upon pIV-stress (Lanes 1-3). Equal numbers of cells were boiled, loaded onto a 12.5 % SDS-gel and subjected to immunoblotting with α-PspA antibodies. Chemi-luminescence was detected using the LAS-3000 Luminescent Image Analyzer (FUJIFILM). ii) The average luminescence intensities of the blot shown in (i) expressed as a percentage of signal intensity with respect to WT PspA (from MG1655 under pIV-stress).

A



B

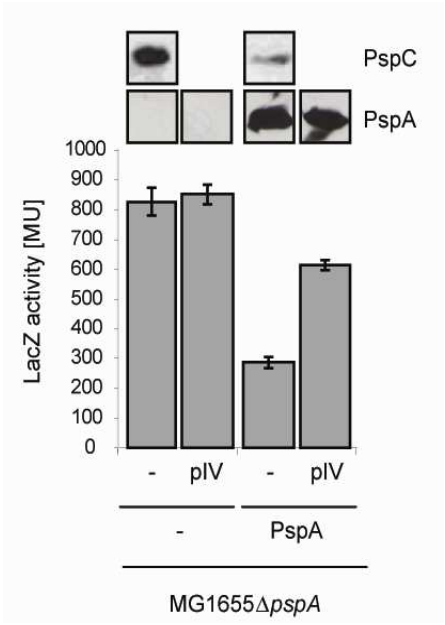


Figure 5.2: Negative regulatory function of GFP-PspA is comparable to plasmid-borne PspA. The negative regulatory function of GFP-PspA **(A)** and plasmid-borne PspA **(B)** was analysed by β-galactosidase assays (see section 2.4.4) in MG1655Δ*pspA* cells containing a ϕ*pspA-lacZ* transcriptional reporter fusion and by immunoblotting with PspC specific antibodies (see section 2.4.3). Both, GFP-PspA and plasmid-borne PspA over-production causes a decrease in PspC levels (indicated by an arrow). In **(B)** immunoblotting with PspA specific antibodies was used to confirm the production of PspA *in trans*.

The effector function of GFP-PspA was tested using a motility assay (see section 2.5.3) (Figure 5.3) since over-production of PspA in WT MG1655 or MG1655Δ*pspF* cells resulted in decreased motility (see section 1.5.4.2.1) (Jovanovic *et al.*, 2006). Importantly, GFP-PspA in MG1655Δ*pspF* cells also caused decreased cell motility (Figure 5.3), demonstrating that GFP-PspA retains its effector functionality. Lloyd *et al.* (2004) identified PspG as an additional effector of the Psp response; over-production of PspG in WT MG1655 or MG1655Δ*pspF* cells also decreased cell motility. In line with this, expression of PspG-GFP in MG1655Δ*pspF* cells also resulted in decreased cell motility (Figure 5.3) demonstrating that the effector function of PspG-GFP is maintained.

Over-expressed GFP fusions can form fluorescent aggregates which reside in inclusion bodies potentially yielding artificial sub-cellular localisation patterns (Bardy and Maddock, 2007). To test inclusion body formation of GFP-PspA and PspG-GFP we performed Triton X-100 based cell fractionations (see section 2.4.6) (Russel and Kazmierczak, 1993). Proteins from MG1655Δ*pspA*/GFP-PspA and MG1655Δ*pspG*/PspG-GFP cells were separated into soluble (periplasmic and cytoplasmic proteins) (Sol), inner membrane (IM), outer membrane (OM) and aggregated (Agg) fractions. Subsequently, the sub-cellular location of GFP-PspA and PspG-GFP was inferred via immunoblotting using GFP specific antibodies (Figure 5.4). GFP-PspA can be detected in soluble and IM fractions (Figure 5.4, Sol & IM) consistent with previous observations that PspA is a peripheral IM protein at the cytoplasmic face of the IM (Brissette *et al.*, 1990).

In silico predictions suggest PspG is an integral IM protein with two trans-membrane helixes and both the N- and C-terminus lie in the cytoplasm (Figure 5.5A). In agreement with this, PspG-GFP was only found in the IM fraction (Figure 5.4, IM), similarly to WT PspG (Figure 5.5B) and neither GFP-PspA nor PspG-GFP showed any detectable aggregates (Figure 5.4, Agg). Taken together, GFP-PspA and PspG-GFP are stably expressed, retain detectable levels of activity and are not located in inclusion bodies indicating that they are suitable for all localisation studies.

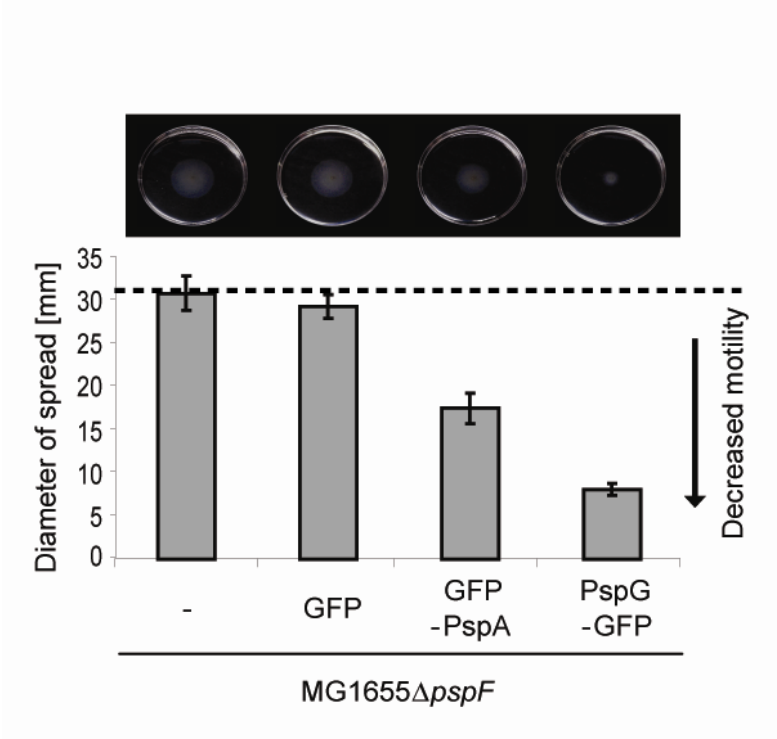


Figure 5.3: GFP-PspA and PspG-GFP are functional effectors of the Psp response. The effector function of the GFP fusions were tested by motility assays using MG1655Δ*pspF* cells expressing either GFP-PspA or PspG-GFP (see section 2.5.3). Both, GFP-PspA and PspG-GFP decrease cell motility and hence are functional effectors of the Psp response.

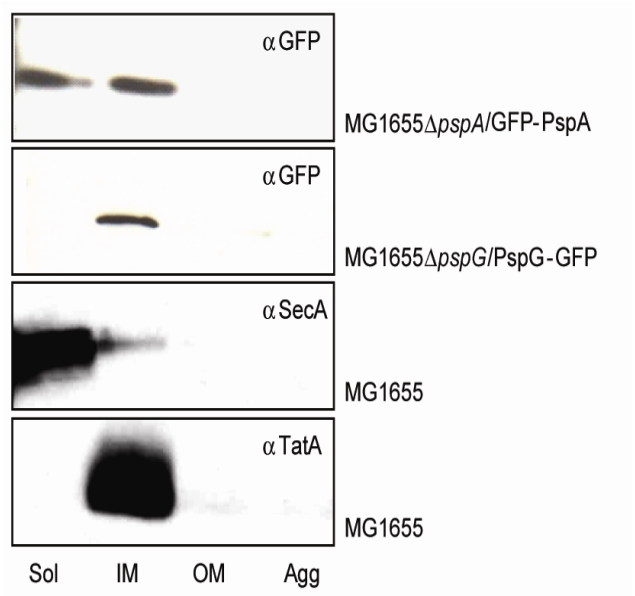


Figure 5.4: GFP-PspA and PspG-GFP are not localised in inclusion bodies. A Triton X-100 based fractionation method (see section 2.4.6) was used to determine the location and amount of inclusion body formation of the fusion proteins. GFP-PspA and PspG-GFP were detected by immunoblotting with GFP-specific antibodies. Sol (soluble fraction; cytoplasmic and periplasmic proteins), IM (inner membrane), OM (outer membrane) and Agg (aggregated) proteins (inclusion bodies). The Triton X-100 fractionation method was validated using SecA and TatA in MG1655 cells as marker proteins. Using α-SecA and α-TatA antibodies, SecA (which is cycling between the cytoplasm and IM; see section 1.3.1.1) was found in the soluble and IM protein fraction whereas TatA (which is an integral IM protein; see section 1.3.1.2) was only detected in the IM protein fraction.

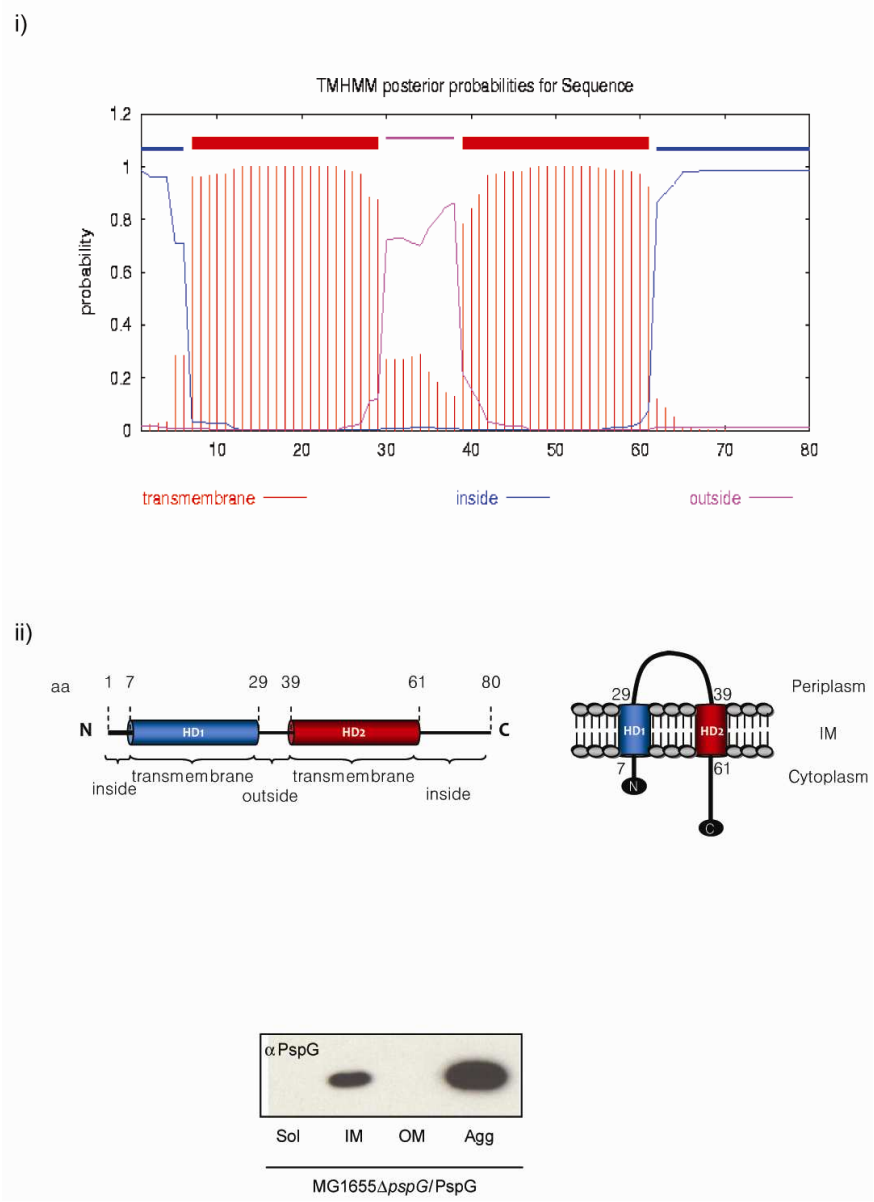


Figure 5.5: PspG is an integral IM protein. (A) HMMTOP *in silico* topology analysis predicts that PspG is an integral IM protein with 2 trans-membrane helices between amino acid residues 7 and 31 and 40 and 61. N- and C-terminus of PspG are predicted to reside within the cytoplasm. **(B)** Triton X-100 based fractionation (see section 2.4.6) of *E. coli* cells containing pLL11 (*pspG* in pBAD18-cm under the control of an arabinose-inducible promoter). Over-expression of WT PspG was induced by 0.4% arabinose. PspG was detected by immunoblotting with α-PspG antibodies (see section 2.4.3) and found in the IM (Lane 2) and inclusion body (Lane 4) fractions. Sol: soluble protein fraction; IM: IM protein fraction; OM: OM protein fraction; Agg: aggregated proteins (inclusion bodies).

5.3.2 GFP-PspA and PspG-GFP are localised to the cell poles and traffic between both poles

In line with their previously established topologies as peripheral (PspA) and integral IM proteins (PspG) (see section 1.5.4), GFP-PspA in MG1655Δ*pspA* and PspG-GFP in MG1655Δ*pspG* cells can be visualised as green fluorescent foci (Figure 5.6A) localised proximal to the IM (Figure 5.6A, red). Epi-fluorescence microscopy indicates that both, GFP-PspA and PspG-GFP (Figure 5.6A, green) appear to accumulate at the cell poles. To quantify these localisation patterns 20 cells (of each strain used) were divided into 6 equally sized cross-sections each covering similar membrane areas in the terminal and lateral sections (approximating the cell poles as hemispheres and assuming an average cell-length of 3 μm and a cell-diameter of 1 μm) and measured the intensity of the fluorescence signal in each segment (Figure 5.6B). In accordance with the fluorescence images, in both MG1655Δ*pspA*/GFP-PspA and MG1655Δ*pspG*/PspG-GFP (Figure 5.6A) cells almost half of the total fluorescence is accounted for by the polar segments 1/6 and 6/6 at the ends of the cells (Figure 5.6B).

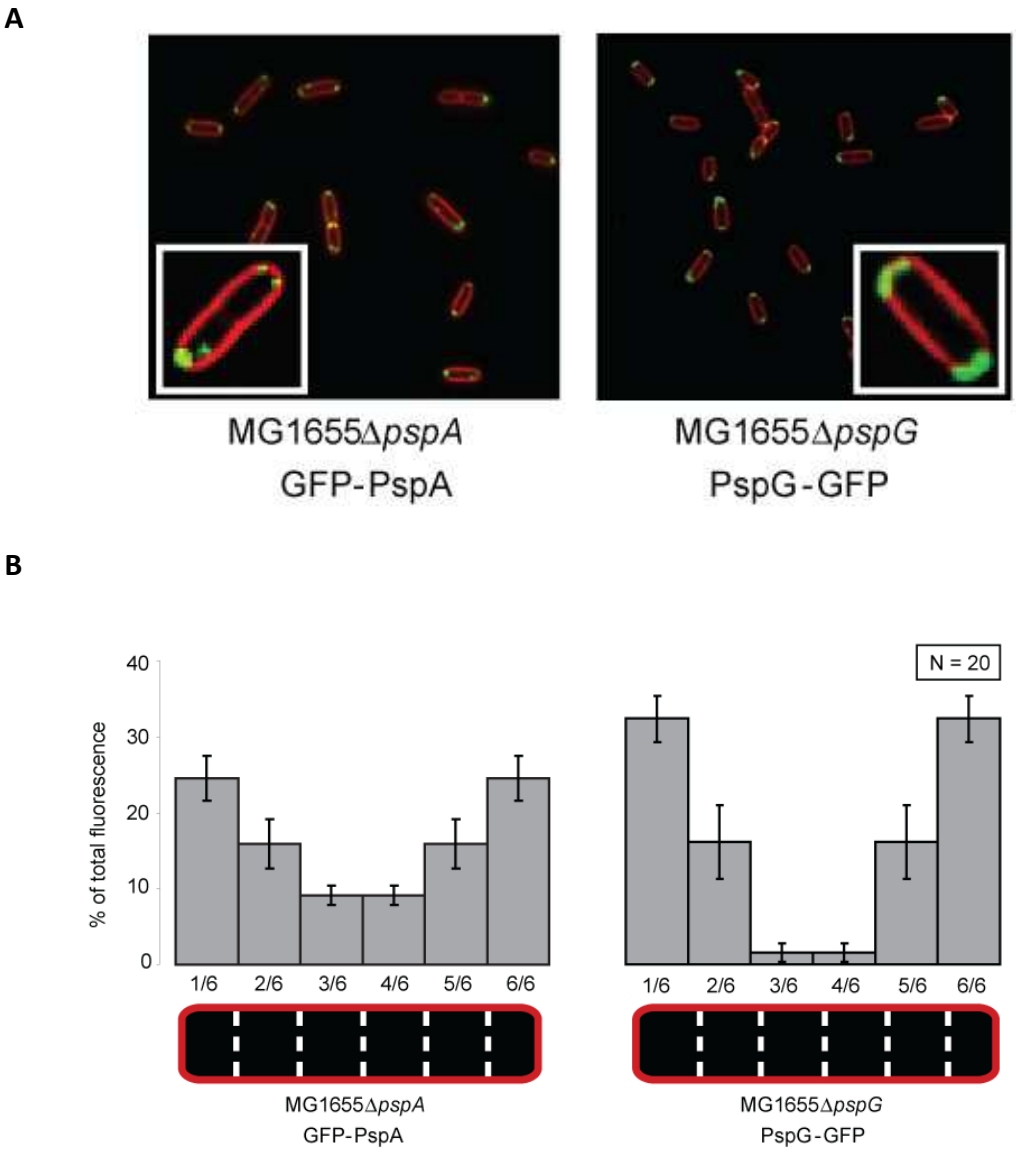


Figure 5.6: GFP-PspA and PspG-GFP localise at both cell poles. (A) Epi-fluorescence images of *E. coli* MG1655Δ*pspA*/GFP-PspA and MG1655Δ*pspG*/PspG-GFP cells. Fluorescent GFP fusion proteins can be seen in green. The IM was stained with FM 5-95 (Molecular Probes; red). Images were taken using a Zeiss Axiovert 200 (inverted) microscope (see section 2.5.8.2). **(B)** The distribution of fluorescence intensity across 6 equally sized cross-segments (1/6 – 6/6) of 20 cells from each strain MG1655Δ*pspA*/GFP-PspA and MG1655Δ*pspG*/PspG-GFP was measured using ImageJ software. Values shown had background fluorescence substracted (measured using MG1655 cells treated with the FM 5-95 IM dye).

To explore the polar localisation further, GFP-PspA and PspG-GFP were visualised in *E. coli* MC1000Δ*minCDE* cells. The MinCDE system is required to maintain the placement of the divisome in mid-cell thereby resulting in 2 equally sized daughter-cells after cell division (Lutkenhaus, 2007) (Figure 5.7). Cells lacking the MinCDE system are characterised by two different cell-types, rod-shaped cells and minicells (Figure 5.8), due to the inappropriate placement of the division site close to one pole (Figure 5.8, DIC, arrow). Hence, minicells represent a polar segment of the parental cell harbouring polar localised proteins (Lai *et al.*, 2004).

Using confocal microscopy, fluorescence could be detected within minicells using either MC1000Δ*minCDE*Δ*pspA*/GFP-PspA (data not shown) or MC1000Δ*minCDE*Δ*pspG/*PspG-GFP (Figure 5.8). Since it is possible to separate minicells from rod-shaped cells by differential centrifugation (see section 2.5.4) (Lai *et al.*, 2004) (Figure 5.8), detection of GFP-PspA and PspG-GFP in minicells by immunoblotting would further validate their polar localisation (Figure 5.8). Consistent with earlier microscopy observation (Figure 5.6A and Figure 5.8) that GFP-PspA and PspG-GFP are concentrated at the cell poles, both fusion proteins can be found in the minicells (Figure 5.8).

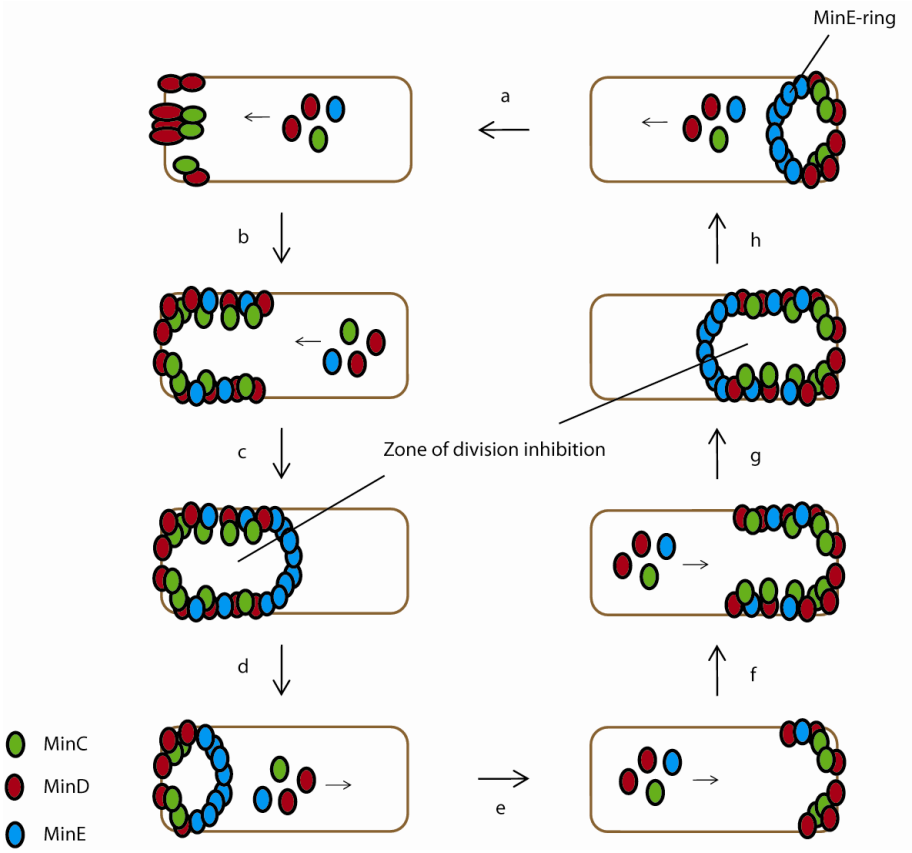


Figure 5.7: Model for the MinCDE system (adapted from Rothfield *et al.*, 2005)**.** The MinCD cluster assembles at a cell pole and oscillates between both poles with alternating cycles of assembling and dis-assembling. The MinE ring forms at the edge of the MinCD cluster. The divisome can only be placed at positions of low MinCD cluster concentration. Pole-to-pole oscillation therefore generates a zone of division inhibition at both poles (high MinCD concentration). Hence, cell division can only occur in mid-cell (low MinCD concentration).

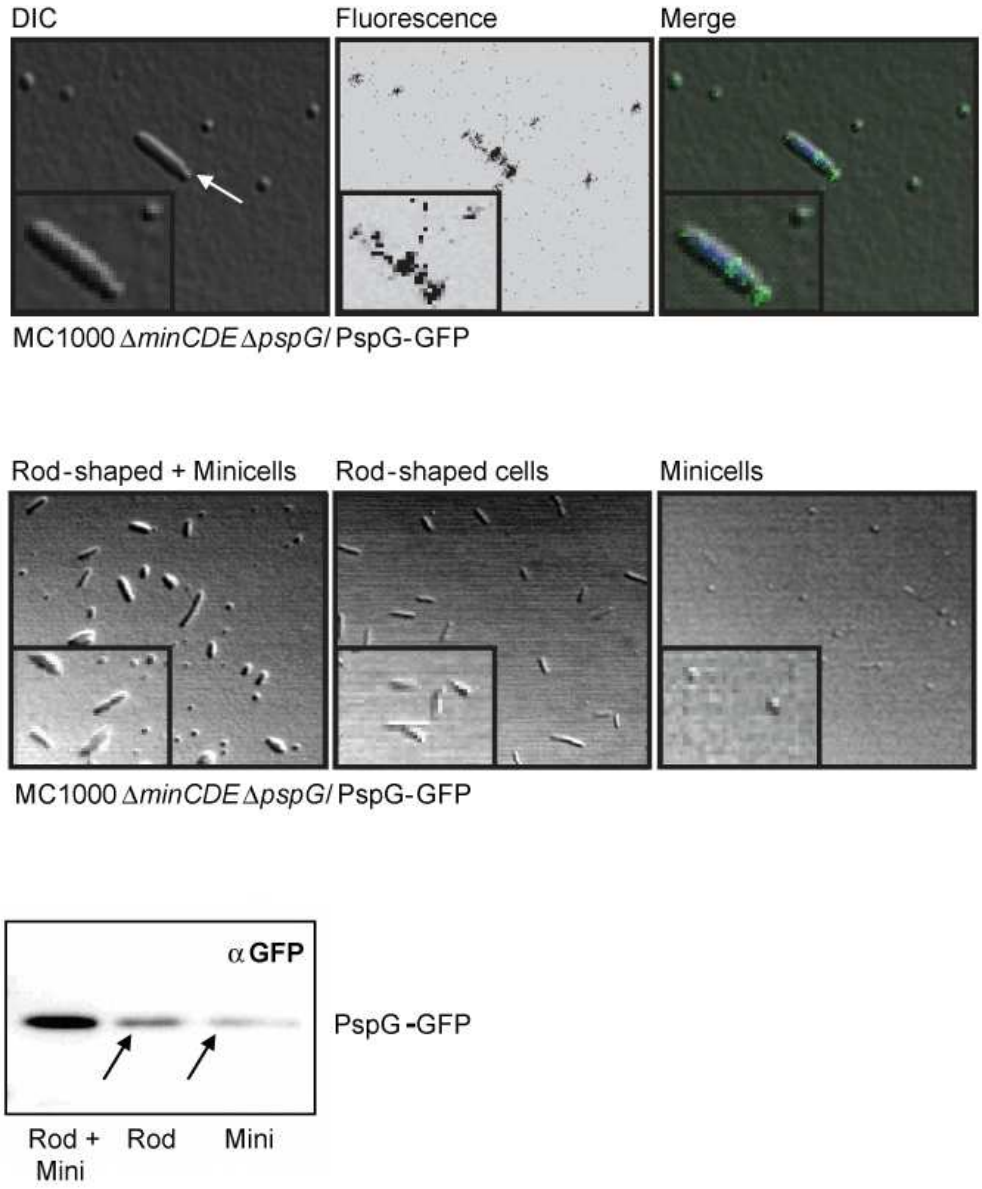


Figure 5.8: PspG-GFP can be found in minicells. *E. coli* MG1655Δ*minCDE*Δ*pspA*/GFP-PspA and MG1655Δ*minCDE*Δ*pspG*/PspG-GFP cells were visualised using confocal fluorescence microscopy (see section 2.5.8.2) (the arrow indicates cell-division at a misplaced division-site close to one cell-pole; DNA was stained using DAPI) and separated into rod-shaped and minicells (see section 2.5.4) (as confirmed by light microscopy), and using GFP-specific antibodies the presence of the fusion proteins was assessed (arrows indicate PspG-GFP found in rod-shaped (Rod) and minicells (Mini)). The results shown refer to MG1655Δ*minCDE*Δ*pspG*/PspG-GFP.

Although fluorescence intensity measurements across the cell indicated that a significant amount of fluorescence is located in the two segments at the ends of the cell (Figure 5.6B, 1/6 and 6/6), fluorescence was detected between the poles (Figure 5.6B, 2/6 – 5/6). Additionally GFP-PspA and PspG-GFP were also present in the rod-shaped MC1000Δ*minCDE* cells (Figure 5.8), implying that GFP-PspA and PspG-GFP may also be present laterally between the cell poles, just not easily visualised.

Therefore, MG1655Δ*pspA*/GFP-PspA and MG1655Δ*pspG*/PspG-GFP strains were examined using a custom-built epi-fluorescence microscopy equipped with a tuneable argon ion laser which improved the resolution of the localisation data (see section 2.5.8.2). In addition to the polar foci (Figure 5.9A, grey arrows) the images obtained clearly revealed lateral fluorescent complexes (Figure 5.9A, black arrows) of both GFP-PspA and PspG-GFP. The non-uniform localisation pattern along the lateral cell wall implies an underlying organisation. Intriguingly, in marked contrast to the polar foci, the lateral complexes were highly mobile displaying a range of curved and linear motions (Figure 5.9A and 5.9B a-j, black arrows; supplementary data) with a track reminiscent of the helical structure of the MreB cytoskeleton (Figure 5.11A). These motions might therefore represent the trafficking of PspA and PspG via an IM route, potentially dependent on the actin-like cytoskeletal protein MreB (Jones *et al.*, 2001; Daniel and Errington, 2003; Shih *et al.*, 2003; Figge *et al.*, 2004; Gitai *et al.*, 2004).

A

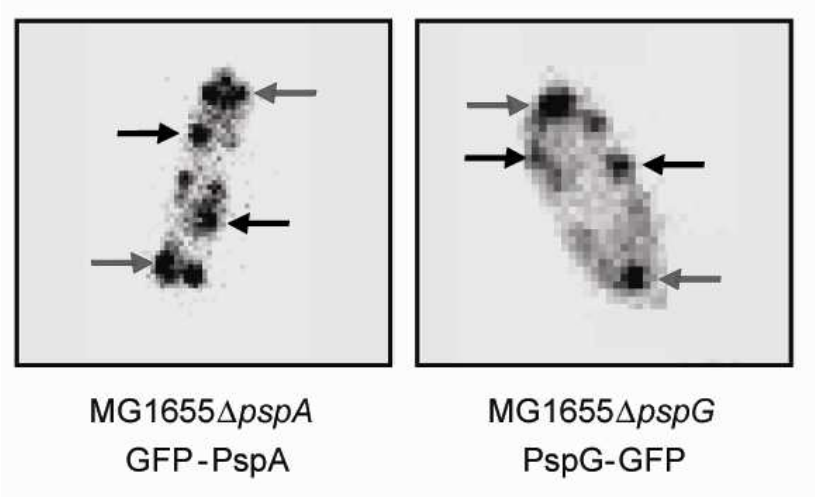


Figure 5.9: GFP-PspA and PspG-GFP traffic between the cell poles. (A) Inverted epi-fluorescence images of *E. coli* MG1655Δ*pspA*/GFP-PspA and MG1655Δ*pspG*/PspG-GFP cells. Polar GFP fusion proteins are indicated with grey arrows, lateral complexes with black arrows. **(B) (see overleaf)** Inverted time-lapsed epi-fluorescence images of MG1655Δ*pspG*/PspG-GFP cells. The movement of one of the mobile lateral complexes is indicated in each image by a black arrow. For clarification, schematic figures were drawn to illustrate the movement of the complex. The spot which represents the mobile fluorescent complex was shaded from black to light grey to indicate increasing time (i.e. black represents t=0s and white with grey outline represents t=5.12s). Composite figures were made to demonstrate the movement of the complex over time (a-e, f-j, a-j). All images were taken using a Nikon TE-2000 inverted optical microscope with a time-resolution of 80 ms / frame (see section 2.5.8.2). (For original images see Apendix G).

B

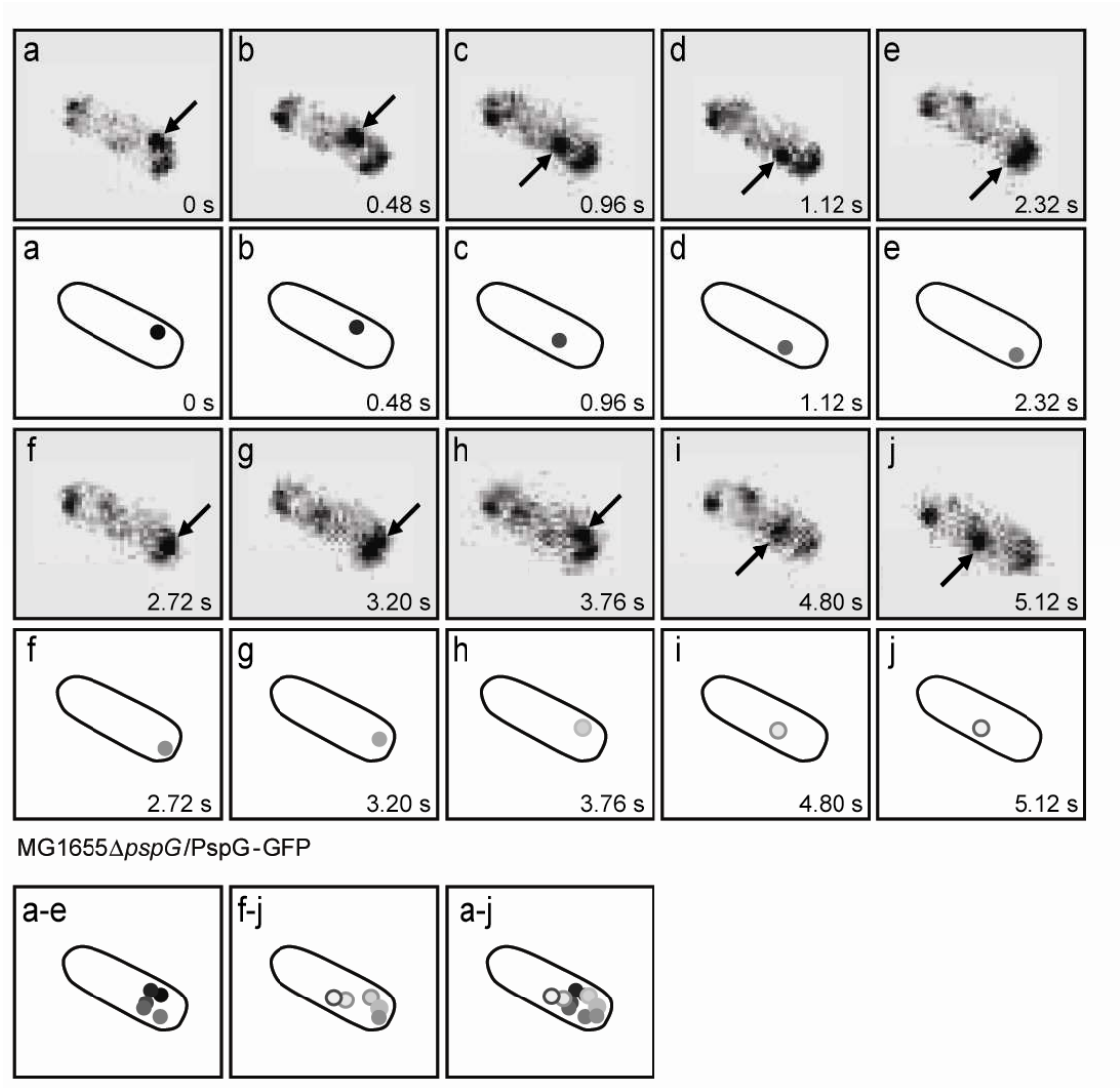


Figure 5.9: GFP-PspA and PspG-GFP traffic between the cell poles. (Figure legend on previous page)

5.3.3 GFP-PspA and PspG-GFP trafficking is affected by A22

To investigate a potential interaction of PspA and PspG with the MreB cytoskeleton, the sub-cellular localisation of GFP-PspA and PspG-GFP was studied in the presence of A22 (S-(3.4-dichlorobenzyl)-isothiourea), a compound that induces MreB depletion-like spherical cell shape (Iwai *et al.*, 2002). Gitai *et al.* (2005) and Kruse *et al.* (2006) showed that A22 treatment prevents MreB from forming a helical structure, which manifests in a delocalised fluorescence pattern of GFP-MreB.

Recently, Taghbalout and Rothfield (2009) observed helical filaments of RNaseE (the main component of the RNA degradosome in *E. coli*) along the length of the cell, similar to the MreB or MinD cytoskeleton. The authors also used A22 to test whether this spatial organisation of RNaseE was dependent on the MreB scaffold. However, RNaseE localisation was not sensitive to A22 and hence it was concluded that the formation of the RNaseE helical filament was independent of the MreB cytoskeleton.

In contrast, and in line with the proposal that PspA and PspG lateral complex formation and their trafficking may somehow involve the MreB cytoskeleton, an A22-dependent change in the sub-cellular localisation of GFP-PspA and PspG-GFP was observed.

Recall that in untreated *E. coli* MG1655Δ*pspA* and MG1655Δ*pspG* cells, GFP-PspA and PspG-GFP is observed largely as polar foci (Figure 5.6A), alongside highly mobile complexes between the poles (Figure 5.9B). After 12 hours incubation with 50 µg/ml A22, the cells lose all detectable mobile lateral complexes but the foci on both poles remain unaffected (Figure 5.10, A22 treated, 12h). This loss of pole to

pole trafficking is specific to A22 treatment and can not be attributed to overnight cell growth as the localisation pattern in these cells is unchanged and similar to untreated cells (Figure 5.10, untreated, 12h). In agreement with A22 affecting the MreB polymerisation (Gitai *et al.*, 2005; Iwai *et al.*, 2002), formation of spherical cells after 24 hours growth in the presence of A22 was observed, confirming that the MreB helical structure is disrupted (Figure 5.10, A22 treated, 24h). These findings indicate that both PspA and PspG not only show 2 spatially (polar and lateral) distinct localisations, but also that the mechanisms behind the positioning of the polar and lateral complexes may differ. Whilst the polar complexes appear to be A22 resistant and therefore MreB-independent, the mobile lateral spots delocalise upon A22 treatment. Hence, PspA and PspG might rely directly upon the MreB cytoskeleton to properly form lateral complexes and move between the cell poles, and the organisation of the MreB cytoskeleton could explain the predominantly curved profile of that route (Figure 5.9).

Imaging of GFP-PspA and PspG-GFP in cells lacking *mreB* (MC1000Δ*mreB*) supported the observations using A22, in which lateral movements were no longer observed and the fluorescent foci appeared dispersed (Figure 5.10, Δ*mreB*). A similar pattern was seen by Shih *et al.* (2005) with polar Tar-GFP in MC1000Δ*mreB,* which the authors concluded may imply that polar localisation the chemoreceptor Tar is dependent on MreB (Figure 5.11). In contrast, Greenfield *et al.* (2009) generated a mathematical model derived from localisation studies using photoactivated localisation microscopy (PALM) suggesting that the formation and maintenance of polar chemoreceptor clusters is a random event, in which these receptors assemble at the poles independently of other cell components (Figure 5.11). In the present

study, it was not possible to distinguish whether the delocalised GFP-PspA and PspG-GFP in MC1000Δ*mreB* (Figure 5.10) corresponds to either the polar or lateral complexes observed in WT *E. coli* cells (Figure 5.9A) and hence whether polar localisation of PspA and PspG is dependent on the MreB scaffold. The resistance of polar foci to A22 however suggests MreB-independent positioning of PspA and PspG at the cell pole.

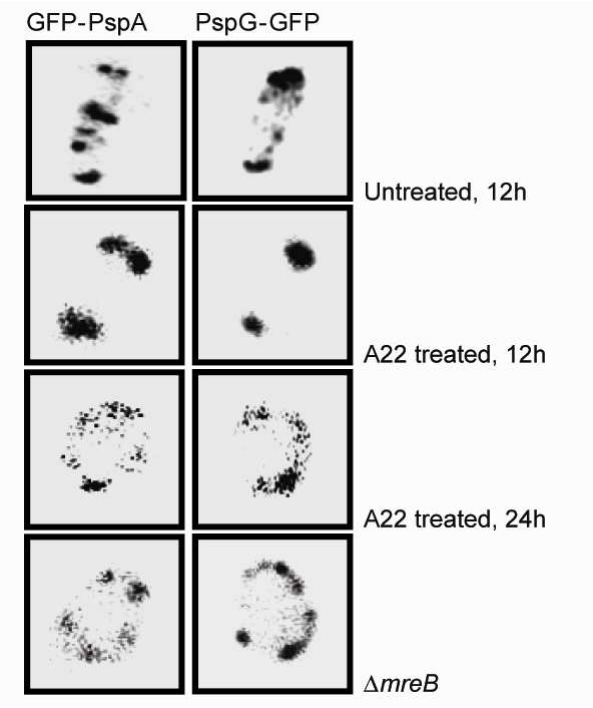
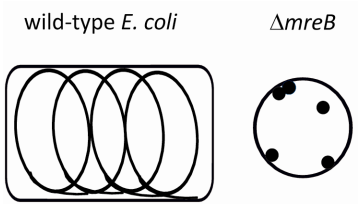


Figure 5.10: Lateral complexes of GFP-PspA and PspG-GFP are affected by A22 treatment. Inverted epi-fluorescence images of *E. coli* MG1655Δ*pspA*/GFP-PspA and MG1655Δ*pspG*/PspG-GFP cells after 12 hours growth without A22 (untreated, 12h), after 12 hours (A22 treated, 12h) and 24 hours (A22 treated, 24h) incubation with 50 µg/ml A22 demonstrate that the lateral complexes are affected by A22 treatment. Consistent with this, *E. coli* MC1000Δ*mreB* cells expressing either GFP-PspA or PspG-GFP also demonstrate that either disruption or removal of MreB results in only static polar GFP-PspA and PspG-GFP complexes being visible, the mobile lateral complexes (seen in Figure 5.9) can no longer be observed All images were taken using Nikon TE-2000 inverted optical microscope with a time-resolution of 80 ms / frame (see section 2.5.8.2). For each condition and strain, 60 cells were analysed. Each cell shown represents the localisation pattern typical of >90% of the population (For original images see Appendix G).

A



B

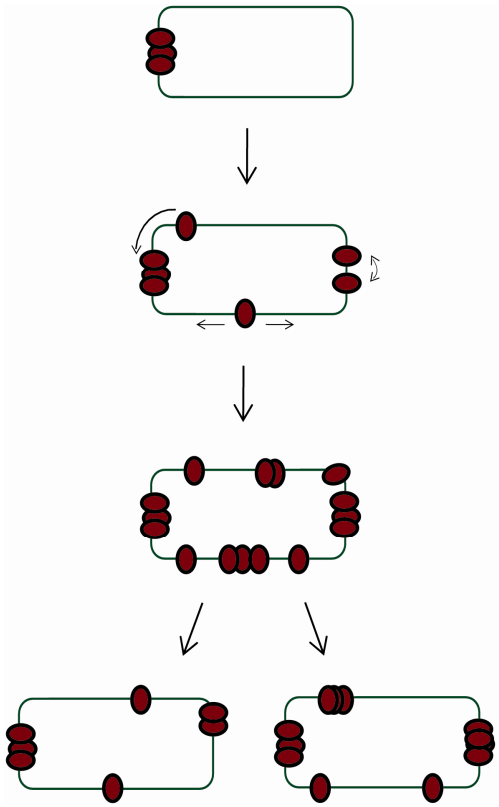


Figure 5.11: Positioning of polar complexes (A: adapted from Shih *et al.*, 2005; B: adapted from Greenfield *et al.*, 2009)**. (A)** Shih *et al.* (2005) propose that polar localisation of the chemoreceptor Tar is dependent on MreB. Loss of MreB results in mislocalisation of polar proteins, either directly (through loss of the cytoskeletal structure) or indirectly (through the altered cell-shape in ΔmreB cells). **(B)** Greenfield *et al.* (2009) suggest, formation and maintenance of polar chemoreceptor (here: Tar) clusters is a random event. Stochastic self-assembly occurs independently of other cell components in a way that maximal distance between 2 clusters is ensured. Hence, a single polar cluster will induce the formation of a cluster at the opposite pole. If clusters are present at both poles, cluster formation will occur in mid-cell.

To determine whether a direct interaction between the Psp system and MreB is occurring, *cya*-based bacterial-two-hybrid assays (BACTH) (Karimova *et al.*, 1998 & 2005) with PspA, PspB, PspC and PspG was performed (see section 2.5.2) (Figure 5.12A). Pair-wise interactions of the 2 proteins of interest were assessed by measuring the β-galactosidase (LacZ) activity. An interaction was scored as positive if the LacZ activity was 2-fold higher (approximately 252 MU) than the negative control, pUT18C + pKT25 (84±13 MU). MreB is known to interact with itself, thereby forming a helical polymer (Jones *et al.*, 2001), which was used as a positive control to score for the functionality of the MreB fusion proteins (T18-MreB and T25-MreB) and was measured as a significant increase in the LacZ activity (1653±75 MU).

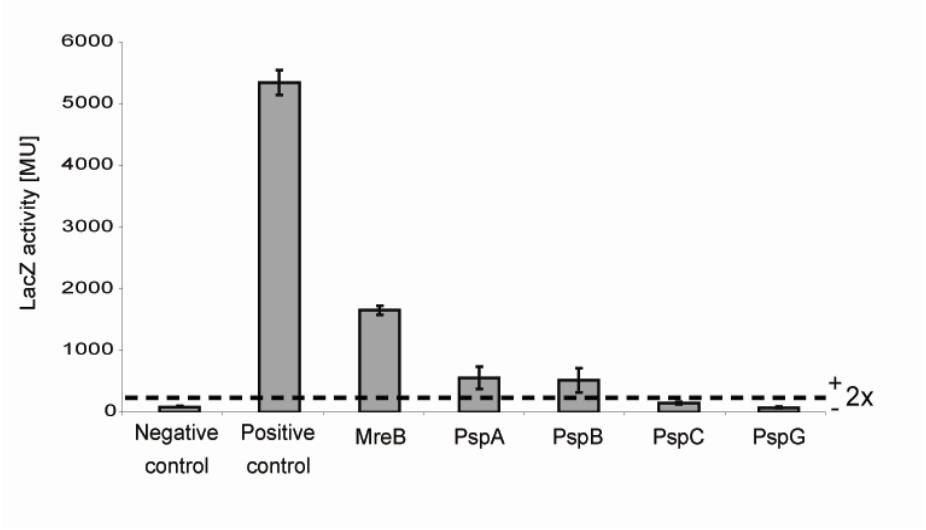
Consistent with the sub-cellular delocalisation of PspA, in the presence of A22 and in MC1000Δ*mreB* cells, the average LacZ activity of cells expressing T18-PspA and T25-MreB (559±183 MU) was well above the 2-fold threshold over the negative control value. Co-expression of T18-MreB and T25-PspB also significantly increased the LacZ activity (521±195 MU). Hence, the data indicate that PspA and PspB associate with MreB, potentially interacting directly or as part of a complex containing additional factors. However, PspC (147±17 MU) and PspG (75±13 MU) do not appear to directly interact with MreB. PspG has been observed to co-purify with PspA (LJL unpublished data), suggesting that PspG might indirectly interact with MreB via PspA, potentially explaining the loss of lateral trafficking of PspG upon A22 treatment. To exclude the possibility of false negatives, the BACTH interactions of PspA with PspB and PspC were also tested (data not shown). The results obtained were consistent with previous findings where PspA interacts with PspB and PspC

(see section 1.5.4.4.2) (Adams *et al.*, 2003), confirming that the lack of interactions with MreB were not the result of mis-folded protein fusions.

To further explore the potential interaction between PspA and MreB (suggested by the BACTH assay) the *in vivo* cross-linking pattern of GFP-PspA in *E. coli* MG1655Δ*pspA*/GFP-PspA and MC1000Δ*pspA*Δ*mreB*/GFP-PspA cells was compared (see section 2.5.5). Following SDS-PAGE, the cross-linked GFP-PspA protein complexes were visualised using antibodies against GFP (Figure 5.12B). In addition to monomeric GFP-PspA (53 kDa), in MG1655Δ*pspA*/GFP-PspA and MC1000Δ*mreB*/GFP-PspA cells treated with DSP (PIERCE) 3 higher molecular weight bands (Figure 5.12B, indicated by asterisks) were observed. These bands could no longer be detected in the presence of DTT (which specifically cleaves the cross-linker) and were absent in the negative controls, MG1655Δ*pspA*/GFP and MC1000Δ*mreB*/GFP (data not shown), indicating that these species are indeed cross-linked GFP-PspA complexes.

If a direct interaction between MreB and PspA was occurring, then one of these cross-linked species (Figure 5.12B) could represent GFP-PspA-MreB. In cells lacking MreB (MC1000Δ*mreB*Δ*pspA*/GFP-PspA) a quantitative change to the cross-linking pattern in the presence of DSP compared to cells harbouring the chromosomal *mreB* gene (MG1655Δ*pspA* / GFP-PspA) was observed, with the middle cross-linked species present at a consistently lower level (Figure 5.12B). These data indicate that MreB (either directly or indirectly) contributes to the formation of complexes containing GFP-PspA, although a single stable MreB-PspA complex is not resolved.

A



B

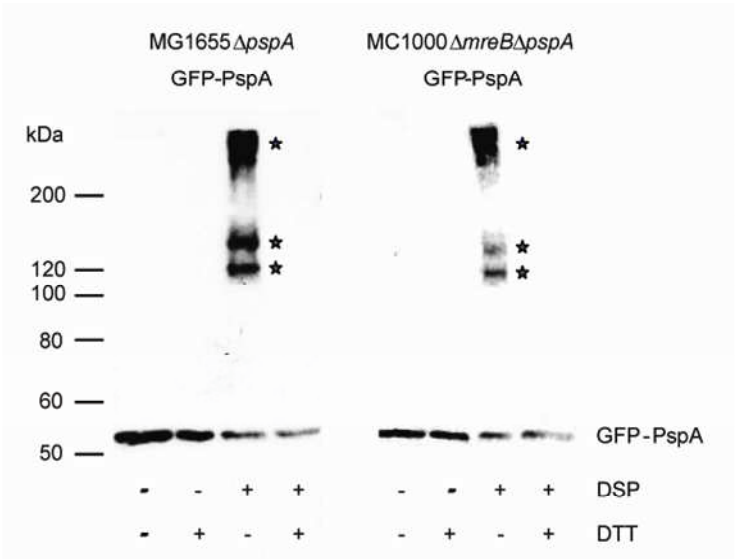


Figure 5.12: Weak or transient interactions occur between PspA or PspB and MreB. (A) Pair-wise interactions of MreB with MreB, PspA, PspB, PspC or PspG were tested using the *cya*-based bacterial-two-hybrid (BACTH) assay (see section 2.5.2) (Karimova *et al.*, 1998 & 2005). A more than 2-fold increase in the LacZ activity above the negative control level (T18+T25) (indicated as dashed line) was scored as positive interaction. Positive control: T18zip + T25zip. **(B)** *In vivo* protein cross-linking (see section 2.5.5) in GFP-PspA expressing MG1655Δ*pspA* and MC1000Δ*mreB* cells indicates the presence of 3 new cross linked species (asterisks) which were determined to contain GFP-PspA using GFP-specific antibodies. The specificity of the cross-linked species was confirmed using the reducing agent DTT.

5.3.4 Psp induction can occur independently of an assembled MreB scaffold whereas PMF maintenance by Psp requires the MreB scaffold

It has been shown recently that A22 inhibits peptidoglycan synthesis during elongation (Uehara and Park, 2008). This might be the consequence of impaired MreB polymerisation and may (by itself) cause IM stress to the cell. In line with this, both A22 and *mreB* gene deletion induces the Psp IM stress response as measured by the β-galactosidase activity from cells harbouring a chromosomal *pspA* promoter *lacZ* fusion (Figure 5.13A). Importantly a further increase in *pspA-lacZ* expression was observed following induction of pIV in the Δ*mreB* mutant. Together with the epi-fluorescence images where GFP-PspA is found only at the poles upon A22 treatment (Figure 5.10), it is conceivable that signalling, sensing and the release of the PspAF inhibitory complex could occur within these complexes found at the cell poles upon A22-treatment, if a cytoplasmic and regulatable PspAF complex does not exist.

Since the Psp system is induced by stresses which interfere with cell envelope integrity and MreB is involved in peptidoglycan synthesis (Osborn and Rothfield, 2007), the potential trafficking of PspA and PspG along the MreB cytoskeleton may therefore coincide with a direct role of the Psp response in cell wall biosynthesis, which in turn might help maintain the PMF of stressed cells. The relationship between the effector functions of PspA and PspG and the lateral complexes was probed by measuring PMF conservation under pIV secretin stress in cells treated

with A22 and in cells deleted for the MreB cytoskeleton (MC1000Δ*mreB*) (Figure 5.13B).

WT *E. coli* cells demonstrate no change in PMF upon pIV-induced IM stress, presumably due to the action of the Psp effectors (see section 1.5.4.2.1) (Jovanovic *et al.*, 2006). Stressed cells lacking the transcriptional activator PspF are unable to produce Psp proteins (see section 1.5.4.4.2) and therefore fail to maintain WT PMF levels. The PMF in WT *E. coli* cells treated with A22 or cells deleted for *mreB* remains high. In contrast to pIV secretin, A22 does not cause a drop in PMF in cells deleted for PspF (MG1655Δ*pspF* A22) but rather causes an increase in PMF. This suggests that some targets of A22, including the Psp effector proteins, will function in PMF homeostasis. When Psp proteins are induced by pIV, in cells treated with A22 or deleted for *mreB* (each a condition where lateral Psp proteins will be lacking) PMF is significantly decreased. This decrease in PMF is strikingly similar to MG1655Δ*pspF* cells expressing pIV, which are unable to mount a Psp response. The PMF drop in pIV expressing cells lacking the lateral Psp complexes implies that the helical Psp trafficking may be important for maintaining PMF under pIV-induced stress (Figure 5.13B). Interestingly, cells deleted for *pspF* show a significant increase in PMF upon A22 treatment compared to WT cells, which may further relate to the absence of lateral Psp protein complexes.

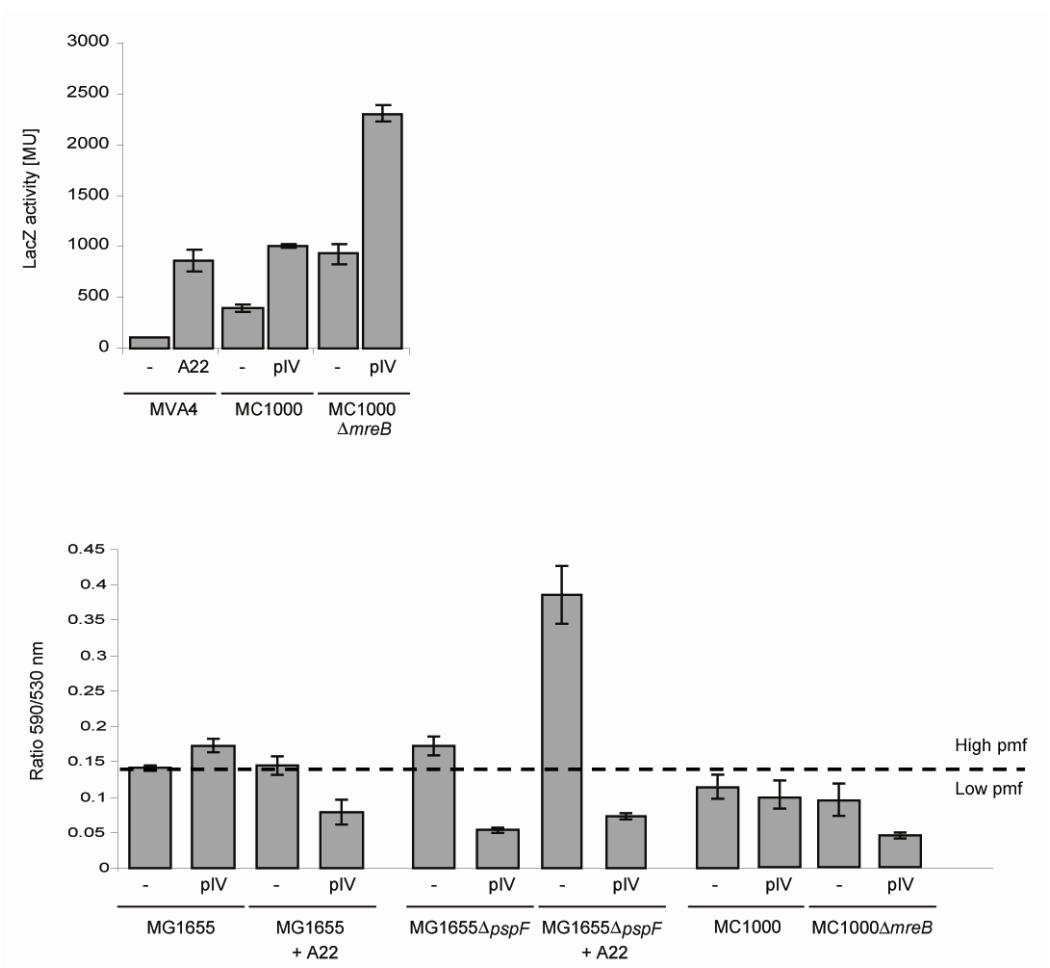


Figure 5.13: Psp induction and maintenance of PMF in cells lacking the MreB scaffold. The effect of impaired trafficking of Psp proteins was analysed in *E. coli* cells treated with A22 and deleted for *mreB*. **(A)** Induction of the Psp response was measured using β-galactosidase assays and a chromosomal ϕ*pspA-lacZ* transcriptional reporter fusion (see section2.4.4). Both, A22 treatment and deletion of *mreB* significantly induce Psp transcription. **(B)** Maintenance of PMF in cells lacking helical Psp trafficking was tested using the electron potential indicator dye JC1 (see section 2.5.6) (Jovanovic *et al.*, 2006). PMF was measured as the 590/530 nm ratio emitted from cells averaged across 3 different microscopic fields. Increase in ratio values corresponds to an increase in electron potential.

5.3.5 PspA and PspG form oligomers in vivo

According to gel-filtration chromatography profiles (Kobayashi *et al.*, 2007; Joly *et al.*, 2009) and structural studies (Hankamer *et al.*, 2004; Standar *et al.*, 2008), PspA can form higher-order oligomers *in vitro*. Kobayashi *et al.* (2007) also showed that oligomeric PspA can directly interact with lipids and somehow block proton leakage of membrane vesicles and liposomes (see section 1.5.4.2.1).

Here, the number of molecules in a fluorescent cluster of GFP-PspA as well as PspG-GFP was estimated by measuring its relative fluorescence intensity within living cells. For this ratio-metric approach, single molecule fluorescence imaging and objective-type total internal reflection fluorescence (TIRF) was used (see section 2.5.8.3), and the fluorescence intensity measured was compared to the fluorescence intensity of GFP foci from cell lysates of *E. coli* MG1655 harbouring pDSW209.

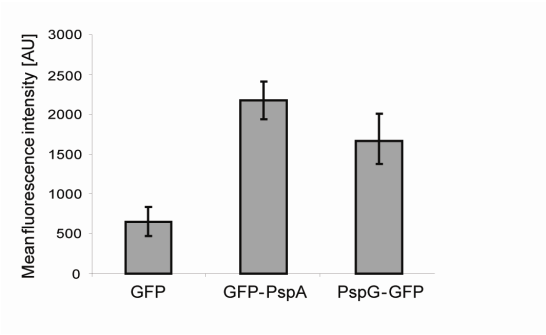
The present study shows for the first time that both, PspA and PspG form oligomers *in vivo* (Figure 5.15), supporting the previous *in vitro* findings on the structure of PspA complexes. Two distinct oligomeric sub-classes of PspA within the living cell were observed. Approximately half of the 50 complexes analysed appeared to have 2- to 3-fold higher fluorescence intensities than GFP alone (Figure 5.15B). The second subclass (~20%) exhibited “off-scale” fluorescence intensities, which were clearly more than 6-fold above GFP alone (Figure 5.15B). This is in full agreement

with reports from gel-filtration experiments, where PspA was observed to form lower-order as well as high-order oligomers (Joly *et al.*, 2009)

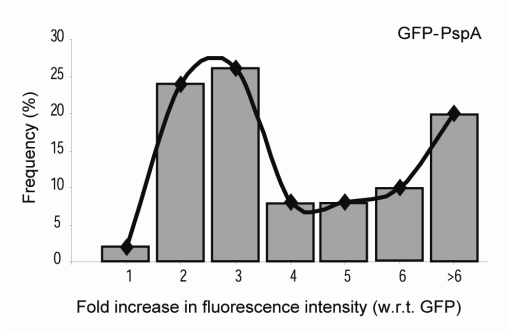
In contrast, PspG-GFP mainly forms one oligomeric class of complexes exhibiting a 3-fold increase in fluorescence intensity with respect to GFP (Figure 5.15B).

Although the TIRF mode may underestimate the number of proteins in the oligomer, since (i) the imaged complex may not be optimally positioned to record its full fluorescence (the TIRF field decays exponentially with distance from the interface and the membrane surface may be a significant distance away from the microscope slide) and (ii) some complexes were larger than those quantitatively analysed, referred to as "off-scale", it is evident, that PspA self-assembles in different oligomeric states *in vivo* whereas PspG appears to form only 1 distinct oligomer.

A



B



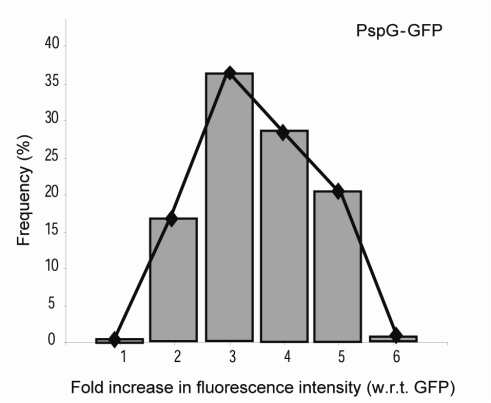


Figure 5.15: GFP-PspA and PspG-GFP form high-order oligomers *in vivo*. Analysis of the *in vivo* oligomerisation state of PspA was performed by single molecule fluorescence imaging using objective-type total internal reflection fluorescence (TIRF) on a Nikon TE-2000 inverted optical microscope (see section 2.5.8.3). The number of molecules in fluorescent complexes was estimated using the ImageJ software. The intensity of a single pixel in a fluorescent GFP-PspA and PspG-GFP cluster expressed in *E. coli* MG1655Δ*pspA* and MG1655Δ*pspG* cells was measured and compared to GFP from cell lysates of WT *E. coli* MG1655 cells harbouring pDSW209. **(A)** The mean fluorescence intensity of 50 GFP-PspA and PspG-GFP complexes within living cells was on average at least 3 times higher than GFP spots, suggesting that PspA can form higher oligomers *in vivo*. **(B)** The frequency distribution amongst the 50 complexes analysed showed that GFP-PspA self-assembles into 2 distinct oligomeric subclasses whereas PspG-GFP can be found mainly in 1 oligomeric form.

5.4 DISCUSSION

Studying the spatial organisation of a protein can provide insights into its function and integration within the network of cellular processes. In the present study, GFP-labelled PspA and PspG, two members of the Phage shock protein (Psp) response, were visualised in *E. coli* using a combination of epi-, confocal and TIRF microscopy. Functional assays with these fusion proteins indicate that the information obtained in this work faithfully represents the native organisation of PspA and PspG within the living *E. coli* cell. This study permitted the analysis of the mode of action and the relationship between the Psp response and other proteins and cellular processes and revealed distinct classes of Psp molecules and a link to cytoskeletal features of the cell.

5.4.1 GFP-PspA and PspG-GFP accumulate at the cell poles

Using fluorescence microscopy, PspA and PspG fusion proteins were observed to localise at cell poles. Polar localisation was confirmed using cells deleted for the MinCDE sytem (*E. coli* MC1000Δ*minCDE*), in which both GFP-PspA and PspG-GFP were found within minicells (which resemble the polar region of the cell). The accumulation of PspA and PspG at the poles was unaffected by A22, suggesting that polar positioning is independent of the MreB cytoskeleton. As discussed below, being localised at the cell pole could be important for the function of PspA and PspG.

Previously, deletion of either PspA or PspG was observed to significantly increase the expression of proteins involved in chemotaxis and motility, e.g the methyl-accepting chemotaxis proteins (MCPs) Tar, Tap and Tsr (see section 1.5.4.2.1) (Jovanovic *et al.*, 2006). These chemoreceptors are part of super-molecular complexes located in the IM at the cell pole (Maddock and Shapiro, 1993) where they sense environmental cues such as attractants or repellents and co-ordinate the chemotactical behaviour of the cell by adjusting the response of the PMF-consuming flagellar motor (see section 1.2.3.1). Polar localised Psp proteins might act in concert with other polar proteins such as chemoreceptors to govern sensory inputs for PMF-consuming key cell properties such as motility, potentially in response to the energy state of the cell.

The Psp system is also implicated in virulence of pathogenic enterobacteria (see section 1.5.4.2.2) (Darwin, 2005). For example, Psp mutants of *Y. enterocolitica* show growth defects and attenuated virulence upon mislocalisation of the secretin from the type III secretion system (Darwin and Miller, 2001), and macrophage infection highly induces *psp* transcription in *S. enterica* and *Sh. flexneri* (Eriksson *et al.*, 2003; Darwin, 2005). Notably, 2 proteins involved in *Shigella* infection, IcsA (enabling intracellular movement within the mammalian host) and IpaC (a component of the T3SS) are also found at the pole (Goldberg *et al.*, 1993; Ebersbach and Jacobs-Wagner, 2007; Jaumouille *et al.*, 2008). It is therefore conceivable that accumulation of Psp proteins at the cell pole is linked to their proposed role in promoting enterobacterial infections.

Interestingly, Strauss *et al.* (2008) proposed that local differences exist in the pH gradient across the IM cristae in mitochondria. According to their model, although a constant electrochemical potential exists along the entire IM surface, the local pH gradient, and hence the ΔpH contribution to the PMF, is significantly higher in regions of high-membrane curvature (Strauss *et al*. 2008). Applied to bacteria, this model suggests that both poles in rod-shaped cells might serve as proton sinks due to the increased pH gradient in this area. Protons leaking into the cytoplasm as a result of impaired IM integrity due to envelope stress might therefore preferentially accumulate at the cell poles. Since the contribution of ΔpH to the PMF appears to be higher in this region, even small changes in the ΔpH might have a stronger effect on PMF at the poles than at lateral regions of the cell. Hence, the poles might be the most sensitive part of the cell to measure changes in the electrochemical gradient. The results from Chapter 4 imply that a drop in PMF alone is not sufficient to induce Psp. However, it can not be ruled out that PMF-dissipation contributes to the inducing signal. Polar localisation of Psp proteins could therefore be important to perceive subtle changes in PMF and subsequently allow for a quick response to IM stress. Importantly, the polar complexes found upon A22 treatment alone are sufficient to mount a “Psp response” in terms of signalling, sensing and release of PspA from PspF (Figure 5.13A).

5.4.2 MreB-dependent lateral complexes and the trafficking of GFP-PspA and PspG-GFP

In addition to the polar localisation of GFP-PspA and PspG-GFP, fluorescence intensity measurement across the cell and their detection in rod-shaped *E. coli* MC1000Δ*minCDE* cells indicated the presence of PspA and PspG along the length of the cell. The movements they displayed were reminiscent of the MreB cytoskeleton, which hence might be involved in the lateral organisation of PspA and PspG. Using A22 and an *E. coli* strain lacking MreB, it could be demonstrated that lateral GFP-PspA and PspG-GFP complexes were no longer visible, implying MreB assists lateral Psp complexes, possibly through their i) formation and/or ii) maintenance or iii) movements. The latter is reflected in the path taken (Figure 5.9B) which resembles the MreB cytoskeletal structure (Figure 5.11). Although BACTH and *in vivo* cross-linking analyses could not establish strong stable direct interactions between Psp proteins and MreB, the data do clearly indicate that PspA as well as PspB might interact weakly/transiently or indirectly with MreB.

The mobility of the lateral complexes of GFP-PspA and PspG-GFP could be one consequence of these weak/transient interactions with the MreB cytoskeleton, which could serve as a scaffold supporting rapid trafficking across the entire cell. Since MreB is thought to have a role in cell wall biogenesis (Kruse *et al.*, 2005) and the trafficking of Psp proteins appears MreB-dependent, Psp effectors may also have a role in cell envelope biosynthesis. This view is supported by findings showing that Psp is induced upon inhibition of lipid biosynthesis in *E. coli* (Bergler *et al.*,

1994) and by cell wall biosynthesis defects in a *glmS* mutant of *Y. enterocolitica* (Maxson and Darwin, 2004).

The data presented in Chapter 4 suggest that Psp may respond to changes in the redox state of the ubiquinone pool. Ubiquinones are electron carriers in the electron transport chain (ETC) transferring electrons from an electron-donor to an electron-acceptor under both, aerobic and microaerobic respiration (see section 1.2.3.2 and 4.1). Lenn *et al.* (2008a) visualised the subcellular localisation of the cytochrome *bd*-I terminal oxidase, a component of the ETC in *E. coli*. Based on their observations of a heterogeneous Cyt*bd*-I distribution, so called "respirazones" were proposed (Lenn *et al.*, 2008b). These are zones within the IM along the length of the *E. coli* cell with an increased local concentration of components of the ETC, such as quinones, in which respiration takes place. Lateral Psp complexes may co-localise with these respirazones where they could sense and respond to changes in the redox state of the ubiquinone pool caused by membrane stress such as pIV production (see Chapter 4).

5.4.3 PspA does not form a scaffold-like structure which evenly coats the IM

Higher-order oligomers of PspA have been proposed to evenly coat the cytoplasmic face of the IM to restore membrane integrity (see section 1.5.4.2.1) (Kobayashi *et al.*, 2007). The present sub-cellular localisation studies of PspA however do not entirely support all aspects of this model. Although the results establish for the first time that PspA (as well as PspG) forms oligomers *in vivo* (broadly in line with

previously reported *in vitro* data (Hankamer *et al.*, 2004; Kobayashi *et al.*, 2007; Standar *et al.*, 2008; Joly *et al.*, 2009), PspA does not evenly coat the IM of the live cell. Instead of uniformly covering the entire cell, PspA (and PspG) is highly organised into what appear to be distinct functional classes (polar and lateral complexes). Together they may maintain the PMF of the cell by regulating PMF consuming processes such as motility and cell envelope biogenesis, as well as by directly restoring membrane integrity (see section 1.5.4.2.1). The PspA and PspG complexes display a dynamic character when in association with the IM, and presumably make interactions with cellular components, in addition to lipids, potentially extending activities beyond their role of binding lipids to "plug" holes within the IM.

CHAPTER 6

OVERVIEW AND FUTURE DIRECTIONS

6.1 OVERVIEW

Bacteria in their natural habitats encounter a variety of stressful conditions that potentially impair the integrity of the cell envelope. In addition to being a barrier between the inside of the cell and the environment, the cell envelope is the site of numerous cellular processes. One of the most important functions of the cell envelope is the generation of energy in form of the PMF. Robustness of the cell envelope is therefore crucial for cell survival. Gram-negative bacteria employ systems to maintain membrane integrity, one of which is the Psp response. In *E. coli,* the Psp response comprises 7 genes organised in a regulon (*pspF pspABCDE* and *pspG*) controlled by a Sigma54-dependent promoter. Psp gene transcription requires activation by PspF, is positively controlled by PspBC and negatively regulated by PspA (Model *et al*., 1997; Darwin, 2005 & 2007). It is assumed that Psp expression is induced upon IM stresses which dissipate PMF. Psp effector proteins help to maintain PMF under stress (Kleerebezem *et al.*, 1996; Jovanovic *et al.*, 2006, Kobayashi *et al.*, 2007). Understanding the mechanism of Psp induction and its biological function is important since the Psp system is significant in protein translocation and in the growth and virulence of pathogenic enterobacteria (Darwin, 2005 & 2007; Rowley *et al.*, 2006). Further, PspA appears to have a fundamental role in membrane biogenesis and energy conservation in all three domains of life. Expression of PspA homologues has been reported in Gram-positive bacteria and archea under environmental stress conditions (Bidle *et al.*, 2008; Vrancken *et al.*, 2008) and a PspA homologue, Vipp1, is essential in plants and *Synechocystis* for thylakoid biogenesis and photosynthesis (Westphal *et al*., 2001).

To date, the mechanism of signal-perception by Psp as well as the nature of the signal is not well understood (Darwin, 2005 & 2007). Jovanovic *et al.* (2006) proposed that ArcB, the sensor kinase of the two-component ArcAB system (a master regulator for the switch from aerobic to anaerobic respiration and fermentation; Malpica *et al.*, 2006), is required for full pIV-dependent *psp* expression in *E. coli* and that *psp*-inducing stresses that dissipate the PMF could initially activate ArcB. However recently, Seo *et al.* (2007) observed ArcB-independent Psp induction in both *E. coli* and *Y. enterocolitica*.

It was proposed that this discrepancy might be explained by differences in growth conditions used in the 2 experimental settings. The effect of changes in growth conditions on the potential relationship(s) between the Psp and Arc system was therefore explored further. The results from Chapter 3 show that the involvement of Arc is indeed conditional, thereby reconciling both observations (Jovanovic *et al.*, 2006; Seo *et al.*, 2007). ArcAB appears to have a major involvement in signal-propagation for induction of the Psp response under microaerobic growth, but not when cells are grown aerobically or anaerobically. The results suggest 2 ways to transduce the Psp-signal via the Arc system under microaerobic growth i) activated ArcB (itself) increases expression of the *psp* genes and ii) phosphorelay from ArcB to ArcA seems to be important for signal-amplification.

BACTH results show that this cross-talk between the ArcAB and the Psp system may be mediated via a direct protein-protein interaction between ArcB and PspB. Notably, in anaerobiosis, pIV-dependent *psp* expression is largely independent of PspBC (positive regulators of the Psp response) and ArcAB proteins, suggesting that

either the repressive PspAF complex is (itself) capable of recognising inducing signals, or that PspBC and ArcAB are substituted by other gene products. This is fully in line with findings that PspBC are only partially required for induction of *psp* gene expression when induced by ethanol treatment or hyperosmotic shock, and redundant upon induction by extreme heat shock (Weiner *et al.*, 1991). This is also consistent with reports indicating that so far only homologues of PspA, and not PspBC, have been found in many other organisms (Westphal *et al*., 2001; Bidle *et al.*, 2008; Vrancken *et al.*, 2008).

The findings that under microaerobic growth Psp signal-perception involves activation of ArcB imply that at least under such conditions the primary signal for Psp induction acts upstream of ArcB. Several studies point to the quinone pool as a candidate for such a signal, since it was reported that ArcB can be activated by changes in the redox state of both ubi- and menaquinones (Georgellis *et al.,* 2001; Malpica *et al.*, 2004; Bekker *et al.*, 2009) and since cells deleted for *ubiG*, part of the ubiquinone-biosynthesis pathway, showed reduced Psp expression (Jovanovic *et al.*, 2006). It was therefore tested by direct quinone measurements under Psp inducing and non-inducing conditions, whether changes in the quinone pool indeed impact on the induction of the Psp response (see Chapter 4).

Electron transport mutants, each with differing ubiquinone content showed variations in the level of Psp induction even in the absence of obvious cell envelope stress. These variations appeared to correlate with a shift of the redox state of ubiquinone towards more reduced state. Additionally, cells with an intact electron transport chain but under pIV stress also showed changes in the ubiquinone pool

when compared to unstressed cells. Production of pIV appears to decrease the percentage of reduced UQ_8-H_2. Intriguingly, these correlations were more pronounced under microaerobic growth, where activation of ArcB is required for Psp induction, than under aerobic growth, a condition under which Psp is induced independently of ArcB. Additionally, the effect is specific for ubiquinone since cells lacking menaquinones showed no marked differences in Psp induction. Accordingly, Psp may, at least under microaerobic growth, respond via ArcB to changes in the redox state of the ubiquinone (but not menaquinone) pool in either direction, towards a more reduced or more oxidised state - indicative of i) a homeostatic role for the Psp response and ii) a ratiometric sensory component. Moreover, on a molecular level, Psp does not seem to differentiate how this change is caused, either by mutations in the ETC or by alterations in the cell envelope integrity (e.g. through pIV production). Both result in a changed ubiquinone pool and hence induce Psp.

The results from Chapter 4 indicate further, that in contrast to what is generally assumed PMF dissipation alone is not sufficient to induce the Psp response. Firstly, the electron transport mutants showed different levels of Psp induction, their PMF however was similar to that of the WT strain, where Psp was not induced. Secondly, individual dissipation of the PMF components $\Delta\psi$ or ΔH^+ by either the K^+-ionophore Valinomycin or by acetate (pH 5) did not increase Psp expression in WT *E. coli* strains. This might explain the following paradox:

The Psp response is still continually induced in pIV-producing cells although Psp functions to maintain PMF and therefore would cause a loss of the inducing signal should it be PMF dissipation.

It is more likely that the Psp response in its "on"-state can not directly confront the inducing signal otherwise Psp would not be continually induced in pIV-producing cells. In contrast to the drop in PMF, the changes in the redox state of the ubiquinone pool caused by pIV prevail even when the Psp response is "on" supporting the idea that these changes may contribute to the signalling activity and are needed for continued *psp* expression under pIV stress.

According to the subcellular localisation study presented in Chapter 5, PspA and PspG are spatially organised in distinct classes and linked to the cytoskeleton of the cell. Some complexes, localised in the polar region of the cell, were rather immobile while other complexes displayed a range of curved and linear motions along the length of the cell. The polar localised complexes may directly communicate with other systems in this area to modulate PMF consuming processes such as chemotaxis or to promote pathogenicity via e.g. type III secretion. Lateral complexes may co-localise with zones composed of components of the ETC (respirazones), where they could sense the above mentioned changes in the redox state of the ubiquinone pool. Lateral trafficking was absent in cells treated with the compound A22 indicating that it is facilitated by the MreB scaffold. This lends support to a role for Psp in cell wall biogenesis in conjunction with other MreB-associated proteins, such as penicillin binding proteins, in order to repair stress-induced membrane damage and maintain PMF. Indeed, PMF is only maintained when PspA and PspG can move along the length of the cell. Counting the number of molecules in the fluorescent complexes indicated that both, PspA and PspG form oligomers *in vivo*. Joly *et al.* (2009) showed by gel-filtration analysis that PspA

assembles into 2 oligomeric states, a lower-order and a high-order oligomer. Notably, only the lower-order oligomer was able to interact with the transcriptional activator PspF. Kobayashi *et al.* (2007) on the other hand showed that only the higher-oligomeric form of PspA can block proton leakage from liposomes and vesicles. This suggests a switch mechanism between PspA negative-regulatory and effector function based on its oligomerisation state. The *in vivo* data on the number of molecules in PspA complexes presented in Chapter 5 is fully in line with this, since it also identified 2 sub-classes of PspA, lower- and higher-order oligomers.

The proposed scaffold-like structure formed by PspA underneath the IM in order to alter the biophysical properties of the cell envelope thereby blocking proton leakage (Kobayashi *et al.*, 2007) however could not be observed.

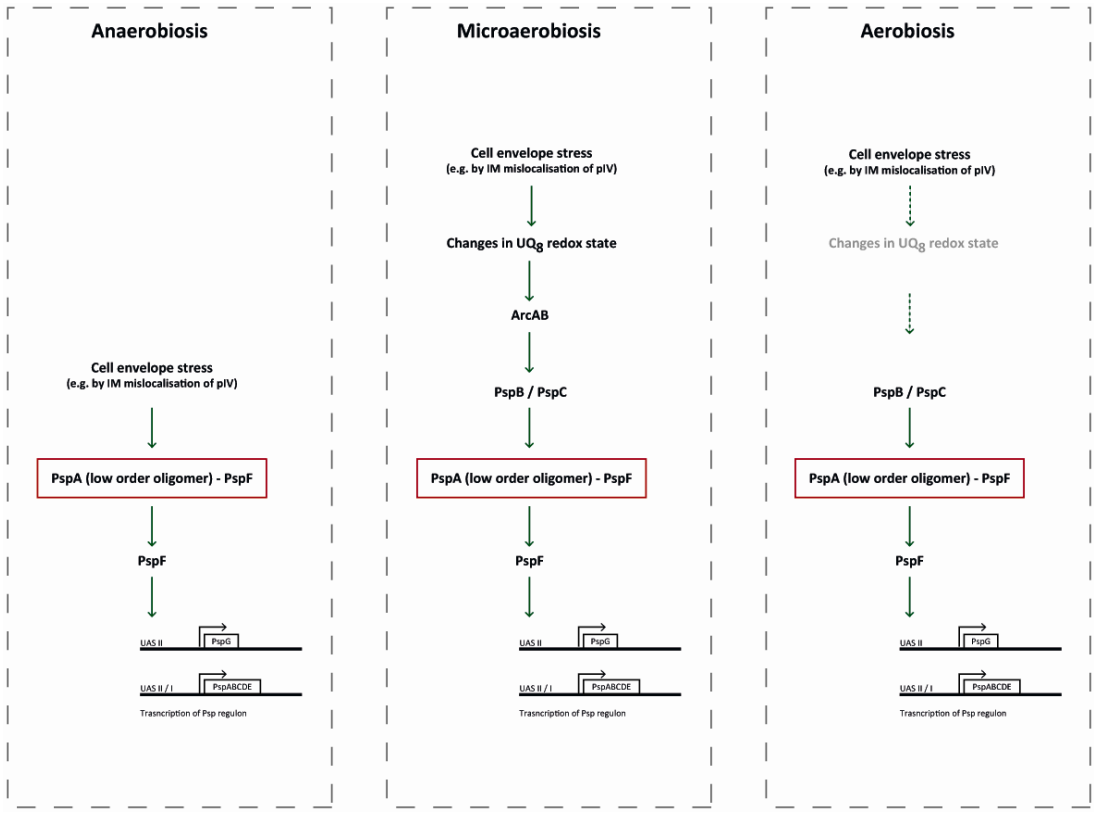


Figure 6.1: Summary of the findings on the signalling pathway of the Psp response. The results from this study lend support to a complex aeration-dependent regulation of the Psp response. Under anaerobic growth, the PspA-PspF inhibitory complex appears to be able to sense the cell envelope stress independently of the positive regulators PspBC and ArcAB. Under microaerobic growth, pIV production causes a continuous change in the redox state of the UQ_8 pool. This change may be sensed by ArcAB, which are required for Psp induction under microaerobic growth. The cross-talk between ArcAB and Psp may be mediated via protein-protein interactions between ArcB and PspB. PspBC then transduce the signal to the PspA-PspF complex and cause release of PspF for activation of Psp transcription. Induction of the Psp response under aerobic growth requires PspBC but is independent of the ArcAB system. Additionally, the change in the redox state of UQ_8 observed under microaerobic growth is less pronounced under aerobic growth and hence it is unclear whether this change is involved in Psp signal transduction under these conditions. Arrows indicate relatiosnships and do not represent order of events.

6.1 FUTURE DIRECTIONS

The experiments in Chapter 3 were conducted in batch cultures, which only allow for a relatively limited control of the growth conditions. However, it appears that ArcAB requirement for Psp induction is strictly dependent on the level of aeration. Future experiments could therefore be done using chemostat cultures at conditions under which the availability of oxygen can be quantified and further varied (Evans *et al.*, 1970; Alexeeva *et al.*, 2000). Cells with and without a functional ArcAB system could be grown under step-wise increasing oxygen levels (from 0% to 100%). Simultaneously at each step, samples could be taken to measure Psp induction by testing *pspA* promoter activity through β-galactosidase assays and by measuring the expression of Psp proteins by immunoblotting. This would allow for a precise mapping of the oxygen level under which ArcAB is required for the Psp signal-transduction and would provide the basis for further analysis of the determinants involved under these conditions. To further investigate the role of the ubiquinones in the Psp signalling cascade upstream of ArcAB, samples could also be taken to analyse the ubiquinones under these conditions in relation to Psp induction. Additionally, a comprehensive screen of the ubiquinone pool alongside measurements of PMF under a wide range of Psp inducing stimuli would also help to further substantiate their proposed involvement in Psp signalling.

The localisation study provides a useful platform to further establish the movements, quantities and oligomeric states of both PspA and PspG *in vivo.* For example, one could visualise PspA and PspG in strains lacking other Psp proteins to determine which members of the Psp response are required for their proper

localisation. Furthermore, recent advances in single-molecule single-cell imaging techniques allow for the quantitative analysis of determinants for the spatial organisation of the Psp response. Using chromosomally encoded fusions of Psp proteins to the rapidly maturing form of the yellow fluorescent protein, Venus, under the native promoter (and hence regulation) one could study the dynamics of *psp* gene expression before and after membrane stress e.g. pIV production. The contribution of regulatory elements such as UAS or IHF binding site (see section 1.5.4.4.2) could also be assessed using such experimental settings. Additionally, measuring the oligomeric state of PspA before and after stress might shed light on whether PspA indeed switches between its 2 functions by changing its oligomeric state.

Finally, attempts should be made to study interactions of Psp proteins with themselves and with lipids and membranes *in vitro*. The absence of any structures of PspBC, and little regarding PspA, should also be addressed by NMR and crystallography studies.

REFERENCES

REFERENCES

Adams, H., Teertstra, W., Koster, M., and Tommassen, J. (2002) PspE (phage-shock protein E) of *Escherichia coli* is a rhodanase. *FEBS Lett.* **518**: 173-176.

Adams, H., Teertstra, W., Demmers, J., Boesten, R., and Tommassen, J. (2003) Interactions between phage-shock proteins in *Escherichia coli*. *J. Bacteriol.* **185**: 1174-1180.

Ades, S.E. (2008) Regulation by destruction: design of the σ^E envelope stress response. *Curr. Opin. Microbiol.* **11**: 535-540.

Alami, M., Luke, I., Deitermann, S., Eisner, G., Koch, H.G., Brunner, J., and Mueller, M. (2003) Differential interactions between a twin-arginine signal peptide and its translocase in *Escherichia coli. Mol. Cell.* **12**: 937-946.

Alba, B.M., and Gross, C.A. (2004) Regulation of the *Escherichia coli* sigma-dependent envelope stress response. *Mol. Microbiol.* **52**: 613-619.

Aldon, D., Brito, B., Boucher, C., and Genin, S. (2000) A bacterial sensor of plant cell contact controls the transcriptional induction of *Ralstonia solanacearum* pathogenicity genes. *EMBO* **19**: 2304-2314.

Alexeeva, S., de Kort, B., Sawer, G., Hellingwerf, K.J., and de Mattos, M.J. (2000) Effects of limited aeration and of the ArcAB system on intermediary pyruvate catabolism in *Escherichia coli*. *J. Bacteriol.* **182**: 4934-4940.

Alexeeva, S., Hellingwerf K. J., and Teixeira de Mattos, M. J. (2003) Requirement of ArcA for redox regulation in *Escherichia coli* under microaerobic but not anaerobic or aerobic conditions. *J. Bacteriol.* **185**: 204-209.

Aoki, S. K., Webb, J. S., Braaten, B. A., and Low, D. A. (2009) Contact-dependent growth inhibition causes reversible metabolic downregulation in *Escherichia coli*. *J. Bacteriol.* **191**: 1777-1786.

Aseeva, E., Ossenbuehl, F., Sippel., C., Cho, W.K., Stein, B., Eichacker, L.A., Meurer, J., Wanner, G., Westhoff, P., Soll, J., and Vothknecht, U.C. (2007) Vipp1 is required for basic thylakoid membrane formation but not for the assembly of thylakoid protein complexes. *Plant Phys. Biochem.* **45**: 119-128.

Baba, T., Ara, T., Hasegawa, M., Takai, Y., Okumura, Y., Baba, M., *et al*. (2006) Construction of *Escherichia coli* K-12 in-frame, single-gene knockout mutants: the Keio collection. *Molecul. Systems Biol.* **2**: 2006.0008.

Baranova, N., and Nikaido, H. (2002) The *baeSR* two-component regulatory system activates transcription of the *yegMNOB* (*mdtABCD*) transporter gene cluster in *Escherichia coli* and increases its resistance to novobiocin and deoxycholate. *J. Bacteriol.* **184**: 4168-4176.

Bardy, S.L., and Maddock, J.R. (2007) Polar explorations. Recent insights into the polarity of bacterial proteins. *Curr. Opin. Microbiol.* **10**: 617-623.

Becker, L. A., Bang, l-S., Crouch, M.-L., and Fang, F. C. (2005) Compensatory role of PspA, a member of the phage shock protein operon, in *rpoE* mutant *Salmonella enterica* serovar Typhimurium. *Mol. Microbiol.* **56**: 1004-1016.

Beckwith, J., and Silhavy, T.J. (1983) Genetic analysis of protein export in *Escherichia coli*. *Methods Enzymol.* **97**: 3-11.

Bekker, M., Kramer, G., Hartog, A.F., Wagner, M.J., de Koster, C.G., Hellingwerf, K.J., and de Mattos, M.J. (2007) Changes in the redox state and composition of the

quinone pool of *Escherichia coli* during aerobic batch-culture growth. *Microbiology* **153**: 1974-1980.

Bekker, M., Alexeeva, S., Laan, W., Sawers, G., Teixeira de Mattos, J., and Hellingwerf, K. (2009) The ArcBA two-component system of *Escherichia coli* is regulated by the redox state of both the ubiquinone and the menaquinone pool. *J. Bacteriol.* Epub ahead of print 20th Nov 2009.

Beloin, C., Valle, J., Latour-Lambert, P., Faure, P., Kzreminski, M., Balestrino, D., Haagensen, J.A., Molin, S., Prensier, G., Arbeille, B., and Ghigo, J.M. (2004) Global impact of mature biofilm lifestyle on *Escherichia coli* K-12 gene expression. *Mol. Microbiol.* **51**: 659-674.

Berg, H.C. (2003) The rotary motor of bacterial flagella. *Annu. Rev. Biochem.* **72**: 19-54.

Bergler, H., Abraham, D., Aschauer, H., and Turnowsky, F. (1994) Inhibition of lipid biosynthesis induces the expression of the *pspA* gene. *Microbiology* **140**: 1937-1944.

Berks, B.C. (1996) A common export pathway for proteins binding complex redox cofactors? *Mol. Microbiol.* **22**: 393-404.

Berks, B.C., Palmer, T., and Sargent, F. (2005) Protein targeting by the bacterial twin-arginine translocation (Tat) pathway. *Curr. Opin. Microbiol.* **8**: 174-181.

Bidle, K. A., Kirkland, P. A., Nannen, J. L., and Maupin-Furlow, J. A. (2008) Proteomic analysis of *Haloferax volcanii* reveals salinity-mediated regulation of the stress response protein PspA. *Microbiology* **154**: 1436-1443.

Blocker, A., Gounon, P., Larquet, E., Niebuhr, K., Cabiaux, V., Parsot, C., and Sansonetti, P. (1999) The tripartite type III secretion of *Shigella flexneri* inserts IpaB and IpaC into host membranes. *J. Cell. Biol.* **147**: 683-693.

Bogsch, E.G., Sargent, F., Stanley, N.R., Berks, B.C., Robinson, C., and Palmer, T. (1998) An essential component of a novel bacterial protein export system with homologues in plastids and mitochondria. *J. Biol. Chem.* **273**: 18003-18006.

Bos, M.,P., Robert, V., and Tommassen, J. (2007) Biogenesis of the gram-negative bacterial outer membrane. *Annu. Rev. Microbiol.* **61**: 191-214.

Brissette, J.L., Russel, M., Weiner, L., and Model, P. (1990) Phage shock protein, a stress protein of *Escherichia coli*. *Proc. Natl. Acad. Sci. USA* **87**: 862-866.

Brissette, J.L., Weiner, L., Ripmaster, T.L., and Model, P. (1991) Characterization and sequence of the *Escherichia coli* stress-induced *psp* operon. *J. Mol. Biol.* **220**: 35-48.

Brueser, T., Yano, T., Brune, D.C., and Daldal, F. (2003) Membrane targeting of a folded and cofactor-containing protein. *Eur. J. Biochem.* **270**: 1211-1221.

Buck. M., Gallegos, M.T., Studholme, D.J., Guo, Y., and Gralla, J.D. (2000) The bacterial enhancer-dependent σ^{54} (sigma N) transcription factor. *J. Bacteriol.* **182**: 4129-4136.

Buck, M., Bose, D., Burrows, P., Cannon, W., Joly, N., Pape, T., Rappas, M., Schumacher, J., Wigneshweraraj, S., and Zhang, X. (2006) A second paradigm for gene activation in bacteria. *Biochem. Soc. Trans.* 34: 1067-1071.

Burns, D.L. (1999) Biochemistry of type IV secretion. *Curr. Opin. Microbiol.* **2**: 25-29.

Callahan, A.M., Frazier, B.L., and Parkinson, J.S. (1987) Chemotaxis in *Escherichia coli*: construction and properties of lambda tsr transducing phage. *J. Bacteriol.* **169**: 1246-1253.

Celebi, N., Yi, L., Facey, S., Kuhn, A., and Dalbey, R.E. (2006) Membrane biogenesis of subunit II of cytochrome bo oxidase: contrasting requirements for insertion of N-terminal and C-terminal domains. *J. Mol. Biol.* **357**: 1428-1436.

Cheng, H., Donahue, J.L., Battle, S.E., Ray, W.K., and Larson, T.J. (2008) Biochemical and genetic characterization of PspE and GlpE, two single-domain sulfurtransferases of *Escherichia coli*. *Op. Microbiol. J.* **2**: 18-28.

Cherepanov, P. P., and Wackernagel, W. (1995) Gene disruption in *Escherichia coli*: Tc^R and Km^R cassettes with the option of Flp-catalyzed excision of the antibiotic-resistance determinant. *Gene* **158**: 9-14.

Clausen, T., Southan, C., and Ehrmann, M. (2002) The HtrA family of proteases: implications for protein composition and cell fate. *Mol. Cell* **10**: 443-455.

Cormack, B.P., Valdivia, R.H., and Falkow, S. (1996) FACS-optimized mutants of the green fluorescent protein (GFP). *Gene* **173**: 33-38.

Cornelis, G.R. (1998) The *Yersinia* Yop virulon, a bacterial system to subvert cells of the primary host defence. *Folia Microbiol. (Praha)* **43**: 253-261.

Cornelis, G.R. (2002) The *Yersinia* Ysc-Yop "type III" weaponery. *Nat. Rev. Mol. Cell. Biol.* **3**: 742-752.

Cotter, S.E., Surana, N.K., and St Geme, J.W., 3rd. (2005) Trimeric autotransporters: a distinct subfamiliy of autotransporter proteins. *Trends Microbiol.* **13**: 199-205.

Craig, L., Pique, M.E., and Tainer, J.A. (2004) Type IV pilus structure and bacterial pathogenicity. *Nat. Rev. Microbiol.* **2**: 363-378.

Cunningham, K., and Wickner, W.T. (1989) Specific recognition of the leader region of precursor proteins is required for the activation of translocation ATPase of *Escherichia coli*. *Proc. Natl. Acad. Sci. USA* **86**: 8630-8634.

Danese, P.N., Snyder, W.B., Cosma, C.L., Davis, L.J., and Silhavy, T.J. (1995) The Cpx two-component signal transduction pathway of *Escherichia coli* regulates transcription of the gene specifying the stress-inducible periplasmic protease, DegP. *Genes Dev.* **9**: 387-398.

Danese, P.N., and Silhavy, T.J. (1997) The σ^E and the Cpx signal transduction systems control the synthesis of periplasmic protein-folding enzymes in *Escherichia coli*. *Genes Dev.* **11**: 1183-1193.

Danese, P.N., and Silhavy, T.J. (1998) Targeting and assembly of periplasmic and outer-membrane proteins in *Escherichia coli*. *Annu. Rev. Genet.* **32**: 59-94.

Daniel, R.A., and Errington, J. (2003) Control of cell morphogenesis in bacteria: two distinct ways to make a rod-shaped cell. *Cell* **113**: 767-776.

Darwin, A.J., and Miller, V.L. (1999) Identification of Yersinia enterocolitica genes affecting survival in an animal host using signature-tagged transposon mutagenesis. *Mol. Microbiol.* **32**: 51-62.

Darwin, A.J., and Miller, V.L. (2001) The *psp* locus of *Yersinia enterocolitica* is required for virulence and for growth in vitro when the Ysc type III secretion system is produced. *Mol. Microbiol.* **39**: 429-444.

Darwin, A. J. (2005) The phage-shock-protein response. *Mol. Microbiol.* **57**: 621-628.

Darwin, A. J. (2007) Regulation of the phage-shock-protein stress response in *Yersinia enterocolitica*. In: *The Genus Yersinia*. *From Genomics to Function*. Perry, R. D., and Fetherston, J. D. (eds.). Advances in Experimental Medicine Biology, Vol. 603. Springer New York, pp. 167-177.

Dartigalongue, C., Missiakas, D., and Raina, S. (2001) Characterization of the *Escherichia coli* σ^E regulon. *J. Biol. Chem.* **276**: 20866-20875.

Das, S., and Chaudhuri, K. (2003) Identification of a unique IAHP (IcmF associated homologous proteins) cluster in *Vibrio cholera* and other proteobacteria through *in silico* analysis. *In Silico Biol.* **3**: 287-300.

Datsenko, K.A., and Wanner, B.L. (2000) One-step inactivation of chromosomal genes in *Escherichia coli* K-12 using PCR products. *Proc. Natl. Acad. Sci. USA* **97**: 6640-6645.

de Graef, M., Alexeeva, S., Snoep, J. L., and de Mattos, M. J. T. (1999) The steady-state internal redox state (NADH/NAD) reflects the external redox state and is correlated with catabolic adaptation in *Escherichia coli. J. Bacteriol.* **181**: 2351-2357.

DeLisa, M.P., Tullman, D., and Georgiou, G. (2003) Folding quality control in the export of proteins by the bacterial twin-arginine translocation pathway. *Proc. Natl. Acad. Sci. USA* **100**: 6115-6120.

DeLisa, M.P., Lee, P., Palmer, T., and Georgiou, G. (2004) Phage shock protein PspA of *Escherichia coli* relieves saturation of protein export via the Tat pathway. *J. Bacteriol.* **186**: 366-373.

Dorel, C., Lejeune, P., and Rodrigue, A., (2006) The Cpx system of *Escherichia coli*, a strategic signaling pathway for confronting adverse conditions and for settling biofilm communities? *Res. Microbiol.* **157**: 306-314.

Drapal, N., and Sawers, G. (1995) Promoter 7 of the *Escherichia coli pfl* operon is a major determinant in the anaerobic regulation of expression by ArcA. *J. Bacteriol.* **177**: 5338-5341.

Duong, F., and Wickner, W. (1997) The SecDFyajC domain of preprotein translocase controls preprotein movement by regulating SecA membrane cycling. *EMBO* **16**: 4871-79.

Dworkin, J., Jovanovic, G., and Model, P. (1997) Role of upstream activation sequences and integration host factor in transcriptional activation by the constitutively active prokaryotic enhancer-binding protein PspF. *J. Mol. Biol.* **273**: 377-388.

Dworkin, J., Jovanovic, G., and Model, P. (2000) The PspA protein of *Escherichia coli* is a negative regulator of sigma(54)-dependent transcription. *J. Bacteriol.* **182**: 311-319.

Ebersbach, G., and Jacobs-Wagner, C. (2007) Exploration into the spatial and temporal mechanisms of bacterial polarity. *Trends Microbiol.* **15**: 101-108.

Edwards, J.C., Johnson, M.S., and Taylor, B.L. (2006) Differentiation between electron transport sensing and proton motive force sensing by the Aer and Tsr receptors for aerotaxis. *Mol. Microbiol.* **62**: 823-837.

Ehrmann, M., and Clausen, T. (2004) Proteolysis as a regulatory mechanism. *Annu. Rev. Genet.* **38**: 709-724.

Elderkin, S., Jones, S., Schumacher, J., Studholme, D., and Buck, M. (2002) Mechanism of action of the *Escherichia coli* phage shock protein PspA in repression of the AAA family transcription factor PspF. *J. Mol. Biol.* **320**: 23-37.

Elderkin, S., Bordes, P., Jones, S., Rappas, M., and Buck, M. (2005) Molecular determinants for PspA-mediated repression of the AAA transcriptional activator PspF. *J. Bacteriol.* **187**: 3238-3248.

Enninga, J., Mounier, J., Sansonetti, P., and Nhieu, G.T. (2005) Secretion of type III effectors into host cells in real time. *Nat. Methods* **2**: 959-965.

Erickson, J.W., and Gross, C.A. (1989) Identification of the σ^E subunit *Escherichia coli* RNA polymerase: a second alternate sigma factor involved in high-temperature gene expression. *Genes Dev.* **3**: 1462-1471.

Eriksson, S., Lucchini, S., Thompson, A., Rhen, M., and Hinton, J.C. (2003) Unravelling the biology of macrophage infection by gene expression profiling of intracellular *Salmonella enterica*. *Mol. Microbiol.* **47**: 103-118.

Evans, C.G.T., Herbert, D., and Tempest, D.W. (1970) The continuous culture of microorganisms. Construction of a chemostat. Vol 2. *Acad. Press.* London, Mew York.

Feng, J.N., Model, P., and Russel, M. (1999) A trans-envelope protein complex needed for filamentous phage assembly and export. *Mol. Microbiol.* **34**: 745-755.

Figge, R.M., Divakaruni, A.V., and Gober, J.W. (2004) MreB, the cell shape-determining bacterial actin homologue, co-ordinates cell wall morphogenesis in *Caulobacter crescentus*. *Mol. Microbiol.* **51**: 1321-1332.

Filloux, A., Hachani, A., and Bleves, S. (2008) The bacterial type VI secretion machine: yet another player for protein transport across membranes. *Microbiology* **154**: 1570-1583.

Finlay, B.B., and Cossart, P. (1997) Exploitation of mammalian host cell functions by bacterial pathogens. *Science* **276**: 718-725.

Flynn, J.M., Levchenko, I., Sauer, R.T., and Baker, T.A. (2004) Modulating substrate choice: the SspB adaptor delivers a regulator of the extracytoplasmic-stress response to the AAA+ protease ClpXP for degradation. *Genes Dev.* **18**: 2292-2301.

Galan, J.E., and Bliska, J.B. (1996) Cross-talk between bacterial pathogens and their host cells. *Annu. Rev. Cell. Dev. Biol.* **12**: 221-255.

Galan, J.E. (2001) *Salmonella* interactions with host cells: type III secretion at work. *Annu. Rev. Cell. Dev. Biol.* **17**: 53-86.

Gao, H., and Xu, X. (2009) Depletion of Vipp1 in Synechocystis sp. PCC 6803 affects photosynthetic activity before the loss of thylakoid membranes. *FEMS Microbiol. Lett.* **292**: 63-70.

Gennis, R. B., and Stewart, V. (1996) Respiration. In: *Escherichia coli* and *Salmonella typhimurium*: Cellular and Molecular Biology. Neidhardt, F. C., Ingraham, J. L., Lin, E. C., Low, K. B., Magasanik, B., Schaechter, M., and Umbarger, H. E (eds.). Washington, D.C.: ASM Press, pp. 217-261.

Gennity, J.M., and Inouye, M. (1991) The protein sequence responsible for lipoprotein membrane localization in *Escherichia coli* exhibits remarkable specificity. *J. Biol. Chem.* **266**: 16458-16464.

Georgellis, D., Kwon, O., and Lin, E. C. (2001) Quinones as the redox signal for the *arc* two-component system of bacteria. *Science* **292**: 2314-2316.

Gerlach, R.G., and Hensel, M. (2007) Protein secretion and adhesins: The molecular armory of Gram-negative pathogens. *Int. J. Med. Microbiol.* **297**: 401-415.

Gitai, Z., Dye, N., and Shapiro, L. (2004) An actin-like gene can determine cell polarity in bacteria. *Proc. Natl. Acad. Sci. U S A* **101**: 8643-8648.

Gitai, Z., Dye, N.A., Reisenauer, A., Wachi, M., and Shapiro, L. (2005) MreB actin-mediated segregation of a specific region of a bacterial chromosome. *Cell* **120**: 329-341.

Goldberg, M.B., Barzu, O., Parsot, C., and Sansonetti, P.J. (1993) Unipolar localization and ATPase activity of IcsA, a *Shigella flexneri* protein involved in intracellular movement. *J. Bacteriol.* **175**: 2189-2196.

Green, R.C., and Darwin, A.J. (2004) PspG, a new member of the *Yersinia enterocolitica* Phage shock protein regulon. *J. Bacteriol.* **186**: 4910-4920.

Greenfield, D., McEvoy, A.L., Shroff, H., Crooks, G.E., Wingreen, N.S., Betzig, E., and Liphardt, J. (2009) Self-organization of the Escherichia coli chemotaxis network imaged with super-resolution light microscopy. *PLoS Biol.* **16;7**:e1000137 Epub.

Grigorova, I.L., Chaba, R., Zhong, H.J., Alba, B.M., Rhodius, V., Herman, C., and Gross, C.A. (2004) Fine-tuning of the *Escherichia coli* σ^E envelope stress response relies on multiple mechanisms to inhibit signal-independent proteolysis of the transmembrane anti-sigma factor, RseA. *Genes Dev.* **18**: 2686-2697.

Guilvout, I., Chami, M., Engel, A., Pugsley, A.P., and Bayan, N. (2006) Bacterial outer membrane secretin PulD assembles and inserts into the inner membrane in the absence of its pilotin. *EMBO* **25**: 5241-5249.

Halic, M., Becker, T., Pool, M.R., Spahn, C.M., Grassucci, R.A., Frank, J., and Beckmann, R. (2004) Structure of the signal recognition particle interacting with the elongation-arrested ribosome. *Nature* **427**: 808-814.

Hankamer, B.D., Elderkin, S.L., Buck, M., and Nield, J. (2004) Organization of the AAA(+) adaptor protein PspA is an oligomeric ring. *J. Biol. Chem*. **279**: 8862-8866.

Hardie, K.R., Seydel, A., Guilvout, I., and Pugsley, A.P. (1996) The secretin-specific, chaperone-like protein of the general secretory pathway: separation of proteolytic protection and piloting functions. *Mol. Microbiol.* **22**: 967-976.

Hardie, K.R., Lory, S., and Pugsley, A.P. (1996) Insertion of an outer membrane protein in *Escherichia coli* requires a chaperone-like protein. *EMBO J.* **15**: 978-988.

Hartl, F.U., Lecker, S., Schiebel, E., Hendrick, J.P., and Wickner, W.T. (1990) The binding cascade of SecB to SecA to SecY/E mediates preprotein targeting to the *E. coli* plasma membrane. *Cell* **63**: 269-279.

Helmann, J.D., and Chamberlin, M.J. (1988) Structure and function of bacterial sigma factors. *Annu. Rev. Biochem.* **57**: 839-872.

Hirakawa, H., Nishino, K., Hirata, T., and Yamaguchi, A. (2003) Comprehensive studies of drug resistance mediated by overexpression of response regulators of two-component signal transduction systems in *Escherichia coli. J. Bacteriol.* **185**: 1851-1856.

Hultgren, S.J., Normark, S., and Abraham, S.N. (1991) Chaperone-assisted assembly and molecular architecture of adhesive pili. *Annu. Rev. Microbiol.* **45**: 383-415.

Huvet, M., Toni, T., Tan, H., Jovanovic, G., Engl, C., Buck, M., and Stumpf, M.P. (2009) Model-based evolutionary analysis: the natural history of phage-shock stress response. *Biochem. Soc. Trans.* **37**: 762-767.

Iwai, N., Nagai, K., and Wachi, M. (2002) Novel S-benzylisothiourea compound that induces spherical cells in *Escherichia coli* probably by acting on a rod-shape-determining protein(s) other than penicillin-binding protein 2. *Biosci. Biotechnol. Biochem.* **66**: 2658-2662.

Isberg, R.R., and Leong, J.M. (1990) Multiple beta 1 chain integrins are receptors for invasion, a protein that promotes bacterial penetration into mammalian cells. *Cell* **60**: 861-871.

Jacob-Dubuisson, F., Fernandez, R., and Coutte, L. (2004) Protein secretion through autotransporter and two-partner pathways. *Biochim. Biophys. Acta* **1694**: 235-257.

Jaumouille, V., Francetic, O., Sansonetti, P.J., and Tran Van Nhieu, G. (2008) Cytoplasmic targeting of IpaC to the bacterial pole directs polar type III secretion in *Shigella*. *Embo J.* **27**: 447-457.

Joly, N., Burrows, P.C., Engl, C., Jovanovic, G., and Buck, M. (2009) A lower-order oligomer form of Phage shock protein A (PspA) stably associates with the hexameric AAA^+ transcription activator protein PspF for negative regulation. *J. Mol. Biol.* **394**: 764-775.

Jones, C.H., Danese, P.N., Pinkner, J.S., Silhavy, T.J., and Hultgren, S.J. (1997) The chaperone-assisted membrane release and folding pathway is sensed by two signal transduction systems. *EMBO J.* **16**: 6394-6406.

Jones, L.J., Carballido-Lopez, R., and Errington, J. (2001) Control of cell shape in bacteria: helical, actin-like filaments in Bacillus subtilis. *Cell* **104**: 913-922.

Jones, S. E., Lloyd, L. J., Tan, K. K., and Buck, M. (2003) Secretion defects that activate the phage shock response of *Escherichia coli*. *J. Bacteriol.* **185**: 6707-6711.

Jovanovic, G., Weiner, L., and Model, P. (1996) Identification, nucleotide sequence, and characterization of PspF, the transcriptional activator of the *Escherichia coli* stress-induced *psp* operon. *J. Bacteriol.* **175**: 1936-1945.

Jovanovic, G., and Model, P. (1997) PspF and IHF bind co-operatively in the *psp* promoter-regulatory region of *Escherichia coli*. *Mol. Microbiol.* **25**: 473-481.

Jovanovic, G., Dworkin, J., and Model, P. (1997) Autogenous control of PspF, a constitutively active enhancer-binding protein of Escherichia coli. *J. Bacteriol.* **179**: 6232-5237.

Jovanovic, G., Rakonjac, J., and Model, P. (1999) *In vivo* and *in vitro* activities of the Escherichia coli sigma54 transcription factor, PspF, and its DNA-binding mutant, PspFDeltaHTH. *J. Mol. Biol.* **285**: 469-483.

Jovanovic, G., Lloyd, L. J., Stumpf, M. P. H., Mayhew, A. J., and Buck, M. (2006) Induction and function of the phage shock protein extracytoplasmic stress response in *Escherichia coli*. *J. Biol. Chem.* **281**: 21147-21161.

Jovanovic, G., Engl, C., and Buck, M (2009) Physical, functional and conditional interactions between ArcAB and phage shock proteins upon secretin-induced stress in Escherichia coli. *Mol. Microbiol.* **74**: 16-28.

Karimova, G., Pidoux, J., Ullmann, A., and Ladant, D. (1998) A bacterial two-hybrid system based on a reconstituted signal transduction pathway. *Proc. Natl. Acad. Sci. USA* **95**: 5752-5756.

Karimova, G., Dautin, N., and Ladant, D. (2005) Interaction network among *Escherichia coli* membrane proteins involved in cell division as revealed by bacterial two-hybrid analysis. *J. Bacteriol.* **187**: 2233-2243.

Kato, A., Mitrophanov, A. Y., and Groisman, E. A. (2007) A connector of two-component regulatory systems promotes signal amplification and persistence of expression. *Proc. Natl. Acad. Sci. U S A* **104**: 12063-12068.

Kato, Y., Nishiyama, K., and Tokuda, H. (2003) Depletion of SecDF-YajC causes a decrease in the level of SecG: implication for their functional interactions. *FEBS Lett.* **550**: 114-118.

Kenny, B., DeVinney, R., Stein, M., Reinscheid, D.J., Frey, E.A., and Finlay, B.B. (1997) Enteropathogenic *E. coli* (EPEC) transfers its receptor for intimate adherence into mammalian cells. *Cell* **91**: 511-520.

Kim, J.-R., and Cho, K.-H. (2006) The multi-step phosphorelay mechanism of unortodox two-component systems in *E. coli* realizes ultrasensitivity to stimuli while maintaining robustness to noises. *Comp. Biol. Chem*. **30**: 438-444.

Kim, S.H., Wang, W., and Kim, K.K. (2002) Dynamic and clustering model of bacterial chemotaxis receptors: structural basis for signalling and high sensitivity. *Proc. Natl. Acad. Sci. USA* **99**: 11611-11615.

Kitagawa, M., Ara, T., Arifuzzaman, M., Ioka-Nakamichi, T., Inamoto, E., Toyonaga, H., *et al.* (2005) Complete set of ORF clones of *Escherichia coli* ASKA library (A Complete Set of *E. coli* K-12 ORF Archive): Unique Resources for Biological Research. *DNA Res.* **12**: 291-299.

Kleerebezem, M., and Tommassen, J. (1993) Expression of the *pspA* gene stimulates efficient protein export in *Escherichia coli*. *Mol. Microbiol.* **7**: 947-956.

Kleerebezem, M., Crielaard, W., and Tommassen, J. (1996) Involvement of stress protein PspA (Phage shock protein A) of Escherichia coli in maintenance of the protonmotive force under stress conditions. *EMBO J.* **15**: 162-171.

Kobayashi, H., Yamamoto, M., and Aono, R. (1998) Appearance of a stress-response protein, phage-shock protein A, in *Escherichia coli* exposed to hydrophobic organic solvents. *Microbiology* **144**: 353-359.

Kobayashi, R., Suzuki, T., and Yoshida, M. (2007) *Escherichia coli* phage-shock protein A (PspA) binds to membrane phospholipids and repairs proton leakage of the damaged membranes. *Mol. Microbiol.* **66**: 100-109.

Kol, S., Nouwen, N., and Driessen, A.J. (2008) Mechanisms of YidC-mediated insertion and assembly of multimeric membrane protein complexes. *J. Biol. Chem.* **283**: 31269-31273.

Koronakis, V., Andersen, C., and Hughes, C. (2001) Channel-tunnels. *Curr. Opin. Struct. Biol.* **11**: 403-407.

Kruse, T., Bork-Jensen, J., and Gerdes, K. (2005) The morphogenetic MreBCD proteins of *Escherichia coli* form an essential membrane-bound complex. *Mol. Microbiol.* **55**: 78-89.

Kruse, T., Blagoev, B., Lobner-Olesen, A., Wachi, M., Sasaki, K., Iwai, N., Mann, M., and Gerdes, K. (2006) Actin homolog MreB and RNA polymerase interact and are both required for chromosome segregation in *Escherichia coli*. *Genes Dev.* **20**: 113–124.

Kubori, T., Matsushima, Y., Nakamura, D., Uralil, J., Lara-Tejero, M., Sukhan, A., Galan, J.E., and Aizawa, S.I. (1998) Supramolecular structure of the *Salmonella typhimurium* type III protein secretion system. *Science* **280**: 602-605.

Kubori, T., Sukhan, A., Aizawa, S.I., and Galan, J.E., (2000) Molecular characterization and assembly of the needle complex of the *Salmonella typhimurium* type III protein secretion system. *Proc. Natl. Acad. Sci. USA* **97**: 10225-10230.

Kuhn, A. (2009) From the Sec complex to the membrane insertase YidC. *Biol. Cem.* **390**: 701-706.

Lai, E.M., and Kado, C.I. (1998) Processed VirB2 is the major subunit of the promiscuous pilus of *Agrobacterium tumefaciens*. *J. Bacteriol.* **180**: 2711-2717.

Lai, E.M., Nair, U., Phadke, N.D., and Maddock, J.R. (2004) Proteomic screening and identification of differentially distributed membrane proteins in *Escherichia coli*. *Mol. Microbiol.* **52**: 1029-1044.

Lee, H.C., and Bernstein, H.D. (2001) The targeting pathway of *Escherichia coli* presecretory and integral membrane proteins is specified by the hydrophobicity of the targeting signal. *Proc. Natl. Acad. Sci. USA* **98**: 3471-3476.

Lenn, T., Laeke, M.C., and Mullineaux, C.W. (2008a) Clustering and dynamics of cytochrome *bd*-I complexes in the *Escherichia coli* plasma membrane *in vivo*. *Mol. Microbiol.* **70**: 1397-1407.

Lenn, T., Laeke, M.C., and Mullineaux, C.W. (2008b) Are *Escherichia coli* OXPHOS complexes concentrated in specialised zones within the plasma membrane? *Biochem. Soc. Trans.* **36**: 1032-1036.

Lessl, M., Balzer, D., Lurz, R., Waters, V.L., Guiney, D.G., and Lanka, E. (1992) Dissection of IncP conjugative plasmid transfer: definition of the transfer region Tra2 by mobilization of the Tra1 region in trans. *J. Bacteriol.* **174**: 2493-2500.

Lindenstrauss, U., and Brueser, T. (2006) Conservation and variation between *Rhodobacter capsulatus* and *Escherichia coli* Tat systems. *J. Bacteriol.* **188**: 7807-7814.

Linderoth, N.A., Simon, M.N., and Russel, M. (1997) The filamentous phage pIV multimer visualized by scanning transmission electron microscopy. *Science* 278: 1635-1638.

Lipinska, B., Sharma, S., and Georgopoulos, C. (1988) Sequence analysis and regulation of the htrA gene of *Escherichia coli*: a σ^{32}-independent mechanism of heat-inducible transcription. *Nucleic Acids Res.* **16**: 10053-10067.

Lloyd, L. J., Jones, S. E., Jovanovic, G., Gyaneshwar, P., Rolfe, M. D., Thompson, A., *et al*. (2004) Identification of a new member of the phage shock protein response in *Escherichia coli*, the phage shock protein G (PspG). *J. Biol. Chem.* **279**: 55707-55714.

Lopez-Campistrous, A., Semchuk, P., Burke, L., Palmer-Stone, T., Brokx, S.J., Broderick, G., Bottorff, D., Bolch, S., Weiner, J.H., and Ellison, M.J. (2005) Localization, annotation, and comparison of the Escherichia coli K-12 proteome under two states of growth. *Mol. Cell. Prot.* **4**: 1205-1209.

Lucchini, S., Liu, H., Jin, Q., Hinton, J.C., and Yu, J. (2005) Transcriptional adaptation of *Shigella flexneri* during infection of macrophages and epithelial cells: insights into the strategies of a cytosolic bacterial pathogen. *Infect. Immun.* **73**: 88-102.

Luirink, J., von Heijne, G., Houben, E., and de Gier, J.W. (2005) Biogenesis of inner membrane proteins in *Escherichia coli*. *Annu. Rev. Microbiol.* **58**: 329-355.

Lutkenhaus, J. (2007) Assembly dynamics of the bacterial MinCDE system and spatial regulation of the Z ring. *Annu. Rev. Biochem.* **76**: 539-562.

Maddock, J.R., and Shapiro, L. (1993) Polar location of the chemoreceptor complex in the *Escherichia coli* cell. *Science* **259**: 1717-1723.

Malpica, R., Franco, B., Rodriguez, C., Kwon, O., and Georgellis, D. (2004) Identification of a quinine-sensitive redox switch in the ArcB sensor kinase. *Proc. Natl. Acad. Sci. U S A* **101**: 13318-13323.

Malpica, R., Peña Sandoval, G. R., Rodríguez, C., Franco, B., and Georgellis, D. (2006) Signaling by the Arc two-component system provides a link between the redox state of the quinone pool and gene expression. *Antioxid. Redox Signal* **8**: 781-795.

Marcino, D.K., Russel, M., and Simon, S.M. (2001) Assembling filamentous phage occlude pIV channels. *Proc. Natl. Acad. Sci. USA* **98**: 9359-9364.

Matsuyama, S., Yokata, N., and Tokuda, H. (1997) A novel outer membrane lipoprotein, LolB (HemM), involved in the LolA (p20)-dependent localization of lipoproteins to the outer membrane of *Escherichia coli*. *EMBO J.* **16**: 6947-6955.

Matsuyama, S., Fujita, Y., and Mizushima, S. (1993) SecD is involved in the release of translocated secretory proteins from the cytoplasmic membrane of *Escherichia coli*. *EMBO J.* **12**: 265-270.

Maxson, M.E., and Darwin, A.J. (2004) Identification of inducers of the *Yersinia enterocolitica* phage shock protein system and comparison to the regulation of the RpoE and Cpx extracytoplasmic stress responses. *J. Bacteriol.* **186**: 4199-4208.

Maxson, M. E., and Darwin, A. J. (2006) PspB and PspC of *Yersinia enterocolitica* are dual function proteins: regulators and effectors of the phage-shock-protein response. *Mol. Microbiol.* **59**: 1610-1623.

Mika, F., and Hengge, R. (2005) A two-component phosphotransfer network involving ArcB, ArcA, and RssB coordinates synthesis and proteolysis of sigmaS (RpoS) in *E. coli*. *Genes Dev.* **19**: 2770-2781.

Miller, J. H. (1992) A short course in Bacterial Genetics: A laboratory manual and handbook for *Escherichia coli* and related bacteria. Cold Spring Harbor Laboratory Press, Cold Spring Harbor, N.Y.

Mitchell, P (1961) Coupling of phosphorylayion to electron and hydrogen transfer by a chemi-osmotic type of mechanism. *Nature* **191**: 144-148.

Model, P., Jovanovic, G., and Dworkin, J. (1997) The *Escherichia coli* phage-shock-protein (*psp*) operon. *Mol. Microbiol.* **24**: 255-261.

Mogensen, J.E., and Otzen, D.E. (2005) Interactions between folding factors and bacterial outer membrane proteins. *Mol. Microbiol.* **57**: 326-346.

Morett, E., and Buck, M. (1989) *In vivo* studies on the interaction of RNA polymerase-sigma 54 with the *Klebsiella pneumonia* and *Rhizobium meliloti nifH* promoters. The role of NifA in the formation of an open promoter complex. *J. Mol. Biol.* **210**: 65-77.

Mougous, J.D., Cuff, M.E., Raunser, S., Shen, A., Zhou, M., Gifford, C.A., Goodman, A.L., Joachimiak, G., Ordonez, C.L., Lory, S., Walz, T., Joachimiak, A., and Mekalanos, J.J. (2006) A virulence locus of *Pseudomonas aeruginosa* encodes a protein secretion apparatus. *Science* **312**: 1526-1530.

Muhlradt, P.F., and Golecki, J.R. (1975) Asymmetrical distribution and artifactual reorientation of lipopolysaccharide in the outer membrane bilayer of *Salmonella typhimurium. Eur. J. Biochem.* **51**: 343-352.

Mukhopadhyay, S., Kapatral, V., Xu, W., and Chakrabarty, A.M. (1999) Characterization of a Hank's type serine/threonine kinase and serine/threonine phosphoprotein phosphatise in *Pseudomonas aeruginosa*. *J. Bacteriol.* **181**: 6615-6622.

Nakayama, S., and Watanabe, H. (1995) Involvement of *cpxA*, a sensor of a two-component regulatory system, in the pH-dependent regulation of expression of *Shigella sonnei virF* gene. *J. Bacteriol.* **177**: 5062-5069.

Natale, P., Brueser, T., and Driessen, A.J.M. (2008) Sec- and Tat-mediated protein secretion across the bacterial cytoplasmic membrane – Distinct translocases and mechanisms. *Biochim. et Biophys. Acta* **1778**: 1735-1756.

Neuwald, A.F., Aravind, L., Spouge, J.L., and Koonin E.V. (1999) AAA+: A class of chaperone-like ATPases associated with the assembly, operation, and disassembly of protein complexes. *Genome Res.* **9**: 27-43.

Nouwen, N., and Driessen, A.J. (2002) SecDFyajC forms a heterotetrameric complex with YidC. *Mol. Microbiol.* **44**: 1397-1405.

Nummelin, H., Merckel, M.C., Leo, J.C., Lankinen, H., Skumik, M., and Goldman, A. (2004) The *Yersinia* adhesin YadA collagen-binding domain structure is a novel left-handed parallel beta-roll. *EMBO J.* **23**: 701-711.

Opalka, N., Beckmann, R., Boisset, N., Simon, M.N., Russel, M., and Darst, S.A. (2003) Structure of the filamentous phage pIV multimer by cryo-electron microscopy. *J. Mol. Biol.* **325**: 461-470.

Osborn, M.J., and Rothfield, L. (2007) Cell shape determination in *Escherichia coli*. *Curr. Opin. Microbiol.* **10(6)**: 606-610.

Paetzel, M., Karla, A., Strynadka, N.C., and Dalbey, R.E. (2002) Signal peptidases. *Chem. Rev.* **102**: 4549-4580.

Pakhomov, A.A., and Martynov, V.I. (2008) GFP family: structural insights into spectral tuning. *Chem. Biol.* **15**: 755-764.

Pallen, M.J., and Wren, B.W. (1997) The HtrA family of serine proteases. *Mol. Microbiol.* **26**: 209-221.

Partridge, J. D., Sanguinetti, G., Dibden, D. P., Roberts, R. E., Poole, R. K., and Green, J. (2007) Transition of *Escherichia coli* from aerobic to micro-aerobic conditions involves fast and slow reacting regulatory components. *J. Biol. Chem.* **282**: 11230-11237.

Paul, K., Erhardt, M., Hirano, T., Blair, D.F., and Hughes, K.T. (2008) Energy source of flagellar type III secretion. *Nature* **451**: 489-492.

Peterson, J.H., Woolhead, C.A., and Bernstein, H.D. (2003) Basic amino acids in a distinct subset of signal peptides promote interaction with the signal recognition particle. *J. Biol. Chem.* **278**: 46155-46162.

Pizarro-Cerda, J., and Cossart, P. (2004) Subversion of phosphoinositide metabolism by intracellular bacterial pathogens. *Nat. Cell. Biol.* **6**: 1026-1033.

Pizarro-Cerda, J., and Cossart, P. (2006) Bacterial adhesion and entry into host cells. *Cell* **124**: 715-727.

Pohlschroeder, M., Hartmann, E., Hand, N.J., Dilks, K., and Haddad, A. (2005) Diversity and evolution of protein translocation. *Annu. Rev. Microbiol.* **59**: 91-111.

Poritz, M.A., Bernstein, H.D., Strub, K., Zopf, D., Wilhelm, H., and Walter, P. (1990) An *E. coli* ribunucleoprotein containing 4.5S RNA resembles mammalian signal recognition particle. *Science* **250**: 1111-1117.

Possot, O., d'Enfert, C., Reyss, I., and Pugsley, A.P. (1992) Pullulanase secretion in *Escherichia coli* K-12 requires a cytoplasmic protein and a putative polytopic cytoplasmic membrane protein. *Mol. Microbiol.* **6**: 95-105.

Price, C.E., and Driessen, A.J.M. (2008) YidC is involved in the biogenesis of anaerobic respiratory complexes in the inner membrane of *Escherichia coli*. *J. Biol. Chem.* **283**: 26921-26827.

Pugsley, A.P, Francetic, O., Possot, O.M., Sauvonnet, N., and Hardie, K.R. (1997) Recent progress and future directions in studies of the main terminal branch of the general secretory pathway in Gram-negative bacteria. *Gene* **192**: 13-19.

Pukatzki, S. Ma, A.T., Sturtevant, D., Krastins, B., Sarracino, D., Nelson, W.C, Heidelberg, J.F., and Mekalanos, J.J. (2006) Identification of a conserved bacterial protein secretion system in *Vibrio cholera* using *Dictyolstelium* host model system. *Proc. Natl. Acad. Sci. USA* **103**: 1528-1533.

Raffa, R.G., and Raivio, T.L. (2002) A third envelope stress signal transduction pathway in *Escherichia coli*. *Mol. Microbiol.* **45**: 1599-1611.

Raivio, T.L., and Silhavy, T.J. (1997) Transduction of envelope stress in *Escherichia coli* by the Cpx two-component system. *J. Bacteriol.* **179**: 7724-7733.

Raivio, T.L., and Silhavy, T.J. (1999) The σ^E and Cpx regulatory pathways: overlapping but distinct envelope stress responses. *Curr. Opin. Microbiol.* **2**: 159-165.

Raivio, T.L., Popkin, D.L., and Silhavy, T.J. (1999) The Cpx envelope stress response is controlled by amplification and feedback inhibition. *J. Bacteriol.* **181**: 5263-5272.

Raivio, T.L., Laird, M.W., Joly, J.C., and Silhavy, T.J. (2000) Tethering of CpxP to the inner membrane prevents spheroblast induction of the cpx envelope stress response. *Mol. Microbiol.* **37**: 1186-1197.

Rappas, M., Schumacher, J., Beuron, F., Niwa, H., Bordes, P., Wigneshweraraj, S., Keetch, C.A., Robinson, C.V., Buck, M., and Zhang, X. (2005) Structural insights into the activity of enhancer binding proteins. *Science* **307**: 1972-1975.

Reitzer, L., and Schneider, B.L. (2001) Metabolic context and possible physiological themes of s54-dependent genes in *Escherichia coli*. *Microbiol. Mol. Biol. Rev.* **65**: 422-444.

Rothfield, L., Taghbalout, A., and Shih, Y.L. (2005) Spatial control of bacterial division-site placement. *Nat. Rev. Microbiol.* **3**: 959-968.

Rowley, G., Spector, M., Kormanec, J., and Roberts, M. (2006) Pushing the envelope: extracytoplasmic stress responses in bacterial pathogens. *Nat. Rev. Microbiol.* **4**: 383-394.

Ruiz, N., and Silhavy, T.J. (2005) Sensing external stress: watchdogs of the *Escherichia coli* cell envelope. *Curr. Opin. Microbiol.* **8**: 122-126.

Russel, M. (1994a) Phage assembly: a paradigm for bacterial virulence factor export? *Science* **265**: 612-614.

Russel, M. (1994b) Mutants at conserved positions in gene IV, a gene required for assembly and secretion of filamentous phages. *Mol. Microbiol.* **14**: 357-369.

Russel, M., and Kazmierczak, B. (1993) Analysis of the structure and subcellular location of filamentous phage pIV. *J. Bacteriol.* **175**: 3998-4007.

Russel, M., Linderoth, N.A., and Sali, A. (1997) Filamentous phage assembly: variation on a protein export theme. *Gene* **192**: 23-32.

Samuelson, J.C., Chen, M., Jiang, F., Moller, I., Wiedmann, M., Kuhn, A., Phillips, G.J., and Dalbey, R.E. (2000) YidC mediates membrane protein insertion in bacteria. *Nature* **406**: 637-641.

Samuelson, J.C., Jiang, F., Yi, L., Chen, M., Kuhn, A., and Dalbey, R.E. (2001) Function of YidC for the insertion of M13 procoat protein in *E. coli*: translocation of mutants that show differences in their membrane potential dependence and Sec-requirement. *J. Biol. Chem.* **276**: 34847-34852.

Sargent, F., Bogsch, E.G., Stanley, N.R., Wexler, M., Robinson, C., Berks, B.C., and Palmer, T. (1998) Overlapping functions of components of a bacterial Sec-independent protein export pathway. *EMBO J.* **17**: 3640-3650.

Sargent, F., Stanley, N.R., Berks, B.C., and Palmer, T. (1999) Sec-independent protein translocation in *Escherichia coli*. A distinct and pivotal role for the TatB protein. *J. Biol. Chem.* **274**: 36073-36082.

Sargent, F., Gohlke, U., De Leeuw, E., Stanley, N.R., Palmer, T., Saibil, H.R. and Berks, B.C. (2001) Purified components of the *Escherichia coli* Tat protein transport system form a double-layered ring structure. *Eur. J. Biochem.* **268**: 3361-3367.

Sauer, F.G., Bamhart, M., Choudhury, D., Knight, S.D., Waksman, G., and Hultgren, S.J. (2000) Chaperone-assisted pilus assembly and bacterial attachment. *Curr. Opin. Struct. Biol.* **10**: 548-556.

Schauer, K., Rodionov, D.A., and de Reuse, H. (2008) New substrates for TonB-dependent transport: do we only see the „tip of the iceberg“? *Trends Biochem. Sci.* **33**: 330-338.

Schmitt, L., Benabdelhak, H., Blight, M.A., Holland, I.B., and Stubbs, M.T. (2003) Crystal structure of the nucleotide-binding domain of the ABC-transporter haemolysin B: identification of a variable region within ABC helical domains. *J. Mol. Biol.* **330**: 333-342.

Schulein, R., Gentschev, I., Mollenkopf, H.J., and Goebel, W. (1992) A topological model fort he haemolysin translocator protein HlyD. *Mol. Gen. Genet.* **234**: 155-163.

Seo, J., Savitzky, D. C., Ford, E., and Darwin, A. J. (2007) Global analysis of tolerance to secretin-induced stress in *Yersinia enterocolitica* suggests that the phage-shock-protein system may be a remarkably self-contained stress response. *Mol. Microbiol.* **65**: 714-727.

Shih, Y.L., Le, T., and Rothfield, L. (2003) Division site selection in *Escherichia coli* involves dynamic redistribution of Min proteins within coiled structures that extend between the two cell poles. *Proc. Natl. Acad. Sci. U S A* **100**: 7865-7870.

Shih, Y.L., Kawagishi, I., and Rothfield, L. (2005) The MreB and Min cytoskeletal-like systems play independent roles in prokaryotic polar differentiation. *Mol. Microbiol.* **58**: 917-928.

Simons, R. W., Houman, F., and Kleckner, N. (1987) Improved single and multicopy *lac*-based cloning vectors for protein and operon fusions. *Gene* **53**: 85–96.

Soballe, B., and Poole, R.K. (1999) Microbial ubiquinones: multiple roles in respiration, gene regulation and oxidative stress management. *Microbiology* **145**: 1817–1830.

Spiess, C., Beil, A., and Ehrmann, M. (1999) A temperature-dependent switch from chaperone to protease in a widely conserved heat shock protein. *Cell* **97**: 339-347.

Standar, K., Mehner, D., Osadnik, H., Berthelmann, F., Hause, G., Lunsdorf, H., and Bruser, T. (2008) PspA can form large scaffolds in *Escherichia coli*. *FEBS Lett* **582**: 3585-3589.

Strauss, M., Hofhaus, G., Schroeder, R.R., and Kuehlbrandt, W. (2008) Dimer ribbons of ATP synthase shape the inner mitochondrial membrane. *EMBO J.* **27**: 1154-1160.

Studholme, D.J., and Dixon, R. (2003) Domain architectures of σ^{54}-dependent transcriptional activators. *J. Bacteriol.* **185**: 1757-1767.

Suvarna, K., Stevenson, D., Meganathan, R., and Hudspeth, M.E. (1998) Menaquinone (vitamin K2) biosynthesis: localization and characterization of the *menA* gene from *Escherichia coli*. *J. Bacteriol.* **180**: 2782-2787.

Szurmant, H., Bu, L., Brooks, C. L. 3rd, and Hoch, J. A. (2008) An essential sensor histidine kinase controlled by transmembrane helix interactions with its auxiliary proteins. *Proc. Natl. Acad. Sci. U S A* **105**: 5891-5896.

Taghbalout, A., and Rothfield, L. (2009) RNaseE and the other constituents of the RNA dgradosome are components of the bacterial cytoskeleton. *Proc. Natl. Acad. Sci. U S A* **104**: 1667-1672.

Tamano, K., Aizawa, S., Katayama, E., Nonaka, T., Imajoh-Ohmi, S., Kuwae, A., Nagai, S., and Sasakawa, C. (2000) Supramolecular structure of the *Shigella* type III secretion machinery: the needle part is changeable in length and essential for delivery of effector. *EMBO J.* **19**: 3876-3887.

Tanaka, S., Narita, S., and Tokuda, H. (2007) Characterization of the *Pseudomonas aeruginosa* Lol system as a lipoprotein sorting mechanism. *J. Biol. Chem.* **282**: 13379-13384.

Terada, M., Kuroda, T., Matsuyama, S., and Tokuda, H. (2001) Lipoprotein sorting signals evaluated as the LolA-dependent release of lipoproteins from the cytoplasmic membrane *Escherichia coli*. *J. Biol. Chem.* **276**: 47690-47694.

Thanabalu, T., Koronakis, E., Hughes, C., and Koronakis, V. (1998) Substrate-induced assembly of a contiguous channel for protein export from *E. coli*: reversible bridging of an inner-membrane translocase to an outer membrane exit pore. *EMBO J.* **17**: 6487-6496.

Thanassi, D.G., Saulino, E.T., and Hultgren, S.J. (1998) The chaperone/usher pathway: a major terminal branch of the general secretory pathway. *Curr. Opin. Microbiol.* **1**: 223-231.

Tokuda, H., Matsuyama, S., and Tanaka-Masuda, K. (2007) Structure, function and transport of lipoproteins in *Escherichia coli*. In "The Periplasm," ed. Ehrmann, M., ASM Press, Washington DC, pp. 67-79.

Tokuda, H. (2009) Biogenesis of outer membranes in Gram-negative bacteria. *Biosci. Biotechnol. Biochem.* **73**: 465-473.

Uehara, T., and Park, J.T. (2008) Growth of *Escherichia coli*: significance of peptidoglycan degradation during elongation and septation. *J. Bacteriol.* **190**: 3914-3922.

Unden, G. (1988) Differential roles for menaquinone and demethylmenaquinone in anaerobic electron transport of *E. coli* and their fnr independent expression. *Arch. Microbiol.* **150**: 499–503.

Urbanus, M.L., Scotti, P.A., Froederberg, L., Saeaef, A., de Gier, J.W.L., Brunnder, J., Samuelson, J.C., Dalbey, R.E., Oudega, B., and Luirink, J. (2001) Sec-dependent membrane protein insertion: sequential interaction of nascent FtsQ with SecY and YidC. *EMBO J.* **2**: 524-529.

van der Laan, M., Urbanus, M.L., Ten Hagen-Jongman, C.M., Nouwen, N., Oudega, B., Harms, N., Driessen, A.J., and Luirink, J. (2003) A conserved function of YidC in the biogenesis of respiratory chain complexes. *Proc. Natl. Acad. Sci. USA* **100**: 5801-5806.

Ventura, S., and Villaverde, A. (2006) Protein quality in bacterial inclusion bodies. *Trends Biotechnol.* **24**: 179-185.

Voulhoux, R., Bos, M.P., Geurtsen, J., Mols, M., and Tommassen, J. (2003) Role of a highly conserved bacterial protein in outer membrane protein assembly. *Science* **299**: 262-265.

Vrancken, K., Van Mellaert, L., Anné, J. (2008) Characterization of the *Streptomyces lividans* PspA response. *J. Bacteriol.* **190**: 3475-3481.

Wallace, B.J., and Young, I.G. (1977) Role of quinones in electron transport to oxygen and nitrate in *Escherichia coli*. Studies with a ubiA- menA- double quinone mutant. *Biochim. Biophys. Acta*. **461**: 84–100.

Wang, Q., Frye, J.G., McClelland, M., and Harshey, R.M. (2004) Gene expression patterns during swarming in *Salmonella typhimurium*: genes specific to surface

growth and putative new motility and pathogenicity genes. *Mol. Microbiol.* **52**: 169-187.

Weiner, L., and Model, P. (1994) Role of an *Escherichia coli* stress-response operon in stationary-phase survival. *Proc. Natl. Acad. Sci. USA* **91**: 2191-2195.

Weiner, L., Brissette, J.L, and Model, P. (1991) Stress-induced expression of the *Escherichia coli* phage shock protein operon is dependent on σ^{54} and modulated by positive and negative feedback mechanisms. *Genes Dev.* **5**: 1912-1923.

Weiner, L., Brissette, J.L, Ramani, N. and Model, P. (1995) Analysis and *cis*-acting elements regulating the stress-induced phage shock protein operon. *Nucleic. Acids Res.* **23**: 2030-2036.

Weiss, D.S., Chen, J.C., Ghigo, J.M., Boyd, D., and Beckwith, J. (1999) Localization of FtsI (PBP3) to the septal ring requires its membrane anchor, the Z ring, FtsA, FtsQ, and FtsL. *J. Bacteriol.* **181**: 508-520.

Westphal, S., Heins, L., Soll, J., and Vothknecht, U. C. (2001) *Vipp1* deletion mutant of *Synechocystis*: a connection between bacterial phage shock and thylakoid biogenesis? *Proc. Natl. Acad. Sci. USA* **98**: 4238-4242.

Wiegert, T., Homuth, G., Versteeg, S., and Schumann, W. (2001) Alkaline shock induces the Bacillus subtilis σ^{W} regulon. *Mol. Microbiol.* **41**: 59-71.

Wigneshweraraj, S., Bose, D., Burrows, P. C., Joly, N., Schumacher, J., Rappas, M., Pape, T., Zhang, X., Stockley, P., Severinov, K., and Buck, M. (2008) Modus operandi of the bacterial RNA polymerasecontaining the sigma54 promoter-specificity factor. *Mol. Microbiol.* **68**: 538-546.

Wild, K., Halic, M., Sinning, I., and Beckmann, R. (2004) SRP meets the ribosome. *Nat. Struct. Mol. Biol.* **11**: 1049-1053.

Wissenbach, U., Ternes, D., and Unden, G. (1992) An *Escherichia coli* mutant containing only demethylmenaquinone, but no menaquinone: effects on fumarate, dimethylsulfoxide, trimethylamine N-oxide and nitrate respiration. *Arch. Microbiol.* **158**: 68–73.

Wolanin, P.M., Thomason, P.A., and Stock, J.B. (2002) Histidine protein kinases: key signal transducers outside the animal kingdom. *Genome Biol.* **3**: R3013.

Wolanin, P.M., and Stock, J.B. (2004) Bacterial chemosensing: cooperative molecular logic. *Curr. Biol.* **14**: R486-487.

Wolfgang, M., van Putten, J.P., Hayes, S.F., Dorward, D., and Koomey, M (2000) Components and dynamics of fiber formation define a ubiquitous biogenesis pathway for bacterial pili. *EMBO J.* **19**: 6408-6418.

Yamaguchi, K., Yu, F., and Inouye, M. (1988) A single amino acid determinant of the membrane localization of lipoproteins in *E. coli*. *Cell* **53**: 423-432.

Zhang, X., Chaney, M., Wigneshweraraj, S.R., Schumacher, J., Bordes, P., Cannon, W., and Buck, M. (2002) Mechanchemical ATPases and transcriptional activation. *Mol. Microbiol.* **45**: 895-903.

APPENDIX

APPENDIX A (STRAINS)

Bacterial strains used in this study are shown below. Bacterial strains were streaked for single colonies from stock onto solid media and grown overnight at 37°C. Liquid cultures were inoculated with single bacterial colonies and grown overnight at 37°C or 30°C with shaking.

Strain	Relevant Characteristics	Reference
GENERAL		
XL1-Blue	*rec*A1 *end*A1 *gyr*A96 *thi*-1 *hsd*R17 *sup*E44 *rel*A1 *lac* F´ *pro*AB l*ac*IqZΔM15 Tn10 (tet^r)	Laboratory collection
MG1655	F$^-$ λ$^-$ *ilvG- rfb-50 rph-1*	CGSC # 7740
MG1655Δ*pspF*	Δ*pspF*	Lloyd *et al.* 2004
MC1061	*hsdR2 hsdM*$^+$ *hsdS*$^+$ *araD139* Δ*(ara-leu)7697* Δ*(lac)X74 galE15 galK16 rpsL* (str^r) *mcrA mcrB1*	CGSC# 6649
MVA4	MC1061 ϕ*pspA-lacZ* (ap^r)	A gift from G. Jovanovic
BTH101	F$^-$ *cya-99 araD139 galE15 galK16 rpsL1* (str^r) *hsdR2 mcrA1 mcrB1*	A gift from D. Ladant
CHAPTER 3 SPECIFIC		
MVA42	MG1655 Δ*pspA* Δ*pspG*::kan (kan^r)	Lloyd *et al.*, 2004
MVA59	MG1655 Δ*arcB*::kan (kan^r)	Jovanovic *et al.*, 2006
JWK4364	BW25113 Δ*arcA:*:kan (kan^r)	Baba *et al.*, 2006
MVA70	MG1655 Δ*arcA*::kan (kan^r)	A gift from G. Jovanovic
MVA61	MG1655 Δ*pspF* Δ*arcB*::kan (kan^r)	Jovanovic *et al.*, 2006
MVA80	MG1655 Δ*pspF* Δ*arcA*::kan (kan^r)	A gift from G. Jovanovic
MVA44	MG1655 ϕ*pspA-lacZ* (amp^r)	Jovanovic *et al.*, 2006
MVA45	MG1655 Δ*pspBC* ϕ*pspA-lacZ* (amp^r)	Jovanovic *et al.*, 2006
MVA63	MVA44 Δ*arcB*::kan (amp^r, kan^r)	Jovanovic *et al.*, 2006
MVA79	MVA44 Δ*arcA*::kan (amp^r, kan^r)	A gift from G. Jovanovic
MVA27	MG1655 Δ*pspA* ϕ*pspA-lacZ* (amp^r)	Jovanovic *et al.*, 2006
MVA62	MVA27 Δ*arcB*::kan (amp^r, kan^r)	Jovanovic *et al.*, 2006
MVA84	MVA27 Δ*arcA*::kan (amp^r, kan^r)	A gift from G. Jovanovic
JWK5536	BW25113 Δ*arcB*::kan (kan^r)	Baba *et al.*, 2006

MVA83	MVA45 Δ*arcB*::kan (amp^r, kan^r)	A gift from G. Jovanovic
MVA92	MVA59 Δ*arcB59* (kan^s, amp^s, cam^s)	A gift from G. Jovanovic
MVA93	MVA92 ϕ*pspA-lacZ* (amp^r)	A gift from G. Jovanovic
MVA94	MVA93 Δ*arcA*::kan (amp^r, kan^r)	A gift from G. Jovanovic
L65	K561 Δ*pspB*::kan (kan^r)	A gift from P. Model
J136	K561 Δ*pspC*::kan (kan^r)	A gift from P. Model
MVA12	MVA4 Δ*pspB*::kan (amp^r, kan^r)	A gift from G. Jovanovic
MVA13	MVA4 Δ*pspC*::kan (amp^r, kan^r)	A gift from G. Jovanovic
MVA77	MVA4 Δ*arcB*::kan (amp^r, kan^r)	A gift from G. Jovanovic
JWK1328	BW25113 Δ*fnr*::kan (kan^r)	Baba *et al.*, 2006
JWK1213	BW25113 Δ*narX*::kan (kan^r)	Baba *et al.*, 2006
JWK1212	BW25113 Δ*narL*::kan (kan^r)	Baba *et al.*, 2006
JWK2453	BW25113 Δ*narQ*::kan (kan^r)	Baba *et al.*, 2006
JWK2181	BW25113 Δ*narP*::kan (kan^r)	Baba *et al.*, 2006
JWK4023	BW25113 Δ*soxS*::kan (kan^r)	Baba *et al.*, 2006
JWK4024	BW25113 Δ*soxR*::kan (kan^r)	Baba *et al.*, 2006
JWK3933	BW25113 Δ*oxyR*::kan (kan^r)	Baba *et al.*, 2006
JWK0669	BW25113 Δ*fur*::kan (kan^r)	Baba *et al.*, 2006
EC1	MVA4 Δ*fnr*::kan (amp^r, kan^r)	This work
EC2	MVA4 Δ*narX*::kan (amp^r, kan^r)	This work
EC3	MVA4 Δ*narL*::kan (amp^r, kan^r)	This work
EC4	MVA4 Δ*narQ*::kan (amp^r, kan^r)	This work
EC5	MVA4 Δ*narP*::kan (amp^r, kan^r)	This work
EC6	MVA4 Δ*soxS*::kan (amp^r, kan^r)	This work
EC7	MVA4 Δ*soxR*::kan (amp^r, kan^r)	This work
EC9	MVA4 Δ*fur*::kan (amp^r, kan^r)	This work
CHAPTER 4 SPECIFIC		
RP437	*thr-1(Am) leuB6 his-4 metF159(Am) eda-50 rpsL1356 thi-1 ara-14 mtl-1 xyl-5 tonA31 tsx-78 lacY1* F$^-$	CGSC # 12122
RP5882	RP437Δ*tsr-7021*	Callahan *et al.*, 1987
BT3402	RP5882 *nuoF::*miniTn*10*Cm; Δ*(cyoABCDE)456*::kan (cm^r, kan^r)	Edwards *et al.*, 2006
BT3406	RP5882 *ndh:erm*; Δ*(cyoABCDE)456*::kan (erm^r, kan^r)	Edwards *et al.*, 2006
BT3408	RP5882 *ndh:erm*; *Zbg-2200::kan* Δ*(cydAB')455* (erm^r, kan^r)	Edwards *et al.*, 2006

EC10	RP437 ϕ*pspA-lacZ* (amp^r)	This work
EC11	BT3402 ϕ*pspA-lacZ* (cm^r, kan^r, amp^r)	This work
EC12	BT3406 ϕ*pspA-lacZ* (erm^r, kan^r, amp^r)	This work
EC13	BT3408 ϕ*pspA-lacZ* (erm^r, kan^r, amp^r)	This work
JW3901	BW25113Δ*menA* (kan^r)	Baba *et al.*, 2006
EC14	MVA4Δ*menA* (kan^r)	This work
CHAPTER 5 SPECIFIC		
MG1655 Δ*pspA*	Δ*pspA*	Lloyd *et al.*, 2004
MVA40	MG1655Δ*pspG*	Lloyd *et al.*, 2004
YLS1	MC1000 Δ*minCDE*	A gift from Yu-Ling Shih
YLS2	MC1000 Δ*mreB*	A gift from Yu-Ling Shih
EC16	YLS1 Δ*pspA*	This work
EC17	YLS1 Δ*pspG*	This work
EC18	YLS2 Δ*pspA*	This work

APPENDIX B (PLASMIDS)

The following plasmids were used in this study:

Plasmid	Relevant Characteristics	Reference
GENERAL		
pBAD18-cm	arabinose-inducible pBAD$_{ara}$ promoter expression vector (cm^r)	A gift from J. Beckwith
pBR325D	Recombinant cloning vector (cm^r, tet^r, amp^r)	Laboratory collection
pGEM®-T Easy	Cloning vector (amp^r)	Promega
pGZ119HE	Expression vector with IPTG-inducible P$_{tac}$ promoter; *lacI*^{q} (cm^r)	Lessl *et al.*, 1992
pPMR129	pGZ119HE harbouring *gIV* (pIV) (cm^r)	A gift from M.Russel
pGJ4	Expression vector with a P$_{lacUV5}$ promoter harbouring *gIV* (pIV) (tet^r)	A gift from G. Jovanovic
pRS415	Promoter-less lac transcription fusion vector (amp^r)	Simons *et al.*, 1987
pUT18	pUC19 encoding T18 (aa 225-339 of CyaA) for N-terminal fusion (amp^r)	Karimova *et al.*, 1998
pUT18C	pUC19 encoding T18 (aa 225-339 of CyaA) for C-terminal fusion (amp^r)	Karimova *et al*., 1998
pUT18Czip	pUT18C encoding leucine zipper of GCN4 (amp^r)	Karimova *et al*., 1998
pKT25	pSU40 encoding T25 (aa 1-224 of CyaA) for C-terminal fusion (kan^r)	Karimova *et al.*, 1998
pKNT25	pSU40 encoding T25 (aa 1-224 of CyaA) for N-terminal fusion (kan^r)	Karimova *et al.*, 1998
pKT25zip	pKT25 encoding leucine zipper of GCN4 (kan^r)	Karimova *et al.*, 1998
CHAPTER 3 SPECIFIC		
pCA24N	Expression vector, PT5/lac promoter (cm^r)	Kitagawa *et al.*, 2005
pCP20	FLP+, λcI857+, λpR Repts, (amp^r, cm^r)	Cherepanov and Wackernagel, 1995
pJW5536(-)	PT5/lac-6xhis-arcB (ArcB$_{WT}$), *lacI*q (cm^r)	Kitagawa *et al.*, 2005
pGJ21	pJW5536(-) encoding ArcB$_{H717A}$ (cm^r)	A gift from G. Jovanovic
pGJ22	pJW5536(-) encoding ArcB$_{LeuZm}$ (L87A L90A	A gift from G. Jovanovic

	L94A M97A) (cm^r)	
pGJ23	pJW5536(-) encoding ArcBC180A/C241A (ArcB*) (cm^r)	A gift from G. Jovanovic
pGJ27	pJW5536(-) encoding ArcB*H717A (cm^r)	A gift from G. Jovanovic
pGJ29	pJW5536(-) encoding ArcBLeuZmH717A (cm^r)	A gift from G. Jovanovic
pGJ30	pJW5536(-) encoding ArcB*H292A (cm^r)	A gift from G. Jovanovic
pGJ31	pJW5536(-) encoding ArcBLeuZmH292A (cm^r)	A gift from G. Jovanovic
pGJ33	pJW5536(-) encoding $ArcB_{H292A}$ (cm^r)	A gift from G. Jovanovic
pJW4364(-)	PT5/lac-6xhis-arcA ($ArcA_{WT}$), $lacI^q$ (cm^r)	Kitagawa *et al.*, 2005
pGJ45	pJW4364(-) encoding ArcAD54A/ΔHTH (cm^r)	A gift from G. Jovanovic
pGJ46	pRS415 harbouring ϕ*pfl-lacZ* with 490 bp of *pfl* promoter region amplified by PCR from MG1655 chromosome (amp^r)	A gift from G. Jovanovic
pAJM1	pBAD18-cm encoding PspB (cm^r)	A gift from A. Mayhew
pGJ48	pBAD18-cm encoding $PspB_{LeuZm}$ (L10A L15A L18) (cm^r)	A gift from G. Jovanovic
pAJM2	pBAD18-cm encoding PspC (cm^r)	A gift from A. Mayhew
CHAPTER 5 SPECIFIC		
pDSW209	IPTG-inducible P_{trc} promoter; $lacI^q$; *gfpmut2*-MCS fusion vector (amp^r)	Weiss *et al.*, 1999
pDSW210	IPTG-inducible P_{trc} promoter; $lacI^q$; MCS-*gfpmut2* fusion vector (amp^r)	Weiss *et al.*, 1999
pLL5	pDSW209 encoding GFP-PspA (amp^r)	A gift from L. Lloyd
pEC1	pLL5 containing -GGGGSGGS- linker between *gfpmut2* and *pspA* (amp^r)	This work
pGJ7	pDSW210 encoding PspG-GFP (amp^r)	A gift from G. Jovanovic
pMR25	*lacZ* transcriptional fusion vector (tet^r)	Jones *et al.*, 2003
pSJ1	pMR25 harbouring ϕ*pspA-lacZ* (tet^r)	Jones *et al.*, 2003
pLL11	pBAD18-cm encoding PspG (cm^r)	Lloyd *et al.*, 2004
pAJM26	pKT25 harbouring *pspA* (kan^r)	A gift from A. Mayhew
pAJM27	pKT25 harbouring *pspC* (kan^r)	A gift from A. Mayhew
pAJM33	pUT18 harbouring *pspB* (amp^r)	A gift from A. Mayhew
pEC2	pKT25 harbouring *mreB* (kan^r)	This work
pEC3	pUT18C harbouring *mreB* (amp^r)	This work
pEC4	pUT18 harbouring *pspG* (amp^r)	This work

APPENDIX C (PRIMER)

The following primers were used in this study:

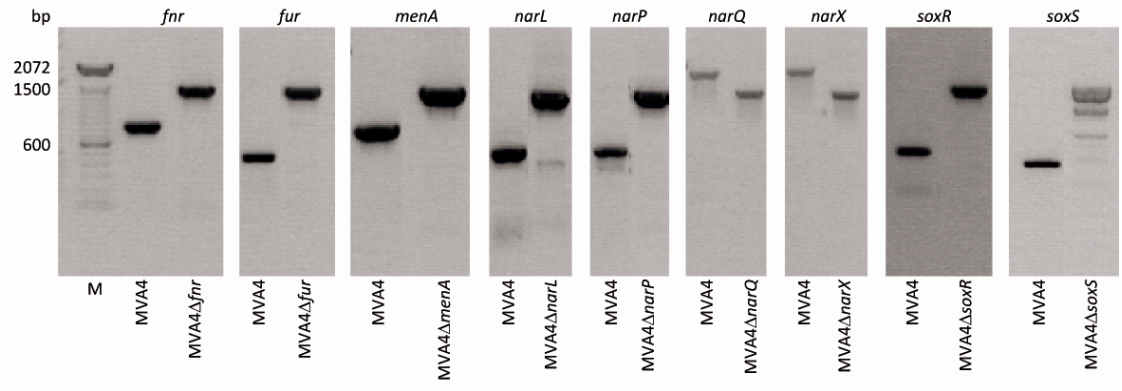
Primer Set	Sequence (5' – 3')	Used For
PspA-GFP1F	5'GCATGGATGAACTATACAAAGGTGGTGGTGGT TCTGGTGGTTCTGAATTCATGGGTATTTTTTCTC3'	Integrating a flexible linker between *gfpmut2* and *pspA*
PspA-GFP1R	5'GAGAAAAAATACCCATGAATTCAGAACCACCAG AACCACCACCACCTTTGTATAGTTCATCCATGC3'	
PspG XbaI F	5'AGCTAGGTCTAGAGATGCTGGAACTACTTTTTGTGATTG GCTTT3'	To clone *pspG* into pUT18 and pKNT25
PspG KpnI R	5'AGCTGTTGGTACCCAGTAACGCCAGCGGTCATAACGCTG ATATTT3'	
MreB XbaI F	5'AGCTAGGTCTAGAGATGTTGAAAAAATTTCGTGG3'	To clone *mreB* into pUT18C and pKT25
MreB KpnI	5'AGCTGTTGGATCCGATTACTCTTCGCTGAACAGGTCG3'	
Kan F	5'-ATTCCGGGGATCCGTCGACC-3'	To analyse gene deletions
Kan R	5'-TGTAGGCTGGAGCTGCTTCG-3'	
MenA F	5'-ATGACTGAACAACAAATTAGC-3'	To analyse *menA* deletion
MenA R	5'-TTATGCTGCCCACTGGCTTAG-3'	
FNR F	5'-ATGATCCCGGAAAAGCGAATTATACG-3'	To analyse *fnr* deletion
FNR R	5'-TCAGGCAACGTTACGCGTATG-3'	
FUR F	5'-ATGACTGATAACAATACCGC-3'	To analyse *fur* deletion
FUR R	5'-TTATTTGCCTTCGTGCGCATG-3'	
NarL F	5'-ATGAGTAATCAGGAACCGGC-3'	To analyse *narL* deletion
NarL R	5'-TCAGAAAATGCGCTCCTGATG-3'	
NarP F	5'-ATGCCTGAAGCAACACCTTTTCAGG-3'	To analyse *narP* deletion
NarP R	5'-TTATTGTGCCCCGCGTTGTTG-3'	
NarQ F	5'-GTGATTGTTAAACGACCCGTCTCG-3'	To analyse *narQ* deletion
NarQ R	5'-TTACATTAACTGACTTTCCTC-3'	
NarX F	5'-ATGCTTAAACGTTGTCTCTCTCC-3'	To analyse *narX* deletion
NarX R	5'-TTACTCATGGGTATCTCCTTG-3'	
SoxR F	5'-ATGGAAAAGAAATTACCC-3'	To analyse *soxR* deletion
SoxR R	5'-TTAGTTTTGTTCATCTTCCAG-3'	
SoxS F	5'-ATGTCCCATCAGAAAATTATTCAGG-3'	To analyse *soxS* deletion
SoxS R	5'-TTACAGGCGGTGGCGATAATC-3'	

APPENDIX D (ANALYSIS OF KNOCK-OUT STRAINS)

Knock-out strains created in this study were analysed for successful deletion of the desired gene by PCR using primers which bind just outside the coding sequence on the chromosome. The chromosomal DNA (the template for the PCR) was purified as described in section 2.3.1.1 and the PCR was performed as described in section 2.3.2.2. Successful replacement of the desired gene in the WT strain (here MVA4, see Appendix A) with the kanamycin cassette from the Keio collection strains can be seen as a PCR product of around 1300 bp amplified by the gene specific primer pair (see Appendix C and Baba *et al.*, 2006).

The sizes of the WT allels of the replaced genes are as follows:

fnr: 753bp; *fur*: 447bp; *menA*: 927bp; *narL*: 651bp; *narP*: 648bp; *narQ*: 1701bp; *narX*: 1797bp; *soxR*: 465bp; *soxS*: 324bp.



In each strain tested, the gene of interest was successfully replaced as seen by the amplification of a DNA fragment of around 1300 bp corresponding to the kanamycin cassette used in the Keio collection strains (Baba *et al.*, 2006). M: TrackIt™ 100 bp DNA ladder (Invitrogen).

APPENDIX E (ANTIBODIES)

Antibody combinations used for detecting the desired proteins are shown below.

Protein	Primary Antibody	Secondary Antibody
ArcB	Rabbit- α-ArcB (1 : 10,000) A gift from D. Georgellis	Goat-α-Rabbit-HRP (1 : 5,000) GE Healthcare
GFP	Mouse-α-GFP (JL-8) (1 : 4,000) Clontech	Sheep-α-Mouse-HRP (1 : 10,000) GE Healthcare
Cya (T18-fragment)	Rabbit- α-Cya(T18) (1 : 1,000) Eurogentec	Goat-α-Rabbit-HRP (1 : 5,000) GE Healthcare
Cya (T25-fragment)	Rabbit- α-Cya(T25) (1 :1,000) Eurogentec	Goat-α-Rabbit-HRP (1 : 5,000) GE Healthcare
PspA	Mouse-α-PspA (1 : 10,000) Lloyd *et al.*, 2004	Sheep-α-Mouse-HRP (1 : 10,000) GE Healthcare
PspB	Rabbit- α-PspB (1 : 5,000) Adams *et al.*, 2003	Goat-α-Rabbit-HRP (1 : 5,000) GE Healthcare
PspC	Rabbit- α-PspC (1 : 5,000) Adams *et al.*, 2003	Goat-α-Rabbit-HRP (1 : 5,000) GE Healthcare
PspD	Rabbit- α-PspD (1 : 1,000) Adams *et al.*, 2003	Goat-α-Rabbit-HRP (1 : 5,000) GE Healthcare

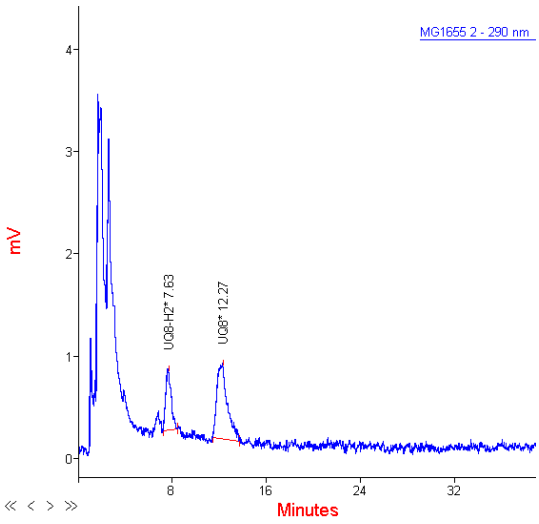
PspF	Mouse-α-PspF (1 : 4,000) Lloyd *et al.*, 2004	Sheep-α-Mouse-HRP (1 : 10,000) GE Healthcare
PspG	Rabbit- α-PspG (1 : 1,000) Eurogentec	Goat-α-Rabbit-HRP (1 : 5,000) GE Healthcare
pIV	Rabbit- α-pIV (1 : 10,000) A gift from M. Russel	Goat-α-Rabbit-HRP (1 : 5,000) GE Healthcare
SecA	Rabbit- α-SecA (1 : 10,000) Minotech	Goat-α-Rabbit-HRP (1 : 5,000) GE Healthcare
TatA	Rabbit- α-TatA (1 : 5,000) A gift from T. Palmer	Goat-α-Rabbit-HRP (1 : 5,000) GE Healthcare

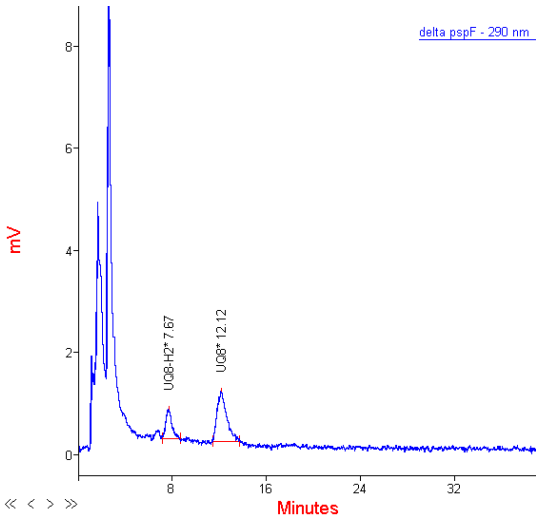
APPENDIX F (HPLC TRACES FROM THE QUINONE MEASUREMENT)

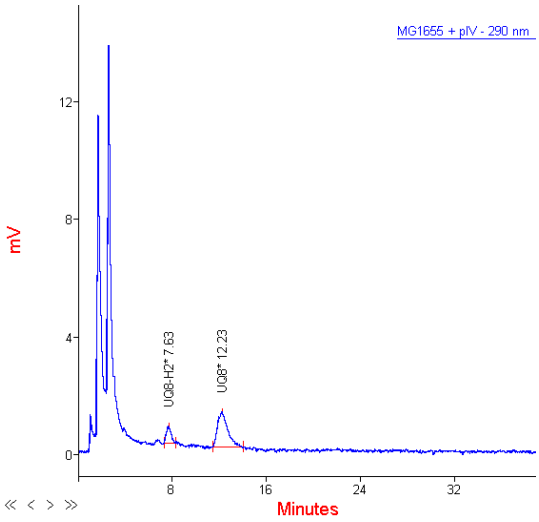
Shown below are the raw data of the HPLC traces obtained from the Quinone measurements in Chapter 4. Ubiquinones are measured at 290 nm and menaquinones at 248 nm. UQ_8-H_2 elutes after 7-8 minutes, UQ_8 after 12-13 minutes, DMK_8 after 18-19 minutes and MK_8 after 21-22 minutes.

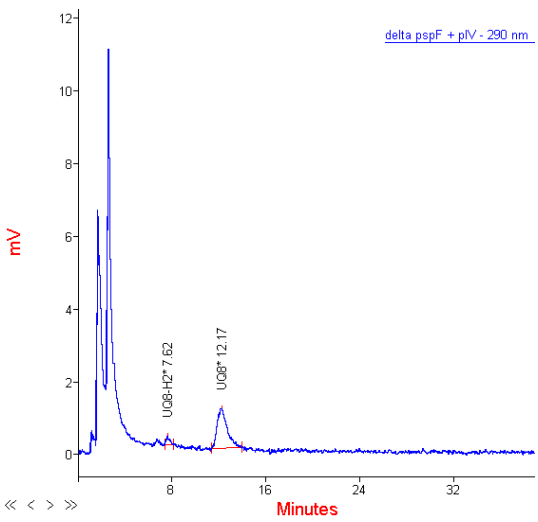
MG1655 strains

UQ_8 and UQ_8-H_2 aerobic

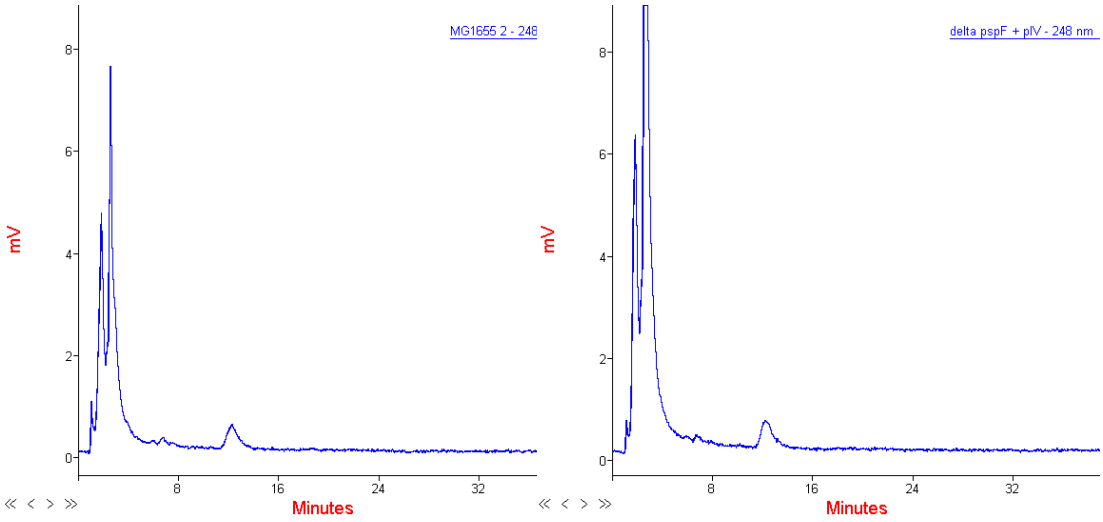




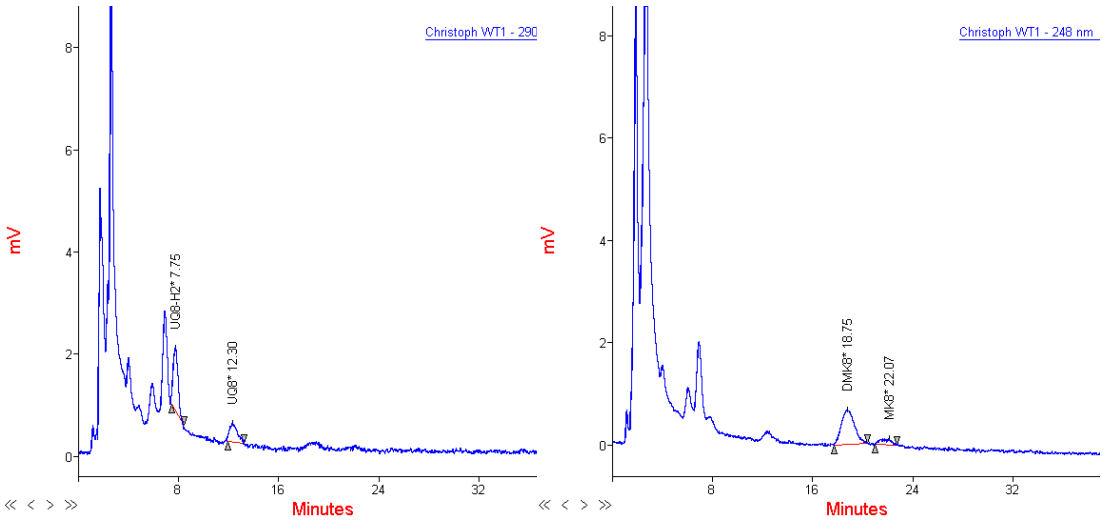


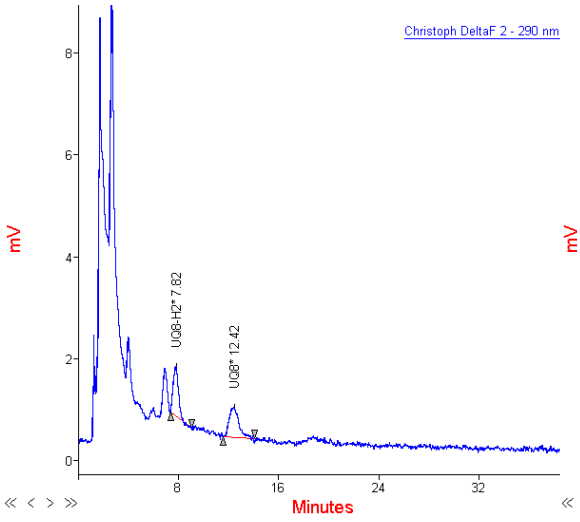


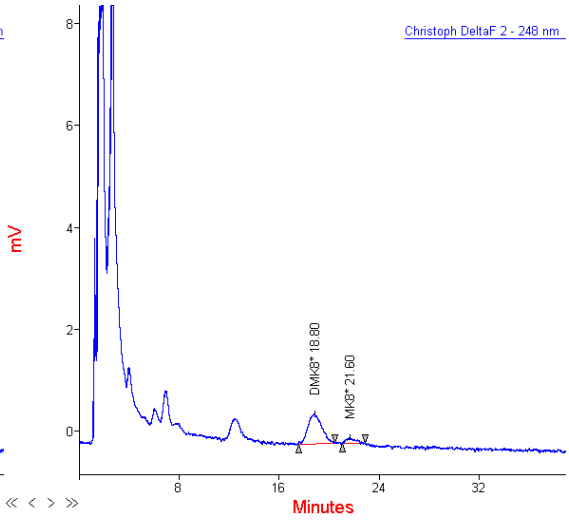
no DMK_8 and MK_8aerobic

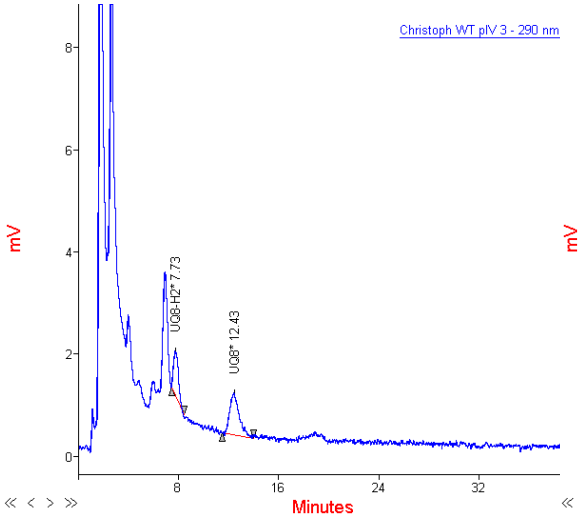


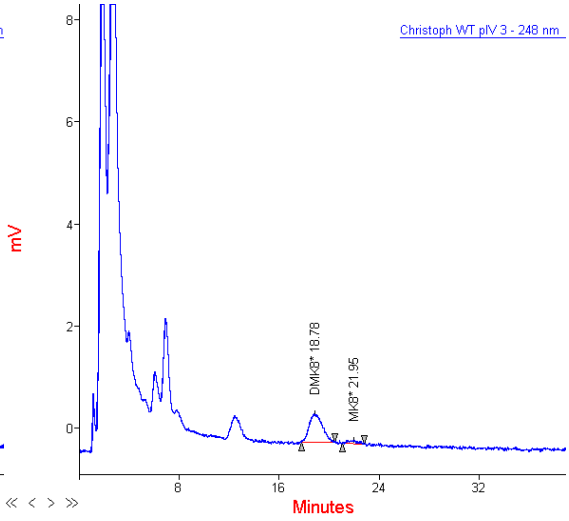
UQ_8, UQ_8-H_2, DMK_8 and MK_8 microaerobic

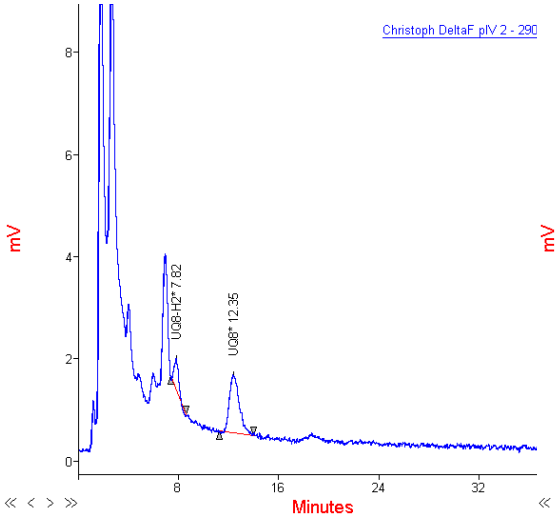


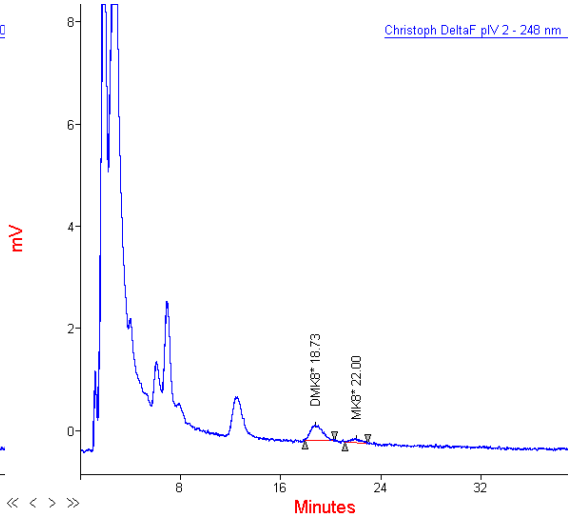

Christoph DeltaF 2 - 290 nm
mV
UQ8-H2* 7.82
UQ8* 12.42
Minutes


Christoph DeltaF 2 - 248 nm
mV
DMK8* 18.80
MK8* 21.60
Minutes


Christoph WT pIV 3 - 290 nm
mV
UQ8-H2* 7.73
UQ8* 12.43
Minutes

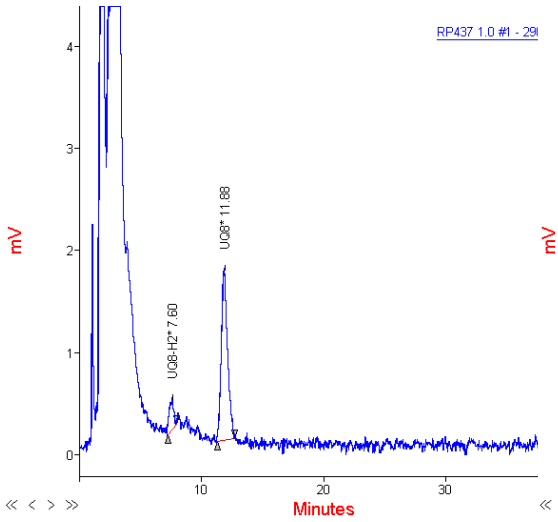

Christoph WT pIV 3 - 248 nm
mV
DMK8* 18.78
MK8* 21.95
Minutes

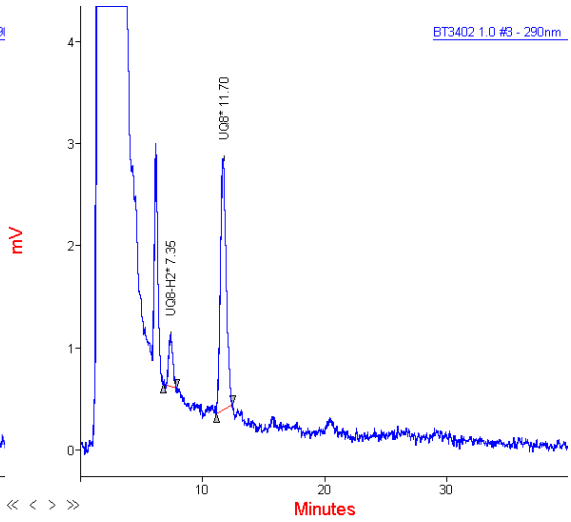

Christoph DeltaF pIV 2 - 290
mV
UQ8-H2* 7.82
UQ8* 12.35
Minutes

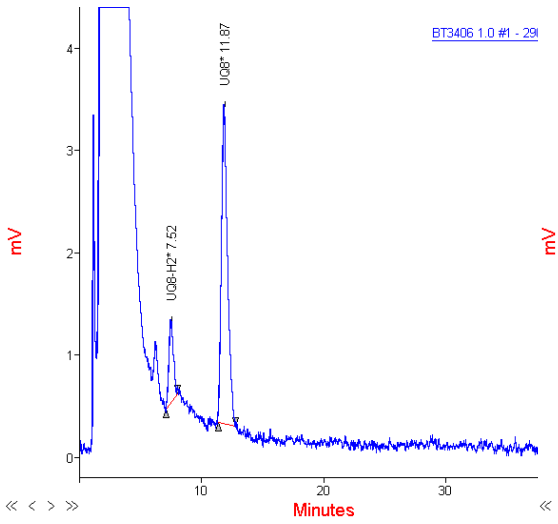

Christoph DeltaF pIV 2 - 248 nm
mV
DMK8* 18.73
MK8* 22.00
Minutes

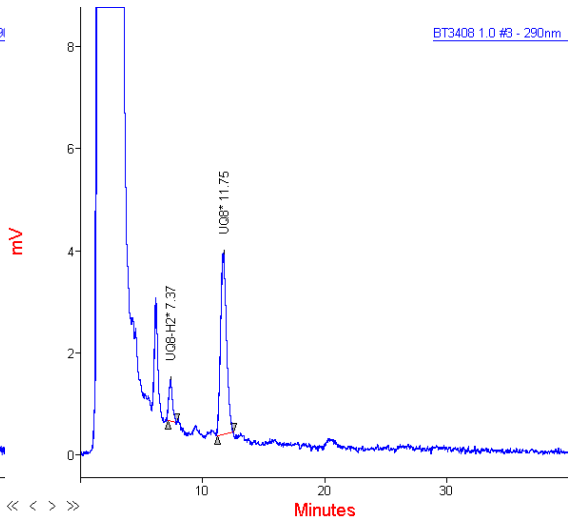
BT strains

$\underline{UQ_8 \text{ and } UQ_8\text{-}H_2 \text{ aerobic}}$

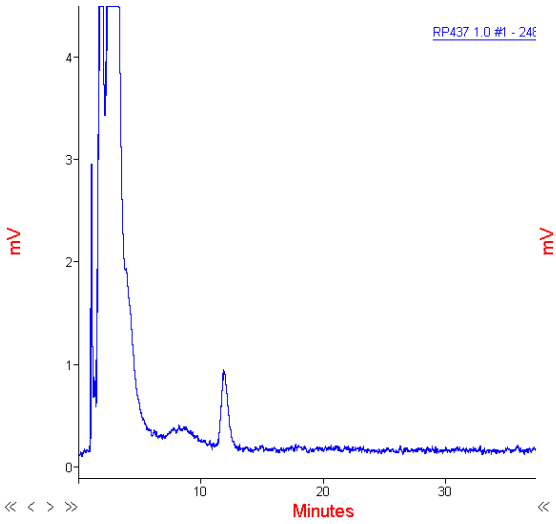


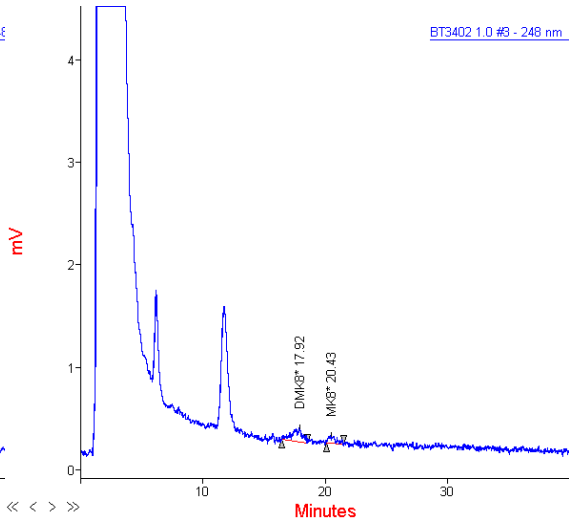


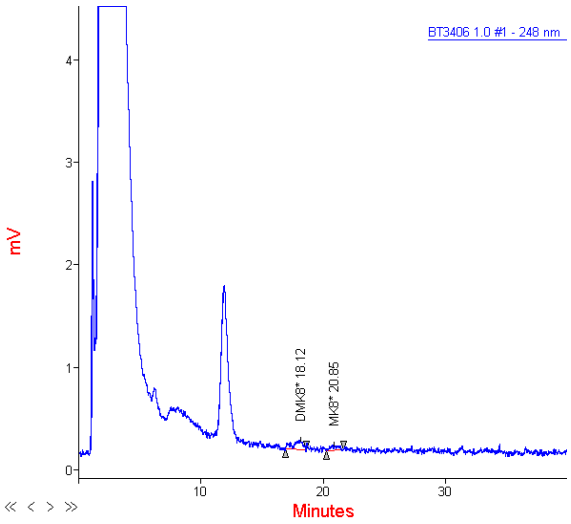


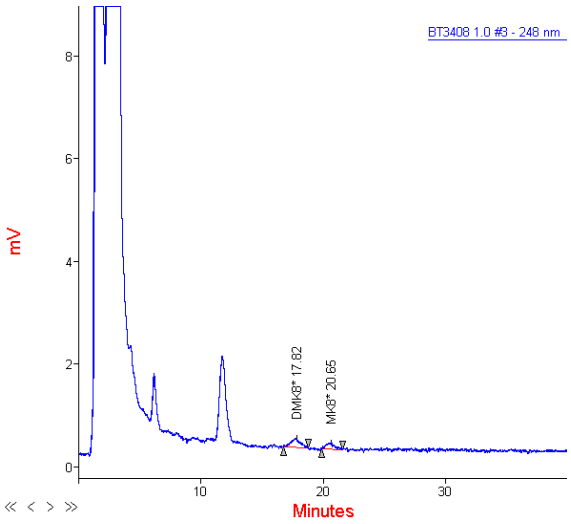


DMK$_8$ and MK$_8$ aerobic (no MK$_8$ in WT RP437, but in BT mutants show some MK$_8$ production)

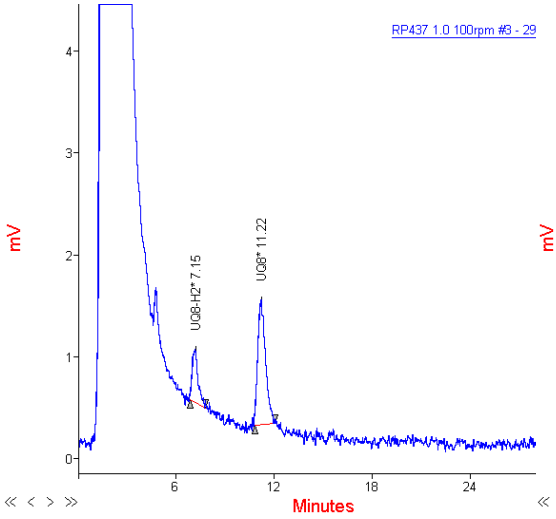


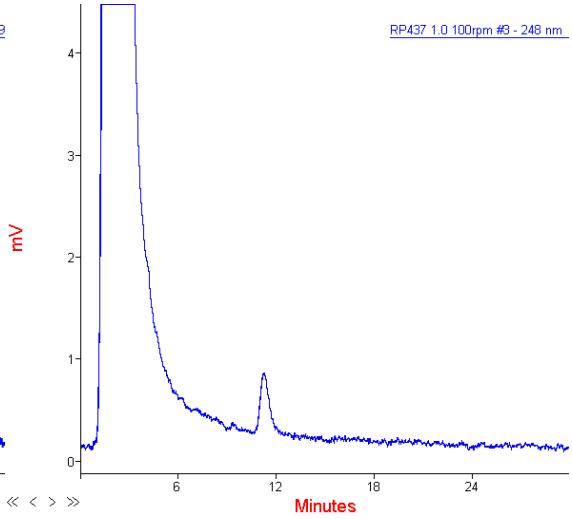


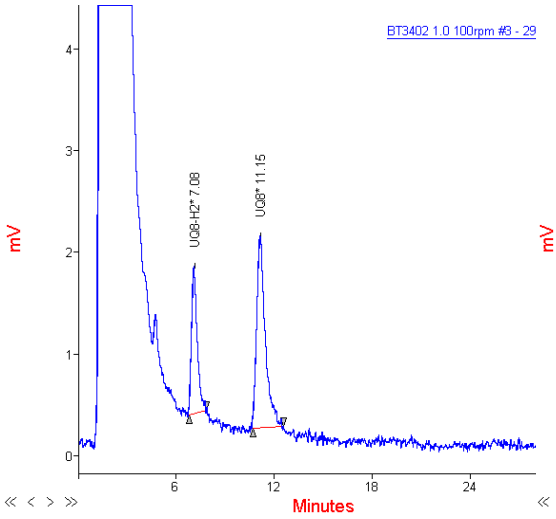


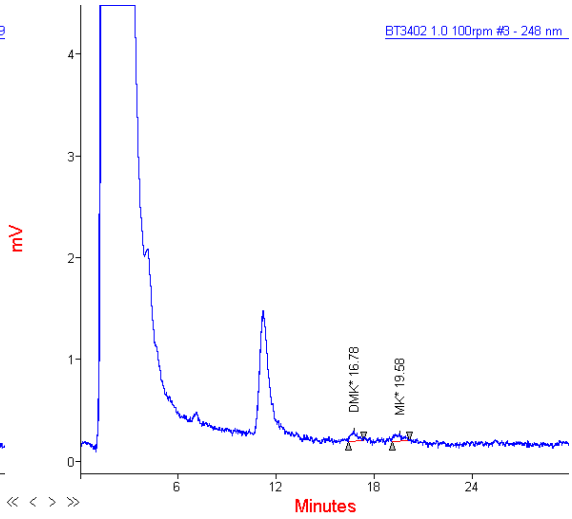


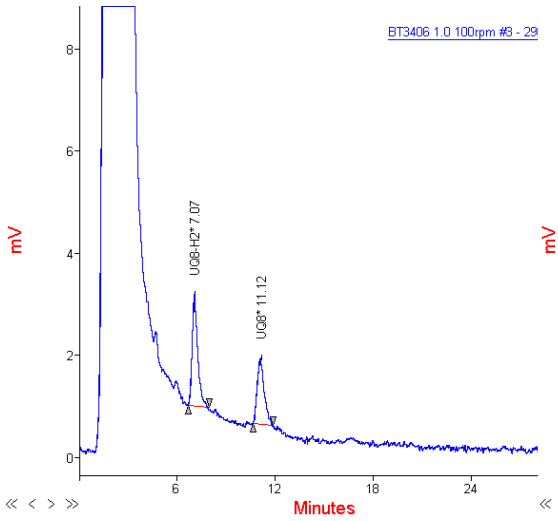
UQ_8, UQ_8-H_2, DMK_8 and MK_8 microaerobic

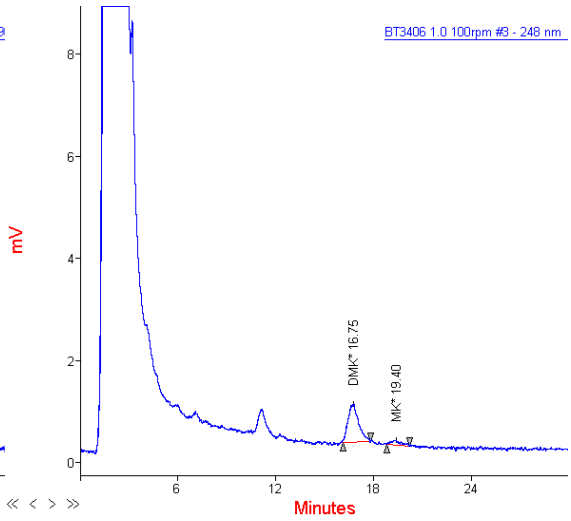


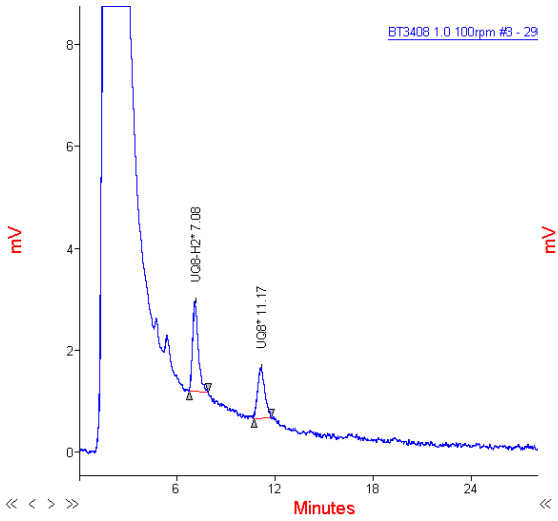


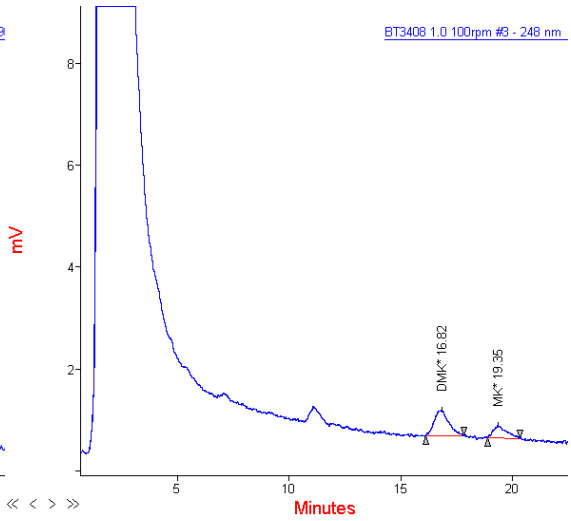




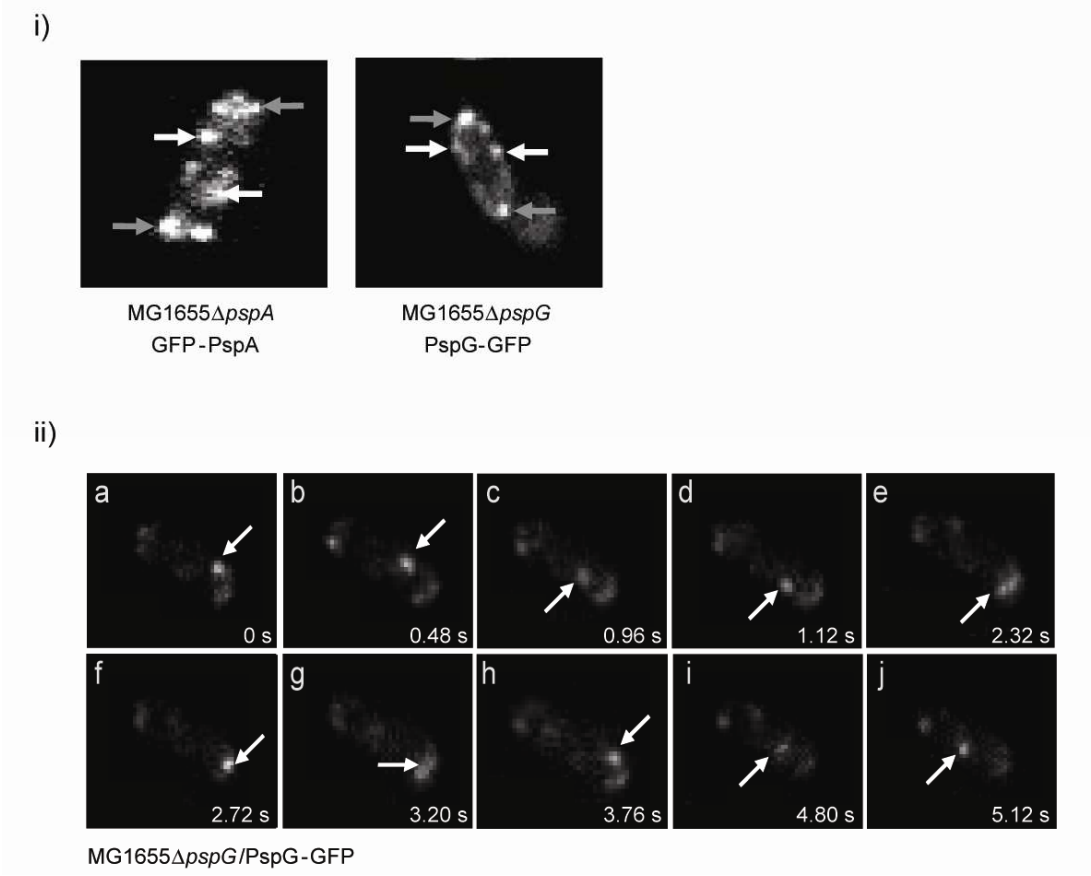

BT3406 1.0 100rpm #3 - 29
mV
UQ6-H2* 7.07
UQ8* 11.12
Minutes


BT3406 1.0 100rpm #3 - 248 nm
mV
DMK* 16.75
MK* 19.40
Minutes

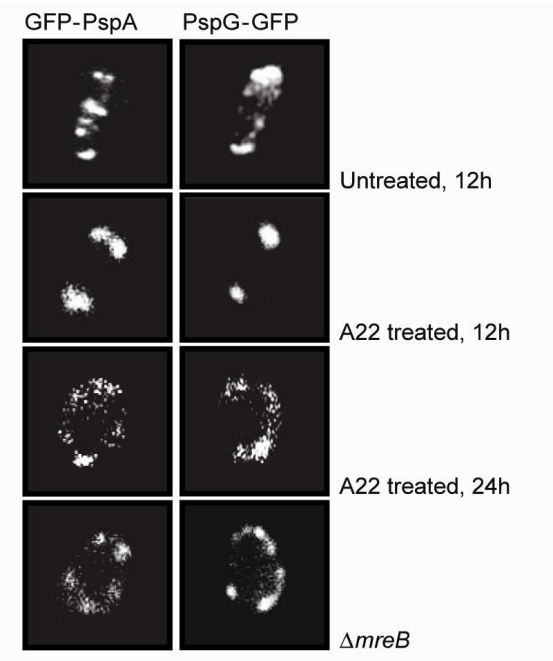

BT3408 1.0 100rpm #3 - 29
mV
UQ6-H2* 7.08
UQ8* 11.17
Minutes


BT3408 1.0 100rpm #3 - 248 nm
mV
DMK* 16.82
MK* 19.35
Minutes

APPENDIX G (ORIGINAL IMAGES FROM THE LOCALISATION STUDY)



Original epi-fluorescence images of Figure 5.9. Shown are the original epi-fluorescence images of *E. coli* MG1655Δ*pspA*/GFP-PspA and MG1655Δ*pspG*/PspG-GFP cells. Polar GFP fusion proteins are indicated with grey arrows, lateral complexes with white arrows. (a-j) Original time-lapsed epi-fluorescence images of MG1655Δ*pspG*/PspG-GFP cells. The movement of one of the mobile lateral complexes is indicated in each image by a black arrow. All images were taken using a Nikon TE-2000 inverted optical microscope.



Original epi-fluorescence images of Figure 5.10. Shown are the original epi-fluorescence images of *E. coli* MG1655Δ*pspA*/GFP-PspA and MG1655Δ*pspG*/PspG-GFP cells before and after A22 treatment and of *E. coli* MC1000Δ*mreB* cells expressing either GFP-PspA or PspG-GFP. Either disruption or removal of MreB results in only polar GFP-PspA and PspG-GFP complexes being visible. All images were taken using Nikon TE-2000 inverted optical microscope.

APPENDIX H (PUBLICATIONS ARISING FROM THIS WORK)

Engl, C., Jovanovic, G., Lloyd, L.J., Murray, H., Spitaler, M., Ying, L., Errington, J., and Buck, M. (2009) *In vivo* localizations of membrane stress controllers PspA and PspG in *Escherichia coli*. *Mol. Microbiol.* **73**: 382-396.

Huvet, M., Toni, T., Tan, H., Jovanovic, G., **Engl, C.**, Buck, M., and Stumpf, M.P. (2009) Model-based evolutionary analysis: the natural history of phage-shock stress response. *Biochem. Soc. Trans.* **37**: 762-767.

Engl, C., Jovanovic, G., and Buck, M. (2009) Physical, functional and conditional interactions between ArcAB and phage shock proteins upon secretin-induced stress in *Escherichia coli*. *Mol. Microbiol.* **74**: 16-28.

Joly, N., Burrows, P.C., **Engl, C.**, Jovanovic, G., and Buck, M. (2009) A lower-order oligomer form of phage shock protein A (PspA) stably associates with the hexameric AAA(+) transcription activator protein PspF for negative regulation. *J. Mol. Biol.* **394**: 764-775.

Jovanovic, G., **Engl, C.**, Mayhew, A.J., Burrows, P.C., and Buck, M. Phage shock protein (Psp) inner membrane regulatory complexes govern signal transduction and induction of the Psp response in *Escherichia coli*. *Submitted*.

Engl, C., Ter Beek, A., Bekker, M., Teixeira de Mattos, J., Jovanovic, G., and Buck, M. Correlations between quinone pools and induction of the Phage shock proteins in *Escherichia coli*. *Submitted*.